

# **Investigation of response and resistance to dasatinib in melanoma cells**

A Thesis submitted for the degree of Ph.D.

by Alexander J. Eustace BSc. MSc.

June 2010

The work in this thesis was carried out under the supervision of

Dr. Norma O'Donovan,  
Prof. Martin Clynes & Prof. John Crown

National Institute for Cellular Biotechnology  
School of Biotechnology  
Dublin City University

*I hereby certify that this material, which I now submit for assessment on the programme of study leading to the award of Ph D. is entirely my own work, that I have exercised reasonable care to ensure that the work is original, and does not to the best of my knowledge breach any law of copyright, and has not been taken from the work of others save and to the extent that such work has been cited and acknowledged within the text of my work.*

**Signed:** \_\_\_\_\_ **ID No.:** 56122578

**Date:** \_\_\_\_\_

## Acknowledgements

I would like firstly to acknowledge the huge commitment made by supervisor Dr. Norma O'Donovan and her unfaltering support which I received as I undertook my PhD. project. Throughout this project I have always been able to call on her for advice, encouragement and support and she has always been both receptive and enthusiastic in her attempts to get me to push on and achieve more. Without her efforts I would not have been able to put together this body of work.

Thank-you to my co-supervisors Prof. John Crown and Prof. Martin Clynes. Firstly I would like to thank Martin for taking me back as a Research Assistant after my travels overseas. My work as a Research Assistant really encouraged me to undertake the PhD, and without Martins support and enthusiasm I would not have been able to proceed with this study. I would also like to thank John for accepting me into the Targeted Therapies group. His appetite for clinical advancement is infectious and played a key role in focusing my thesis towards developing clinically relevant results.

I would like to acknowledge the many people who have assisted me with the numerous assays in my study. Dr. Niall Barron's help with the molecular work including my PCR and siRNA studies was invaluable. Thanks also to Dr. Paul Dowling, Dr. Paudie Doolin and Michael Henry for their help with my proteomic analysis and literature mining. What was a potentially very complicated set of experiments ran very smoothly thanks to their supervision and support. I would also like to acknowledge the efforts of Dr. Anne-Marie Larkin and Dr. Susan Kennedy for their help with the immunohistochemistry work. Anne-Marie taught me the complexities of IHC whilst Susan Kennedy very kindly agreed to score the slides. I wonder though if each of them knew how much work was involved in each of the studies before they all agreed to take it on!

Thanks as well to all those who have helped me on the way. From Joe's tireless work in the Prep room, to the invaluable support I received from Carol, Yvonne and Mairead in the office. I would also like to thank all those who contributed to my enjoyment of the PhD. Process. From the people in the Targeted Therapies group Denis, Aoife, Brendan, Brigid, Martina and Thamir, to those who made me smile on the days when it mattered most. In retrospect, i think that it is easier a couple of months after completion to say that I enjoyed the PhD!

Finally I'd like to thank my family for believing in me especially my Dad, John, for accepting that I might never leave the University system, and my late Mum Penny, to whom I would like to dedicate this body of work. Then to my wife Rachel for always being there and believing in me, and for bearing me the two most beautiful children, Liam and Conor. For that, this has all been worth it.

## Abbreviations

2-D DIGE	- 2 dimensional differential gel electrophoresis
5-FU	- 5-fluoro uracil
ACN	- Acetonitrile
AJCC	- American Joint Committee on Cancer
AK	- Actinic keratosis
AMN	- Acquired melanocytic nevus
ANXA1	- Annexin-A1
ANXA2	- Annexin-A2
APC	- Antigen presenting cells
ATase	- O <sup>6</sup> Alkyl-transferase
ATCC	- American Type Culture Collection
ATP	- Adenosine triphosphate
ABC	- ATP binding cassette
BCA	- Bicinchoninic acid
BCC	- Basal cell carcinoma
BCL-2	- B-cell CLL/lymphoma 2
BCNU	- Carmustine
Bcr-Abl	- C-abl oncogene 1
BCRP	- Breast cancer resistance protein
bFGF	- Basic fibroblast growth factor
BRAF	- V-raf murine sarcoma viral oncogene homolog B1
BrdU	- 5-bromo-2-deoxyuridine
BVA	- Biological variation analysis
CAV-1	- Caveolin-1
CAV-2	- Caveolin-2
CCNU	- Lomustine
cDNA	- Complimentary DNA
C.I.	- Combination index
c-Kit	- V-kit Hardy-Zuckerman 4 feline sarcoma viral oncogene homolog
c-MET	- Met proto-oncogene
CTLA-4	- Cytotoxic T-lymphocyte associated antigen 4 receptors

DEPC	- Diethyl pyrocarbonate
DIA	- Differential in-gel analysis
DMF	- Dimethylformamide
DN	- Dysplastic nevus
DNA	- Deoxyribonucleic acid
dNTP	- Deoxyribonucleotide triphosphate
DTIC	- Dacarbazine
ECACC	- European Association Culture Collection
ED	- Effective dose
EphA	- Ephrin-A
ERK	- MAPK
ERP	- Endoplasmic reticulum protein
FAK	- Focal adhesion kinase
FCT	- Fumitremorgin C
HEPES	- 4-(2-hydroxyethyl)-1-piperazineethanesulfonic acid
HGF	- Hepatocyte growth factor/scatter factor
HMB45	- Melanoma antibody
HPV	- Human papilloma virus
HR	- hazard ratio
HRP	- Horseradish peroxidase
HSP60	- Heat shock protein 60
IAP	- Inhibitor of apoptosis
IC <sub>50</sub>	- Inhibitory concentration 50 %
IFN- $\alpha$ 2b	- Interferon $\alpha$ 2b
IGF	- Insulin growth factor
IGFBP2	- IGF binding protein 2
IHC	- Immunohistochemistry
IL	- Interleukin
INK4A	- Cyclin-dependent kinase inhibitor 4A
IP	- Immunoprecipitated
kDa	- Kilo Dalton
LC-MS	- Liquid chromatography- mass spectrometry
LDH	- Lactate dehydrogenase

MALDI-ToF-MS - Matrix-assisted laser desorption/ionisation-time of flight mass spectrometry

MAPK	- Mitogen activated protein kinase
MART-1	- Melan-A
MCAM	- Melanoma cell adhesion molecule
MDR	- Multi-drug resistance
MEK	- MAPK/ERK kinase
MIA	- Melanoma inhibitory activity
MMLV-RT	- Moloney murine leukaemia virus reverse transcriptase
MMS	- Mohs microscopic surgery
mRNA	- messenger RNA
MRP	- Multi-drug resistance protein
MTIC	- Methyl-triazeno imidazole carboxiamide
mTOR	- Mammalian target of rapamycin
NCBI	- National Centre for Biotechnology Information
NCI	- National Cancer Institute
OD	- Optical density
p-protein	- Phosphorylated-protein
PANTHER	- Protein ANALYSIS THrough Evolutionary Relationships
PBS	- Phosphate buffered solution
PCR	- Polymerase chain reaction
PDGF	- Platelet derived growth factor
PEG-IFN- $\alpha$ 2b	- pegylated IFN- $\alpha$
P-gP	- P-glycoprotein
PI3/AKT	- Phosphoinositide 3-kinase
PMSF	- Phenylmethanesulphonylfluoride
PNP	- Paranitrophenol phosphate
PTEN	- Phosphatase and tension homolog
PTRF	- Polymerase I and transcript release factor
qRT-PCR	- Qualitative RT-PCR
RGP	- Radial growth phase
RNA	- Ribonucleic acid
RNase	- Ribonuclease

RT	- Room temperature
RTK	- Receptor tyrosine kinases
RT-PCR	- Reverse transcriptase-PCR
S100	- S100 calcium binding protein
SCC	- Squamous cell carcinoma
SCF	- Stem cell factor
SDS	- Sodium dodecyl sulphate
SFM	- Serum free medium
SiRNA	- Small interfering RNA
SMM	- Superficial spreading melanoma
SRC	- V-src sarcoma (Schmidt-Ruppin A-2) viral oncogene
homolog	
STAT	- Signal transducer and activator of transcription
SVUH	- Saint Vincents University hospital
TFA	- Trifluoro acetic acid
TGF- $\beta$	- Transforming growth factor- $\beta$
TKI	- Tyrosine kinase inhibitor
TMZ	- Temozolomide
TUNEL	- Terminal DNA transferase-mediated dUTP nick end labelling
UV	- Ultra violet
VEGF	- Vascular endothelial growth factor
VGP	- Vertical growth phase

Acknowledgements.....	2
Abstract.....	14
1. Introduction and background.....	15
1.1 The structure and function of skin.....	17
1.2 Skin Cancer.....	19
1.2.1 Basal Cell Carcinoma.....	19
1.2.2 Actinic Keratosis.....	20
1.2.3 Squamous cell carcinoma <i>in situ</i> .....	21
1.2.4 Squamous cell carcinoma.....	21
1.2.5 Melanoma skin cancer.....	22
1.2.5.1 Aquired melanocytic nevus.....	22
1.2.5.2 Dysplastic nevus.....	23
1.2.5.3 Radial Growth Phase.....	24
1.2.5.4 Vertical Growth Phase.....	24
1.2.6 Classification of cutaneous malignant melanoma.....	25
1.2.7 Clinical variables and prognostic markers in malignant melanoma.....	26
1.3 From melanocyte to melanoma, the road to metastasis.....	30
1.3.1 Cadherin expression in melanoma progression.....	30
1.3.2 Growth factor dependence in melanoma development.....	31
1.3.3 Role of receptor tyrosine kinases in melanoma progression.....	32
1.3.4 Mitogen activating protein kinase pathway (MAPK).....	35
1.3.5 AKT Pathway.....	37
1.4 Current therapies for metastatic melanoma.....	38
1.4.1 Chemotherapy.....	38



1.5 Drug resistance in melanoma.....	42
1.5.1 Multi-drug resistance protein (MRP) and P-glycoprotein (P-gP).....	42
1.6 Immuno-therapy.....	46
1.6.1 Interleukin-2 therapy.....	47
1.6.2 Interferon- $\alpha$ therapy.....	49
1.6.3 CTLA-4 therapy.....	50
1.6.4 Chemotherapy combined with immunotherapy.....	51
1.7 Targeted therapies for melanoma treatment .....	53
1.7.1 Targeting the RAS/RAF/MAPK Pathway in Melanoma.....	53
1.7.2 Targeting the PI3/AKT Pathway in Melanoma .....	55
1.7.3 Novel tyrosine kinase targets in melanoma .....	58
1.7.3.1 C-Kit receptor .....	58
1.7.3.2 SRC Kinase.....	59
1.8 Summary.....	60
2. Materials and Methods.....	63
2.1 Cells and Reagents.....	64
2.2 Invasion assays.....	65
2.3 Proliferation assay.....	66
2.4 RNA Extraction .....	66
2.5 Reverse Transcriptase Reaction.....	67
2.6 Polymerase Chain Reaction (PCR).....	67
2.7 Real-Time PCR.....	69
2.8 Establishing temozolomide resistant cell lines .....	70
2.9 Establishing taxotere resistant cell line.....	70
2.10 Terminal DNA transferase-mediated dUTP nick end labelling (TUNEL) assay	71

2.11 Cell Cycle Assays .....	72
2.12 Protein Extraction and Western blotting.....	73
2.13 Immunoprecipitation.....	74
2.14 Immunohistochemistry .....	75
2.15 Phosphoprotein preparation .....	77
2.16 Protein Precipitation and Quantification.....	77
2.17 Protein labelling and two-dimensional differential gel electrophoresis (DIGE) .	78
2.18 Gel Imaging .....	80
2.19 Spot digestion.....	80
2.20 MALDI-ToF-ToF Mass Spectrometry and Protein Identification.....	81
2.21 One dimensional (1D) reverse phase chromatography for simple protein mixtures .....	82
2.22 Pro-Q Diamond phosphostaining.....	83
2.23 Bioinformatics analysis and literature mining .....	84
2.24 Small interfering RNA (siRNA) transfection .....	84
2.25 Statistical analysis.....	85
3. Characterisation of invasion and drug sensitivity in melanoma cell lines.....	87
3.1 Introduction.....	88
3.2 Invasion and motility of melanoma cell lines .....	89
3.3 Chemo-sensitivity .....	91
3.3.1 Chemotherapy drug sensitivity in melanoma cell lines .....	91
3.3.2 Comparison of chemo-sensitivity in cancer cell lines .....	92
3.4 Expression of ABC transporters in melanoma cell lines .....	94
3.5 Acquired temozolomide resistance in melanoma cell lines.....	95
3.5.1 Induction of temozolomide resistance in pulse selected melanoma cells.....	95

3.5.2 Expression of ABC transporters in temozolomide resistant cell lines.....	96
3.5.3 Cross resistance of temozolomide pulse selected variants .....	97
3.6 Acquired taxotere resistance in melanoma cell lines.....	98
3.6.1 Induction of taxotere resistance in melanoma cell lines .....	98
3.6.2 Expression of ABC transporters in taxotere resistant cell lines.....	99
3.7 BCRP inhibition in melanoma cell lines.....	100
3.8 MRP-2 inhibition in melanoma cell lines .....	103
3.9 Summary .....	105
4. <i>In vitro</i> evaluation of the effects of dasatinib in melanoma cells .....	106
4.1 Introduction.....	107
4.2 Sensitivity to dasatinib and imatinib.....	107
4.3 Effect of dasatinib on invasion and migration .....	109
4.4 Effect of dasatinib on apoptosis.....	111
4.5 Effect of dasatinib on cell cycle arrest.....	111
4.6 Dasatinib effects on cell signalling .....	115
4.6.1 SRC kinase.....	115
4.6.2 EphA2 .....	116
4.6.3 Focal adhesion kinase .....	118
4.6.4 MAPK and AKT .....	120
4.7 Summary .....	121
5. Evaluation of dasatinib in combination with current therapies in melanoma.....	123
5.1 Introduction.....	124
5.2 Dasatinib in combination with chemotherapy .....	124
5.3 Sensitivity to sorafenib in melanoma cells .....	130
5.4 Sensitivity of TMZ resistant melanoma cell lines to dasatinib.....	133

5.5 Summary.....	137
6. Biomarkers for dasatinib treatment in melanoma.....	138
6.1 Introduction.....	139
6.2 Evaluation of Src, EphA2 and FAK as biomarkers for dasatinib therapy in melanoma cell lines.....	139
6.3 Evaluation of a 6-gene predictive biomarker panel by qRT-PCR.....	141
6.4 Protein expression of biomarker panel in melanoma cell lines.....	144
6.5 Immunohistochemistry analysis of selected biomarkers.....	149
6.5.1 Patient characteristics.....	149
6.6.1 Caveolin-1 expression in melanoma samples.....	150
6.6.2 Percentage of tumour cells positive for CAV-1 expression in melanoma samples.....	153
6.6.3 Intensity of Caveolin-1 expression in melanoma samples.....	155
6.7.1 SRC kinase expression in melanoma samples.....	157
6.7.2 Percentage of tumour cells positive for SRC expression in melanoma samples.....	159
6.7.3 Intensity of SRC kinase expression in melanoma samples.....	161
6.8 Summary.....	163
7. Phosphoproteomic analysis of dasatinib sensitive WM-115 and dasatinib resistant WM266-4 melanoma cells.....	164
7.1 Introduction.....	165
7.2 2-D DIGE analysis.....	165
7.3 Phosphoprotein identification by LC-MS and MALDI-ToF-MS.....	168
7.4 Phosphoproteins uniquely associated with dasatinib treatment in sensitive and resistant cell lines.....	175

7.4.1 Phosphoproteins uniquely altered in response to dasatinib treatment in sensitive WM-115 cells.....	176
7.4.2 Phosphoproteins uniquely altered in response to dasatinib treatment in resistant WM-266-4 cells .....	177
7.5 PANTHER analysis of identified phosphoproteins .....	178
7.6 Pathway Studio analysis of phosphoproteins altered in dasatinib treated melanoma cells .....	181
7.7 Selection of phosphoproteins for further investigation.....	183
7.8 Identification of phosphorylated peptides.....	187
7.9 Pro-Q Diamond staining of phosphoproteins in WM-266-4 cells.....	188
7.10 Summary .....	192
8. Analysis of targets implicated in dasatinib sensitivity and resistance in melanoma cell lines .....	195
8.1 Introduction.....	196
8.2 Optimisation studies for siRNA knockdown in melanoma cell lines .....	197
8.3 SRC siRNA.....	198
8.3.1 SRC siRNA in WM-115 .....	198
8.3.2 SRC siRNA in WM-266-4.....	200
8.4 Validation of targets identified by Pro-Q Diamond staining.....	202
8.5 Validation of ANXA2 in melanoma cell lines.....	204
8.5.1 ANXA2 siRNA in WM-115 .....	206
8.5.2 ANXA2 siRNA in WM-266-4.....	209
8.6 Summary .....	212
9. Discussion.....	214
9.1 Characterisation of melanoma cell lines.....	215

9.2 <i>In vitro</i> evaluation of dasatinib and imatinib in melanoma .....	219
9.3 Dasatinib in combination with current targeted therapies .....	222
9.4 Biomarkers for dasatinib treatment in melanoma .....	225
9.5 Proteomic profiling of dasatinib sensitive and resistant melanoma cells and functional validation of targets identified from phosphoproteomic analysis.....	228
9.6 Summary and Conclusion .....	239
References.....	241

## Abstract

Metastatic melanoma is highly chemotherapy resistant but the use of targeted therapies alone and in combination with chemotherapy may improve response.

We examined expression of ABC transporters and their relationship to chemosensitivity in melanoma cell lines. We found that melanoma cell lines showed better responses to chemotherapy drugs, such as taxotere, than has been reported in the clinical setting. This may be related to altered expression of ABC transporters in cell lines compared to *in vivo* tumours.

We tested dasatinib and found that it had anti-proliferative and anti-invasive effects in melanoma cell lines. Combinations of dasatinib with temozolomide or with sorafenib and temozolomide were more effective than testing single agents alone. We studied the effect of dasatinib on the protein levels and phosphorylation status of the dasatinib targets SRC and EphA2, and on downstream signalling pathways including FAK, MAPK and AKT. Our results demonstrated that FAK inhibition by dasatinib may correlate with inhibition of migration and invasion whilst EphA2 expression may correlate with dasatinib sensitivity.

We found that the combined expression of ANXA1, CAV-1 and EphA2 predicted response to dasatinib in melanoma cell lines. Expression of both SRC and CAV-1 was also examined by immunohistochemical staining in tumours from 120 melanoma patients. SRC was detected in 73 % of tumours and CAV-1 was detected in 44 %.

Two phosphoproteomic approaches were used to identify phosphoproteins associated with dasatinib response/resistance in melanoma cell lines. Dasatinib altered levels of 31 unique phosphoproteins in WM-115 cells and 5 unique phosphoproteins in WM-266-4 cells. ANXA2 phosphoprotein levels were altered in WM-115 cells but not in WM-266-4 cells. We used siRNA transfection to examine the effect of ANXA2 knockdown on proliferation in both WM-115 and WM-266-4 cell lines and found ANXA2 plays a role in proliferation and may play a role in mediating response to dasatinib in WM-115 cells.

# **Chapter 1**

## **1. Introduction and background**



Metastatic melanoma in its disseminated form is largely untreatable by cytotoxic chemotherapy and the prognosis is almost certainly fatal. The incidence of melanoma has increased over the last four decades, with current rates varying between 15-60 per 100,000 [1]. In 2006 there were 60,000 new cases of cutaneous melanoma, in the European Union, resulting in 13,000 deaths ([www.europeancancerleagues.org](http://www.europeancancerleagues.org)).

Melanoma has become a more prevalent cancer over the past twenty years. This can be explained by work and social practices; people are spending more time outside, in direct contact with the sun. The associated exposure to powerful sunshine has been identified as a major cause of melanoma development [2]. Sunlight is made up of UV-rays and can be separated into two UV classes, UV-A, which is the more abundant, and UV-B, which has been shown to have a strong association with melanoma development. However, both UV-A and UV-B have been proven to have links with melanoma progression [3, 4].

Localised disease can be effectively treated by wide excision, however upon metastasis the rate of survival drops dramatically. Patients with advanced disease, such as those with lymph node involvement, have a 30 % survival rate over 5 years. However, those with Stage IV disease which includes distant metastasis have only a 10 % chance of surviving more than 5 years [5, 6], and cure rates are reported in less than 1 % of advanced melanoma patients [2].

The reason for the poor prognosis of this disease may be related to the limited effect of chemotherapy. Metastatic melanoma is largely untreatable and over the past 30 years alkylating drugs such as dacarbazine and more recently temozolomide, have not

changed the long-term prognosis of the disease. Analysis of the response to drugs rather than their survival rates revealed that no more than 10 % to 15 % of patients demonstrated any benefit from drug chemotherapy [7].

The advent of newer therapies, such as those targeting kinases or signalling pathways alone or in combination with chemotherapy offer hope of better tolerated, more efficient therapies.

### 1.1 The structure and function of skin

The human skin is made up of two distinct layers, the epidermis and the dermis, which are separated by the basement membrane. The dynamic interactions that occur between the melanocytes and the microenvironment of the skin, which include keratinocytes, fibroblasts, endothelial cells and the extra cellular matrix maintain a balance between the various components of the skin [2] (Figure 1.1).

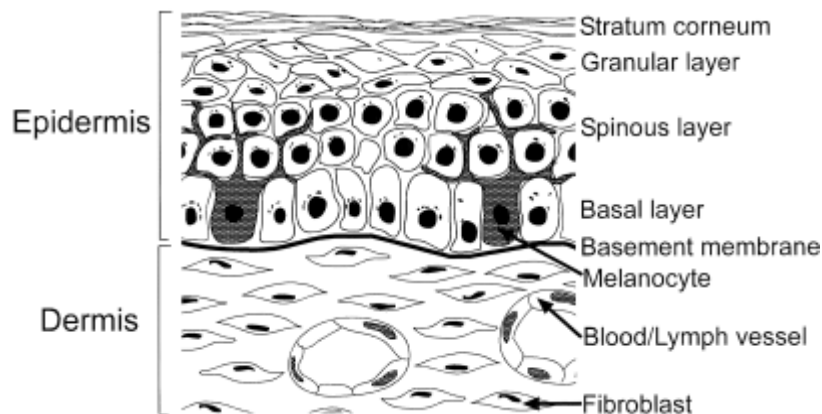


Figure 1.1: The structure of the human skin [8].

Keratinocytes are found in the epidermal layer. These keratinocytes provide a barrier to the outside environment by self-renewal. They can control the proliferation and

differentiation of the un-differentiated basal cells, and can help form a stratified multilayered cohesive tissue. This tissue is then able to produce molecules that are involved in cell growth and the maintenance of the skin's defence [8].

Melanocytes, which are pigment synthesising cells, are part of the neural crest lineage. The neural crest lineage undergoes epithelial/mesenchymal conversion and migrates below the epidermis where they give rise to melanocytes. This entire process is closely regulated by multiple, perhaps sequential receptor tyrosine kinases [9]. During normal growth melanocytes inhabit and are confined to the basal layer, above the basement membrane, and are interspersed along every 5-10 keratinocytes. The ratio of keratinocytes to melanocytes is 35: 1 and is tightly controlled in normal skin. Melanocytes have dendritic processes, which can spread out and contact the keratinocytes. These dendritic processes allow the melanocytes to transfer pigment-containing melanosomes to the keratinocytes. These melanosomes once in the keratinocytes protect the skin from UV radiation by absorbing and scattering the solar radiation [8]. The pigment melanin protects the skin from the negative effects of the sun. Melanin is a free oxygen radical scavenger which prevents damage of the DNA of keratinocytes and melanocytes during cell division [10]. Melanin is produced in melanocytes by the conversion of tyrosine into dopa and subsequently to dopaquinone via the bi-functional enzyme tyrosinase which is then oxidised into melanin [10].

The relationship between keratinocytes and melanocytes is one of importance in the development of melanoma. Despite the dynamic environment of the normal epidermal layer, the number of melanocytes in the basal layer is controlled only by the basal keratinocytes. This was confirmed by Hsu and Meier, (2004) who showed

that neither fibroblasts nor carcinoma cells could reinstate control over the melanocytes when keratinocytes are removed [8].

## **1.2 Skin Cancer**

Skin cancer is increasing in its prevalence and is now the most frequent form of cancer found in young people. Whilst melanoma skin cancer occurs worldwide at a rate of 132,000 cases each year [11], non-melanoma skin cancer makes up the majority of recorded cases with between 2 to 3 million cases diagnosed each year ([www.who.int](http://www.who.int)). Non-melanoma skin cancer includes basal cell carcinoma, actinic keratosis, squamous cell carcinoma *in situ* and squamous cell carcinoma. However, the most dangerous form of skin cancer is melanoma. Treatment options for non-melanoma skin cancer include excision surgery which in greater than 90 % of cases results in adequate removal of low risk tumours [12].

Non-melanoma skin types are divided into four sub-types which are classified according to the specific type of cells which become cancerous.

### **1.2.1 Basal Cell Carcinoma**

Basal cell carcinoma (BCC) is the most common form of skin cancer in the Caucasian population. It accounts for nearly 80 % of all non-melanoma skin cancer cases, and at present its incidence is increasing in Australia at a rate of 1 - 2 % per year, with a 30 % chance of BCC occurring in a person's lifetime [13]. It is rare to see a sporadic case of BCC occurring before the age of 20 and the recorded rate of mortality of BCC is low due to its limited ability to metastasise [14, 15].

BCC is caused mainly by UV-B radiation from the sun and normally occurs *de novo* without a precursor. Certain phenotypic traits can increase susceptibility to the disease, such as fair skin, blue or green eyes, and fair or red hair. Also at higher risk are people who are immuno-suppressed or have a familial history of skin cancer [16].

80 % of BCCs are found on the head or neck, with the remainder occurring on the limbs or trunk [16]. BCC is typically a slow growing tumour that can be treated by surgery such as Mohs micrographic surgery (MMS), radiotherapy, cryotherapy and the use of topical ointments containing 5-fluoro-uracil (5-FU) [12]. Patients with a history of BCC have an increased chance of developing recurrent BCC [13] or even progressing to squamous cell carcinoma (SCC) [14].

### **1.2.2 Actinic Keratosis**

Actinic keratosis (AK) is not a malignancy but can be a precursor to SCC. Progression from a single AK to an invasive SCC ranges from 0.25 % to 20 % per year [17]. It occurs on photo-damaged skin and is related to exposure to UV-B sunlight. AK is recognised as a partial thickness atypia of the keratinocytes, which begins at the basal layer but does not reach the granular layer [18]. Actinic keratosis is a serious condition in Australia, with a 60% incidence in the population over the age of 40 years [18].

### **1.2.3 Squamous cell carcinoma *in situ***

Intra-epidermal squamous cell carcinoma, also commonly known as Bowen's disease, is the next stage in the progression of AK to SCC [19]. Bowen's disease may arise *de novo* or may be associated with human papilloma virus (HPV) [20]. Lesions normally appear on skin that is sun exposed such as the trunk, legs, neck and head. Its appearance is slightly keratocytic with a barely elevated plaque. SCC *in situ* is usually treated with topical creams such as 5-FU or cryotherapy [16].

### **1.2.4 Squamous cell carcinoma**

SCC occurs 5 times less frequently than BCC [19] and is more common in men than women. It has a low mortality rate; however when tumours appear on the scalp or lip the chance of metastasis is increased. 50 % of SCC occur on the head and neck, and are recognisable by a keratocytic papule, which commonly ulcerates [19]. Histologically, keratinocytes invade the dermal layer, with some keratinocytes detaching from the overlying dermis. SCC incidence has been linked to immunosuppression, arsenic exposure, radiation and chronic ulceration [19]. Due to the propensity of SCC to metastasise, treatment options are more aggressive than for BCC. Therefore, advanced tumours are commonly treated by microsurgery and lymph node dissection [21]. Depending on the severity of the cancer, SCC can be treated with either excision and topical creams, but with deeply invasive SCC adjuvant therapies may be considered [12].

### **1.2.5 Melanoma skin cancer**

Melanomas can be classified according to location, stage and progression and are defined in 5 stages.

#### **1.2.5.1 Acquired melanocytic nevus**

The common acquired melanocytic nevus (AMN) which is a benign growth, is assumed to be the earliest hyperplastic melanocytic lesion and is common in humans [8]. They are usually recognisable as brown areas on the skin of varying size and shape. This pigmented nevus, which is commonly called a mole, develops as a proliferation of melanocytes which are clumped into nests rather than being placed singly along the basement membrane [10].

AMN are commonly divided into three groups depending on the position they occupy in the skin. They can be junctional nevi, which are situated along the dermal-epidermal junction, compound nevi, which are in the dermal epidermal junction and the dermis, or intra-dermal nevi, which are in the dermal layer.

AMN, however, can also be classified by age of appearance. There are two classes, the congenital nevi, which appear within the first six months after birth, and the acquired nevi, which appear when the patient is over 1 year of age. The difference and clinical importance of this classification is that congenital nevi are thought to be more likely to become malignant in life [22]. This can be related to the fact that congenital nevi, whilst clustered at the dermal-epidermal junction, go deeper into the dermis than acquired nevi. They tend to have more neural differentiation and can invade blood vessels, nerves and erector pilli muscles [10].

AMN grows in a consistent manner, with a regular progression. The cells proliferate at the dermal junction and with time invade the upper dermis. This stage is called the compound stage and after time the cells lose contact with the dermal junction and become an intra-dermal nevus.

#### **1.2.5.2 Dysplastic nevus**

The second stage described as the dysplastic nevus (DN) has increased abnormal growth compared to the common acquired nevus. The risk of developing DN is estimated to be around 7 - 18 % in a lifetime [23]. They are commonly found on the trunk and have irregular asymmetrical borders. The clinical importance of DN is that in some cases they are thought to represent a precursor to cutaneous melanoma [23].

The nevi are associated with an increased risk of progressing to melanoma. The presence of DN or a familial history of the disease can cause a 7 - 20 fold increase risk of developing the disease [23]. It is estimated that 22 - 36 % of malignant melanomas found on patients originated as DN [23]. However, it is important to state that not all DN become melanoma, as most DN do not progress or become malignant [24]. Because DN is phenotypically flexible it has been suggested that melanocytic transformation is not genetically controlled, but this phenotypical flexibility can cause the loss of control by the keratinocytes, which is secondary to spatial growth [23].



### 1.2.5.3 Radial Growth Phase

The third stage, radial growth phase (RGP), is the first recognisable malignant stage. During RGP the cells remain confined to the epidermis. They can be locally invasive but do not have the ability to rapidly divide or metastasise [24]. The cells in RGP are still dependant on exogenous growth factors supplied by the keratinocytes, and are incapable of anchorage independent growth [8].

### 1.2.5.4 Vertical Growth Phase

The fourth stage is called the vertical growth phase (VGP) in which the melanoma cells are able to invade and infiltrate as an expanding mass into the dermal layer and below the basement membrane, with an obvious risk of systemic dissemination [8]. The cells have now fully escaped growth control by keratinocytes. They establish a close network with fibroblasts and are able to acquire growth factors and grow without anchorage (Figure 1.2).

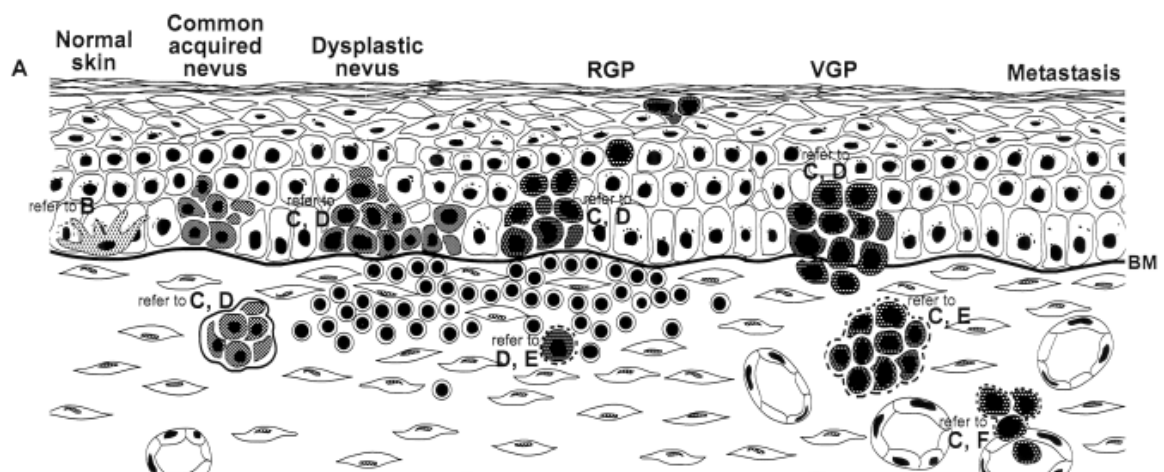


Figure 1.2: The different stages of melanoma skin cancer development, [8].

### 1.2.6 Classification of cutaneous malignant melanoma

Four major types of malignant melanoma are currently clinically recognised, superficial spreading melanoma, nodular melanoma, lentigo maligna melanoma and amelanocytic melanoma.

Superficial spreading melanoma (SMM) accounts for over 70 % of all cutaneous malignant melanoma, and usually arises from a pre-existing dysplastic nevus [5]. Diagnosis of SMM mainly occurs in patients' 4<sup>th</sup> or 5<sup>th</sup> decade and is equally prevalent in both men and women. SMM initially displays a radial growth phase in patients where it is confined to the epidermal layer. It then progresses to the vertical phase of growth whereby the lesion expands into the dermis. The development of SMM usually occurs over a period of 7 years [5].

Nodular melanoma accounts for between 15 – 30 % of malignant melanoma cases. It is the most aggressive form of melanoma and clinically affects men mainly in their 5<sup>th</sup> decade [5]. Nodular melanoma usually arise *de novo*; however it can also develop from a pre-existing nevus. Nodular melanoma lacks a radial growth phase, meaning it is more aggressive and offers a worse prognosis. This is related to the fact that the vertical growth phase is more difficult to diagnose [25].

Lentigo maligna melanoma or melanoma *in situ*, occurs on extremely sun damaged skin, and is the least aggressive and least common melanoma type, accounting for 5 % of melanoma cases [5]. The benign precursor of melanoma *in situ*, lentigo maligna grows slowly for 3 – 15 years achieving a final size of 3 – 6 cm. Less than 5 % of melanoma *in situ* cases display any vertical growth phase. Interestingly despite

melanoma *in situ* accounting for only 5 % of all melanoma cases, it accounts for between 35 - 65 % of all cases of melanoma in darkly pigmented populations (e.g. African Americans, Asians, etc.) [5].

Amelanocytic melanomas which do not contain any pigment, account for between 2 – 8 % of all malignant melanoma cases. They usually go undiagnosed due to their uncharacteristic appearance [26]. For example desmoplastic melanoma, a rare amelanocytic melanoma variant, is usually not diagnosed due to it being mistaken as scar tissue.

There are also a group described as acral lentiginous melanoma which account for less than 5 % of the total case numbers. This type is most commonly found on the palms of the hands and soles of the feet or around the big toenail. It can also grow under the nails. It is much more common on the feet than on the hands and is the most common type of melanoma in dark skinned people [27]. Melanomas from acral lentiginous, mucosal, and chronic sun-damaged sites frequently harbor activating mutations and/or increased copy number in the KIT tyrosine kinase receptor gene, which are very rare in the more common cutaneous tumors [28].

### **1.2.7 Clinical variables and prognostic markers in malignant melanoma**

The melanoma tumour, node, metastasis system (TNM) categorises and stages melanoma cases from over 60,000 cases in 17 cancer centres. This system can be used to determine the outcome of patients with cutaneous melanoma [29]. The

staging system looks at clinical factors such as tumour thickness, ulceration, mitotic activity and lymph node metastasis.

In stage IV melanoma several factors have been clinically linked to survival. The location of the metastasis significantly influences the prognosis of the disease. For example visceral site metastasis excluding lung metastasis have been associated with poorer 1 year survival rates compared to tumours that metastasise to the skin [6].

Ulceration of the tumour has also been linked with worse outcome. Ulceration may directly affect the local environment of the tumour which may favour melanoma progression. However ulceration may also provide melanoma cells with an effective way of interrupting keratinocyte mediated control, leading to far greater proliferation rates [30].

The biological significance of a melanoma cells mitotic activity has been previously associated with disease progression. Most genes associated with metastasis are linked to DNA repair or replication. Melanomas with poorer outcome have overexpression of genes associated replication origins firing (ROF), whilst expression of mini-chromosome maintenance protein 4 (MCM4) and MCM6 have been associated with metastasis free survival. The importance of both ROF and MCM genes is that even when age, sex, location of the primary tumour, thickness of tumour and ulceration are taken into account, their predictive value remains strong [30].

Factors such as the thickness of the tumour and the number of metastasis at distant sites have also been associated with poorer outcome. However the current AJCC

staging of melanoma does not include these in their system. A lack of a definite link between these factors and patient outcome means that whilst they may have some clinical relevance, they are not robust enough markers [29].

Prognostic markers provide an essential tool in the early detection of melanoma. Many markers have been studied in both melanoma tumour and serological samples. The aim is to identify either one protein or a panel of protein markers that will allow the reproducible identification of different forms of melanoma.

For the diagnosis of melanoma there are a small panel of melanocytic lineage markers (S100, MART-1 and gp100/HMB45) which are used to distinguish melanoma from non-melanocytic cancers [31]. These markers however, cannot distinguish all types of melanoma from other cancer types. Ki67 remains the most useful adjunct to the melanocytic lineage markers in distinguishing benign from malignant melanocytic tumours [31].

It remains difficult to obtain one true prognostic tissue marker for melanoma due to the cumulative genetic alterations that are associated with disease. The expression of several molecules has been associated with impaired prognosis of melanoma. These include increased levels of c-Kit and p-AKT [32, 33] and decreased levels of PTEN and E-cadherin [34, 35]. However, none of these have been validated as prognostic markers for clinical use.

Serological markers have several advantages over tissue sample biomarkers, including the ease to obtain samples and the numerous methods that can be used to detect them.

The melanocytic lineage differentiation markers S100-beta and melanoma inhibitory activity (MIA) are frequently used for early detection of melanoma [31]. Both S100-beta and MIA detect melanoma based on the tumour load. S100-beta levels are also elevated in melanoma patient sample sera [36]. When MIA and S100-beta are compared, S100 beta is the stronger serological marker, as it can provide early indication of tumour progression, relapse or metastasis. However both markers fail to provide prognostic information in early stages of melanoma especially in patients who are tumour free after surgical resection [37].

In advanced metastatic melanoma the strongest prognostic serum marker is lactate dehydrogenase (LDH) which can determine high tumour load in several cancer types including melanoma. Due to its prognostic significance and the multiple detection methodologies, it is currently the only marker included in the current melanoma staging classification system of the American Joint Committee on Cancer (AJCC) [31]. YKL40 a heparin and chitin binding lectin secreted by macrophages and neutrophils in the late stage of differentiation is another marker of poor survival in breast, kidney and lung cancer [30]. In 234 melanoma patients the level of YKL-40 at the time of diagnosis was an independent prognostic factor for overall survival. Despite these findings YKL-40 has not been cleared by the Food and Drug Administration as a biomarker for cancer [30].

### **1.3 From melanocyte to melanoma, the road to metastasis**

#### **1.3.1 Cadherin expression in melanoma progression**

The genetic and cellular differences that result in progression from RGP to VGP are not fully understood however, one factor crucial to the progression to melanoma is a change in cadherin expression [2]. Cadherins are a family of cell surface glycoproteins that promote calcium dependant cell-cell adhesion. E-cadherin acts as a mediator between keratinocytes and normal melanocytes. Expression of E-cadherin plays a key role in melanoma development and is lost during melanoma metastasis. Upon losing expression of E-cadherin, cells have increased mobility and invasiveness and keratinocytes no longer control melanocytes [38].

The motile melanoma cells express N-cadherin, which acts as a survival factor for the melanoma cells as they move through the dermis allowing them to change cellular partners and develop gap junctions with fibroblasts, which can allow electrolyte transport [2].

N-cadherin also allows melanoma cells adhere to each other. Co-receptors like melanoma cell adhesion molecule (MCAM) facilitate cluster formation. Increased expression of N-cadherin leads to the increased association of melanoma cells with stromal fibroblasts and endothelial cells and changes the expression of cell surface receptors. For example, expression of vitronectin receptor  $\alpha V\beta 3$  can facilitate binding of 11 other matrix proteins involved in cell-to-cell adhesion, which influences migration of melanoma cells [2].

Metastasis is the final stage of melanoma development. At this point the melanoma cells are able to establish a tumour at a secondary site. This is the stage where treatment is most difficult, due to the genotypic and phenotypic changes that the cells have gone through. In fact the development of melanoma, whilst certainly due to cumulative genetic events, is also related to disruptions in the normal molecular dialogue between the two epidermal layers which may indirectly cause these phenotypic and genotypic changes [8].

### **1.3.2 Growth factor dependence in melanoma development**

Normal melanocytes are relatively inactive in growth factor production even after stimulation. Nevus cells are known to produce basic fibroblast growth factor (bFGF) and hepatocyte growth factor (HGF) [39].

When melanocytes undergo transformation to melanoma cells they show an increase in growth factor receptors and cytokine receptors. Ruiter et al, (2002) [40] proposed that growth factor production by melanoma cells is the driving force for progression from RGP to VGP. Autocrine growth factors such as bFGF, platelet derived growth factor A (PDGF-A) and Interleukin-8 (IL-8) are associated with proliferation and migration of melanoma cells [39]. Paracrine growth factors such as vascular endothelial growth factor (VEGF) and transforming growth factor- $\beta$  (TGF- $\beta$ ) are associated with modulation of the microenvironment, especially stromal fibroblasts. This modulation of the microenvironment favours the malignant cell and is associated with invasion and metastasis.



bFGF is the most significant autocrine growth factor in melanoma progression. Blocking bFGF can stop melanoma proliferation. bFGF binds to matrix proteins such as heparin sulphate proteoglycan, which then stimulates fibroblasts and endothelial cells. bFGF not only plays a role in the survival of melanoma cells but is also involved in regulating motility by up-regulating serine proteinases and metalloproteinases [41].

PDGF-A plays an important role in tumour angiogenesis and stromal formation [41]. By organising the stroma and inducing VEGF it is able to orchestrate angiogenesis. VEGF is important in the progression from RGP to VGP because of its strong angiogenic properties. VEGF can stimulate endothelial cell growth, migration and invasion [40].

TGF- $\beta$  is constitutively expressed in melanoma cells and its expression can be a biological marker of melanoma progression *in situ* [41]. TGF- $\beta$  exerts a negative control on cell proliferation of normal melanocytes, however advanced melanoma becomes resistant to its anti-proliferative effects. TGF- $\beta$  can also promote growth through paracrine regulation; by regulating melanogenesis, inducing angiogenesis and potentiating the effects of bFGF [41].

### **1.3.3 Role of receptor tyrosine kinases in melanoma progression**

Receptor tyrosine kinases (RTK) play a pivotal role in the normal regulation of all basic cellular functions, including cell proliferation, differentiation, migration and survival. RTKs are trans-membrane polypeptides that contain both an extra-cellular ligand binding domain and a cytoplasmic tyrosine kinase domain, which has the

ability to regulate signalling via a number of key pathways, including the Ras/MAPK and the PI3/AKT pathways. An increasing number of RTK stimulated pathways are implicated in melanocyte development, which reflects the unique cooperative role they have in melanoma [42].

RTKs and the components of their signalling pathways are common targets for transformation (Figure 1.3). RTKs can stimulate the production of growth factors such as fibroblast growth factor and platelet-derived growth factor, which exert their influences on the microenvironment around the melanoma through paracrine signalling processes. The association of RTKs with processes including angiogenesis, matrix degradation and adhesive interactions have accounted for the association of active RTKs and melanoma development [42].

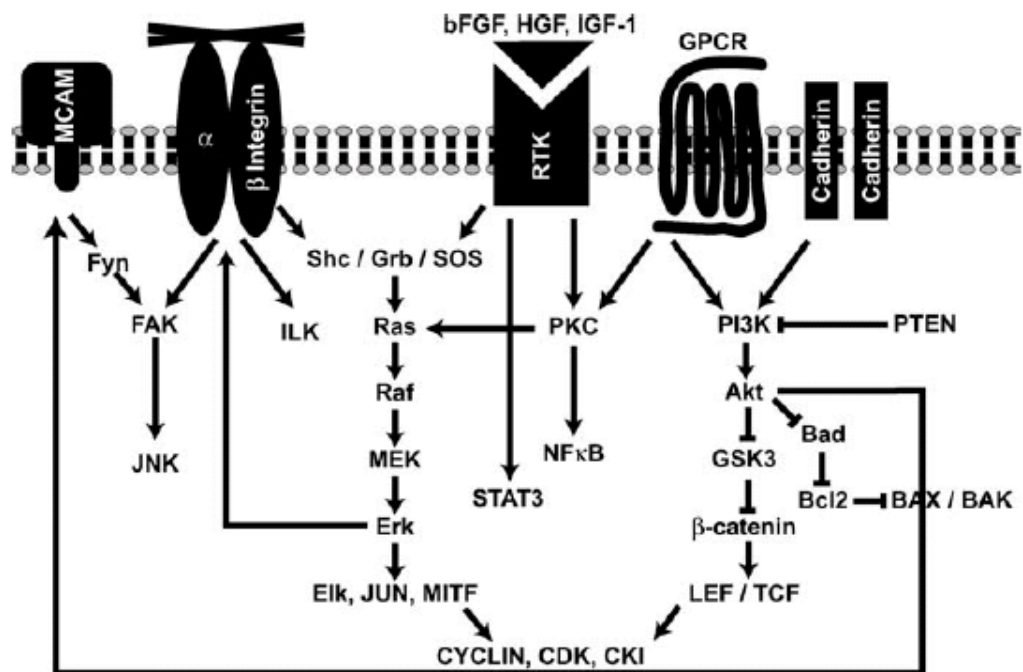


Figure 1.3: Receptor signalling pathways in melanocytic transformation [43]

Hepatocyte growth factor/scatter factor (HGF) acts through its tyrosine kinase receptor (C-Met), which is present on epithelial cells and melanocytes. HGF stimulates proliferation and motility of melanoma cells in culture [44]. However, it has also been implicated in the disruption of adhesion between melanocytes and keratinocytes via down regulation of E-cadherin and demogelin-1 [9]. The decoupling of melanocytes to keratinocytes is involved in the deregulation of proliferation and scattering of melanocytes. Studies performed in mice with ubiquitous expression of HGF showed induction of various tumours including subcutaneous melanoma [9].

Stimulation of the C-Kit receptor tyrosine kinase by its ligand, stem cell factor (SCF), leads to activation of intracellular signalling pathways including Ras/Raf/MAPK, SRC and PI3K/Akt signalling [45]. It is expressed at high levels in normal melanocytes [46] and is essential for normal melanocyte development and homeostasis [47]. Until recently it was believed that C-Kit expression was lost with melanoma progression [48]. However recent studies have shown that C-Kit is over-expressed in a small percentage of melanoma patients [46, 49-51]. Patients who have mutated c-Kit are generally not V-raf murine sarcoma viral oncogene homolog B1 (BRAF) mutated and are defined as being mucosal, acral or chronic sun damaged [52-54].

The biological functions of IGF1 are mediated by the ligand induced activation of IGF1R a trans-membrane tyrosine kinase linked to the Ras-Raf mitogen activated protein kinase (MAPK) and PI3K/AKT signal transduction pathways [55]. It is

constitutively active in nearly every cell [56] and shares approximately 70 % homology with insulin receptor [57].

IGF1R is important for developing the malignant phenotype [58] and IGF1R expression increases with tumour progression [59]. Down regulation of IGF1R expression or activity causes growth arrest and apoptosis in melanoma cell lines [60]. In melanoma IGF1R increases sensitivity of mouse melanoma cells to radiotherapy, and IGF is able to promote resistance to apoptosis by the up regulation of anti-apoptotic members of the BCL-2 family and the IAP survivin [55]. Silencing of IGF1R in melanoma caused significant inhibition of survival, enhanced apoptosis and increased by 2 fold the sensitivity of melanoma cells to cisplatin and temozolomide. These effects were independent of BRAF status and were also associated with a decrease in AKT and MAPK activity [61].

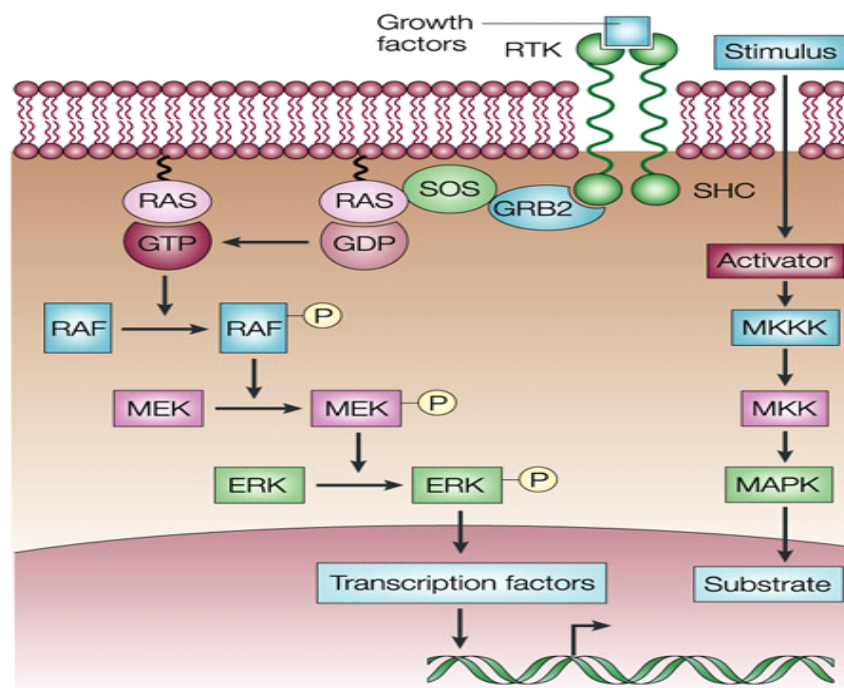
#### **1.3.4 Mitogen activating protein kinase pathway (MAPK)**

The MAPK pathway regulates cell proliferation, differentiation and survival. Activation of the MAPK pathway is a frequent and early event in melanoma [44].

The MAPK pathway is activated via sequential phosphorylation of a number of kinases, which alter cellular behaviour in response to diverse environmental stimuli (Figure 1.4). The extra cellular signal regulated kinases (ERK1 and ERK2) belong to one branch of the cascade that is responsible for sensing external stimuli such as UV light. Stimuli of the RAS family of proto-oncogenes cause the activation of the RAF family of serine/threonine kinases (e.g. BRAF, CRAF and ARAF). RAF then

phosphorylates the MAPK kinase MEK, which can lead to activation of the MAPKs, ERK1 and ERK2.

Activation of the RAS/RAF/MAPK pathway is a frequent and early event in melanoma [44]. BRAF, a key player in the pathway, is mutated in 60-70 % of melanoma cases [62]. The mutation valine-600-glutamic acid (V600E) accounts for approximately 80 % of BRAF mutations [63]. Analysis of BRAF mutation status showed that the presence of the mutated BRAF in primary tumours (n=114) did not impact on prognosis or survival but was associated with a significantly poorer prognosis (n=86) when detected in metastatic melanomas [64].



Nature Reviews | Cancer

Figure 1.4: The mitogen activated protein kinase pathway (MAPK) [9]

RAS mutations, particularly NRAS, are also associated with melanoma. Studies have found that approximately 10-12 % of all melanoma mutations are Ras mutations [9].

Oncogenic RAS is involved in the activation of the RAF and PI3K cascades. BRAF and NRAS mutations appear to be equivalent in MAPK activation with mutations generally found to appear separately in a cell. However one study recorded that coupled BRAF and NRAS mutations have been identified in 6 out of 1300 melanoma specimens [44].

### **1.3.5 AKT Pathway**

Constitutive activation of the phosphatidylinositol-3-kinase (PI3K)/AKT pathway has been implicated in chemoresistance in many human cancers, including melanoma [65]. Although PI3K itself is rarely mutated [66] or overexpressed [67] in melanoma, activation of downstream signalling components, e.g. AKT, have been implicated in melanoma progression [68]. In one study, phosphorylated AKT was detected in 17, 43, 49, and 77% of normal nevi (n=12), dysplastic nevi (n=58), primary melanoma (n=170) and melanoma metastases (n=52), and strong p-AKT staining correlated inversely with overall and 5-year survival of patients with primary melanoma ( $p < 0.05$ ) [33].

The AKT pathway stimulates cell cycle progression by controlling G1 progression, cell proliferation and inhibition of apoptosis. Phosphatase and tension homolog (PTEN) is a tumour suppressor gene, which encodes a lipid/protein phosphatase with dual specificity. With the lipid phosphatase activity PTEN can down-regulate the AKT pathway. However, PTEN has also been implicated in the MAPK pathway. Studies have revealed that the protein phosphatase activity of PTEN can inhibit MAPK signalling [44, 69].

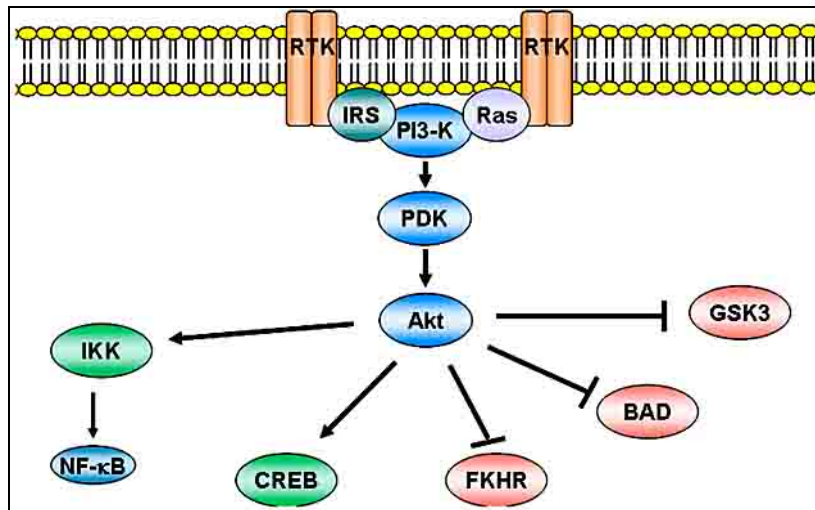


Figure 1.5: The Phosphoinositide 3-kinase (PI3/AKT) pathway [70].

Loss or mutation of PTEN has been found in approximately 30-40% of melanoma cell lines [9]. Loss of PTEN expression is associated with activation of the AKT pathway. Consistent with the *in vitro* results phosphorylated AKT is detected in most metastatic melanomas but not in nevi [9]. Loss of PTEN can also cooperate with inactivation of the INK4A pathway, which can induce melanoma neoplasia. These roles of PTEN help to confirm the role of the AKT pathway in the development of metastatic melanoma. Studies by Rodolfo et al (2004) [44] indicated that PTEN mutations may occur early in melanoma development.

## 1.4 Current therapies for metastatic melanoma

### 1.4.1 Chemotherapy

Systemic cytotoxic chemotherapy is a common treatment for patients with advanced disseminated metastasis. The success with chemotherapy treatment varies in

metastatic melanoma, depending on where the cancer exists. Patients with metastatic tumours in the subcutaneous skin or distant lymph node have a better survival rate than those whose disease occurs in any other anatomic site. [6, 71].

The classical mono-chemotherapeutic regimen used in the treatment of metastatic melanoma is dacarbazine. Dacarbazine (DTIC) is a non-classical alkylating agent. It is inactive when administered to the patient but undergoes activation in the liver via oxidative metabolism to methyl-triazeno imidazole carboxiamide (MTIC). The response rate for dacarbazine in patients is around 10-20 % with an estimated complete response rate of around 0 % [71].

DTIC, however, has advantages over other chemotherapeutics in that it is cheap, easy to administer and well tolerated by the patient. It however, does cause side effects such as neutropenia, thrombocytopenia, nausea and vomiting, but these are dose dependent and not cumulative.

Other drugs have been tested in melanoma in an attempt to improve response rates in patients. The most successful of these in monotherapy is temozolomide. Temozolomide (TMZ) is an imidazotetrazine pro-drug that is spontaneously activated at physiological pH to MTIC. This spontaneous activation is of great advantage in the use of TMZ, as the drug does not need hepatic activation and can be orally administered [71].

TMZ acts by methylating DNA producing three adducts, N<sup>7</sup>-methylguanine, N<sup>3</sup>-methyladenine and O<sup>6</sup>-methylguanine. O<sup>6</sup>-Methylguanine is the cytotoxic lesion, as



during replication it is incorrectly paired with thymine by DNA polymerase. This incorrect pairing is recognised by the DNA mismatch repair system, which leads to the activation of apoptosis [72]. The DNA repair protein O<sup>6</sup>-alkylguanine-DNA alkyltransferase (AGT) is the primary defence against O<sup>6</sup>-methylguanine adducts and is a recognised mechanism of resistance to TMZ. AGT directly removes the O<sup>6</sup>-methyl adduct from the O<sup>6</sup> position of guanine in a suicide reaction that reduces the toxicity of TMZ [72]. Another important mechanism of resistance to TMZ is DNA repair mediated by the damage-reversal suicide enzyme O<sup>6</sup>-methylguanine-DNA methyltransferase (MGMT). It repairs the pre-toxic DNA lesion O<sup>6</sup>-methylguanine by transfer of the methyl group from guanine to an own cysteine residue. This causes, in an expression-dependent manner, resistance to methylating agents that produce O<sup>6</sup>-Methyl guanine [73]. No dosing schedule of TMZ or DTIC has been clinically proven to be more effective than a single administration of either drug [74], however current treatments still favour a 5-day schedule [75].

In patients the response to TMZ is similar to that of dacarbazine but its use is associated with fewer side effects [76], such as nausea and vomiting which are easily treatable. TMZ is also able to cross the blood brain barrier, where it converts to MTIC, and gains its alkylating activity. As it is found in higher levels in the cerebrospinal fluid, it may be more effective at treating melanomas that have metastasised to the brain [75], however no direct evidence to support this hypothesis has been found to date.

Several other chemotherapeutic agents have been tested in melanoma cells due to their effects in other cancer types. Cytotoxic agents such as the nitrosoureas group,

which include carmustine (BCNU), lomustine (CCNU) and fotemustine, give 10-20 % response rates in melanoma [71, 77, 78].

Fotemustine is a nitrosourea agent that has been associated with a consistent response to melanoma in the central nervous system. It gives a 6-60 % response rate in patients with central nervous system melanoma [79]. Fotemustine has an amino acid phosphoryl adduct, which makes it lipophilic and allows it to easily cross the blood brain barrier. However the drug has strong side effects, with leukopenia and thrombocytopenia occurring in 15-45 % of patients and associated problems with the gastro intestinal tract including serious vomiting and nausea commonly occurring [79].

Taxanes have also been tested in melanoma, however they only achieve response rates of 12-18 % [71]. They act by stabilising the polymerised microtubules, which results in mitotic arrest in G<sub>2</sub> and M phases of the cell cycle. These drugs are also associated with severe toxicity such as neuropathy, neutropenia and acute hypersensitivity.

Whilst many mono-chemotherapy regimes have been tested, one group joined the mediocre responses of dacarbazine and cisplatin into the Dartmouth regime. Initial testing of this combination, which comprised DTIC, cisplatin, carmustine and tamoxifen, yielded responses of 40-50 % in stage IV melanoma. This regime became so popular that in certain centres in the USA it was the common treatment for metastatic melanoma [71]. Further testing and randomised trials however tell a different story. The trials have shown that the Dartmouth regime has actually little or

no benefit compared to the single agent dacarbazine treatment. The associated toxicity with the treatment is so severe that high fatality rates were recorded. The response rate of the regimen was short and long-term remissions from the disease were rare [71]. As a result no reported clinical trials testing the Dartmouth regime in melanoma have been identified since the year 2000.

Finally TMZ was combined with thalidomide in 6 phase I and phase II trials. Responses ranged from 8-42 % with complete responses in 0-11 % and median survival of 4 – 12.3 months [75]. Because of the favourable results a phase II trial including greater than 60 patients was undertaken, but failed to demonstrate any benefit [80].

## **1.5 Drug resistance in melanoma**

Melanoma is known to be very resistant to common chemotherapeutics, and the disease is very difficult to treat once it has metastasised. Resistance to chemotherapy in melanoma may be caused by intrinsic or acquired resistance. The ATP binding cassette (ABC) family of transporters have been implicated in chemotherapy resistance due to their ability to efflux specific substrate drugs out of cancer cells.

### **1.5.1 Multi-drug resistance protein (MRP) and P-glycoprotein (P-gp)**

The ABC super family is the largest most broadly expressed super family known in humans [81]. Most of the ABC transporters are ATP dependant, that is, the binding and hydrolysis of ATP is required to provide energy for the transport of the substrate across the membrane.

Chemo-resistance has been observed in many different cancer types and originally P-gP was identified as the major cause of drug resistance, but the isolation of a second distantly related member of the ABC family, multi-drug resistance protein (MRP) which is also involved in drug efflux, led to the discovery of 9 more genes, 7 of which are involved in drug transport mechanisms [81, 82]. MRP1, MRP2 and P-gP are also expressed in non-malignant tissues and are involved in the protection of the cells from xenobiotic accumulation.

P-gP, a product of the multi-drug resistance (MDR) associated protein gene MDR-1, is a 170-kDa trans membrane glycoprotein which is over expressed in various tumours. P-gP functions as an energy dependant transmembrane efflux pump and is responsible for removing compounds from the cell and it also plays an important role in the blood brain barrier. P-gP is able to transport several classes of compounds including anthracyclines, epipodophyllotoxin, taxanes and vinca alkaloids. However, P-gP is rarely expressed in melanoma cell lines [83], despite being previously detected in melanoma tumour samples (unpublished data). Treatment with chemotherapeutics has not been reported to increase the expression of P-gP in melanoma [84].

MRP1 is a 190-kDa trans-membrane glycoprotein which acts as an energy dependant efflux pump, decreasing the intracellular concentration of cytostatic agents. MRP1 was detected immunohistologically in almost 50 % of primary and metastatic melanoma specimens but studies are conflicting over whether treatment with chemotherapeutics increases the levels of MRP-1 expression [85]. Helmbach et al, (2001) [84] stated that in the cell lines tested no real increase was found after

chemotherapy treatment. However, in the cell lines tested by Ichihashi et al (2001) [86] treatment with various chemotherapeutics, including dacarbazine, increased MRP1 mRNA expression.

MRP2 and MRP1 share 49 % amino acid homology [81]. MRP2 is synthesised in the endoplasmic reticulum, processed in the Golgi apparatus and translocated to the apical plasma membrane [87]. Interestingly, MRP2 like P-gP has a more limited tissue distribution than MRP1 but expression of MRP2 has been found in brain endothelial cells, the liver and the kidney [82, 88]. MRP2 has the ability to export a spectrum of drugs from the cell including endobiotics and xenobiotics. Cell lines which express high levels of MRP2 can transport chemotherapeutics such as cisplatin [89]. This effect has also been noted in melanoma cell lines [90].

ABCG2 or breast cancer resistance protein (BCRP) is a half size ABC transporter that is usually found as a dimer [89]. BCRP is usually localised in the liver, intestinal epithelium and the blood brain barrier, but has also been found to be expressed in stem cell populations [91]. Expression of BCRP has also been identified in melanoma cell lines [92]. Up regulation of BCRP has been implicated in causing drug resistance. BCRP has a broad spectrum of substrates such as irinotecan, taxanes, mitoxantrone and has recently been implicated in the transport of tyrosine kinase inhibitors (TKIs) imatinib and gefitinib [91]. Both gefitinib and imatinib are transported at low concentrations by BCRP. However at higher concentrations the TKIs inhibit the function of BCRP [91]. Therefore, expression of BCRP may significantly alter the absorption, metabolism and toxicity of these TKIs.

ABCB5 is a novel human ABC transporter and was the third identified member of the P-gP family next to its structural paralogs ABCB1 and ABCB4. ABCB5 acts as an energy dependant drug efflux transporter for the fluorescent probe rhodamine-123. In studies on physiological progenitor cells, ABCB5 acted to maintain membrane hyper polarisation, which meant it was able to act as a negative regulator of cell fusion, culture growth and differentiation [93]. ABCB5 was further shown to be a major efflux mediator of doxorubicin in melanoma cell lines [93].

There are other potential mechanisms of resistance in particular alterations in apoptosis proteins such as inhibitor of apoptosis proteins (IAPs) and the BCL family of proteins.

BCL-2 has been well studied in melanoma but results have been conflicting. Whilst certain studies have noted an up regulation of BCL-2, others have noticed a down regulation of BCL-2 in melanoma, and some have even stated that BCL-2 levels did not change during melanoma development [94]. This has led to a lot of confusion of the role of BCL-2 in melanoma development. BCL-2 expression is not solely linked to melanoma development as it is expressed in normal melanocytes as well as melanoma cells. However, BCL-2 may instead be a marker of tumour resistance to chemotherapy, radiation and common treatments in melanoma [95].

IAPs have been found to suppress apoptosis induced by a variety of stimuli including TNF, UV Radiation and the Fas ligand [95]. IAP are able to block apoptosis mainly through their ability to bind specific caspases [96].

Survivin, a member of the IAP family, has been detected in melanoma cell lines but is absent from most normal adult tissues [97]. Its expression has been detected early in melanoma development and it is thought that survivin expression is an important early step in melanocyte transformation. Livin like survivin is normally associated with the cytoskeleton and nucleus and is required for melanoma cell viability. It is localised predominantly in the nucleus and in a filamentous pattern throughout the cytoplasm [98]. Livin like survivin is an anti-apoptotic protein. There is a correlation between livin over-expression, *in vitro* drug resistance and patient clinical response [96]. Hussein et al., (2003) stated that livin had anti-apoptotic effects that were more robust than those of survivin. However Satyamoorthy et al., (2001) suggested that survivin and livin whilst not redundant are distinct factors in apoptosis, and that they could both be playing an important role in apoptosis.

## **1.6 Immuno-therapy**

With the elucidation of T-cell and antigen presentation pathways, it has become clear that melanoma cells are not only immunogenic [99], but probably one of the most immunogenic of all solid tumours [100]. T-cells are essential for anti-tumour responses as they recognise tumour antigens after presentation and processing by professional antigen presenting cells (APC).

The presence of tumour antigen specific cytotoxic T cells in the peripheral blood of melanoma patients has been previously identified [101] and the ability of the T lymphocytes especially CD8 T cells to prevent tumour formation is well documented [102]. To achieve maximum benefit from immunotherapy, an effective anti tumour CD8 T-cell response must be initiated. This requires sufficient numbers of anti-tumour specific CD8 cells; the CD8 T cells generated must be able to permeate the tumour and finally the CD8 T cells must be sufficiently activated within tumours [103].

Multiple approaches to stimulating CD8 T cells are currently being investigated. We will focus on the non-specific stimulation of anti-tumour immune responses by agents such as interleukin-2 and interferon- $\alpha$ , and the use of anti-cytotoxic T-lymphocyte antigen-4 antibodies which are currently being tested in metastatic melanoma.

### **1.6.1 Interleukin-2 therapy**

Interleukin-2 (IL-2) was the first immunotherapeutic treatment to demonstrate a durable clinical response in metastatic melanoma. IL-2 is important in immunotherapy as it promotes proliferation, differentiation and recruitment of immature T and B cells, as well as innate response cells such as natural killer cells. It is also involved in the initiation of cytolytic activity in a subset of lymphocytes mediating interactions between the immune system and malignant cells [99].

IL-2 is known for its potent ability to activate CD8 T lymphocytes and natural killer cells, which results in the development of lymphokine-activated killer cells [103].



Analysis of 8 trials of high dose IL-2 performed between 1985 and 1993 on 270 metastatic melanoma patients reported objective responses in 16 % of patients and complete responses in 6 % of patients [104]. Of the patients who had a complete response, 86% of those remained in complete remission for 39-148 months and many were cured permanently [99]. The obvious benefit of this therapy was that patients could maintain a durable response unlike that seen with chemotherapy [105]. A recent high dose bolus IL-2 regimen was tested in 33 previously treated melanoma patients. Objective durable responses were seen in 12.5 % of patients. 2 melanoma patients with mixed responses remain disease free after 23 and 29 months respectively [106].

IL-2 has been tested with variable doses and schedules, however the original National Cancer Institute (NCI) trial, which gave intermittent high doses of IL-2 [104] to patients has proven to be the most effective and is still used in clinical trials to this day. The benefits of IL-2 (Proleukin) led to its approval for use in metastatic melanoma in the USA in 1998. It has yet to be granted a licence for treatment OF melanoma in Europe [107]. The cost of IL-2 therapy; the limitations of its use to only patients with good organ function and the associated toxicities that the therapy causes including hypotension, cardiovascular and neurological problems limit its use in metastatic melanoma [108]. However, IL-2 therapy remains one of the few therapies which yield remission in metastatic disease. Further studies to elucidate the causes of resistance or sensitivity to IL-2 therapy in melanoma will potentially increase the response rate to the therapy in a subset of patients [109].

### 1.6.2 Interferon- $\alpha$ therapy

Interferon  $\alpha$ 2b (IFN- $\alpha$ 2b) is a pleiotropic cytokine, which has a variety of modulating effects in the inflammatory response and can alter STAT signalling in melanoma [110]. IFN- $\alpha$ 2b therefore can impact the effector immune response and play a role in effecting tumour progression [111].

IFN- $\alpha$ 2b is commonly used as an immunotherapy option in early to mid-stage melanoma patients. In high risk patients with early stage melanoma IFN- $\alpha$ 2b reduces the risk of recurrence by almost 26 % [112]. A review of clinical data for IFN- $\alpha$ 2b published in 2008 showed that it can significantly improve 5 year survival rates by almost 3 % in melanoma patients [111].

However, IFN- $\alpha$ 2b is rarely used as a single agent in advanced melanoma, but when tested has achieved response rates of between 10-15 % regardless of dose and schedule [107, 113]. The limitations of this therapy include the associated toxicity, the short half life and the selection criteria for trials [107, 114]. Newer generation drugs though such as pegylated IFN- $\alpha$  (PEG-IFN- $\alpha$ 2b) have improved half-lives and better bioavailability. Pegylation is the covalent binding of polyethylene glycol to IFN- $\alpha$ , which can reduce the immunogenicity of IFN- $\alpha$  and also prolong its lifetime in the patients circulation. Phase I studies have shown that PEG-IFN- $\alpha$ 2b showed dose-dependent response rates in the range 6–12% and in combination with TMZ showed response rates of 18 % [107]. Combinations of PEG-IFN- $\alpha$ 2b and IL-2 have also failed to produce improvements in response rates [115].

### 1.6.3 CTLA-4 therapy

Activation of a T-cells immune response requires recognition of the antigen by T cell receptors and the presence of co-stimulatory signals. For full T-cell activation, co-stimulatory B7 molecules on the APC must also be bound to their ligand CD28 on the T-cell [116]. This results in a signal cascade and initiation of the immune response. Following antigen stimulation of the T-cells, cytotoxic T-lymphocyte associated antigen 4 receptors (CTLA-4) are up-regulated and move to the surface of the cell. CTLA-4 receptors have a greater affinity for B7 molecules than CD28 and once CTLA-4 receptors have bound B7 molecules a decrease in the immune response occurs (Figure 1.5) [117]. Therefore, CTLA-4 receptors can act as negative regulators of T-cell activation and can control the immune response returning T-cells to homeostasis.

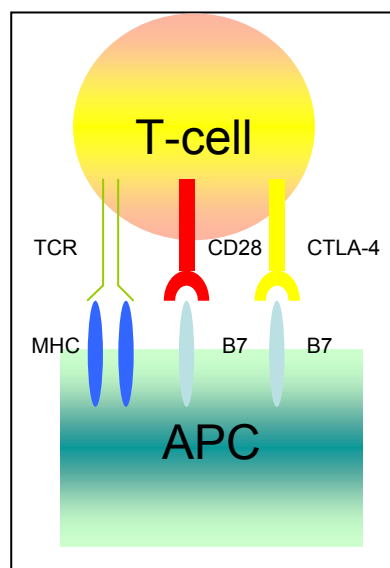


Figure 1.5: The receptors and ligands involved in the initiation and control of an immune response. Adapted from [117].

Monoclonal antibodies to CTLA-4 act to block the binding of CTLA-4 receptors to B7 molecules [117]. This results in the maintenance of the immune response which

can then be used to provide an anti-tumour response. Two monoclonal antibodies ipilimumab and tremelimumab have been designed to target CTLA-4 and have been tested alone and in combination in several melanoma clinical trials.

Anti-CTLA-4 mono-therapy using either ipilimumab or tremelimumab in Phase I or Phase II trials has achieved response rates of between 7-15 % in heavily pre-treated patients with metastatic melanoma [103]. In trials of ipilimumab approximately 10 % of patients tested were alive between 2 to 4 years after therapy [103]. The studies of ipilimumab also reported immune related adverse effects including diarrhoea and dermatitis. However, the induction of manageable auto-immunity as a result of ipilimumab therapy may be a marker of objective and durable response [107]. Tremelimumab was tested in comparison to chemotherapy (DTIC or TMZ) in a Phase III randomised trial. However, the trial was stopped for futility and conclusions were drawn that the antibody failed to improve overall response when compared to chemotherapy [107].

It was disappointing to find that mono-therapy using tremelimumab did not improve overall survival rates when compared to DTIC or TMZ, however future testing of CTLA-4 therapy in combination with chemotherapy is ongoing ([www.clinicaltrials.gov](http://www.clinicaltrials.gov)).

#### **1.6.4 Chemotherapy combined with immunotherapy**

Combined treatment with TMZ and immunotherapy is an option for melanoma. TMZ has been combined with IFN- $\alpha$ 2b in 6 trials to date. The response rates of the combination have ranged between 13-23 % with complete responses in 3-7 % of

patients. Median survival ranges from 8.5 to 12 months [75]. A phase III trial of IFN- $\alpha$ 2b and TMZ compared to TMZ alone showed that the combination produced higher response rates, however overall survival was the same for both treatments [118].

Two Phase II trials of PEG-IFN- $\alpha$ 2b combined with either dacarbazine [119] or TMZ [120] produced response rates of 24 % and 18 % respectively, however no change in overall survival was observed.

Phase III trials which combine IL-2 and chemotherapy, including dacarbazine and cisplatin, have failed to improve the effectiveness of IL-2 therapy. Combinations did not improve either the response rate or the survival rates when compared to IL-2 therapy on its own [76].

Biochemotherapy which combines IL-2 or IFN- $\alpha$  with chemotherapy such as dacarbazine, TMZ, or cisplatin failed to produce any benefit over single agent treatment and has been associated with increased toxicity [121]. The combination using DTIC, tamoxifen and cisplatin with or without IL-2 and IFN- $\alpha$ 2b was assessed. Initial response rates were found to be around 44 % to 27 % in favour of the biochemotherapy arm, however overall survival was improved in the chemotherapy arm compared to biochemotherapy [122]. Therefore it is thought that PEG-IFN- $\alpha$ 2b combined with chemotherapy or other immuno-therapies would not be recommended for metastatic melanoma.

## **1.7 Targeted therapies for melanoma treatment**

Several novel targets are currently being investigated in melanoma. Our increasing knowledge of the molecular alterations associated with melanoma progression provides rational druggable targets for development of novel therapeutic strategies, including alterations in key intracellular signalling pathways and growth factor receptors.

At present, the best studied kinase is BRAF which is frequently mutated in melanoma. A multi-target tyrosine kinase inhibitor, sorafenib, which targets BRAF and CRAF, has shown promising activity in preclinical studies. Sorafenib is being tested in combination with chemotherapy in patients with metastatic disease but so far has shown only limited response [123]. In addition to BRAF, therapies which target other components of the RAF/RAS/MAPK pathway are being investigated. Other novel targets currently being investigated include components of the PI3/AKT pathway and tyrosine kinases (Figure 1.6).

### **1.7.1 Targeting the RAS/RAF/MAPK Pathway in Melanoma**

A number of BRAF inhibitors are currently in clinical development (Table 1.1). Sorafenib (BAY43-9006, Bayer) is a bi-aryl urea small molecule inhibitor of vascular endothelial growth factor receptor (VEGFR) and RAF kinase, which also has activity against C-Kit and platelet derived growth factor receptor beta (PDGFR- $\beta$ ). Preclinical studies demonstrated that sorafenib can inhibit BRAF in melanoma cell lines resulting in blocking of MAPK activity and inhibition of melanoma cell growth *in vitro* and *in vivo* [124]. Sorafenib also exerts anti-angiogenic effects by blocking RAS/RAF/MAPK signalling in endothelial cells [125]. Sorafenib showed no

significant anti-tumour activity as a single agent in advanced melanoma [126], however, a recent randomised phase II study of sorafenib in combination with dacarbazine produced significantly improved progression free survival (21.1 weeks versus 11.7 weeks, hazard ratio (HR), 0.619) compared to dacarbazine alone. No improvement in overall survival was observed [127]. The addition of sorafenib to paclitaxel and carboplatin as second line treatment for advanced melanoma did not improve progression free survival or overall response rates [128]. This regimen is currently being evaluated in a phase III trial in chemotherapy-naïve advanced melanoma. Several phase II trials of sorafenib in combination with chemotherapy or with other targeted agents are currently ongoing ([www.clinicaltrials.gov](http://www.clinicaltrials.gov)).

Two specific mutant BRAF inhibitors, PLX-4032 and PLX-4720 (Plexxikon Inc.) have been developed and are being tested in melanoma. PLX-4720, a 7-azaindole derivative, reduced MAPK activation in V600E mutated melanoma cell lines but did not alter MAPK activation in BRAF wild type cell lines suggesting that PLX-4720 has the ability to specifically target cancer cells with mutant BRAF. *In vivo* studies confirmed the inhibition of melanoma cell growth and no toxicity was reported [129]. RAF-265 (Novartis) a pan RAF inhibitor is currently recruiting patients for phase I trials in metastatic melanoma.

PLX-4032 recently completed Phase I studies in 55 cancer patients which included 24 BRAF mutation positive melanoma patients. Results are promising with 4 patients achieving minor responses with tumour size reducing by 10-30 %. A further 9 patients achieved partial responses with treatment reducing tumour size by greater than 30 %. Overall PLX-4032 resulted in a degree of tumour size reduction in

metastatic melanoma patients. Patients who responded to PLX-4032 treatment had stable disease for up to 14 months with an interim progression free survival of 6 months. PLX-4032 is currently recruiting patients for Phase II studies in melanoma (<http://www.medicalnewstoday.com/articles/152309.php>).

MEK (MAPK/ERK kinase), downstream of BRAF may be a potential target in melanoma. BRAF-induced hyperactivation of MEK has been implicated in melanoma [130]. A number of MEK inhibitors are being investigated in solid tumours, including RO5126766 (Hoffman-La Roche), and AZD6244 (AstraZenca) which has been shown to be cytostatic as monotherapy, and cytotoxic in combination with docetaxel in preclinical evaluation in melanoma [6]. AZD6244 was tested in Phase I studies and reported stable disease in 9 out of 51 patients for greater than 5 months including tumour shrinkage in 1 melanoma patient [131]. AZD6244 was also tested in a Phase II trial which compared its efficacy against TMZ in advanced melanoma patients. Despite achieving partial response in some patients, overall survival was similar for both treatments [132].

### **1.7.2 Targeting the PI3/AKT Pathway in Melanoma**

Constitutive activation of the phosphatidylinositol-3-kinase (PI3K)/AKT pathway (Figure 1.5) has been implicated in chemo-resistance in many human cancers, including melanoma [65]. Although PI3K itself is rarely mutated [52] or over expressed [67] in melanoma, activation of downstream signalling components, e.g. AKT, have been implicated in melanoma progression [124]. In one study, phosphorylated AKT was detected in 17%, 43%, 49%, and 77% of normal nevi (n=12), dysplastic nevi (n=58), primary melanoma (n=170) and melanoma metastases



(n=52), and strong p-AKT staining correlated inversely with overall and 5-year survival of patients with primary melanoma ( $p < 0.05$ ) [33], however these results have not been corroborated as yet.

Increased AKT activation can be caused by mutation or loss of phosphatase and tensin homolog (PTEN), a tumour suppressor which can down-regulate the AKT pathway [133]. Loss of PTEN reduces apoptosis and promotes cell survival and thereby promotes melanoma tumour development, and has been reported in 20-40 % of melanomas [134, 135]. Increased mTOR (mammalian target of rapamycin) activation has also been implicated in melanoma cell growth. Proliferation of melanoma cells lines was blocked by the mTOR inhibitor rapamycin [136]. mTOR is a downstream target of the PI3K/AKT kinase signalling pathway and regulates cancer cell growth and metabolism [137, 138].

Rapamycin (sirolimus) and its analogs, temsirolimus (CCI-779, Wyeth Pharmaceuticals), everolimus (RAD-001, Novartis) and deforolimus (AP23573, ARIAD Pharmaceuticals, Inc. and Merck & Co., Inc.), which inhibit mTOR have shown promising activity in several cancers [139]. Rapamycin has been shown to inhibit melanoma cell growth *in vitro* and *in vivo*, and synergistically enhances apoptosis and chemo-sensitivity in melanoma cells [140-143]. Temsirolimus also inhibits growth and enhances response to dacarbazine and cisplatin in melanoma cell lines and mouse models of melanoma [144, 145]. Temsirolimus did not demonstrate any clinical benefit as a single agent in the treatment of metastatic melanoma [146]. Phase II trials of temsirolimus and everolimus in combination with chemotherapy or other targeted agents, are currently recruiting patients ([www.clinicaltrials.gov](http://www.clinicaltrials.gov)).

The pan-PI3K inhibitor, LY294002, which has been restricted to preclinical studies [139], showed anti-tumour activity in preclinical models of melanoma [147, 148], demonstrating the potential benefits of targeting the PI3K/AKT pathway in melanoma. Although specific PI3K inhibitors have not yet been tested in melanoma patients, a number of inhibitors are undergoing trials in other solid tumours and may be potential therapies for melanoma. For example NVP-BEZ 235, a dual PI3K/mTOR inhibitor, has shown anti-proliferative effects in glioblastoma, multiple myeloma and breast cancer cell lines [149-151], and is currently in phase I/II trials in solid tumours and breast cancer ([www.clinicaltrials.gov](http://www.clinicaltrials.gov)). XL765 (Exelixis) has recently completed Phase I trials in 19 patients. XL765 was well tolerated and resulted in stable disease in two patients for greater than 6 months. It also resulted in the reduction of the proliferation marker Ki67 [152]. Several other PI3K inhibitors are also in phase I trials, including SF1126 (Semofore), XL147 (Exelixis Inc.) and GDC-0941 (Genentech).

Perifosine (AOI Pharma Inc. and Keryx Biopharmaceuticals), an alkylphosphocholine analogue, inhibits phosphorylation of AKT, which results in the blocking of AKT membrane translocation [139]. A phase II trial of single-agent perifosine as first line treatment in metastatic melanoma patients produced no objective responses [153]. Further trials of perifosine in combination with chemotherapy and targeted agents in other solid tumours are ongoing.

Targeting either the MAPK or AKT pathway individually may be beneficial, but there is substantial preclinical evidence to support targeting both pathways simultaneously

in melanoma [143, 154]. Indeed, Cheung et al showed that AKT3 and mutant BRAF cooperate to promote melanoma development [129]. Dual inhibition of MAPK and PI3K/AKT/mTOR has shown anti-tumour activity in melanoma cell lines [143, 154, 155]. The combination of MAPK and AKT inhibitors completely suppressed invasive growth of melanoma cells in regenerated human skin [156]. A phase I/II trial of combined BRAF and mTOR inhibition by sorafenib and temsirolimus, is currently recruiting melanoma patients ([www.clinicaltrials.gov](http://www.clinicaltrials.gov)).

### **1.7.3 Novel tyrosine kinase targets in melanoma**

#### **1.7.3.1 C-Kit receptor**

Imatinib mesylate (Gleevec, Novartis), which targets c-Kit in addition to Bcr-Abl, inhibited proliferation in melanoma cell lines due to cell cycle arrest in the G<sub>2</sub>M phase [157]. Imatinib had been tested in phase II trials in metastatic melanoma patients without success [158]. A recent study of 21 melanoma patients who had tumours which expressed greater than 25 % positivity for c-Kit were selected for imatinib therapy. Patients were treated with 400 mg twice daily for 6 weeks. Results were poor however with 4 patients achieving stable disease for 12 weeks and 1 patient achieving a partial response for 12.8 months. In most cases though disease progressed quickly and as a result the trial was stopped [159]. Trials which target acral melanoma patients who have c-Kit over expression, exclusive of BRAF mutation, are underway [53]. However it is the presence of mutated form of c-Kit that is important for imatinib therapy and trials which selected for this have not yet been initiated.

### 1.7.3.2 SRC Kinase

Members of the SRC kinase family have been implicated in melanoma progression [160-164] and both SRC and Yes are reported to be elevated in melanoma cells compared to normal melanocytes [160, 165]. The many functions of SRC kinase may be attributable to its relationships with several oncogenes such as the non receptor tyrosine kinase, focal adhesion kinase (FAK) and Stat3 [166]. SRC kinase regulates Stat3 which is active in melanoma but not in normal or benign melanocytes [167]. Blocking SRC kinase leads to inhibition of Stat3, and as a result induction of apoptosis in melanoma cells [168].

Dasatinib, a multi-target tyrosine kinase inhibitor, which targets BCR-Abl, SRC kinases, C-Kit, PDGFR and ephrin-A receptor kinases, is the most potent SRC kinase inhibitor currently in clinical development with an  $IC_{50}$  of 0.5 nM for SRC kinase ( $IC_{50}$  of < 30 nM for the other targets) [169]. In melanoma cell lines, dasatinib has shown anti-proliferative effects and significantly reduced tumour cell migration and invasion [170]. Dasatinib has also shown preclinical activity in prostate cancer [171], triple negative breast cancer [172] and colon cancer cells [173]. Dasatinib is currently being tested in phase I trials in metastatic melanoma.

AZD0530 (AstraZeneca), a selective SRC kinase inhibitor, reduced tumour formation in a skin carcinogenesis model [174], and reduced tumour growth in a SRC-transfected 3T3-fibroblast xenograft model [175]. A phase II clinical trial of AZD0530, as a single agent, is currently recruiting patients with stage III/IV melanoma. SKI-606, a SRC/Abl kinase inhibitor has shown anti-tumour effects in breast cancer *in vitro* and *in vivo* [176], but has not yet been tested in melanoma.

## **1.8 Summary**

Metastatic melanoma is at present one of the fastest growing cancers in Europe and is almost certainly fatal. One reason for melanomas high mortality rate is the failure of the disease to respond to the available treatments. Several factors including cumulative genetic mutations and the alteration of key signalling pathways have been implicated in melanoma progression and drug resistance.

Targeted therapies which are undergoing testing in metastatic melanoma may lead to improvements in prognosis for this aggressive disease. The use of newer targeted therapies alone and in combination with chemotherapy might also offer new hope of improving response to treatment.

Challenges for the future of novel targeted therapies in melanoma include identification of the key molecular alterations which predict sensitivity to a particular targeted agent, to ensure appropriate patient selection, and optimisation of combinations of targeted therapies either with chemotherapy or with other targeted therapies.

Table 1.1. Molecularly targeted agents currently being evaluated in malignant melanoma.

<b>Drug name</b>	<b>Targets</b>	<b>Clinical trials status<sup>a</sup></b>
<b>Sorafenib</b>	B-Raf, VEGF, PDGFR, c-Kit,	Phase III
<b>RAF-265</b>	Raf, VEGFR	Phase I
<b>PLX-4032</b>	Mutant B-Raf	Phase II
<b>RO5126766</b>	MEK	Phase I/II
<b>Perifosine</b>	AKT	Phase II
<b>Rapamycin</b>	mTOR	Phase II
<b>Temsirolimus</b>	mTOR	Phase II
<b>Everolimus</b>	mTOR	Phase II
<b>Deforolimus</b>	mTOR	Phase I
<b>Imatinib mesylate</b>	c-Kit, BCR-Abl, PDGFR	Phase II
<b>Sunitinib</b>	VEGFR, PDGFR, c-Kit, FLT3, CSF-1R, RET	Phase II
<b>Dasatinib</b>	BCR-Abl, Src, c-KIT, PDGFR, Ephrin-A receptors	Phase II
<b>AZD0530</b>	Src, Abl	Phase II

<sup>a</sup> Clinical trial status obtained from [www.clinicaltrials.gov](http://www.clinicaltrials.gov). (5<sup>th</sup> November 2009)

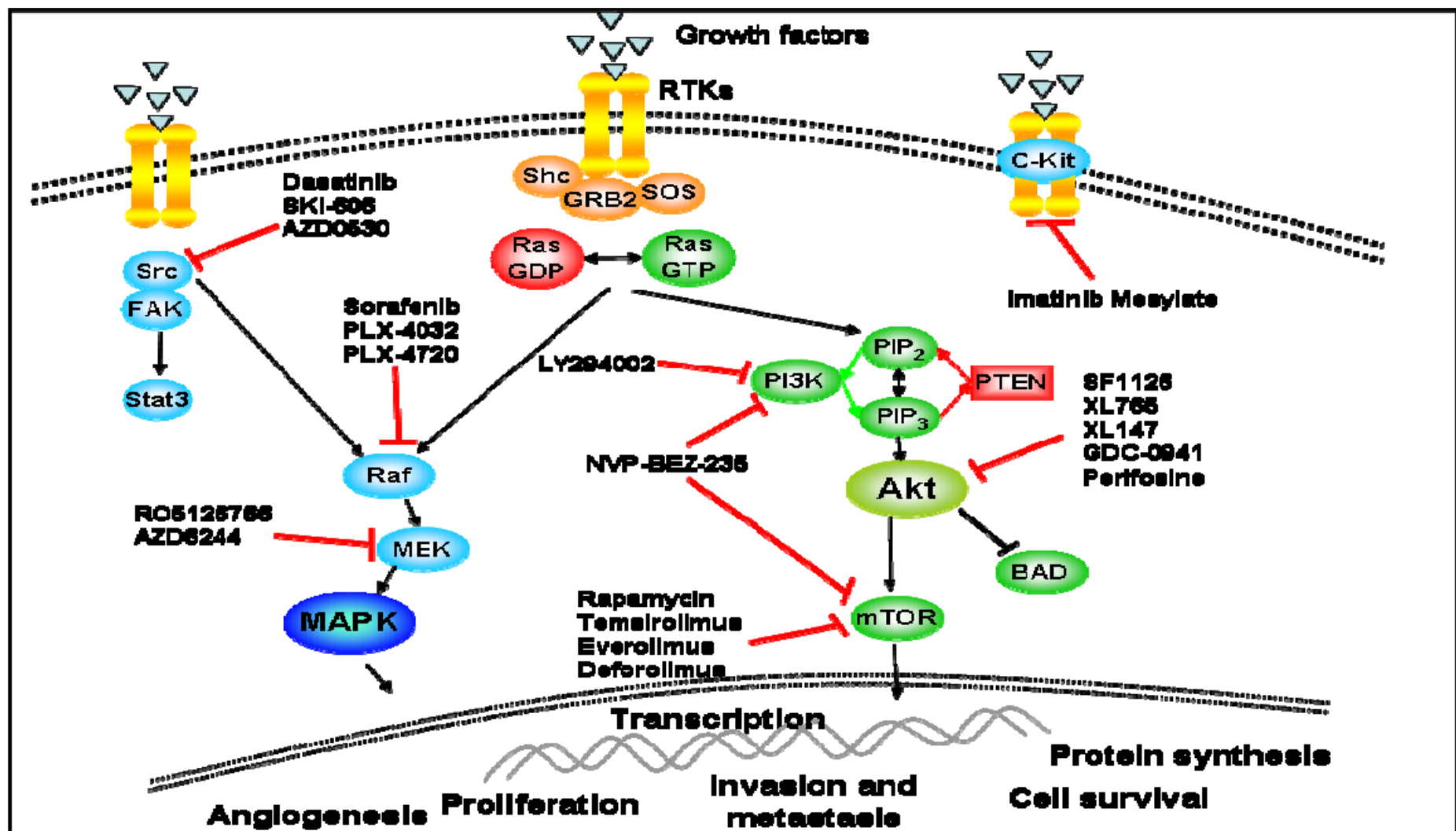


Figure 1.5: Signalling pathways and molecules that are potential targets for melanoma therapy.

## **Chapter 2**

### **2. Materials and Methods**



## 2.1 Cells and Reagents

Melanoma cell lines were obtained from the Department of Developmental Therapeutics, National Cancer Institute, the American Type Culture Collection (ATCC) and the European Association Culture Collection (Table 2.1). All cell lines were maintained at 37 °C with 5 % CO<sub>2</sub> and medium requirements for each cell line are detailed in Table 2.1. Cell lines were centrally tested for possible Mycoplasma contamination every three months approximately, using the Hoechst indirect staining procedure [177].

Table 2.1: Details of the melanoma cell lines including the source and growth medium.

Cell name	Cancer type	Source	Media + % Serum
HT144	<b>Melanoma</b>	ATCC	McCoy's 5A + 10 % FCS
Lox-IMVI	<b>Melanoma</b>	NCI	RPMI + 10 % FCS
Malme-3M	<b>Melanoma</b>	NCI	RPMI + 10 % FCS
M14	<b>Melanoma</b>	NCI	RPMI + 10 % FCS
Sk-Mel-5	<b>Melanoma</b>	NCI	RPMI + 10 % FCS
Sk-Mel-28	<b>Melanoma</b>	NCI	RPMI + 10 % FCS
WM-115	<b>Melanoma</b>	ECACC	MEM + 2 mM L-Glut, 1 mM NEAA, 1 mM Sodium Pyruvate + 10 % FCS
WM-266-4	<b>Melanoma</b>	ECACC	MEM + 2 mM L-Glut, 1 mM NEAA, 1 mM Sodium Pyruvate + 10 % FCS
DLKP-Mitox	<b>Lung</b>	NCTCC	ATCC + 5 % FCS
MRP2-2008	<b>Ovarian</b>	University Hospital Amsterdam	RPMI + 10 % FCS

The chemical compounds listed in Table 2.2 were prepared as stock solutions in dimethyl sulfoxide (Sigma).

Table 2.2: Sources and stock concentrations of chemotherapy drugs and inhibitors used in this project.

<b>Drug Name</b>	<b>Source</b>	<b>Stock Conc.</b>
<b>Dasatinib</b>	Sequoia Chemicals	10 mM
<b>Sorafenib</b>	Sequoia Chemicals	10 mM
<b>Epirubicin</b>	Department of Pharmacy Saint Vincent's University Hospital	3.43 mM
<b>Fumitremorgin C</b>	Sigma	10 mM
<b>Imatinib</b>	Novartis	16.9 mM
<b>MK571</b>	Calbiochem	9.3 mM
<b>Mitoxantrone</b>	SVUH	4.5 mM
<b>MTIC</b>	NCI	50 mM
<b>PP2</b>	Calbiochem	10 mM
<b>Taxotere</b>	SVUH	11.6 mM
<b>Temozolomide</b>	NCI	50 mM
<b>Vincristine</b>	SVUH	1.21 mM

## 2.2 Invasion assays

Invasion and migration assays were performed using the Boyden chamber method as previously described [178]. We used  $1 \times 10^5$  cells in 1mg / ml matrigel-coated (Sigma) 24-well invasion inserts for invasion assays and uncoated inserts for migration assays. To test the effects of dasatinib in invasion/migration, cells were incubated for 6 hours before dasatinib treatment to allow cells to attach and then incubated at 37 °C with dasatinib at varying concentrations for 24 hours. Cells were stained with 0.5 % crystal violet (Sigma) and the number of invading/migrating cells was estimated by counting 10 fields of view at 200 X magnification. The average count was multiplied by the conversion factor 140 (growth area of membrane divided by field of view area, viewed at 200 X magnification) to determine the total number of invading/migrating cells. All assays were performed in triplicate.

### **2.3 Proliferation assay**

Proliferation was measured using an acid phosphatase assay.  $1 \times 10^3$  cells/well were seeded in 96-well plates, except for HT144 and Malme-3M which were seeded at  $2 \times 10^3$  cells/well. Plates were incubated overnight at 37 °C followed by addition of drug at the appropriate concentrations and incubated for a further 5 days until wells were 80 % to 90 % confluent. All media was removed and the wells were washed once with PBS (Sigma). 10 mM paranitrophenol phosphate substrate (Sigma-Aldrich) in 0.1 M sodium acetate buffer with 0.1 % Triton X (Sigma) pH 5.5 was added to each well and incubated at 37 °C for 2 hours. 50  $\mu$ l of 1 M NaOH was added and the absorbance was read at 405 nM (reference – 620 nM), as previously described [179].

### **2.4 RNA Extraction**

RNA extraction was achieved using Tri reagent (Sigma-Aldrich). Cells were grown until confluent in a 90 mm petri-dish. Media was removed and the cells washed twice with PBS. 1 ml of Tri reagent was added to the cells and the resulting lysate passed through a pipette to create a homogenous mixture. The lysate was transferred to a sterile eppendorf and 200  $\mu$ l of chloroform was added. The sample mixed vigorously for 30 seconds by vortexing, then allowed to stand for 15 minutes followed by centrifugation at 12,000 g for 15 minutes at 4 °C. The upper layer containing the RNA was removed to a clean eppendorf and 0.5 ml isopropanol added. The sample was incubated at -20 °C overnight. The samples were centrifuged at 12,000 g for 10 minutes at 4 °C. The supernatant was removed and the RNA pellet washed with 1 ml 75 % ethanol. The RNA was air dried, then resuspended in 20  $\mu$ l of diethyl pyrocarbonate (DEPC)-treated dH<sub>2</sub>O (Sigma). RNA was quantified spectrophotometrically at 260nm and 280nm using the NanoDrop® (ND-1000

spectrophotometer). The ND-1000 software automatically calculated the quantity of RNA in the sample based on an OD<sub>260</sub> of 1 being equivalent to 40mg/mL RNA. The software simultaneously measured the OD<sub>280</sub> of the samples allowing the purity of the sample to be estimated from the ratio of OD<sub>260</sub>/OD<sub>280</sub>. This was typically in the range of 1.8-2.0. A ratio of <1.6 indicated that the RNA may not be fully in solution. RNA samples were stored at -80 °C.

## **2.5 Reverse Transcriptase Reaction**

To synthesise cDNA, 2 µl oligo dT<sub>18</sub> (0.5 µg/ µl) (Sigma), 1 µl DEPC water and 1 µl RNA (1 µg) were heated to 72 °C for 10 min and then cooled to 37 °C. 2 µl 10x MMLV-RT Buffer (Sigma), 0.5 µl RNAsin (40 U/ µl) (Sigma), 1.0 µl 10 mM dNTPs (Sigma), 11 µl DEPC water and 0.5 µl Moloney murine leukaemia virus reverse transcriptase (MMLV-RT) (40,000 U/ µl) (Sigma) were added and the reaction incubated at 37 °C for 1 hour. The cDNA samples were then stored at -20 °C until use.

## **2.6 Polymerase Chain Reaction (PCR)**

PCR amplification of target genes was performed using 1 µl of cDNA, 1.5 µl MgCl<sub>2</sub> (Sigma), 2.5 µl PCR buffer (Sigma), 9.0 µl DEPC water and 0.5 µl of both the forward and reverse primers and 10 µl of the Taq mixture consisting of 0.5 µl 10mM dNTPs (10 mM of each dNTP, 0.25 µl of 5U/ µl *Taq* DNA Polymerase enzyme and 9.25 µl of dH<sub>2</sub>O). Primers were designed and purchased from Eurofins MWG Operon. The PCR amplifications conditions for each primer set are listed in Table 2.3.

Table 2.3: Oligonucleotide sequences and annealing temperatures for primers for RT-PCR analysis of the ABC transporters MRP1, MRP2, BCRP, PgP, ABCB5 and the endogenous control GAPDH.

Oligo Name	Forward and Reverse Sequence	Program settings	Annealing temp
<b>ABCC1 (MRP1)</b>	<b>For:</b> AGT GGA ACC CCT CTC TGT TTA AG <b>Rev:</b> CCT GAT ACG TCT TGG TCT TCA TC	<b>Step 1:</b> 94 °C 2 mins <b>Step 2:</b> 94 °C for 30 secs 55 °C for 30 secs 72 °C for 30 secs	68
<b>ABCC2 (MRP2)</b>	<b>For:</b> TCC TTG CGC AGC TGG ATT ACA T <b>Rev:</b> TCG CTG AAG TGA GAG TAG ATT G	<b>Step 1:</b> 94 °C 2 mins <b>Step 2:</b> 94 °C for 30 secs 58 °C for 30 secs 72 °C for 30 secs	66
<b>ABCG2 (BCRP)</b>	<b>For:</b> CCG CGA CAG TTT CCA ATG ACC T <b>Rev:</b> GCC GAA GAG CTG CTG AGA ACT GTA	<b>Step 1:</b> 94 °C 2 mins <b>Step 2:</b> 94 °C for 30 secs 55 °C for 30 secs 72 °C for 30 secs	68
<b>ABCB1 (PgP)</b>	<b>For:</b> GTT CAA ACT TCT GCT CCT GA <b>Rev:</b> CCC ATC ATT GCA ATA GCA GG	<b>Step 1:</b> 94 °C 2 mins <b>Step 2:</b> 94 °C for 30 secs 55 °C for 30 secs 72 °C for 30 secs	58
<b>ABCB5 Alpha/Beta</b>	<b>For:</b> AAT GCT TCT CGG CCT TTT GGC TAA G <b>Rev:</b> GGG CTA TTG CGA AGG TTT CAA AGT G	<b>Step 1:</b> 94 °C 2 mins <b>Step 2:</b> 94 °C for 30 secs 60 °C for 30 secs 72 °C for 30 secs	72
<b>GAPDH</b>	<b>For:</b> GCC TCA AGA TCA TCA GCA A <b>Rev:</b> CAG AAT C CATC CTT TAG GGT CAC A	<b>Step 1:</b> 94 °C 2 mins <b>Step 2:</b> 94 °C for 30 secs 58 °C for 30 secs 72 °C for 30 secs	56

PCR samples were separated on a 1.5 % agarose gel (1.5% agarose (Sigma) in 1 X TBS buffer with 0.00002 % ethidium bromide (Sigma)) and run at 100 V for 20 minutes. PCR products were visualised using the Epi Chemi II Darkroom gel documentation system (UVP).

## 2.7 Real-Time PCR

RNA was extracted and cDNA synthesised as per Section 2.4. Taqman® Real Time PCR analysis was performed using the Applied Biosystems Assays on Demand PCR kits (TaqMan® gene expression assays) for ANXA1, CAV1, CAV2, EPHA2, PTRF, IGFBP2, BCRP and MRP-2 on a 7900 fast real-time PCR instrument (Applied Biosystems).

Real-Time PCR was performed by adding 22.5 µl of qPCR master mix to the relevant wells of a 96-well PCR plate. qPCR master mix consists of 12.5 µl of 2X TaqMan universal PCR mastermix (Applied Biosystems), 1.25 µl of 20X gene expression assay mix (Applied Biosystems) and 8.75 µl of RNase free water. 5 µl of each cDNA sample was added to give a final reaction volume of 25 µl. Each cDNA sample was analysed in triplicate for measurement of target gene expression and endogenous control (GAPDH).

For analysis of the dasatinib 6 gene marker set, expression of each gene was standardized using GAPDH as a reference gene, and relative expression levels for the panel of cell lines were quantified by calculating  $2^{-\Delta\Delta C_T}$ , where  $\Delta\Delta C_T$  is the difference in  $C_T$  between target and reference genes. Control pooled samples consisting of equal volumes of mRNA of each cell line tested were also prepared. The control pool allowed us to compare the relative expression of a target gene in a target cell line against the average expression of all the cell lines.

## **2.8 Establishing temozolomide resistant cell lines**

Malme-3M cells were seeded at a density of  $2.5 \times 10^4$  cells in a 75 cm<sup>2</sup> flask. After 24 hours the medium was replaced with medium containing 300  $\mu$ M temozolomide. The cells were treated for 6 hours and the medium replaced with drug-free medium. Cells were allowed to grow until confluent, then trypsinised and reseeded at a density of  $2.5 \times 10^4$  cells per flask. Treatment was repeated 6 times.

HT144 cells were seeded at a density of  $2.5 \times 10^4$  cells in a 75 cm<sup>2</sup> flask. After 24 hours medium was replaced with 300  $\mu$ M temozolomide. The cell were treated for 6 hours, the medium was replaced and the cells were incubated at 37 °C overnight. The next day the cells were treated again with 300  $\mu$ M temozolomide for 6 hours. This treatment was repeated for 7 days. After 7 days the drug was removed and replaced with fresh drug-free medium. Cells were allowed to grow until confluent, then trypsinised and seeded at a density of  $2.5 \times 10^4$  cells in a 75 cm<sup>2</sup> flask. This treatment was repeated four times.

## **2.9 Establishing taxotere resistant cell line**

Malme-3M cells were seeded at a density of  $2.5 \times 10^4$  cells in a 75 cm<sup>2</sup> flask. After 24 hours the medium was replaced with fresh medium containing 1 nM taxotere. After 6 hours the medium was replaced with fresh medium. Cells were allowed to grow until confluent, then trypsinised and reseeded at a density of  $2.5 \times 10^4$  cells. Treatment was repeated 6 times.

## **2.10 Terminal DNA transferase-mediated dUTP nick end labelling (TUNEL) assay**

The Guava® TUNEL Assay detects apoptosis-induced DNA fragmentation through a quantitative fluorescence assay. Terminal deoxynucleotidyl transferase (TdT) catalyzes the incorporation of bromo-deoxyuridine (BrdU) residues into the fragmenting nuclear DNA at the 3'-hydroxyl ends by nicked end labeling. A TRITC-conjugated anti-BrdU antibody can then label the 3'-hydroxyl ends for detection by a Guava System.  $2.5 \times 10^4$  cells were seeded per well in 24-well plates and incubated overnight at 37°C, followed by addition of drug at the appropriate concentrations. After 72 hours, media was collected and the wells washed once with PBS. Cells were trypsinised and added to the media collected for each sample. Cells were centrifuged at 300 x g for 5 minutes and the medium was aspirated. The pellet was re-suspended in 150 µl of PBS and transferred to a round bottomed 96 well plate. 50 µL of 4% para-formaldehyde (Sigma) made up in PBS was added to the wells and mixed. Cells were incubated at 4 °C for 60 minutes. The plate was centrifuged at 300 x g for 5 minutes and the supernatant aspirated leaving approximately 15 µL in each well. The remaining volume was used to resuspend the cells and 200 µL of ice cold 70 % ethanol (Fluka) was added to the cells. The plates were then stored at – 20 °C for 2 hours. After fixation, the cells including positive and negative controls were spun at 300 g for 5 minutes. The supernatant was aspirated, and the cells washed with 200 µL of wash buffer and then spun again at 300 g for 5 minutes. The wash buffer was aspirated and 25 µL of DNA labelling mix was added to each well and the cells mixed. The plates were covered with parafilm and incubated for 60 minutes at 37 °C. 200 µL of rinsing buffer were then added to each well and the plates spun at 300 g for 5 minutes. The supernatant was aspirated and 50 µL of anti-BrdU staining mix added



to each well, with the plate stored in the dark at room temperature for 30 minutes. At the end of the incubation 150  $\mu$ L of rinsing buffer was added to each well. Cells were analysed on the Guava EasyCyte (Guava Technologies). Positive and negative controls were performed with each assay.

## **2.11 Cell Cycle Assays**

The Guava Cell Cycle Assay uses the nuclear DNA stain, propidium iodide (PI), to measure cell cycle. Resting cells (G0/G1) contain two copies of each chromosome. Cycling cells synthesize chromosomal DNA (S phase), which results in increased fluorescence intensity. When all chromosomal DNA has doubled (G2/M phase), cells fluoresce with twice the intensity of the initial population.  $2.5 \times 10^4$  cells were seeded per well in 24-well plates and incubated overnight at 37°C. After 24 hours cells were synchronised by removing the media and replacing it with serum free medium (SFM) for a further 24 hours. SFM was removed and the cells incubated for 6 hours in media containing serum before the drug was added at the appropriate concentrations. Plates were then incubated at 37 °C for a further 24 hours. Media was collected and the wells washed once with PBS. Cells were trypsinised and added to the media collected for each sample. Cells were centrifuged at 300 x g for 5 minutes and the media was aspirated. The cell pellet was re-suspended in 150  $\mu$ L PBS and transferred to a round bottomed 96 well plate. The plate was centrifuged at 300 x g for 5 minutes and the supernatant aspirated leaving approximately 15  $\mu$ L in each well. The remaining volume was used to resuspend the cells and 200  $\mu$ L of ice cold 70 % ethanol was added. The plates were then stored at – 20 °C for 2 hours. After fixing the cells were spun at 450 x g for 5 minutes, the supernatant removed, washed with 200  $\mu$ L of PBS

and spun again at 450 g. The PBS was then removed and 200  $\mu$ L of Guava Cell Cycle reagent were added to the plates. The cells were mixed by pipetting and stored at room temperature shielded from the light for 30 minutes. Cells were analysed on the Guava EasyCyte and the data was analysed using Modfit LT software (Verity).

## **2.12 Protein Extraction and Western blotting**

500  $\mu$ L RIPA buffer (Sigma-Aldrich) with 1 X protease inhibitors, 2 mM phenylmethanesulphonylfluoride (PMSF) and 1 mM sodium orthovanadate (Sigma-Aldrich) was added to cells and incubated on ice for 20 minutes. Following centrifugation at 16,000 g for 5 minutes at 4°C the resulting lysate was stored at -80°C. Protein quantification was performed using the Bicinchoninic acid (BCA) assay (Pierce). 40  $\mu$ g of protein in sample buffer (2.5 ml 1.25 M Tris HCl; 1 g Sodium dodecyl sulphate (SDS); 2.5ml betamercaptoethanol; 5.8 ml glycerol; 0.1% bromophenol blue made up to 20 ml with dH<sub>2</sub>O) was heated to 95 °C for 5 minutes and proteins were separated on 7.5 or 10 % gels (Lonza). The protein was transferred to Hybond-ECL nitrocellulose membrane (Amersham Biosciences) using a semi-dry transfer unit (Atto). The membrane was blocked with 5 % milk powder (Biorad) in 0.1 % PBS-Tween at room temperature for 1 hour, then incubated overnight at 4 °C in primary antibody (Table 2.4) with 0.1 % PBS-Tween in 5 % milk powder. The membrane was washed three times with 0.5 % PBS-Tween and then incubated at room temperature with secondary antibody (Table 2.4) in 5 % milk powder with 0.5 % PBS-Tween for 1 hour. The membrane was washed three times with 0.5 % PBS-Tween followed by one wash with PBS alone. Detection was performed using Luminol (Santa Cruz Biotechnology).

Table 2.4: Details of antibodies used, including phosphorylation sites, suppliers, host species and concentration of primary and secondary antibodies used.

<b>Antigen</b>	<b>Phospho Site</b>	<b>Supplier</b>	<b>2° Ab Species</b>	<b>1° Ab µg/ml</b>	<b>2° Ab µg/ml</b>
<b>Caveolin-1</b>	n/a	Millipore	Mouse	1	1.0
<b>EPHA2</b>	n/a	Millipore	Mouse	1	1.0
<b>p-FAK</b>	Y 861	Biosource	Mouse	1	1.0
<b>p-FAK</b>	Y 397	Biosource	Rabbit	1	0.3
<b>FAK</b>	n/a	Biosource	Rabbit	1	0.3
<b>p-SRC</b>	Y 418	Biosource	Rabbit	2	0.3
<b>SRC</b>	n/a	Millipore	Mouse	1	1.0
<b>Akt</b>	n/a	Cell Signalling Technology	Rabbit	1	0.3
<b>p-AKT</b>	Ser 473	Cell Signalling Technology	Rabbit	1	0.3
<b>MAPK</b>	n/a	Cell Signalling Technology	Rabbit	1	0.3
<b>p-MAPK</b>	Y 42 / 44	Cell Signalling Technology	Rabbit	1	0.3
<b>HSP-60</b>	n/a	Millipore	Mouse	1	1.0
<b>ERP-29</b>	n/a	AbCam	Rabbit	1	0.3
<b>p-Tyrosine</b>	n/a	Millipore	Mouse	1	1.0
<b>p-Serine</b>	n/a	Millipore	Mouse	1	1.0
<b>Annexin-2</b>	n/a	BD Biosciences	Mouse	1	1.0
<b>Annexin-1</b>	n/a	BD Biosciences	Mouse	1	1.0
<b>PTRF</b>	n/a	AbCam	Rabbit	1	0.3
<b>IGFBP2</b>	n/a	AbCam	Mouse	1	1.0
<b>α-tubulin</b>	n/a	Sigma-Aldrich	Mouse	1	1.0
<b>Caveolin-2</b>	n/a	BD Biosciences	Mouse	1	1.0

### 2.13 Immunoprecipitation

Immunoprecipitation was performed using the Catch and Release® reversible immunoprecipitation system (Millipore). Briefly, spin columns were washed 3 times

with 400 µl of 1 X Catch and Release wash buffer. 500 µg of cell lysate was added to the column together with 2-3 µg of antibody per sample, 10 µl of Catch and Release antibody ligand and the final volume was made up to 500 µl with 1X wash buffer. Capped sample columns were then incubated overnight on a shaker at 4 °C. The caps were removed and sample columns spun at 2000 g for 30 seconds to remove all unbound protein and antibody. The column was then washed with 400 µl of 1X wash buffer. The column was centrifuged again at 2000 g for 30 seconds and the supernatant removed. This process was repeated twice. To elute protein in its denatured form 70 µl of denaturing elution buffer with 5 % beta-mercaptoethanol was added to the sample column and incubated for 5 minutes. The column was then centrifuged for 1 minute at 2000 g. This procedure was repeated three times and each eluent collected into a separate tube. Samples were then heated to 95 °C for 5 minutes and the sample stored at - 20 °C until used.

## **2.14 Immunohistochemistry**

All immunohistochemical (IHC) staining was performed using the DAKO Autostainer (DAKO). Deparaffinisation and antigen retrieval was performed using Epitope Retrieval 3-in-1 Solution (pH 6) (DAKO) and the PT Link system (DAKO) for EphA2, Src kinase and Annexin-A1. For Caveolin-1 deparaffinisation and antigen retrieval was performed using Epitope Retrieval 3-in-1 Solution (pH 9) (DAKO) and the PT Link system (DAKO). For epitope retrieval, slides were heated to 97 °C for 20 minutes and then cooled to 65 °C. The slides were then immersed in wash buffer (DAKO). On the Autostainer (DAKO) slides were blocked for 10 minutes with 200 µL HRP Block (DAKO). Cells were washed with 1X wash buffer and 200 µL of antibody added to the slides for 30 minutes. Slides were washed again with 1X wash

buffer and then incubated with 200 µL Real EndVision (DAKO) for 30 minutes. Slides were washed again with 1X wash buffer and then stained with 200 µL AEC substrate chromagen (DAKO) for 10 minutes and this procedure was repeated twice. A positive control slide was included in each staining run. A negative control was also tested for each sample, using antibody diluent without the primary antibody, to allow for evaluation of non-specific staining. All slides were counterstained with haematoxylin (DAKO) for 5 minutes, and rinsed with deionised water, followed by wash buffer. Once staining was completed each slide was mounted with a coverslip using Faramount mounting solution (DAKO). Staining was assessed by consultant Pathologist, Dr. Susan Kennedy. Slides were assessed for both the percentage of tumour cells that were positive for staining (0 = not present; 1 = < 25 %; 2 = < 50 %; 3 = >50 %) and for the intensity of the positive staining (0 = not present; 1 = weak; 2 = moderate; 3 = intense).

Table 2.5: Positive control tissue samples used for each antibody.

<b>Antigen</b>	<b>Antibody supplier</b>	<b>Positive control tissue</b>
<b>Annexin-1</b>	BD Biosciences	Tonsil
<b>Caveolin-1</b>	Cell signalling	Head and Neck Cancer
<b>EphA2</b>	Santa Cruz Biotechnology	Metastatic Breast Cancer
<b>Src kinase</b>	Cell Signalling	Head and Neck Cancer

Table 2.6: Antibody concentrations used for immunohistochemical staining.

<b>Antigen</b>	<b>Primary Antibody Conc.</b>
<b>ANXA1</b>	1: 200
<b>Cav-1</b>	1: 150
<b>EphA2</b>	1: 15
<b>Src kinase</b>	1: 100

## **2.15 Phosphoprotein preparation**

WM-115 and WM266-4 cells were grown in 175 cm<sup>2</sup> flasks until 90% confluent. Each cell line was then either treated for 6 hours with dasatinib at a concentration of 100 nM or with control growth media. Triplicate samples of each treatment were prepared. Total protein was extracted and the phosphoprotein fragments were isolated using the Pierce<sup>TM</sup> Phosphoprotein Enrichment Kit (Pierce Biotechnology). Cells were washed twice with cold HEPES buffer (50 mM, pH 7), and lysed using the Lysis/Binding/Wash buffer provided. The lysis buffer was supplemented with CHAPS (0.25%), sodium dodecyl sulphate, 0.1% SDS, 1X Halt Protease Inhibitor EDTA-free and 1X Halt Phosphatase Inhibitor Cocktail (Pierce Biotechnology). After cell scraping the lysates were transferred to eppendorfs, and placed on ice for 45 minutes, vortexing every 5 minutes with the resulting lysate being passed through an 18-gauge needle. The lysate was centrifuged at 10,000 x g for 20 minutes at 4 °C and the supernatant collected and stored at -80 °C. After protein quantification by BCA assay, the concentration of each lysate was adjusted to 0.5 mg/ml and the phosphoprotein fraction of each was enriched using phosphoprotein enrichment columns supplied with the kit, according to the protocol provided. The eluted phosphoprotein fractions were then concentrated using iCON concentrators (Thermo scientific), yielding 100-150 µl of concentrated phosphoprotein for each sample. The samples were stored at -80°C.

## **2.16 Protein Precipitation and Quantification**

Cell lysates suspended in the 1x storage buffer were precipitated using the ReadyPrep 2-D Cleanup kit (Bio-Rad), following the manufacturer's instructions. The resulting pellet was resuspended in DIGE lysis buffer (7

M urea, 2 M thiourea, 4% CHAPS, and 30 mM Tris-HCl, pH 8.5). Total protein concentration was determined using the Quick start Bradford dye reagent (Bio-Rad).

## **2.17 Protein labelling and two-dimensional differential gel electrophoresis**

### **(DIGE)**

All proteomic analysis detailed in this thesis was carried out under the supervision of Dr. Paul Dowling. DIGE was performed using three CyDye DIGE Fluor Minimal dyes Cy3, Cy5 and Cy2 (GE Healthcare) [180]. In this technique, 25 µg of each phosphoprotein sample was added to microcentrifuge tubes and labelled with Cy3 or Cy5 dye (200 pico mole (pmol) in 1 µl anhydrous dimethylformamide (DMF)). Each tube was mixed by vortexing, and placed on ice for 30 minutes in the dark. Under these conditions approximately 1% of the lysine residues of the protein are covalently conjugated to the CyDyes. The reaction was quenched by the addition of a 50-fold molar excess of free lysine to the dye for 10 minutes on ice in the dark. The labelled samples were stored at -80 °C.

Each gel compared two samples, one labelled with Cy3 and the other with Cy5 (Table 2.7). Triplicate gels were run for each comparison. A Cy2-labelled pool was prepared containing 12.5 µg of protein from each of the 18 samples. This pool was used on all gels as an internal standard to allow for accurate quantification [180]. A mix of each sample was also prepared to run on a preparative gel to facilitate protein identification after electrophoresis.

Table 2.7: DIGE experimental design, showing gel number and the Cy dye used for each sample. Triplicate gels were run for each comparison.

<b>Gel no.</b>	<b>Cy2 (50 µg)</b>	<b>Cy3 (50 µg)</b>	<b>Cy5 (50 µg)</b>
<b>1</b>	Cy2 pool	WM-115 Ctrl	WM-115 Dasat
<b>2<sup>a</sup></b>	Cy2 pool	WM-115 Dasat	WM-115 Ctrl
<b>3</b>	Cy2 pool	WM-115 Ctrl	WM-115 Dasat
<b>4</b>	Cy2 pool	WM-266-4 Ctrl	WM-266-4 Dasat
<b>5<sup>a</sup></b>	Cy2 pool	WM-266-4 Dasat	WM-266-4 Ctrl
<b>6</b>	Cy2 pool	WM-266-4 Ctrl	WM-266-4 Dasat

<sup>a</sup> Gel no.s 2 and 5 are examples of reverse labelling, and are introduced to avoid any slight bias caused because of the different molecular weights of the Cy dyes.

An equal volume of 2x sample buffer (2.5 ml rehydration buffer stock solution (7 M urea, 2 M thiourea, 4 % CHAPS), pharmalyte broad range pH 4-7 (2%) (GE Healthcare), DTT (2%)) (Sigma) was added to the labelled protein samples. The mixture was incubated on ice for 10 minutes.

The protein samples were then passively rehydrated into immobiline 24-cm linear pH gradient strips (IPG, pH 3-11) (GE Healthcare) using rehydration buffer solution (7 M urea, 2 M thiourea, 4 % CHAPS, 0.5% IPG buffer, 50 mM DTT). Each strip was overlaid with 3 ml IPG Cover Fluid (GE Healthcare) and allowed to rehydrate overnight at RT. Isoelectric focussing (IEF) was then performed using the IPGphor apparatus (40 kv/hr @ 20 °C with resistance set at 50mA) (GE Healthcare).

For second dimension separation, the strips were equilibrated by incubating in equilibrium solution (50 mM Tris-HCL, pH 8.8, 6 M urea, 30% glycerol, 1% SDS) (All Sigma) containing 65 mM DTT for 20 minutes, followed by 20 minutes incubation in the same buffer containing 240 mM iodoacetamide (both at room



temperature). 12.5 % acrylamide gel solutions (acrylamide/bis 40 %, 1.5 M Tris pH 8.8, 10 % SDS) (All Sigma) were prepared, and prior to pouring, 10 % ammonium persulfate (Sigma) and 100  $\mu$ l TEMED (Sigma) were added. The gels were overlaid with 1 ml saturated butanol (BDH), and left to set for at least three hours at RT. Equilibrated IPG strips were transferred onto 24 cm 12.5% uniform polyacrylamide gels poured between low fluorescence glass plates. Strips were overlaid with 0.5% low melting point agarose (Sigma) in running buffer containing bromophenol blue (Sigma). Gels were run at 2.5 W/gel for 30 min and then 100 W total at 10 °C until the dye front had run off the bottom of the gels.

### **2.18 Gel Imaging**

All of the gels were scanned using the Typhoon 9400 Variable Mode Imager (GE Healthcare) to generate gel images at the appropriate excitation and emission wavelengths from the Cy2-, Cy3- and Cy5-labelled samples. The resultant gel images were cropped using the ImageQuant software tool and imported into Decyder 6.5 software. The biological variation analysis (BVA) module of Decyder 6.5 was used to compare the control versus test samples to generate lists of differentially expressed proteins.

### **2.19 Spot digestion**

Preparative gels containing 400 mg of protein were fixed and then poststained with colloidal coomassie blue stain (Sigma). The subsequent gels were scanned using the Typhoon 9400 Variable Mode Imager (GE Healthcare) to generate gel images at the appropriate excitation and emission wavelengths for the colloidal CBB stain.

Preparative gel images were then matched to the Master gel image generated from the DIGE experiment. Spots of interest were selected and a pick list was generated and imported into the software of the Ettan Spot Picker robot (GE Healthcare). Gel plugs were placed into presiliconised microtitre plates and stored at 47 °C until digestion. Tryptic digestions were performed using the Ettan Digester robot (GE Healthcare). Excess liquid was removed from each plug, and washed for three cycles of 20 min using 50 mM NH<sub>4</sub>HCO<sub>3</sub> (Sigma) in 50% methanol (Romil) solution. The plugs were then washed for two cycles of 15 min using 70% Acetonitrile (ACN) (Fluka) and left to air dry for 1 h. Lyophilised sequencing grade trypsin (Promega) was reconstituted with 50 mM acetic acid (Fluka) as a stock solution and then diluted to a working solution with 40 mM NH<sub>4</sub>HCO<sub>3</sub> in 10% ACN solution, to a concentration of 12.5 ng trypsin per mL. Samples were digested at 37°C overnight and were then extracted twice with 50% ACN and 0.1% trifluoro acetic acid (TFA) (Sigma) solution for 20 min each. All extracts were pooled and concentrated by SpeedVac (Thermo Scientific) for 40 min.

## **2.20 MALDI-ToF-ToF Mass Spectrometry and Protein Identification**

One fifth of the peptide extract solution from the digest was added to a 384 spot MALDI sample plate (Applied Biosystems) and supplemented with 0.5 µl of a 5 mg/ml solution of recrystallised  $\alpha$ -cyano-4-hydroxy-trans-cinnamic acid matrix (Laser Biolabs) plus 10mM NH<sub>4</sub>H<sub>2</sub>PO<sub>4</sub> in 50% acetonitrile/water containing 0.1% TFA and allowed to air dry prior to analysis. MALDI mass spectra were generated using a 4800 TOF/TOF Proteomics Analyzer instrument (Applied Biosystems). An internal sample mix, Pep4 (Laser Biolabs) was also spotted onto target slides and used as an internal calibrant. All MS and MS/MS experiments were carried out in positive reflectron

mode. Ten precursor ions for MS/MS were selected automatically on the basis of intensity from the MS spectra. The MS and MS/MS data were combined and searched against a number of databases using GPS Explorer software (Applied Biosystems) and a local MASCOT (Matrix Science) search engine for protein identification. A mass window of 20 parts per million was set for database searching on all precursors.

### **2.21 One dimensional (1D) reverse phase chromatography for simple protein mixtures**

Prior to analysis columns were equilibrated in Solvent A (2% acetonitrile in LC-MS grade water containing 0.1% formic acid (Sigma)) for 10 min and the column set to a temperatures of 25°C using a column oven. 5 µL of digested protein samples in sample loading buffer (0.1 % TFA) was loaded using the injection pickup of the LC system onto a PepMap C18 trap cartridge (300 µm x 5 mm) (LC Packings/Dionex) at a flow rate of 25 µL/min for 5 min to desalt and concentrate the sample.

Peptides from the trap column were eluted at a flow rate of 350 nL/min acetonitrile/water gradient (2-50% Solvent B (2% LC-MS grade water in acetonitrile containing 0.1% formic acid (Sigma)) in 30 min) onto a PepMap C18 capillary column (300 µm x 15 cm, 3 µm particles) directly into the electrospray tip. Peptides were eluted directly off the column into the LTQ Orbitrap XL mass spectrometer (Thermo Fisher Scientific).

The columns were re-equilibrated in Solvent A for 10 minutes prior to analysis of the next sample. The scan sequence of the MS is based on a data dependent method. The full scan was acquired in the Orbitrap at a resolution of 60,000 and we then acquired

subsequent MS/MS scans of the 5 most abundant peaks in the spectrum in the linear ion trap using dynamic exclusion to exclude multiple MS/MS of the same peptide. We set the dynamic exclusion to a repeat count of 1, a repeat duration of 30 s and an exclusion list of 500. The general MS conditions we used were: electrospray voltage of 1.6kV, ion transfer tube temperature of 200°C, collision gas pressure of 1.3 mTorr, normalised collision energy of 35%, and an ion selection threshold of 500 counts for MS2. An activation q-value of 0.25 and an activation time of 30 ms for MS2 acquisitions were also used.

We identified the peptides using the tandem mass spectrum (MS/MS) data generated by mass spectrometry. We searched each tandem mass spectrum against a database using database-searching software packages. Peptide identifications were reported in terms of XCorrelation scores and probability scores, as in the case for the SEQUEST algorithm (Thermo Fisher Scientific). If several statistically significant peptides were identified from the same protein then generally this protein identification is accepted.

## **2.22 Pro-Q Diamond phosphostaining**

Fluorescent staining of 2-DE gels using Pro-Q Diamond phosphoprotein gel stain kit (Molecular Probes, Eugene, OR) was performed according to the manufacturer's guidelines on WM-266-4 untreated and dasatinib treated cells. Briefly, the gels were fixed in 50% methanol, 10% acetic acid overnight, washed with three changes of deionized water for 15 min per wash, followed by incubation in Pro-Q Diamond phosphoprotein gel stain for 195 min. They were then destained with three changes of 20% acetonitrile in 5 mM sodium acetate (pH 4.0) for 1 h. This was done three times. Useful images could be obtained at 3 h after staining. Images were acquired using a

Typhoon™ 9400 imager (Amersham Biosciences) with an excitation of 532 nm and an emission of 580 nm to determine the phosphostain reacting proteins.

### **2.23 Bioinformatics analysis and literature mining**

Genes were annotated to Genbank gene symbols using an in-house annotation tool, yielding a total of 22 annotated transcripts on which ontology and literature mining analysis was carried out using PANTHER (Protein ANalysis THrough Evolutionary Relationships) (<http://www.pantherdb.org/>). Additionally we undertook literature mining analysis using Pathway Studio (Ariadne Genomics) on this list to determine previously-established links to productivity-related cell processes and analyses.

### **2.24 Small interfering RNA (siRNA) transfection**

A siRNA molecule targeting kinesin, and a scrambled sequence siRNA molecule (Ambion) were used as positive and negative transfection controls. Each siRNA molecule was transfected at a final concentration of 30 nM.  $5 \times 10^4$  and  $1.5 \times 10^5$  cells were resuspended in MEM media for 96-well and 6-well plates respectively and allowed to incubate overnight at 37 °C. Each siRNA and Lipofectamine 2000 transfection agent (3 µl for 6 well plates; 0.75 µl for 24 well plates) were diluted in Gibco™ Opti-MEM reduced serum medium (Invitrogen), and incubated at room temperature (RT) for 5 minutes. Diluted Lipofectamine 2000 was then added to each diluted siRNA and incubated for a further 20 minutes at RT. The transfection mix was then added to the cells. After 24 hours, the transfection media was replaced with 10 % MEM. 6-well plates were used to prepare lysates after 72 hours. Cells in 24-

well plates were harvested after four days and counted using Guava Viacount (Millipore) on the Guava EasyCyte.

Table 2.8. Sequences of three anti-SRC siRNA molecules, with the Ambion siRNA ID number, and the number (1-3) assigned to each.

ID	No.	Sense	Antisense
683	1	GGCUGAGGAGUGGUAUUUUtt	AAAAUACCACUCCUCAGCCtg
684	2	GGCCCUUUGUGUAAGGUGUtt	ACACCUUACACAAAGGGCCtt
103417	3	GGUCAUGAAGAAGCUGAGGtt	CCUCAGCUUCUUCAUGACCtg

Table 2.9: Sequences of the 4 individual anti ANXA2 siRNA molecules that comprise the ON-TARGETplus SMART pool.

Product code	Location	Target Sequence
J-010741-07	ORF	CGACGAGGACUCUCUCAUU
J-010741-08	3' UTR	AUCCAAGUGUCGCUAUUUA
J-010741-09	3' UTR	AAAACCAGCUUGCGAAUAA
J-010741-10	3' UTR	GGAAGAAAGCUCUGGGACU

## 2.25 Statistical analysis

IC<sub>50</sub> values were calculated using CalcuSyn software (BioSoft). For Lox-IMVI, combination index (CI) values were calculated using CalcuSyn software. C.I. values were used to determine synergy in cell lines (Table 2.10)

Table 2.10: Recommended symbols for describing synergism or antagonism in drug combination studies analyzed with the Combination Index (CI) method

Range of CI	Symbol	Description
<0.1	+++++	Very strong synergism
0.1-0.3	++++	Strong synergism
0.3-0.7	+++	Synergism
0.7-0.85	++	Moderate synergism
0.85-0.90	+	Slight synergism
0.90-1.10	±	Nearly additive
1.10-1.20	-	Slight antagonism
1.20-1.45	--	Moderate antagonism
1.45-3.3	---	Antagonism
3.3-10	----	Strong antagonism
>10	-----	Very strong antagonism

CI values were not calculated for the other cell lines, as dasatinib did not achieve 50 % inhibition of growth at concentrations up to 1  $\mu$ M. The Student's *t* test was used to compare temozolomide IC<sub>50</sub>s alone and in combination with dasatinib in migration/invasion assays and cell cycle assays. *P* < 0.05 was considered statistically significant.

## **Chapter 3**

### **3. Characterisation of invasion and drug sensitivity in melanoma cell lines**



### 3.1 Introduction

In this study, we examined how the *in vitro* melanoma phenotype relates to the *in vivo* behaviour of metastatic melanoma, in particular with respect to melanoma cell invasion and drug resistance. Utilising the *in vitro* Boyden chamber invasion assay, we characterised the ability of our melanoma cell lines to migrate and invade. By examining the sensitivity of the melanoma cell lines to common chemotherapeutics we aimed to determine how response to chemotherapy drugs *in vitro* relates to the chemo-resistant phenotype of the disease.

We examined expression of a panel of ABC transporters and how they relate to chemo-sensitivity in the melanoma cell lines. We also examined whether repeated exposure of melanoma cells to chemotherapy, in particular temozolomide and taxotere, results in the development of resistance *in vitro* and whether the ABC transporters play a role in the development of acquired resistance.

### 3.2 Invasion and motility of melanoma cell lines

Invasion and migration assays were performed using matrigel-coated 24-well invasion inserts for invasion assays and uncoated inserts for migration assays (Figure 3.1 and Figure 3.2).

All of the melanoma cell lines displayed the ability to migrate and invade *in vitro*. Apart from Sk-Mel-5 which shows a low level of migration, the remaining melanoma cell lines are highly migratory. Lox-IMVI, Sk-Mel-28 and M14 are highly invasive cell lines, Malme-3M and HT144 less invasive, and Sk-Mel-5 is poorly invasive.

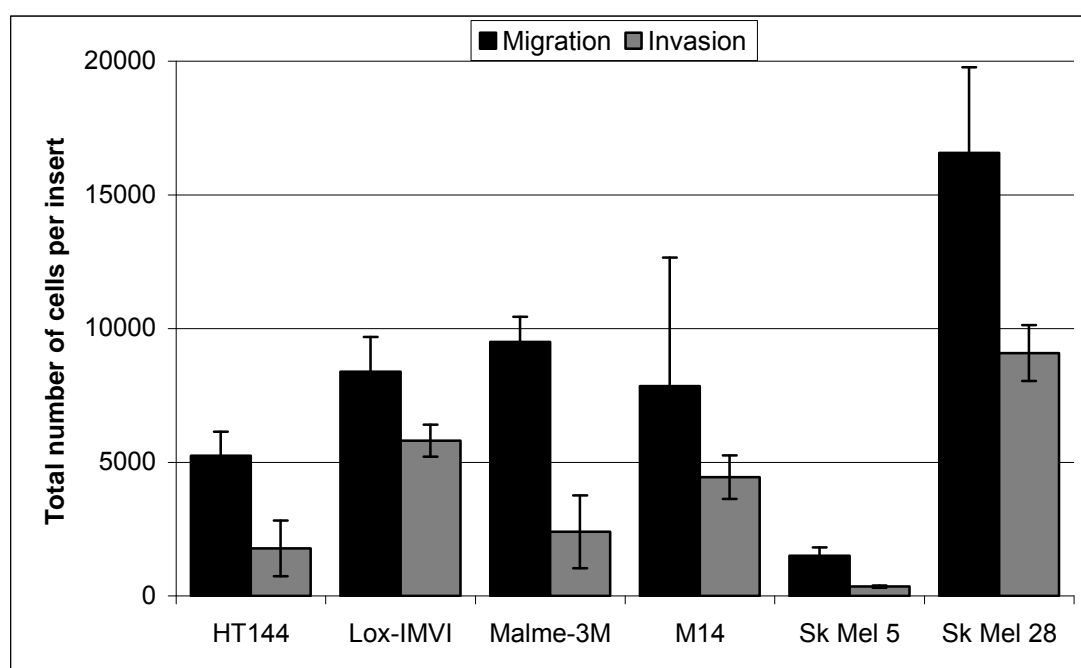


Figure 3.1: Analysis of the level of invasion and migration in the melanoma panel.

Error bars represent the standard deviation of triplicate assays.

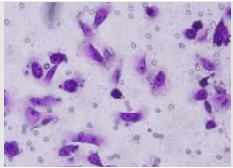
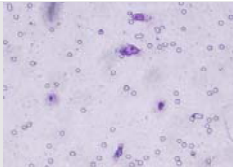
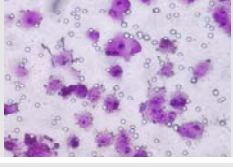
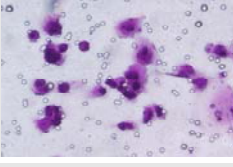
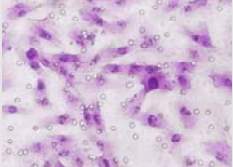
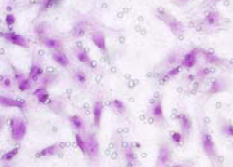
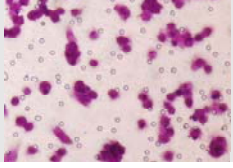
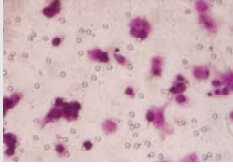
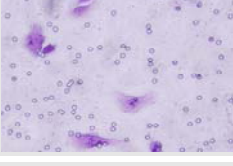
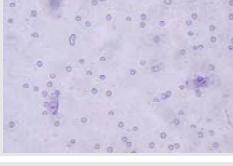
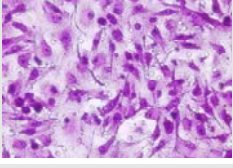
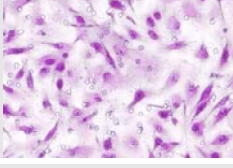
Cell Line	Migration	Invasion
<b>HT144</b>		
Total number of cells	<b>5241 ± 902</b>	<b>1778 ± 1036</b>
<b>Lox-IMVI</b>		
Total number of cells	<b>8381 ± 1310</b>	<b>5805 ± 597</b>
<b>Malme-3M</b>		
Total number of cells	<b>9497 ± 939</b>	<b>2403 ± 1364</b>
<b>M14</b>		
Total number of cells	<b>7849 ± 4802</b>	<b>4447 ± 809</b>
<b>Sk Mel 5</b>		
Total number of cells	<b>1503 ± 318</b>	<b>355 ± 45</b>
<b>Sk Mel 28</b>		
Total number of cells	<b>16576 ± 3198</b>	<b>9086 ± 1043</b>

Figure 3.2: Visual analysis of the level of invasion and migration in the melanoma panel. Numbers of cells ± the standard deviation are displayed.

### 3.3 Chemo-sensitivity

#### 3.3.1 Chemotherapy drug sensitivity in melanoma cell lines

IC<sub>50</sub> values for four chemotherapeutic drugs were determined in the melanoma cell line panel (Table 3.1). The melanoma cell lines tested are sensitive to epirubicin. Sk-Mel-5 was the most responsive cell line tested with an IC<sub>50</sub> of 8.1 nM ( $\pm$  0.9 nM) whilst Lox-IMVI was the most resistant, with an IC<sub>50</sub> of 48.3 nM ( $\pm$  7.0 nM). Sk-Mel-28 displayed the greatest resistance to temozolomide (TMZ) (IC<sub>50</sub> = 791  $\mu$ M ( $\pm$  153  $\mu$ M)). Most of the cell lines displayed similar responses to TMZ and 5-(3-methyltriazene-1-yl)imidazole-4-carboximide (MTIC), the active form of TMZ, except Sk-Mel-28 which was significantly more resistant to MTIC than TMZ, ( $p$  = 0.04). Sk-Mel-28 has an IC<sub>50</sub> of 1184  $\mu$ M ( $\pm$  168  $\mu$ M) for MTIC, whilst Malme-3M and Lox-IMVI had more sensitivity to MTIC with IC<sub>50</sub>s of 271  $\mu$ M ( $\pm$  40  $\mu$ M) and 313  $\mu$ M ( $\pm$  76  $\mu$ M) respectively. Taxotere was also tested in the melanoma cell panel and all cell lines displayed sensitivity to taxotere with IC<sub>50</sub>s of less than 5 nM.

Table 3.1: IC<sub>50</sub> values for epirubicin, temozolomide, MTIC and taxotere in the melanoma cell line panel. Standard deviations for triplicate assays are presented.

<b>Cell line</b>	<b>Epirubicin (nM)</b>	<b>Temozolomide (<math>\mu</math>M)</b>	<b>MTIC (<math>\mu</math>M)</b>	<b>Taxotere (nM)</b>
<b>HT144</b>	<b>13.1</b> $\pm 3.5$	<b>393</b> $\pm 2$	<b>427</b> $\pm 60$	<b>0.70</b> $\pm 0.02$
<b>Lox-IMVI</b>	<b>48.3</b> $\pm 7.0$	<b>223</b> $\pm 55$	<b>313</b> $\pm 76$	<b>0.70</b> $\pm 0.10$
<b>Malme-3M</b>	<b>33.8</b> $\pm 4.3$	<b>258</b> $\pm 46$	<b>271</b> $\pm 40$	<b>0.80</b> $\pm 0.06$
<b>M14</b>	<b>32.0</b> $\pm 22.0$	<b>455</b> $\pm 51$	<b>553</b> $\pm 50$	<b>2.00</b> $\pm 0.33$
<b>Sk-Mel-5</b>	<b>8.1</b> $\pm 0.9$	<b>263</b> $\pm 69$	<b>363</b> $\pm 90$	<b>0.70</b> $\pm 0.14$
<b>Sk-Mel-28</b>	<b>46.5</b> $\pm 4.8$	<b>791</b> $\pm 153$	<b>1184</b> $\pm 168$	<b>0.70</b> $\pm 0.06$

### 3.3.2 Comparison of chemo-sensitivity in cancer cell lines

A comparative review of *in vitro* sensitivity to chemotherapeutics was performed using data available in our laboratory for breast, glioma, lung and pancreatic cancer cell lines (Table 3.2).

Table 3.2: IC<sub>50</sub> results for epirubicin, taxotere and temozolomide in lung, breast and pancreatic cancer cell lines and in glioma primary cell lines. Standard deviations for triplicate assays are presented. ND = not determined.

Cancer type	Cell line	Epirubicin (nM)	Temozolomide (μM)	Taxotere (nM)
Lung	DLKP	170.0 ± 0.8	ND	0.38 ± 0.02
	A549	380.0 ± 4.5	ND	0.25 ± 0.02
Glioma	893	ND	1167.0 ± 17.7	9.30 ± 0.70
	978	ND	1167.0 ± 1.0	3.00 ± 0.20
	152	ND	494.5 ± 1.4	0.50 ± 0.01
	314	ND	575.6 ± 7.1	24.80 ± 0.01
Breast	MCF7	42.5 ± 6.5	ND	3.75 ± 1.41
	MDA-MB-231	16.0 ± 2.0	ND	ND
	MDA-MB-453	67.0 ± 4.4	ND	0.78 ± 0.03
Pancreatic	Mia-PaCa-2	25.8 ± 4.1	ND	0.50 ± 0.05
	BxPc-3	68.5 ± 12.3	ND	0.50 ± 0.06
	KCI-MOH1	10.3 ± 1.3	ND	0.53 ± 0.12

Melanoma cell lines display similar sensitivity to epirubicin as breast and pancreatic cancer cell lines, whilst the lung cancer cell lines display significant resistance to epirubicin. Lung cancer and pancreatic cancer cell lines display a similar sensitivity to taxotere as the melanoma cell lines. The glioma primary cell lines display less sensitivity to taxotere, although the IC<sub>50</sub>s are still in the nanomolar range. TMZ IC<sub>50</sub> values are higher for primary glioma cell lines than for melanoma cell lines.

### 3.4 Expression of ABC transporters in melanoma cell lines

Expression of MRP-2, ABCB5, MRP-1, P-gP, BCRP and GAPDH were analysed by conventional RT-PCR (section 2.6) (Figure 3.3) due to their involvement in drug resistance in cancer cells [91].

MRP-2 mRNA was not detected in normal melanocytes whereas the metastatic melanoma cell lines express low levels of MRP2. ABCB5 mRNA is expressed in normal melanocytes and in 5 of the 6 melanoma cell lines. Lox-IMVI is the only melanoma cell line that does not express ABCB5. MRP-1 mRNA is expressed in the normal melanocytes, Sk-Mel-5 and Sk-Mel-28 but was not detected in HT144 and M14. P-gP expression is low in the melanoma panel with only Sk-Mel-5 and M14 showing detectable levels of P-gP mRNA. BCRP mRNA was detected at very low levels in the normal melanocytes but BCRP mRNA was detected in all of the melanoma cell lines apart from Lox-IMVI.

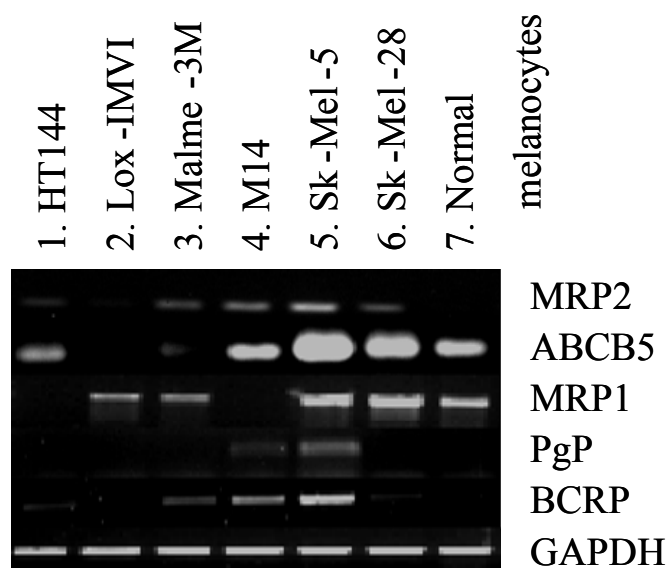


Figure 3.3: RT-PCR for the ABC transporters MRP-2, ABCB5, MRP-1, P-gP, BCRP and the endogenous control GAPDH in the melanoma cell lines and normal melanocytes.

### 3.5 Acquired temozolomide resistance in melanoma cell lines

#### 3.5.1 Induction of temozolomide resistance in pulse selected melanoma cells

Malme-3M was ‘pulse selected’ in duplicate (A and B) using 5-daily pulse treatments to create temozolomide resistant Malme-3M cell lines (section 2.8). The  $IC_{50}$  for temozolomide in Malme-3M is  $306 \mu\text{M}$  ( $\pm 29 \mu\text{M}$ ) (Figure 3.5). Malme-TMZ (A) and Malme-TMZ (B) display significantly increased  $IC_{50}$ s for temozolomide of  $440 \mu\text{M}$  ( $\pm 21 \mu\text{M}$ ) (1.44 fold increase ( $p = 0.004$ )) and  $515 \mu\text{M}$  ( $\pm 45 \mu\text{M}$ ) (1.68 fold increase ( $p = 0.04$ )).

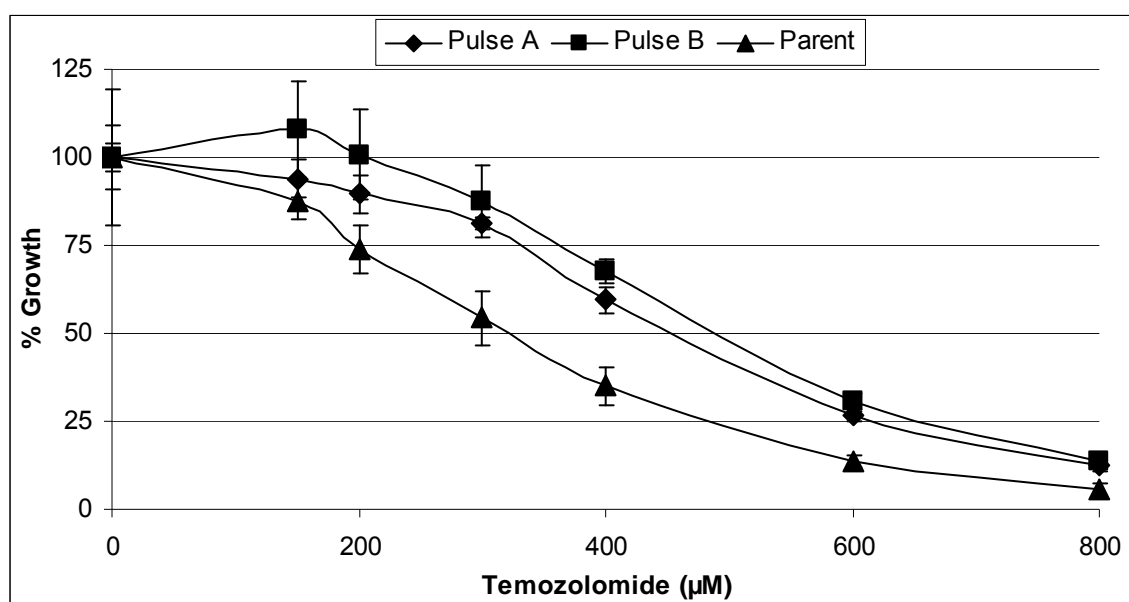


Figure 3.5: Effect of temozolomide in Malme-3M melanoma cell line and the temozolomide ‘pulse selected’ variants Malme-TMZ (A) and Malme-TMZ (B). Error bars represent the standard deviation of triplicate assays.

HT144 cells were ‘pulse selected’ with TMZ to establish a resistant cell line which could be used to investigate TMZ resistance in melanoma cell lines (section 2.8). The  $IC_{50}$  for TMZ in HT144 cells is  $338 \mu\text{M}$  ( $\pm 25 \mu\text{M}$ ) (Figure 3.4). In HT144-TMZ, the



pulse selected variant of HT144, the  $IC_{50}$  increased to  $490 \mu\text{M}$  ( $\pm 15 \mu\text{M}$ ) which represents a 1.45 fold increase in resistance to TMZ ( $p = 0.002$ ).

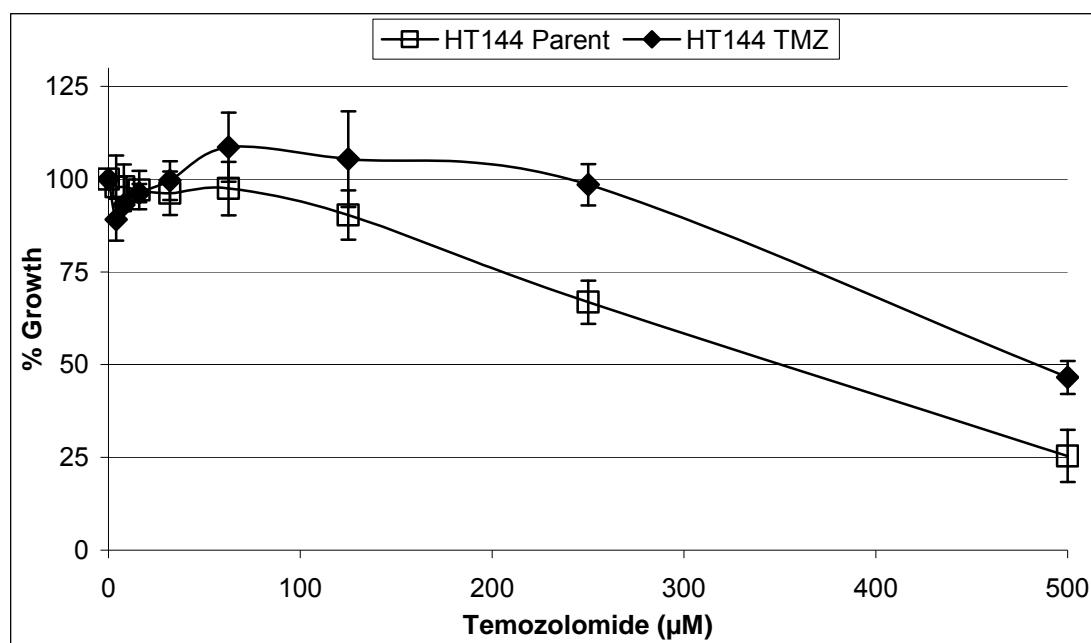


Figure 3.4: Effect of temozolomide on growth of HT144 melanoma cell line and the temozolomide pulse selected variant HT144-TMZ. Error bars represent the standard deviation of triplicate assays.

### 3.5.2 Expression of ABC transporters in temozolomide resistant cell lines

Levels of mRNA expression of ABC transporters were measured in the parent and resistant cell lines by conventional RT-PCR (section 2.6) (Figure 3.6). Malme-3M expresses ABCB5, MRP-2 and MRP-1 mRNA but not BCRP or P-gP. In Malme-TMZ expression of ABCB5, MRP-2 and MRP-1 mRNA is reduced compared to the parent cell line, whilst BCRP expression remains unchanged and P-gP is slightly increased.

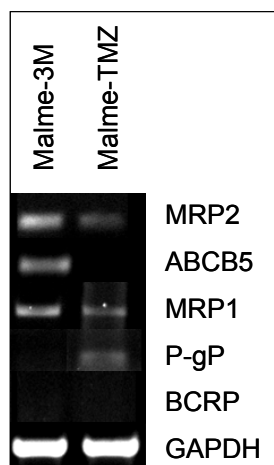


Figure 3.6: RT-PCR for the ABC transporters ABCB5, BCRP, MRP-2 P-gP and MRP-1 in Malme-3M and Malme-TMZ cell lines.

### 3.5.3 Cross resistance of temozolomide pulse selected variants

During drug selection of cell lines, cells can acquire altered sensitivity to other chemotherapeutic drugs. The two temozolomide selected cell lines were tested with 4 drugs to examine the chemo-sensitivity between the parent and the resistant cell lines.

The melanoma cell line HT144 and the temozolomide selected variant HT144-TMZ display similar sensitivity to cisplatin, epirubicin and taxotere whilst the resistant cell line is significantly more sensitive to mitoxantrone (Table 3.3) ( $p = 0.02$ ). Malme-3M and the pulse selected cell line Malme-TMZ have similar  $IC_{50}$ s for epirubicin and mitoxantrone. Malme-TMZ is significantly more resistant to cisplatin ( $p = 0.001$ ) and both HT144-TMZ and Malme-TMZ are significantly more resistant to taxotere than the parent cell lines Malme-3M and HT144 ( $p=0.02$ ;  $p = 0.02$ ), although the  $IC_{50}$  values are still in the very low nanomolar range.

Table 3.3: IC<sub>50</sub> values for cisplatin, epirubicin, mitoxantrone and taxotere in HT144 and Malme-3M and in the temozolomide resistant cell lines HT144-TMZ and Malme-TMZ. ‘\*’ indicates p < 0.05.

Cell name	Cisplatin (nM)	Epirubicin (nM)	Mitoxantrone (nM)	Taxotere (nM)
<b>HT144 Parent</b>	<b>724</b> ± 82	<b>8.2</b> ± 3.6	<b>39.7</b> ± 9.4	<b>0.94</b> ± 0.08
<b>HT144-TMZ</b>	<b>996</b> ± 197	<b>10.5</b> ± 3.6	<b>6.7 *</b> ± 0.9	<b>1.31 *</b> ± 0.08
<b>Malme-3M Parent</b>	<b>2843</b> ± 390	<b>33.8</b> ± 4.3	<b>27.6</b> ± 1.1	<b>0.74</b> ± 0.02
<b>Malme-TMZ</b>	<b>5678 *</b> ± 265	<b>26.6</b> ± 1.4	<b>36.3</b> ± 9.5	<b>0.90 *</b> ± 0.06

### 3.6 Acquired taxotere resistance in melanoma cell lines

#### 3.6.1 Induction of taxotere resistance in melanoma cell lines

HT144 cells were ‘pulse selected’ with taxotere to establish a resistant cell line which could be used to investigate taxotere resistance in melanoma cell lines (section 2.9).

The IC<sub>50</sub> for taxotere in HT144 is 1.27 nM (± 0.03 nM). HT144-Tax (A) and HT144-Tax (B), the duplicate taxotere pulse selected variants of HT144 have taxotere IC<sub>50</sub>s of 1.93 nM (± 0.28 nM) and 2.11 nM (± 0.32 nM) respectively (Figure 3.7). The IC<sub>50</sub>

for taxotere was not significantly increased in HT144-Tax A ( $p = 0.054$ ) but was significantly increased in HT144-Tax (B) ( $p = 0.043$ ) compared to the parent cell line.

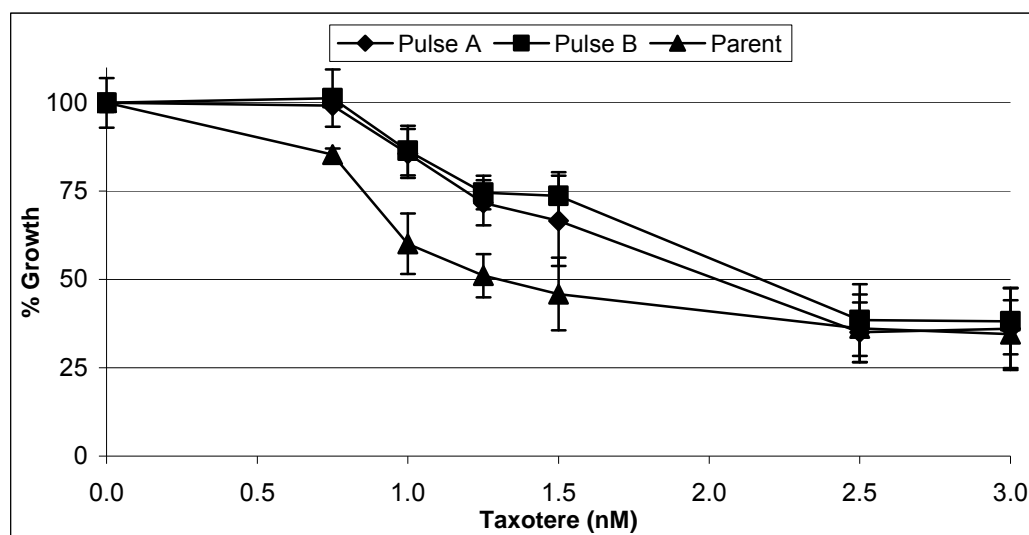


Figure 3.7: Effect of taxotere on the growth of HT144 melanoma cell line and the taxotere pulse selected variants HT144-Tax (A) and HT144-Tax (B). Error bars represent the standard deviation of triplicate assays.

### 3.6.2 Expression of ABC transporters in taxotere resistant cell lines

HT144 cells express low levels of ABCB5, BCRP, MRP-2, P-gP and MRP-1 mRNA (Figure 3.8). In the taxotere pulse selected cell line HT144-Tax (B) levels of BCRP, MRP-2 and MRP-1 are increased.

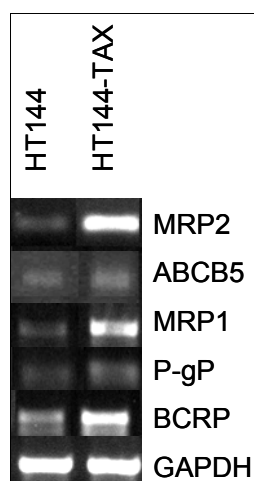


Figure 3.8: RT-PCR for the ABC transporters ABCB5, BCRP, MRP-2 P-gP and MRP-1 in HT144 and HT144-Tax cell lines.

### 3.7 BCRP inhibition in melanoma cell lines

BCRP mRNA was detected in 5 of the 6 melanoma cell lines and not in the normal melanocytes. We tested BCRP inhibition in combination with mitoxantrone to determine if BCRP inhibition would enhance the response to chemotherapy in melanoma cells. Two BCRP positive cells, Malme-3M and Sk-Mel-5 were selected for this analysis. In addition DLKP-Mitox has been previously shown by western blotting to be positive for BCRP expression (Aoife Devery, unpublished data) and as such was used as positive control for BCRP expression.

DLKP-Mitox is a lung cancer cell line that has been pulse selected with mitoxantrone a BCRP substrate. DLKP-Mitox has an  $IC_{50}$  for mitoxantrone of 70.3 nM ( $\pm$  11.4 nM). In combination with the BCRP inhibitor fumitremorgin C (FTC), DLKP-Mitox has an  $IC_{50}$  for mitoxantrone of 41.0 nM  $\pm$  (9.3 nM). Combination of a non-toxic combination of FTC and mitoxantrone in DLKP-Mitox reduced the  $IC_{50}$  of mitoxantrone, however the difference was not significant ( $p = 0.07$ ).

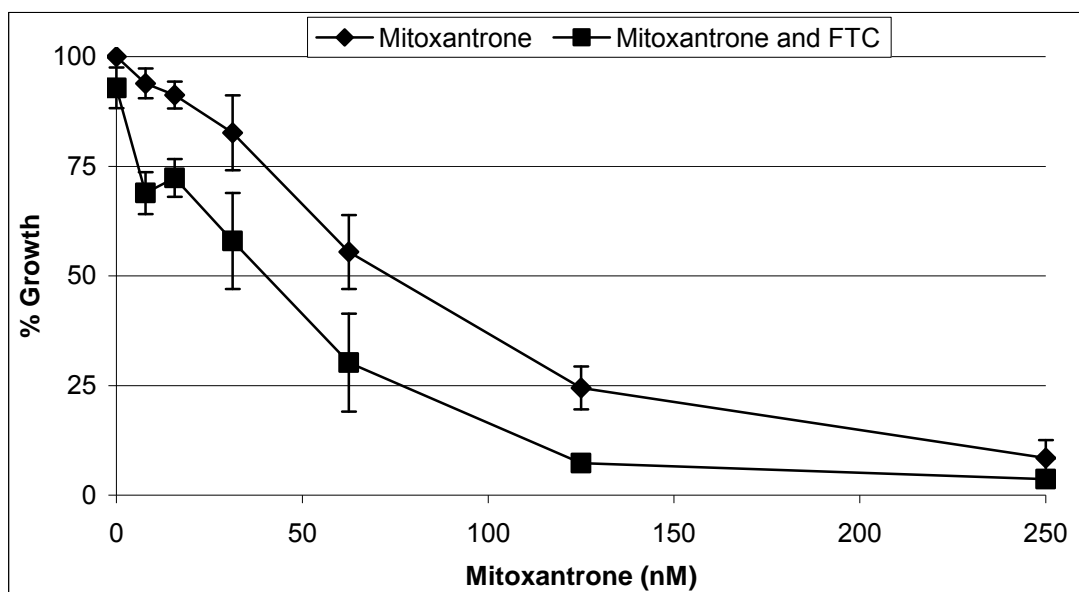


Figure 3.10: Analysis of DLKP-Mitox sensitivity to mitoxantrone and in combination with 20  $\mu\text{M}$  of fumitremorgin C. Error bars represent the standard deviation of triplicate assays.

Combination of FTC and mitoxantrone in Malme-3M did not increase the sensitivity of Malme-3M to mitoxantrone compared to cells tested with mitoxantrone alone (Figure 3.11). In fact combination of FTC and mitoxantrone in Malme-3M increased the  $\text{IC}_{50}$  value of mitoxantrone ( $\text{IC}_{50}$  of mitoxantrone alone = 63 nM ( $\pm 17$  nM);  $\text{IC}_{50}$  of mitoxantrone in combination with FTC 119 nM ( $\pm 29$  nM)).

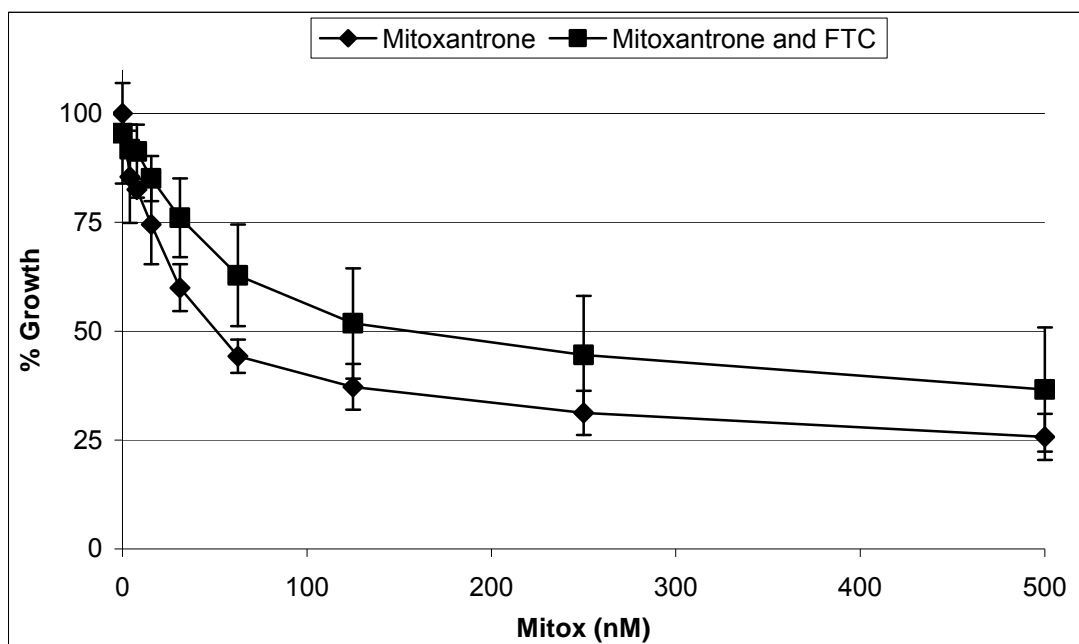


Figure 3.11: Analysis of Malme-3M sensitivity to mitoxantrone and the combination of 20  $\mu\text{M}$  of the specific BCRP inhibitor FTC and mitoxantrone. Error bars represent the standard deviation of triplicate assays.

The  $\text{IC}_{50}$  for mitoxantrone is 6.57 nM ( $\pm$  0.69 nM) in Sk-Mel-5. Mitoxantrone in combination with FTC yielded an  $\text{IC}_{50}$  value of 11.3 nM ( $\pm$  3.5 nM) ( $p = 0.3$ ) (Figure 3.12).

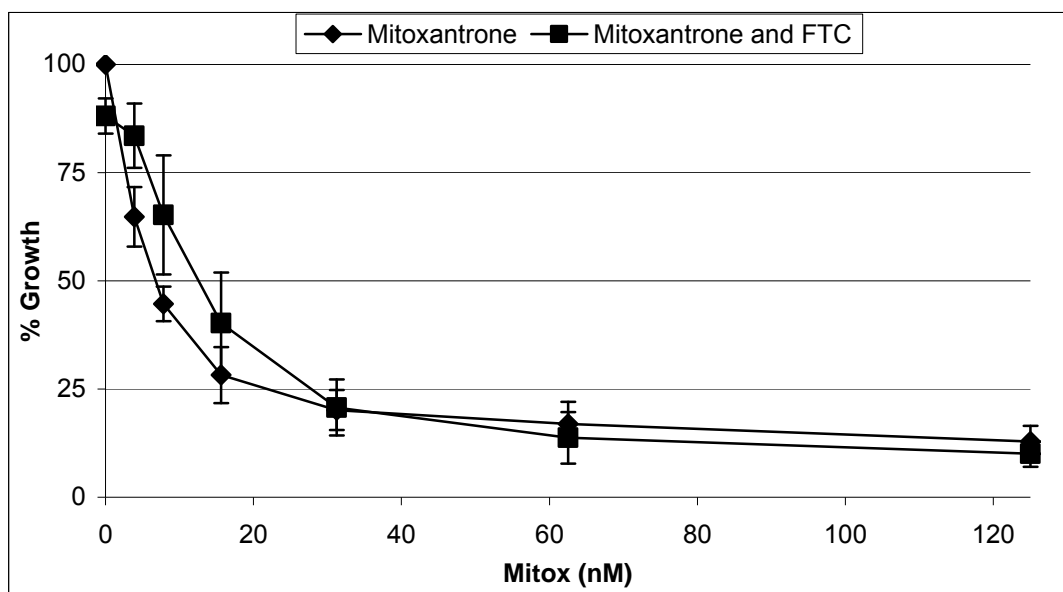


Figure 3.12: Sk-Mel-5 sensitivity to mitoxantrone alone and in combination with 20  $\mu$ M of FTC. Error bars represent the standard deviation of triplicate assays.

### 3.8 MRP-2 inhibition in melanoma cell lines

MRP-2 mRNA was detected in all 6 melanoma cell lines tested and not in normal melanocytes. We tested MRP-2 inhibition in combination with an MRP-2 substrate drug vincristine, to determine if MRP-2 inhibition could improve response to chemotherapy in melanoma cells. The combinations were also tested in Malme-3M. MRP-2 2008 an ovarian cancer cell line that over expresses MRP-2 was used as a positive control to study inhibition of MRP-2 [181] (Figure 3.13).

The  $IC_{50}$  for vincristine in MRP-2 2008 cells is 12.8 nM ( $\pm$  1.9 nM). However the addition of the specific MRP-1/MRP-2 inhibitor MK-571 to the cells did not significantly reduce the  $IC_{50}$  of vincristine when tested in the MRP-2 2008 cells (10.1 nM ( $\pm$  2.0 nM)) (Figure 3.13).



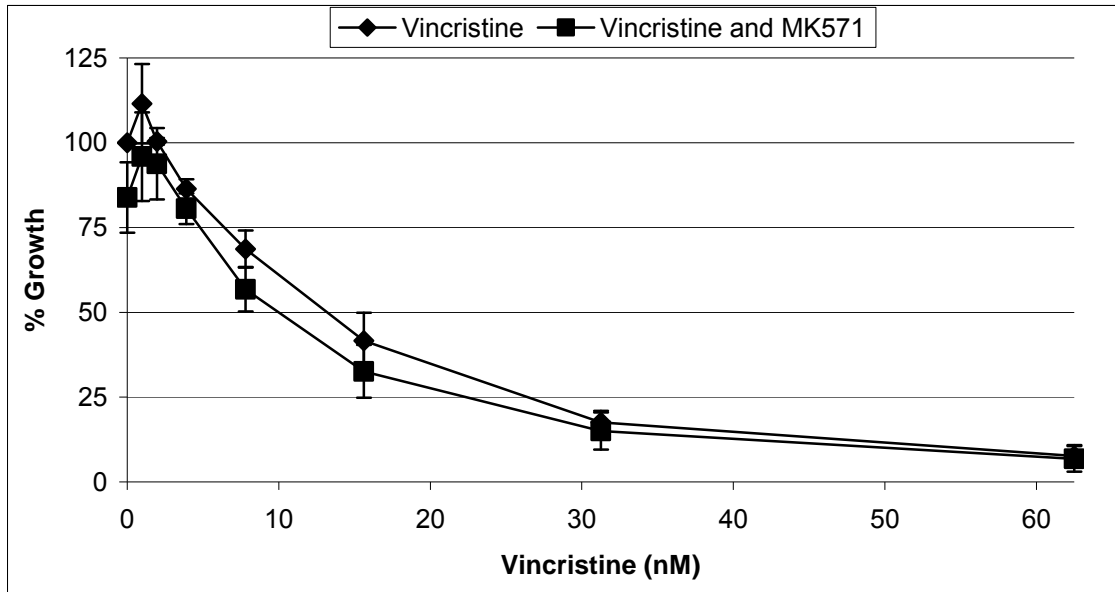


Figure 3.13: Analysis of MRP-2-2008 sensitivity to vincristine alone and in combination with 7.5  $\mu$ M of MK-571. Error bars represent the standard deviation of triplicate assays.

The  $IC_{50}$  for vincristine in Malme-3M cells is 0.53 nM ( $\pm$  0.03 nM). In combination with MK-571 vincristine had an  $IC_{50}$  of 0.46 nM ( $\pm$  0.9 nM) ( $p = 0.32$ ) (Figure 3.14).

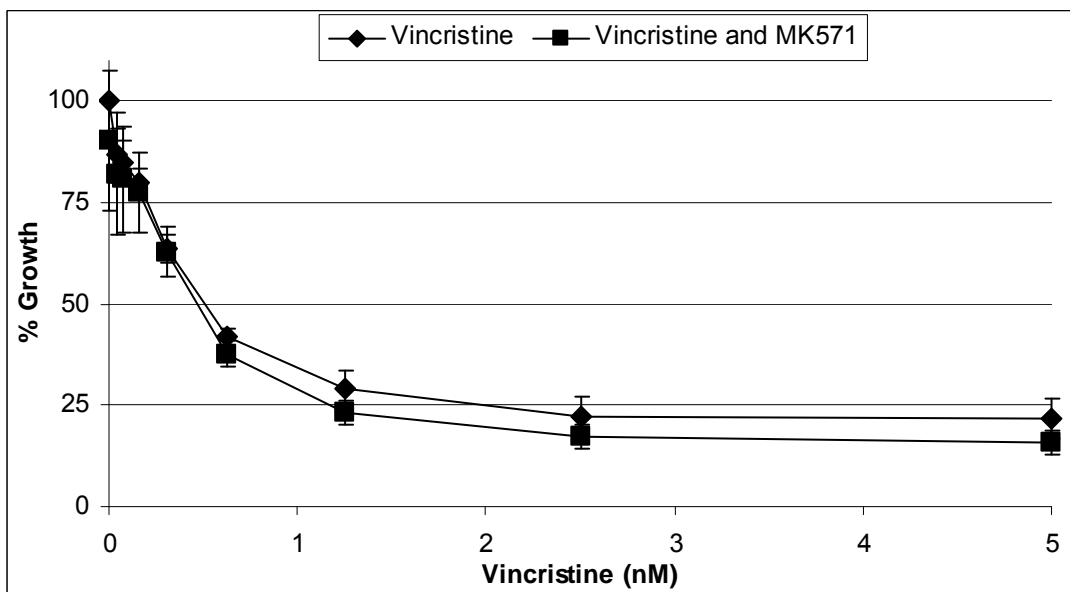


Figure 3.14: Analysis of Malme-3M sensitivity to vincristine alone and in combination with 7.5  $\mu$ M of MK-571. Error bars represent the standard deviation of triplicate assays.

### 3.9 Summary

Each member of the melanoma cell line panel displayed varying degrees of migration and invasion. Drug sensitivity testing showed that melanoma cells are relatively resistant to TMZ treatment *in vitro*. The melanoma cell lines displayed *in vitro* sensitivity to taxotere and epirubicin. This is also the case for the pancreatic and glioma cell lines which display sensitivity to the taxanes.

ABC transporters including BCRP and MRP-2 were found to be expressed in the melanoma cell line panel. Despite inhibiting BCRP we found no alteration in mitoxantrone sensitivity in the melanoma cell lines. Inhibition of MRP-2 with MK571 was ineffective even in the positive control cell line.

We successfully established two *in vitro* models of temozolomide resistance. Although the taxotere selected cell lines display some resistance, the IC<sub>50</sub>s for the pulse selected cell lines were still in the low nanomolar range.

TMZ is not known to be a substrate for any ABC transporter but the TMZ variant cell line Malme-TMZ did show alteration in the expression of some ABC transporters. P-gP expression is slightly increased which may account for the very small decrease in sensitivity to taxotere observed in this cell line. The increase in BCRP levels observed in HT144-Tax may contribute to the slight decrease in sensitivity to taxotere observed as taxotere is also a substrate for BCRP.

## **Chapter 4**

### **4. *In vitro* evaluation of the effects of dasatinib in melanoma cells**

## **4.1 Introduction**

Dasatinib, a multi-tyrosine kinase inhibitor which is currently licensed as a first line treatment for chronic myeloid leukaemia, was assessed for its efficacy as an anti-proliferative/ pro-apoptotic agent in the melanoma cell line panel.

We studied the effect of dasatinib on proliferation, cell cycle and apoptosis induction in a panel of melanoma cell lines (section 2.3, 2.10 and 2.11). Previous studies revealed that dasatinib inhibits migration and invasion of other cancer cells [182, 183], so using the Boyden chamber method we also determined the effect of dasatinib on motility and invasion in melanoma cell lines.

Imatinib and dasatinib target similar kinases including PDGF-R, c-Kit and BCR-Abl. However, dasatinib also targets other kinases including ephrin A receptors and SRC kinase (section 1.7.3.2). We studied the effect of dasatinib on the protein levels and phosphorylation status of the dasatinib targets SRC and EphA2, and on downstream signalling pathways including FAK, MAPK and Akt, by immunoblotting (section 2.12).

## **4.2 Sensitivity to dasatinib and imatinib**

The effect of dasatinib on proliferation was tested in a panel of ten melanoma cell lines (Figure 4.1 and Table 4.1) (section 2.3). The response to dasatinib varies significantly across the panel of cell lines. Lox-IMVI and WM-115 display the greatest sensitivity to dasatinib with  $IC_{50}$  values of 35.4 nM ( $\pm$  8.8 nM) and 79.3 nM ( $\pm$  11.7 nM), respectively. HT144 and Malme-3M also display some sensitivity to

dasatinib with maximum growth inhibition of 40 % and 25 %, respectively, achieved in these cell lines at 250 and 300 nM dasatinib respectively. Growth of WM266-4 and M14 appear to be unaffected by dasatinib, whilst growth of Sk-Mel-28 was substantially and Sk-Mel-5 slightly increased in response to dasatinib treatment.

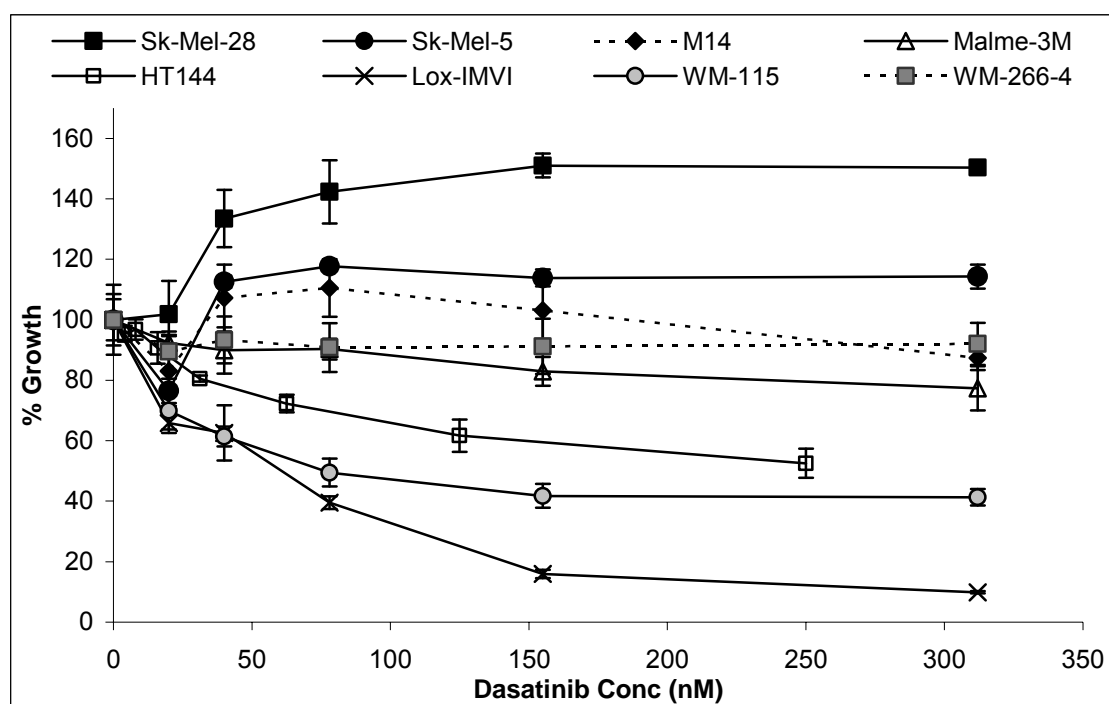


Figure 4.1: Percentage growth inhibition by dasatinib in a panel of melanoma cell lines. Error bars represent the standard deviation of triplicate experiments.

Table 4.1: Percentage growth inhibition achieved when the melanoma cell line panel was treated with 300 nM dasatinib. IC<sub>50</sub> values are included where they are achieved.

Cell line	% Growth @ 300 nM
HT144	50 %
Lox-IMVI	10 % IC <sub>50</sub> = 35.4 nM (± 8.8 nM)
Malme-3M	75 %
M14	87 %
Sk-Mel-5	115 %
Sk-Mel-28	150 %
WM-115	40 % IC <sub>50</sub> = 79.3 nM (± 11.7 nM)
WM-266-4	92 %

The effect of imatinib, which targets Bcr-Abl, C-Kit and PDGFR, on proliferation was also tested in HT144 and Lox-IMVI melanoma cell lines (Figure 4.2). At concentrations up to 5  $\mu$ M, imatinib did not inhibit proliferation in either cell line tested.

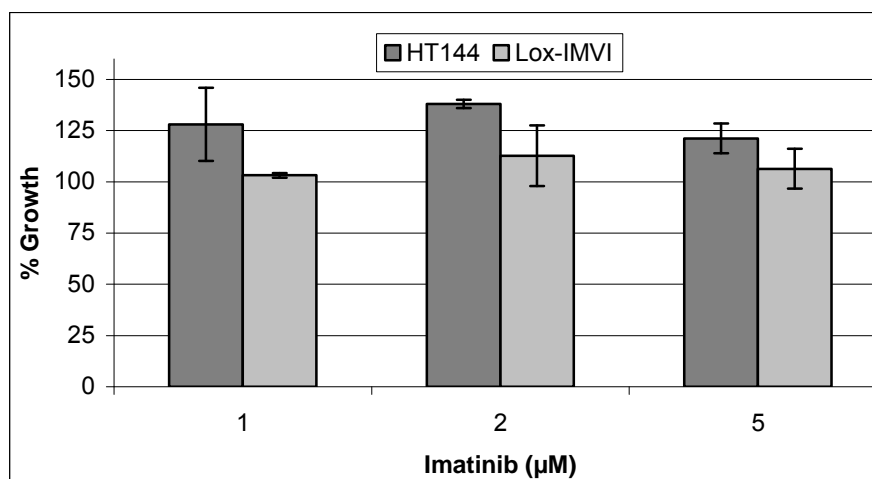


Figure 4.2: Proliferation assay showing percentage growth of HT144 and Lox-IMVI cells treated with 1, 2 and 5  $\mu$ M imatinib, relative to the control. Error bars represent the standard deviation of triplicate experiments.

### 4.3 Effect of dasatinib on invasion and migration

Three cell lines were selected to test the effects of dasatinib on migration and invasion in the melanoma panel. The cell lines were selected based on their invasive capacity; one which displayed a low level of invasion (HT144); one moderately invasive (M14); and one highly invasive (Sk-Mel-28) (section 3.2). The three cell lines also represent varying degrees of sensitivity to dasatinib (Table 4.1). The Boyden chamber assay was used to assess migration and invasion (section 2.2). Dasatinib significantly decreased invasion and migration of HT144, M14 and Sk-Mel-28 cells (invasion: 25 nM dasatinib: HT144  $p = 0.05$ ; M14  $p = 0.005$ ; Sk-Mel-28  $p = 0.016$ )

(Figure 4.3A), (migration: 25 nM dasatinib: HT144  $p = 0.001$ ; M14  $p = 0.004$ ; Sk-Mel-28  $p = 0.019$ ) (Figure 4.3B). The concentrations of dasatinib used in the invasion/migration assays were non-toxic to the cells.

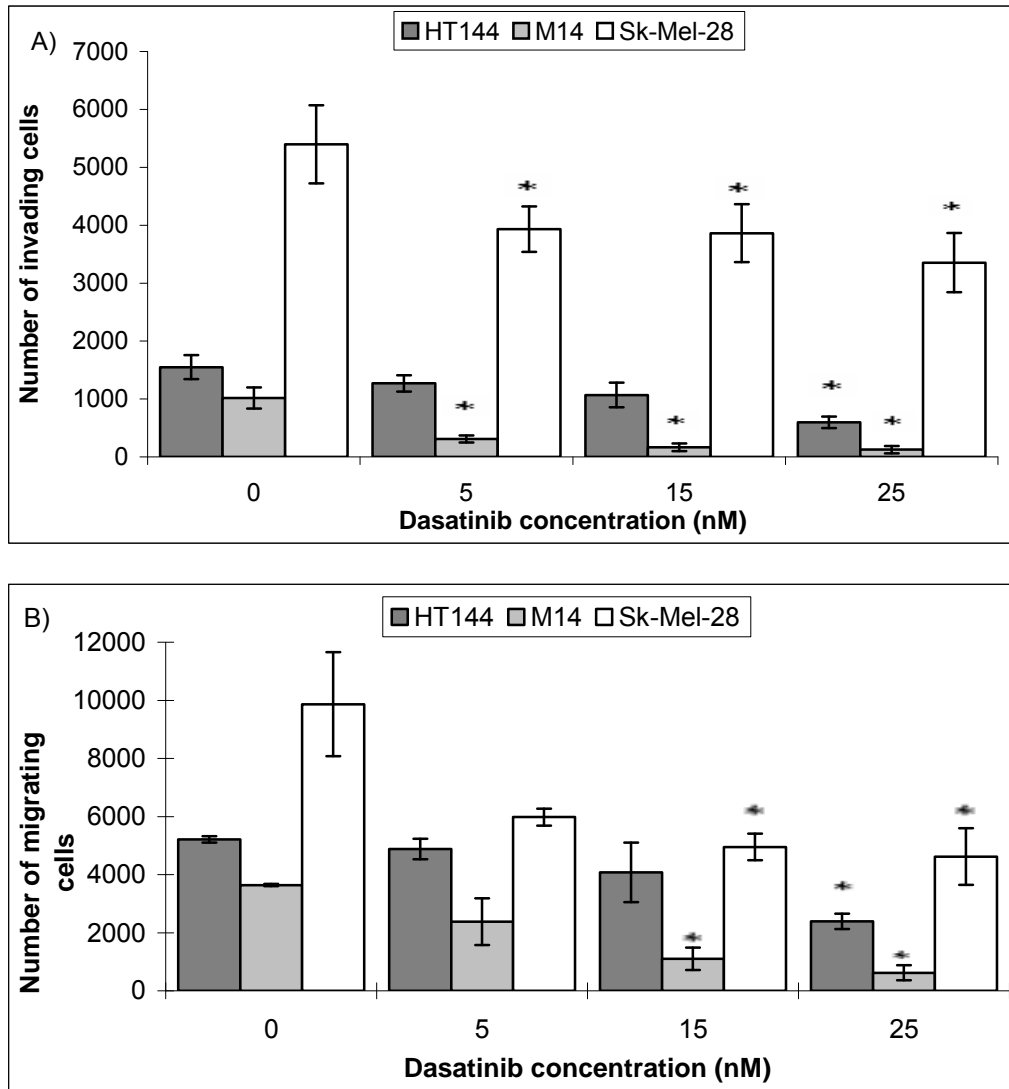


Figure 4.3: Effect of dasatinib on (A) invasion and (B) migration in HT144, M14 and Sk-Mel-28 melanoma cell lines. Error bars represent the standard deviation of triplicate assays. ‘\*’ indicates  $p < 0.05$  for treated cells compared to controls, using the Student’s T-test.

#### 4.4 Effect of dasatinib on apoptosis

Apoptosis induction was measured in three dasatinib sensitive cell lines using a TUNEL assay (section 2.10) (Figure 4.4). With increasing concentrations of dasatinib, Lox-IMVI and Malme-3M cell lines display increasing apoptosis. However, in HT144 cells dasatinib does not appear to induce apoptosis with concentrations up to 200 nM for 72 hours.

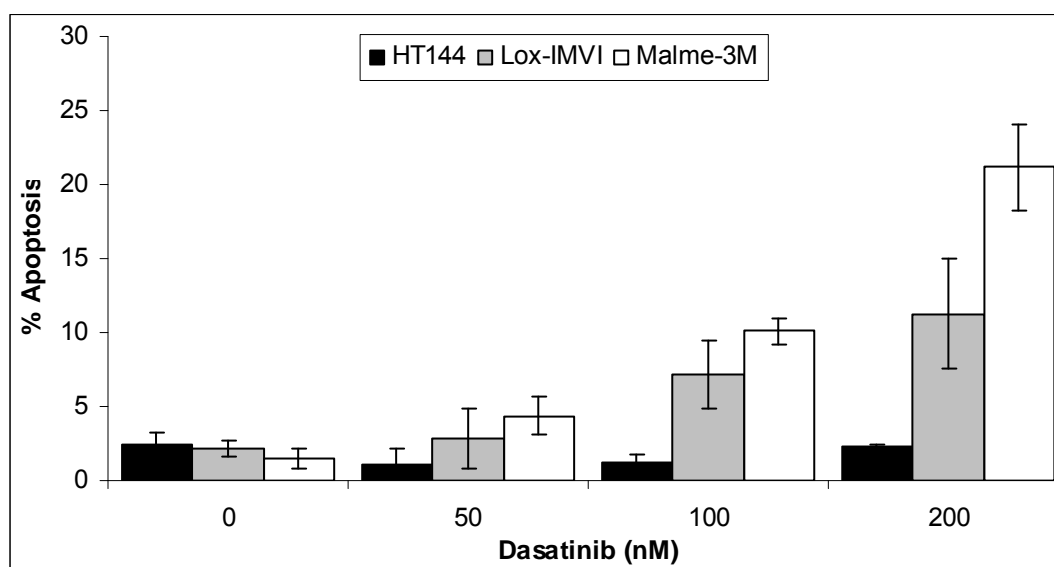


Figure 4.4: Measurement of dasatinib induced apoptosis in HT144, Lox-IMVI and Malme-3M after 72 hours of treatment using the TUNEL assay. Error bars represent the standard deviation of triplicate assays.

#### 4.5 Effect of dasatinib on cell cycle arrest

The effect of dasatinib treatment on cell cycle arrest was analysed in the melanoma cell lines HT144, Lox-IMVI, Malme-3M and Sk-Mel-5. After 24 hours treatment with dasatinib, the cells were analysed for G1 cell cycle arrest. Images of cellular morphology were also acquired at 24 hours to assess if dasatinib, imatinib mesylate or PP2 (a SRC kinase inhibitor) altered cell appearance.



Treatment with 100 nM dasatinib for 24 hours altered cellular morphology of HT144, Lox-IMVI and Sk-Mel-28 cells resulting in a more ‘rounded’ morphology (Figure 4.5). This effect was not observed for Malme-3M cells. Treatment with either imatinib mesylate or PP2 inhibitor did not affect the cellular morphology after 24 hours treatment.

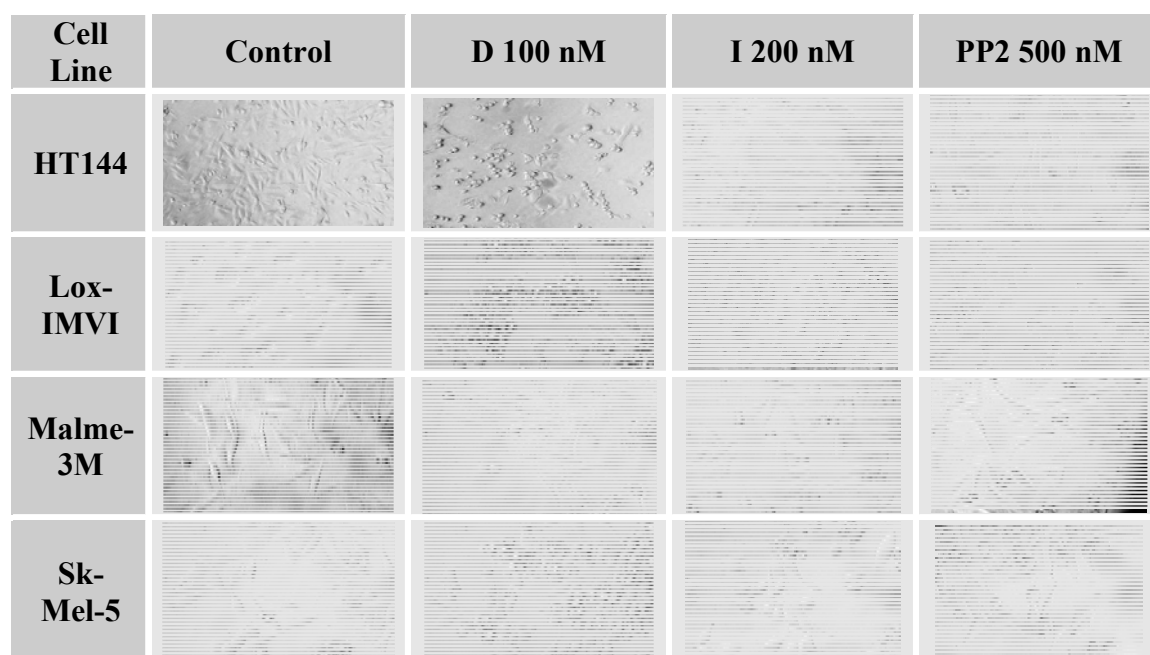


Figure 4.5: Analysis of the change in cellular morphology of melanoma cell lines HT144, Lox-IMVI, Malme-3M and Sk-Mel-5 when treated with 100 nM dasatinib (D), 200 nM imatinib (I) or 500 nM PP2 inhibitor, compared to control untreated samples.

Dasatinib treatment resulted in a slight increase in the percentage of cells in G1 in HT144 ( $p = 0.07$ ) (Figure 4.6) and significantly increased G1 in Lox-IMVI ( $p = 0.0045$ ). Dasatinib did not alter the percentage of cells in G1 phase in Malme-3M ( $p = 0.59$ ) or Sk-Mel-5 ( $p = 0.97$ ). In HT144 treatment with dasatinib resulted in a slight decrease in G2/M (D100: G2/M phase  $p = 0.08$ ). In Lox-IMVI, dasatinib at both the

50 nM (D50) and 100 nM (D100) caused a significant decrease in both G2/M and S-phase (G2/M phase: D50:  $p = 0.01$ , D100:  $p = 0.02$ ; S phase: D50:  $p = 0.01$ , D100:  $p = 0.01$ ). Treatment with imatinib and PP2 inhibitor did not affect the percentage of cells in G1, G2/M or S phase in any of the cells lines tested.

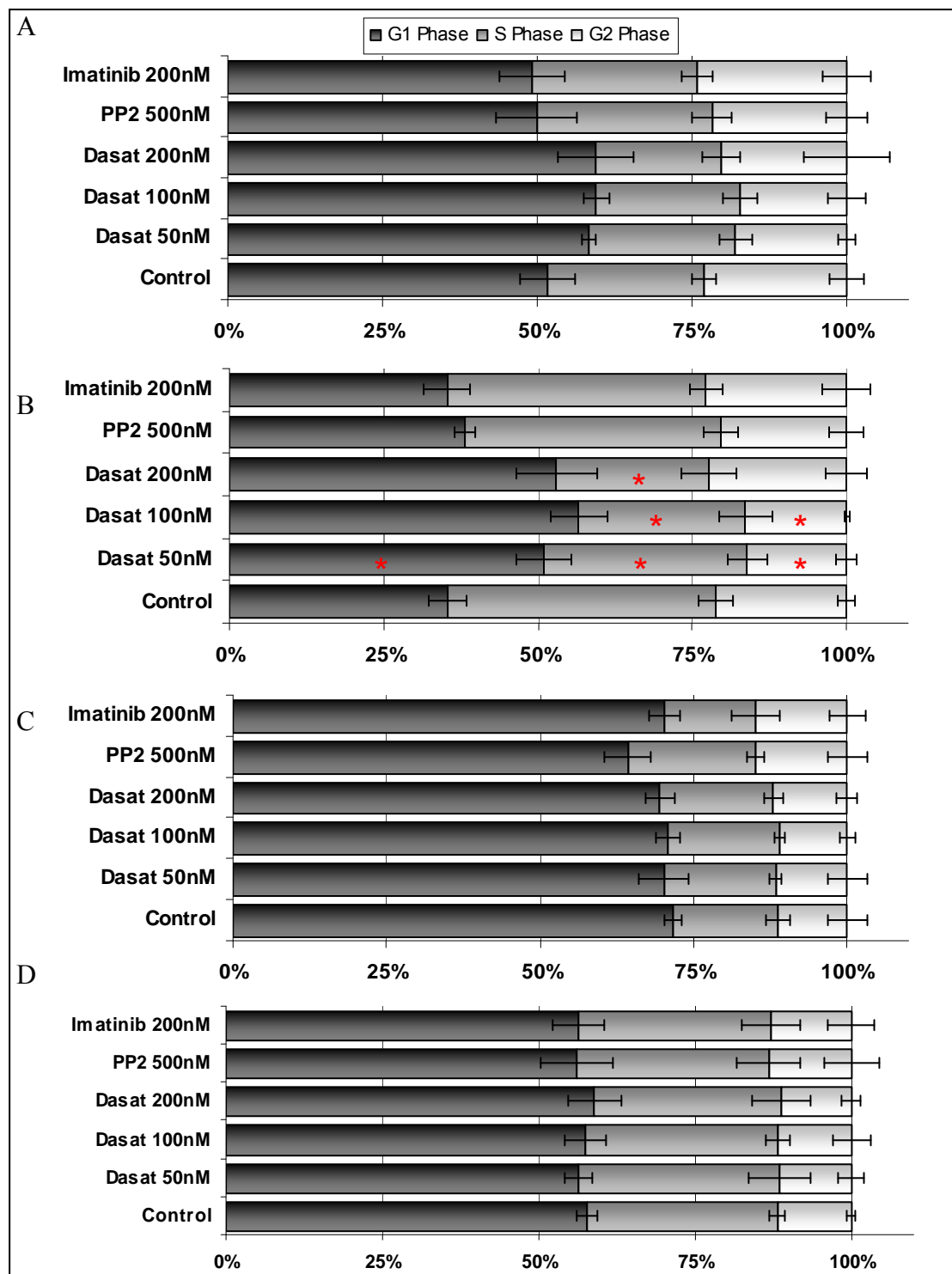


Figure 4.6: Percentage of A) HT144, B) LoX-IMVI, C) Malme-3M and D) Sk-Mel-5 cells in the G1, S and G2/M phases of cell cycle. Cells were untreated or treated with dasatinib (50, 100, 200 nM), imatinib (200 nM) or PP2 (500 nM). Error bars represent the standard deviation of triplicate assays and ‘\*’ indicates  $p < 0.05$  for treated cells compared to controls, using the Student’s T-test.

## 4.6 Dasatinib effects on cell signalling

The effects of dasatinib on cell signalling were assessed by immunoblotting with antibodies for both total proteins and phospho-proteins, for the dasatinib targets SRC and EphA2, and the downstream signalling pathways FAK, MAPK and Akt.

### 4.6.1 SRC kinase

Total SRC kinase protein levels were unaffected by treatment with dasatinib, imatinib or PP2 (a specific SRC kinase inhibitor) (Figure 4.7). Phosphorylated-SRC kinase (p-SRC) was detected at low levels in all melanoma cell lines. Treatment with increasing doses of dasatinib decreased the phosphorylation of SRC kinase in HT144, Lox-IMVI, Malme-3M and Sk-Mel-5 cell lines. However, increasing doses of dasatinib up to 200 nM dasatinib only slightly reduced SRC kinase phosphorylation in Sk-Mel-28. Both imatinib and PP2 reduced p-SRC in Lox-IMVI and Malme-3M but did not affect p-SRC in the remaining cell lines. P-SRC was reduced in all cell lines after 30 minutes treatment with 100 nM dasatinib; in Sk-Mel-28 there was a slight reduction in p-SRC. Results for western blotting of  $\alpha$ -tubulin are displayed in figure 4.7. However, the  $\alpha$ -tubulin blots represented are also relevant to the results obtained for EphA2, FAK, MAPK and AKT. In all cases  $\alpha$ -tubulin was unaffected by dasatinib treatment.

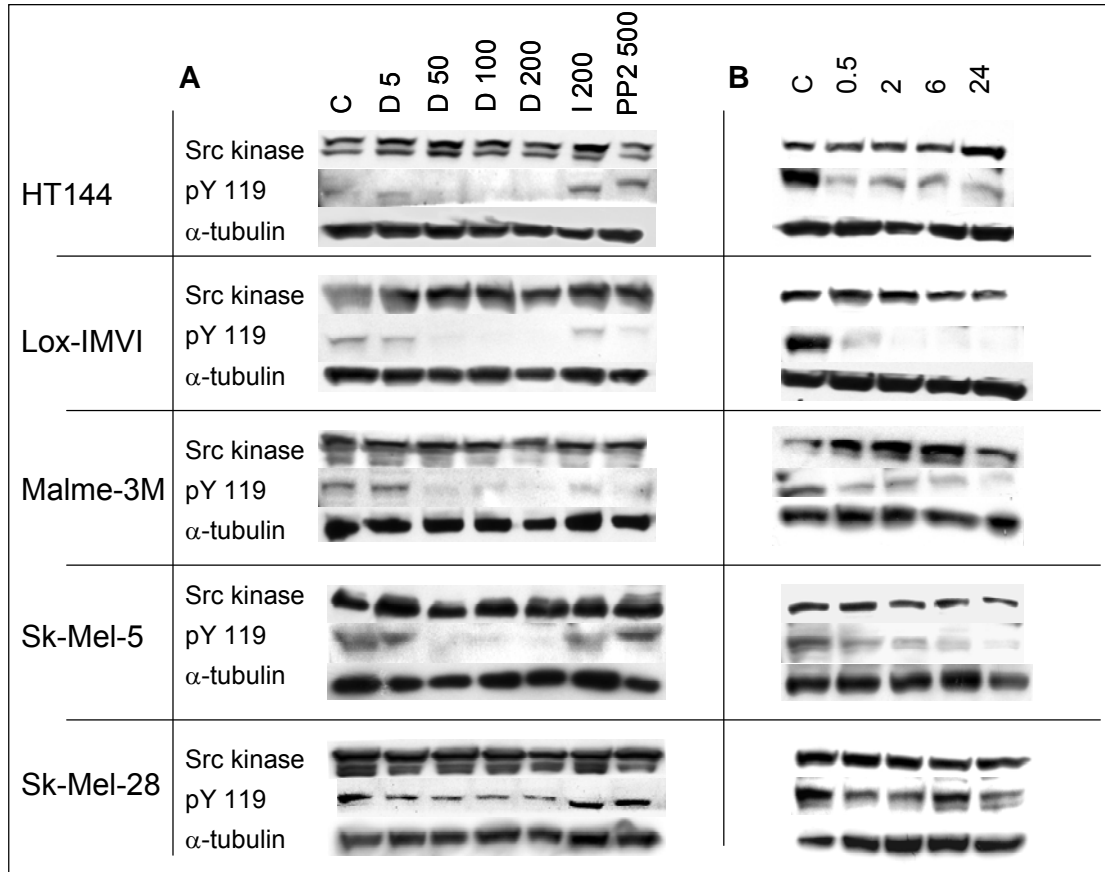


Figure 4.7: Western blotting for total SRC kinase, p-SRC kinase pY119 and  $\alpha$ -tubulin in (A) HT144, Lox-IMVI, Malme-3M, Sk-Mel-5 and Sk-Mel-28 untreated (control) or treated with increasing doses of dasatinib, imatinib (200 nM) or PP2 inhibitor (500 nM) for 6 hours; and in (B) HT144, Lox-IMVI, Malme-3M Sk-Mel-5 and Sk-Mel-28 untreated (control) or treated with 100 nM dasatinib for increasing duration (hours).

#### 4.6.2 EphA2

Treatment with dasatinib reduced the level of EphA2 protein in Malme-3M, however, basal levels appear to be restored after 48 hours of treatment with 100 nM dasatinib. Treatment with either imatinib or PP2 did not affect the level of EphA2 protein. EphA2 levels were also reduced in Sk-Mel-28 when treated with 100 nM dasatinib for 24 or 48 hours.

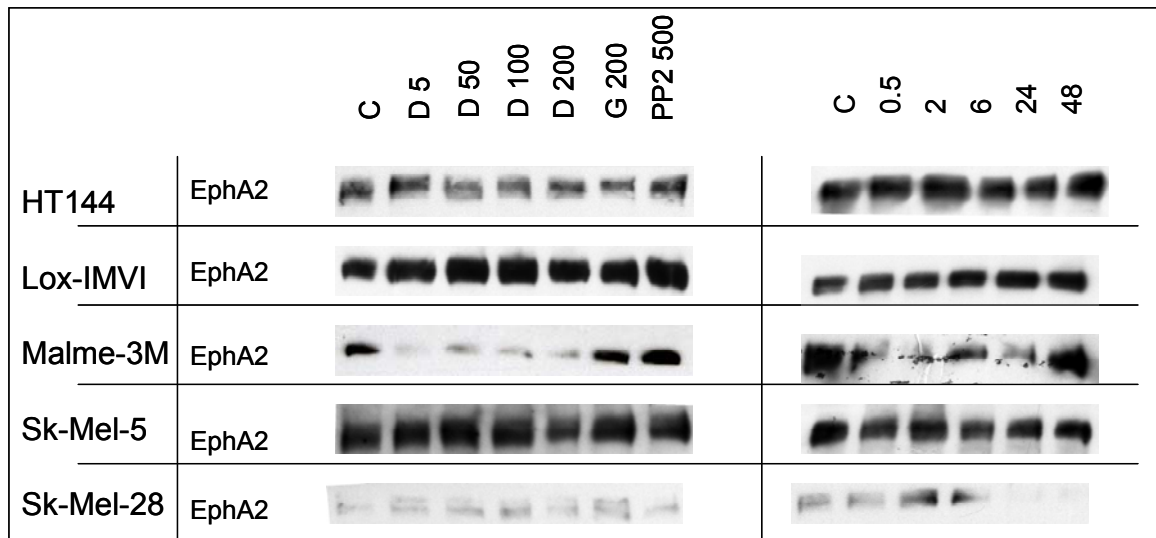


Figure 4.8: Western blotting for total EphA2 in the panel of melanoma cell lines; and in (A) HT144, Lox-IMVI, Malme-3M, Sk-Mel-5 and Sk-Mel-28 untreated (control) or treated with increasing doses of dasatinib for 6 hours or imatinib (200 nM) or PP2 inhibitor (500 nM) ; and in (B) HT144, Lox-IMVI, Malme-3M Sk-Mel-5 and Sk-Mel-28 untreated (control) or treated with 100 nM dasatinib for increasing duration (hours).

The effect of dasatinib on EphA2 phosphorylation was also analysed in Lox-IMVI by immunoprecipitation followed by blotting with a phosphotyrosine antibody (section 2.13). Treating cells with 100 nM dasatinib for up to 48 hours resulted in a slight increase in EphA2 phosphorylation compared to time zero controls (Figure 4.9).

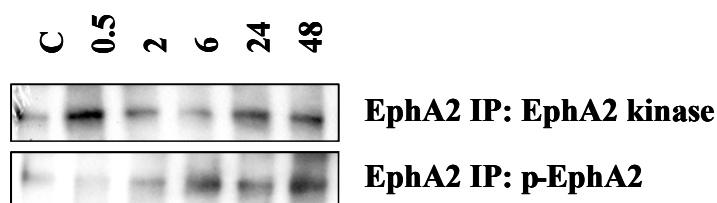


Figure 4.9: Western blotting for total EphA2 and phosphorylated EphA2 in Lox-IMVI melanoma cell line untreated or treated with dasatinib for increasing duration (hours).

### **4.6.3 Focal adhesion kinase**

Treatment with 200 nM dasatinib for 6 hours reduced FAK levels in HT144 and Malme-3M; however, FAK levels remain unchanged in all other cell lines tested both in the dose response and time course assays (Figure 4.10). Both imatinib and PP2 reduced FAK levels in HT144 and Malme-3M, but did not affect FAK levels in other cell lines tested.

FAK has multiple phosphorylation sites of which FAK Y397 and Y861 are associated with proliferation and motility. They have also both been identified as being important in SRC kinase signalling. FAK Y397 is an auto-phosphorylation site and its activity is required for FAK to function, whilst FAK Y861 is directly phosphorylated by SRC kinase. We therefore studied the effect of dasatinib treatment on both phosphorylation sites, to determine the effect on FAK activity.

Dasatinib reduced phosphorylation of FAK Y861 in all cell lines tested and at concentrations as low as 5 nM in HT144 and Sk-Mel-28. Treatment with imatinib reduced phosphorylation of FAK Y861 in HT144 and Sk-Mel-28, whilst PP2 reduced phosphorylation of FAK Y861 in HT144 and Lox-IMVI.

Treatment with imatinib reduced phosphorylation of FAK Y397 in Malme-3M but increased phosphorylation in Sk-Mel-5. PP2 reduced phosphorylation of FAK Y397 in HT144 and Lox-IMVI but did not alter phosphorylation in the remaining cell lines. In HT144, treatment with up to dasatinib did not reduce phosphorylation of FAK

Y397. In Sk-Mel-5 treatment with 100 nM dasatinib for greater than 30 minutes appears to increase FAK Y397 phosphorylation.

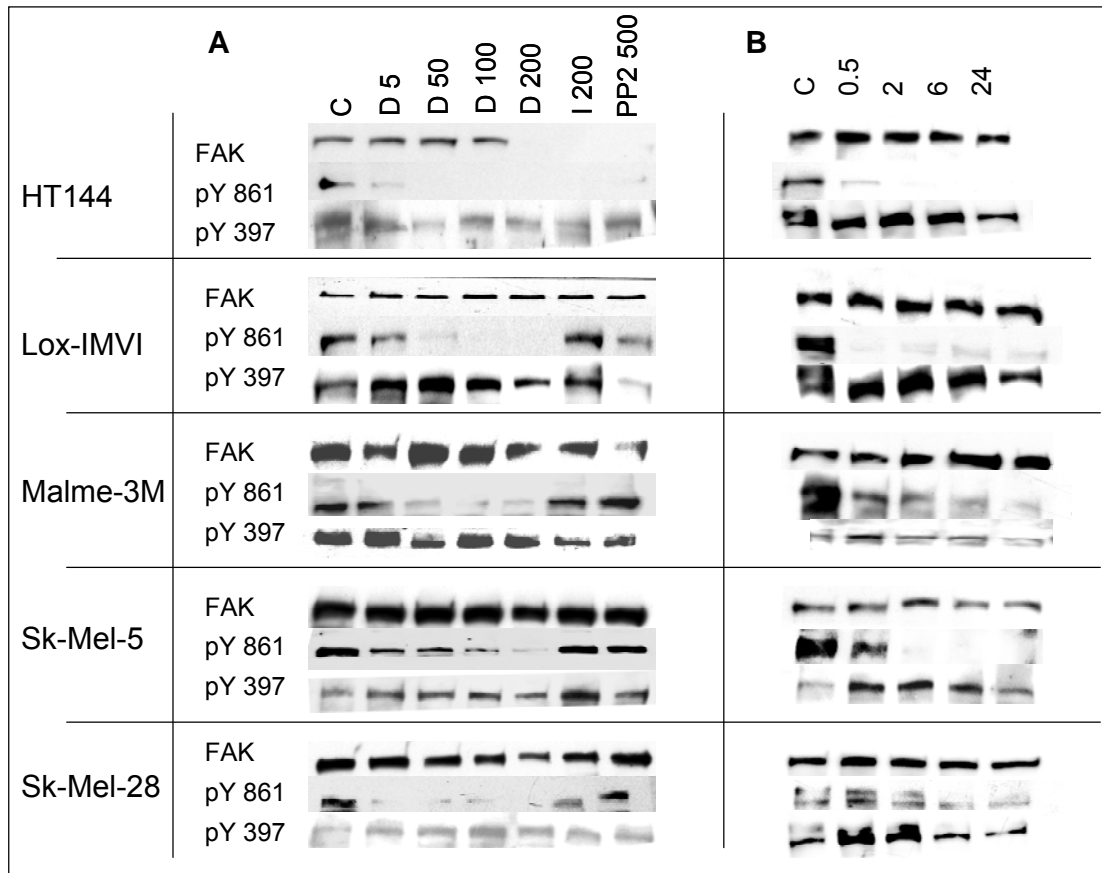


Figure 4.10: Western blotting for total FAK, FAK pY 861 and FAK pY 397 in (A) HT144, Lox-IMVI, Malme-3M, Sk-Mel-5 and Sk-Mel-28 untreated (control) or treated with increasing doses of dasatinib for 6 hours or imatinib (200 nM) or PP2 inhibitor (500 nM); and in (B) HT144, Lox-IMVI, Malme-3M, Sk-Mel-5 and Sk-Mel-28 untreated (control) or treated with 100 nM dasatinib for increasing duration (hours).



#### **4.6.4 MAPK and AKT**

Dasatinib, imatinib and PP2 did not alter the level of MAPK in the melanoma cell lines (Figure 4.11). Treatment with concentrations over 100 nM dasatinib resulted in a reduction in p-MAPK in HT144 and Lox-IMVI cell lines. Treatment with imatinib or PP2 also reduced p-MAPK in Lox-IMVI.

Treatment with 200 nM dasatinib slightly decreased levels of AKT in Malme-3M cells; however dasatinib treatment up to 200 nM did not significantly affect the levels of AKT in the other cell lines (Figure 4.11). Phosphorylated-AKT (p-AKT) levels were low in HT144, Lox-IMVI and Sk-Mel-5. There was a reduction in the levels of p-AKT in response to dasatinib in Malme-3M and Sk-Mel-28. Imatinib decreased p-AKT in HT144, Lox-IMVI and Malme-3M cell lines whilst PP2 decreased p-AKT in Lox-IMVI, Sk-Mel-5 and Sk-Mel-28.

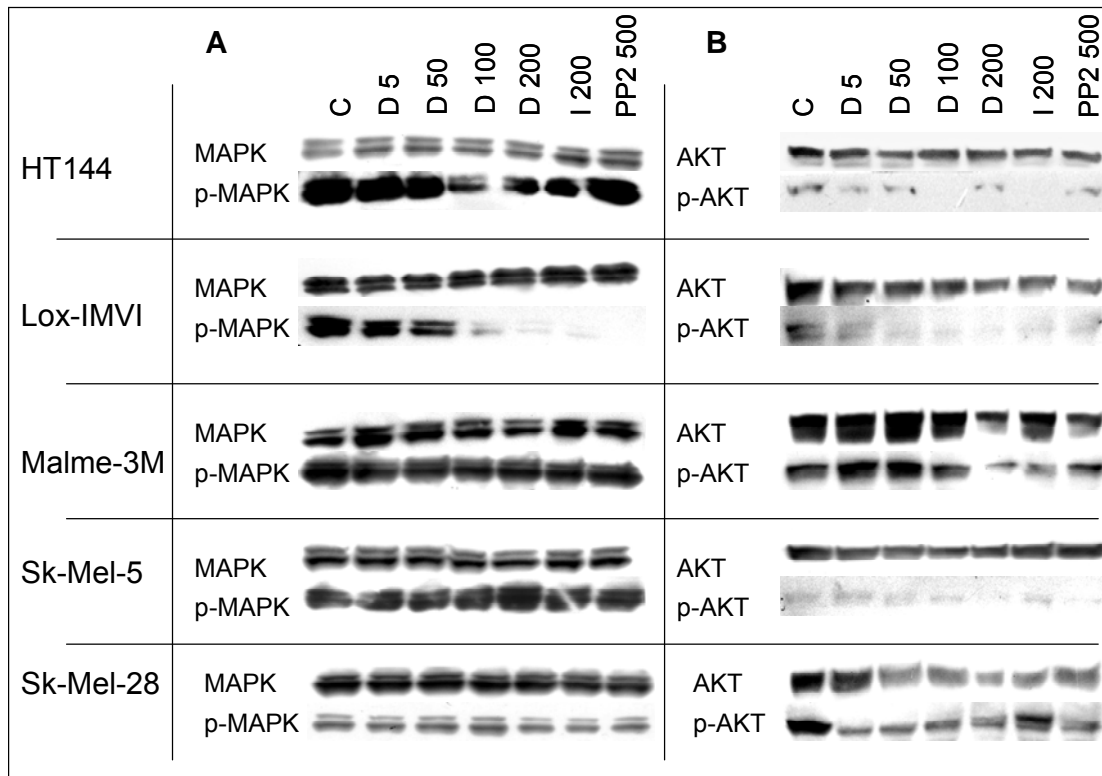


Figure 4.11: Western blotting for (A) total MAPK and p-MAPK and (B) total AKT and p-AKT in HT144, Lox-IMVI, Malme-3M, Sk-Mel-5 and Sk-Mel-28 untreated (control) or treated with increasing doses of dasatinib for 6 hours or imatinib (200 nM) or PP2 (500 nM).

#### 4.7 Summary

Dasatinib inhibited growth of five of the 10 melanoma cell lines tested. In the dasatinib sensitive cell line, Lox-IMVI dasatinib treatment induced cell cycle arrest, whilst in HT144 dasatinib induced apoptosis. Dasatinib also significantly inhibited cell migration and invasion in the three melanoma cell lines tested.

Dasatinib testing reduced p-SRC in all cell lines tested apart from Sk-Mel-28 where p-SRC was unaffected by dasatinib. Treatment with imatinib or PP2 only appeared to reduce p-SRC in dasatinib sensitive cell lines.

Dasatinib treatment resulted in the increase in phosphorylation of EphA2 in Lox-IMVI, however this was in contrast with results seen in Malme-3M and Sk-Mel-28 where dasatinib treatment reduced the total protein levels of EphA2.

Dasatinib reduced phosphorylation of FAK Y861 in all cell lines regardless of their sensitivity to the drug. In contrast, PP2 only reduced phosphorylation of FAK Y861 in dasatinib sensitive cell lines, whilst imatinib only reduced phosphorylation of FAK Y861 in HT144.

Increasing doses of dasatinib reduced p-MAPK in HT144 and Lox-IMVI only. Imatinib and PP2 also reduced p-MAPK in Lox-IMVI but had no effect on MAPK levels or phosphorylation in the remaining cell lines. Imatinib treatment reduced the phosphorylation of AKT in the dasatinib sensitive cell lines, whilst PP2 reduced phosphorylation in Lox-IMVI and the dasatinib resistance cell lines.

## **Chapter 5**

### **5. Evaluation of dasatinib in combination with current therapies in melanoma**

## **5.1 Introduction**

In general, greater clinical benefit is observed with tyrosine kinase inhibitors when they are combined with other therapies, such as chemotherapy, radiotherapy or other targeted therapies. Therefore, we tested dasatinib in combination with chemotherapy drugs and in combination with sorafenib, a B-Raf targeted therapy which is currently in clinical trials for melanoma.

We tested dasatinib in combination with temozolomide (TMZ), taxotere and epirubicin in an attempt to identify synergistic combinations for melanoma treatment. We also tested dasatinib in combination with sorafenib in dasatinib sensitive cell lines, and the triple combination of dasatinib with TMZ and sorafenib.

We have previously shown that our TMZ resistant cell lines have altered sensitivity to certain chemotherapy drugs compared to the parent cell lines (section 3.5.3). We also tested these TMZ resistant cell lines to determine if sensitivity to dasatinib was altered.

## **5.2 Dasatinib in combination with chemotherapy**

The effect of dasatinib in combination with chemotherapy was examined in three dasatinib responsive cell lines, Lox-IMVI, HT144, Malme-3M, and in two dasatinib-resistant cell lines, M14 and Sk-Mel-28. In Lox-IMVI, combination index (CI) values (section 2.25) revealed the combination of dasatinib and TMZ was nearly additive (CI value at Effective Dose 50 ( $ED_{50}$ ) =  $0.88 \pm 0.03$ ) (Table 5.1, Figure 5.1). CI values could not be calculated for the remaining cell lines as dasatinib alone did not achieve

an IC<sub>50</sub> at the concentrations tested. However, in both HT144 and Malme-3M, dasatinib enhanced response to TMZ (Table 5.1 and Figure 5.1). The IC<sub>50</sub> for TMZ was significantly reduced when TMZ was tested in combination with dasatinib (HT144 p = 0.038; Malme-3M p = 0.024). In M14, which shows the weakest response to dasatinib, there appears to be a significant enhancement of the effect of TMZ when combined with dasatinib (p = 0.001).

Table 5.1: Comparison of the IC<sub>50</sub> value of TMZ tested alone and in combination with dasatinib in the melanoma panel. p-values were determined using the Student's t-test. Combination index (CI) values were determined in Lox-IMVI as IC<sub>50</sub> values were achieved for both dasatinib and temozolomide

<b>Cell Line</b>	<b>TMZ IC<sub>50</sub></b>	<b>TMZ IC<sub>50</sub> when tested in combination with dasatinib</b>	<b>p value</b>
<b>HT144</b>	<b>359 ± 53 μM</b>	<b>227 ± 53 μM</b>	<b>0.038</b>
<b>Lox-IMVI</b>	<b>204 ± 30 μM</b>	<b>CI @ ED<sub>50</sub> = 0.88 ± 0.03</b>	<b>n/a</b>
<b>Malme-3M</b>	<b>274 ± 35 μM</b>	<b>170 ± 13 μM</b>	<b>0.024</b>
<b>M14</b>	<b>519 ± 17 μM</b>	<b>351 ± 25 μM</b>	<b>0.001</b>
<b>Sk-Mel-28</b>	<b>465 ± 19 μM</b>	<b>412 ± 45 μM</b>	<b>0.170</b>

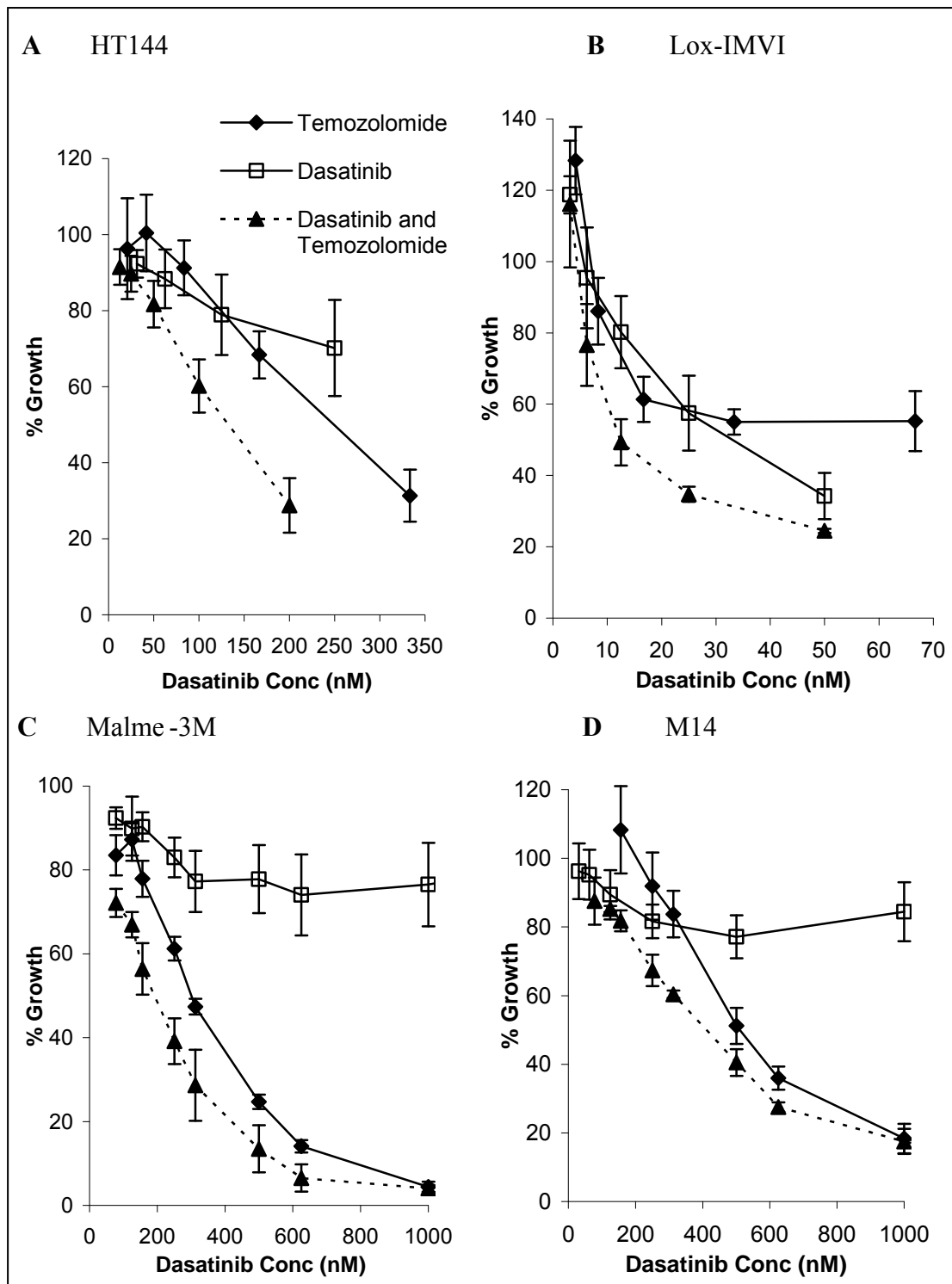


Figure 5.1: Combination assays testing dasatinib with TMZ at the specified ratios in (A) HT144 (ratio 1:1500), (B) Lox-IMVI (ratio 1:3000), (C) Malme-3M (ratio 1:800) and (D) M14 (ratio 1:800) cells. Concentrations of TMZ are represented as a ratio of the dasatinib concentration. Error bars represent the standard deviation of triplicate experiments.

In Sk-Mel-28, which is resistant to dasatinib, TMZ combined with dasatinib produces a similar response to TMZ alone (Figure 5.2).

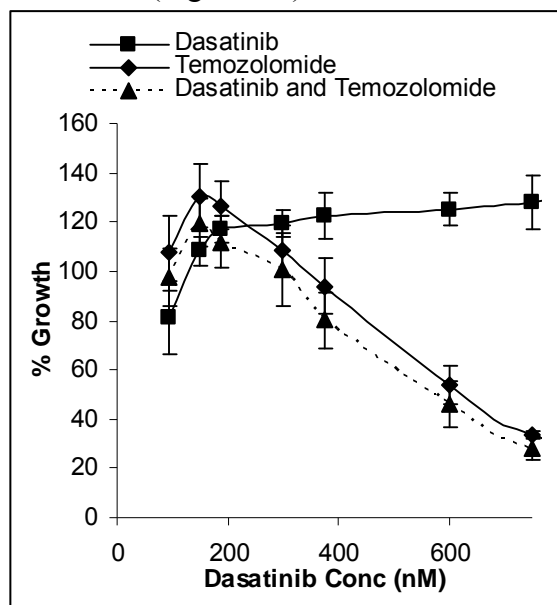


Figure 5.2: Combination assay testing dasatinib with TMZ at the specified ratio in Sk-Mel-28 (ratio 1:800) cells. Concentrations of TMZ are represented as a ratio of the dasatinib concentration. Error bars represent the standard deviation of triplicate experiments.

The effects of dasatinib in combination with epirubicin and taxotere were also examined in HT144, Lox-IMVI and M14 (Figure 5.3). In HT144 dasatinib combined with epirubicin had a significantly greater inhibitory effect than either drug tested alone (Table 5.2). However, the combination of taxotere and dasatinib did not significantly enhance inhibition compared to taxotere alone in HT144. In Lox-IMVI, the combination of 25 nM dasatinib and 25 nM epirubicin significantly reduced growth compared to either drug alone; however at higher concentrations the combination was ineffective. Finally, combining taxotere and dasatinib in Lox-IMVI did not significantly increase inhibition compared to testing either drug alone. Dasatinib had no effect on response to epirubicin or taxotere in M14 cells.



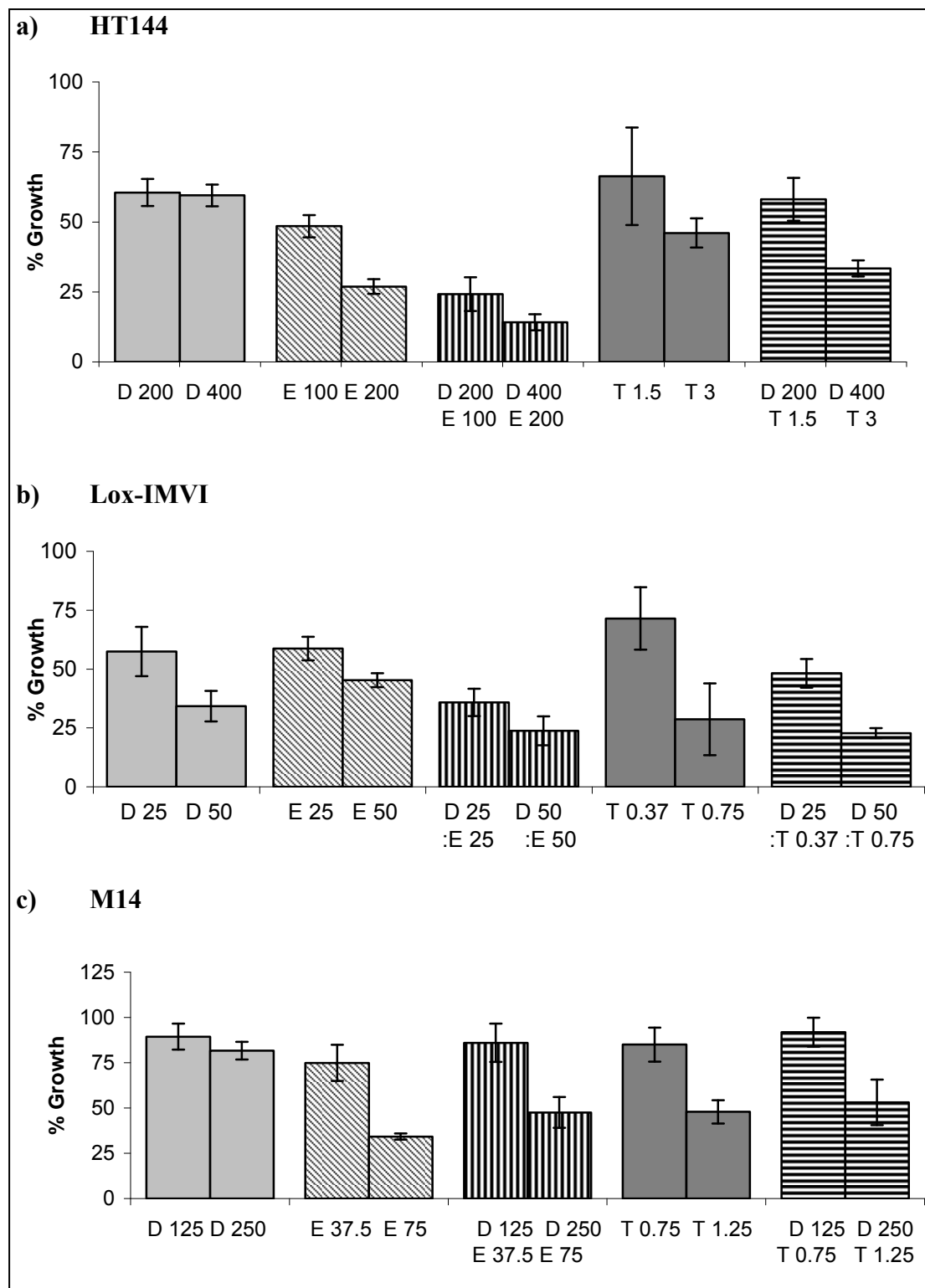


Figure 5.3: Combination assays of dasatinib (D) with epirubicin (E) or taxotere (T) in a) HT144, b) Lox-IMVI and c) M14. Drug concentrations are in nM. Error bars represent standard deviations of triplicate experiments.

Table 5.2: Comparison of percentage growth inhibition caused by testing either epirubicin or taxotere alone and in combination with dasatinib in HT144 melanoma cell line. p-values were determined using the Student's T-test.

HT144	Chemo only	200 nM dasatinib	400 nM dasatinib	dasatinib + chemo	p values
<b>Epirubicin 100 nM</b>	55.6 ± 4.0	58.5 ± 4.8	-	24.2 ± 6.0	<b>E vs DE</b> p < 0.01 <b>D vs DE</b> p < 0.01
<b>Epirubicin 200 nM</b>	48.5 ± 2.7	-	58.2 ± 3.9	14.2 ± 2.9	<b>E vs DE</b> p < 0.01 <b>D vs DE</b> p < 0.01
<b>Taxotere 1.5 nM</b>	63.9 ± 17.4	58.5 ± 4.8	-	58.1 ± 7.6	<b>T vs DT</b> p = 0.63 <b>D vs DT</b> p = 0.93
<b>Taxotere 3 nM</b>	46.0 ± 7.9	-	58.2 ± 3.9	33.4 ± 2.8	<b>T vs DT</b> p = 0.15 <b>D vs DT</b> p < 0.01

Table 5.3: Comparison of the percentage growth inhibition caused by testing either epirubicin or taxotere alone and in combination with dasatinib in LoX-IMVI melanoma cell line. p-values were determined using the Student's T-test.

Lox-IMVI	Chemo alone	25 nM dasatinib	50 nM dasatinib	dasatinib + chemo	p values
<b>Epirubicin 25 nM</b>	58.8 ± 5.0	57.5 ± 10.5	-	35.8 ± 5.8	<b>E vs DE</b> p = 0.01 <b>D vs DE</b> p = 0.05
<b>Epirubicin 50 nM</b>	45.3 ± 2.9	-	34.2 ± 6.5	23.8 ± 6.1	<b>E vs DE</b> p = 0.01 <b>D vs DE</b> p = 0.11
<b>Taxotere 1.5 nM</b>	84.0 ± 24.2	57.5 ± 10.5	-	48.1 ± 6.1	<b>T vs DT</b> p = 0.12 <b>D vs DT</b> p = 0.27
<b>Taxotere 3 nM</b>	78.8 ± 22.3	-	34.2 ± 6.5	17.0 ± 3.8	<b>T vs DT</b> p = 0.19 <b>D vs DT</b> p = 0.02

### 5.3 Sensitivity to sorafenib in melanoma cells

Sorafenib, a multi-target tyrosine kinase inhibitor, is currently in clinical trials in combination with TMZ for the treatment of melanoma. We tested sorafenib as a single agent, combinations of sorafenib with dasatinib and finally the triple combination of sorafenib, dasatinib and TMZ in melanoma cell lines.

The response to sorafenib was similar across the panel of six melanoma cell lines tested. Sk-Mel-5 displays the greatest sensitivity to sorafenib with an  $IC_{50}$  of  $1.8 \mu M$  ( $\pm 0.3 \mu M$ ). HT144 and Sk-Mel-28 are the most resistant cell lines to sorafenib with  $IC_{50}$  values of  $3.9 \mu M$  ( $\pm 0.6 \mu M$ ) and  $4.1 \mu M$  ( $\pm 0.4 \mu M$ ), respectively.

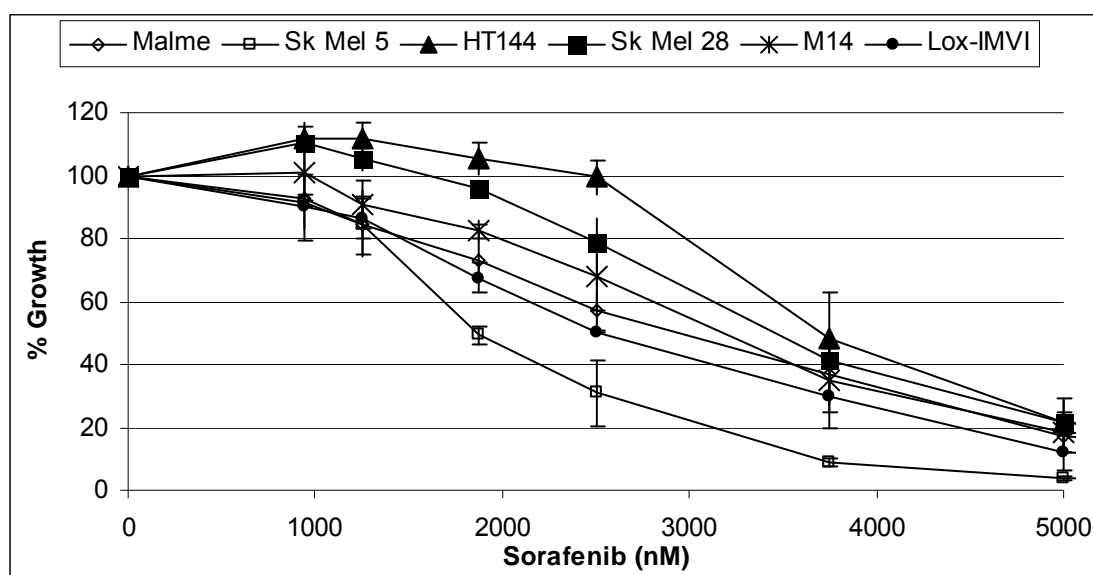


Figure 5.4: Percentage growth inhibition by sorafenib in the melanoma cell lines, HT144, Lox-IMVI, Malme-3M, M14, Sk-Mel-5 and Sk-Mel-28. Error bars represent the standard deviation of triplicate experiments.

In Lox-IMVI, the combination of dasatinib and sorafenib enhanced growth inhibition compared to either inhibitor tested alone (Figure 5.5). CI values ( $CI @ ED_{25} = 1.21$

$\pm 0.08$ ; CI @ ED<sub>50</sub> = 1.11  $\pm$  0.04; CI @ ED<sub>75</sub> = 1.05  $\pm$  0.10) revealed the combination of dasatinib and sorafenib was nearly additive at ED<sub>50</sub> and ED<sub>75</sub>. The combination of dasatinib and sorafenib was also tested in a single experiment in HT144 and M14; however the combination did not improve response compared to sorafenib or dasatinib alone.

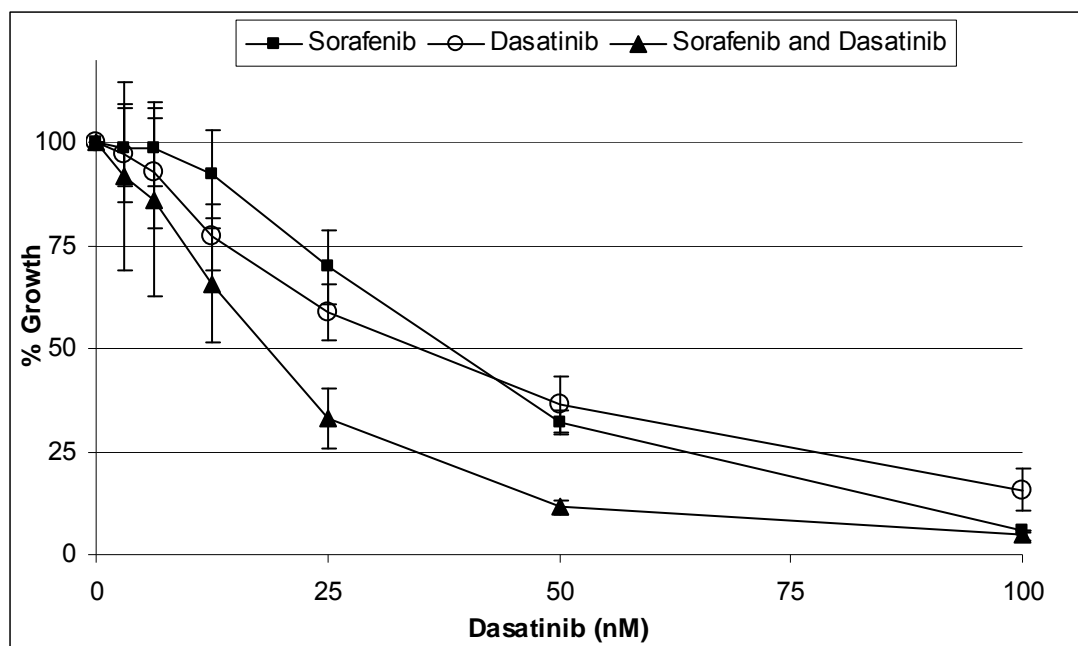


Figure 5.5: Combination assays of dasatinib with sorafenib at the specified ratio in Lox-IMVI (dasatinib: sorafenib 1:60) cells. Concentrations of sorafenib are represented as a ratio of the dasatinib concentration. Error bars represent the standard deviation of triplicate experiments.

The triple combination of dasatinib and sorafenib enhanced growth inhibition in Lox-IMVI compared to either inhibitor or TMZ alone (Figure 5.6). CI values revealed that at ED<sub>50</sub> the combination of dasatinib, sorafenib and TMZ produced a nearly additive response (CI @ ED<sub>25</sub> = 1.25  $\pm$  0.17; CI @ ED<sub>50</sub> = 0.97  $\pm$  0.16; CI @ ED<sub>75</sub> 0.79  $\pm$  0.15) and at ED<sub>75</sub> the combination produced a slightly synergistic affect.

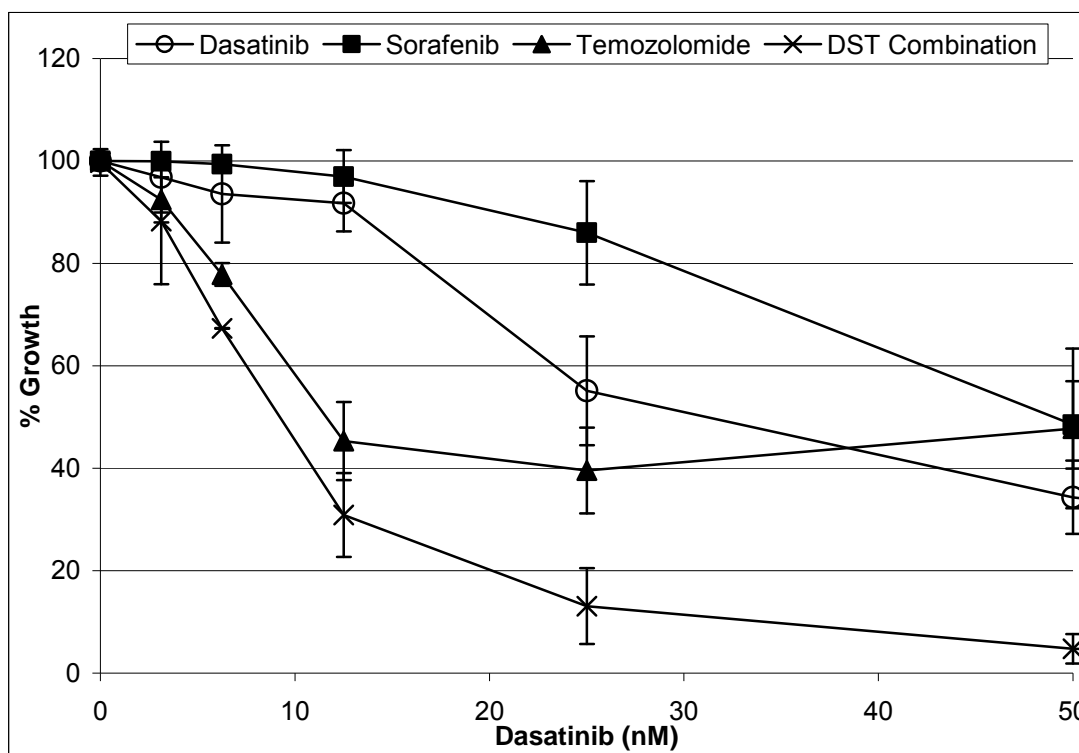


Figure 5.6: Triple combination assays of dasatinib with sorafenib and TMZ at the specified ratio in Lox-IMVI (dasatinib: sorafenib: TMZ 1:60:3000) cells. Concentrations of sorafenib and TMZ are represented as a ratio of the dasatinib concentration. Error bars represent the standard deviation of triplicate experiments.

The combination of dasatinib, sorafenib and TMZ was also tested in Malme-3M (Figure 5.7). The combination of drugs enhanced growth inhibition when compared to each of the drugs alone. One-way ANOVA analysis confirmed that combinations of dasatinib, sorafenib and TMZ were more effective than each drug on its own at concentrations of 37.5 nM ( $p = 0.008$ ), 75 nM ( $p = 0.001$ ) and 150 nM ( $p = 0.002$ ) dasatinib in Malme-3M cells. CI values were not calculated as dasatinib does not achieve greater than 50% growth inhibition in this cell lines, at the concentrations tested.

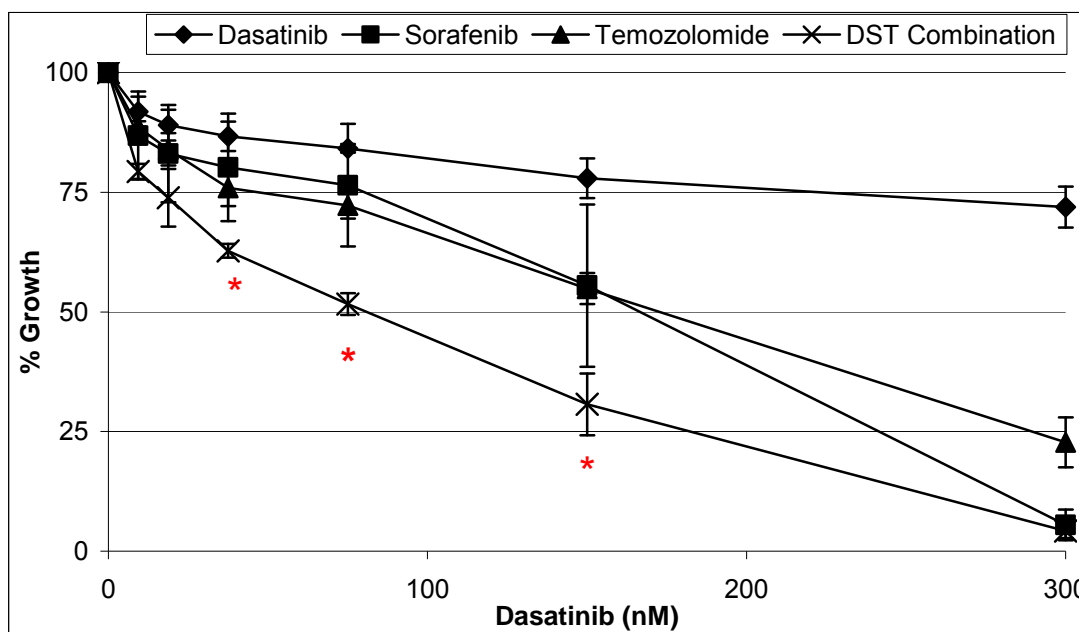


Figure 5.7: Triple combination assays of dasatinib with sorafenib and TMZ at the specified ratio in Malme-3M (dasatinib: sorafenib: TMZ 1:60:3000) cells. Concentrations of sorafenib and TMZ are represented as a ratio of the dasatinib concentration. Standard error bars represent the average result of triplicate assays. ‘\*’ indicates that the combination of dasatinib, sorafenib and TMZ is significantly more effective than testing dasatinib, sorafenib or TMZ on its own, as determined by one-way ANOVA analysis.

#### 5.4 Sensitivity of TMZ resistant melanoma cell lines to dasatinib

We have shown that dasatinib in combination with TMZ has a greater effect on proliferation of melanoma cells than either drug alone (section 5.2). We examined whether the TMZ resistant cell lines displayed altered sensitivity to dasatinib (Table 5.4) and secondly whether the combination of TMZ and dasatinib was effective in the resistant cell lines.

HT144-TMZ is approximately 3-fold more sensitive and Malme-TMZ is approximately 5-fold more sensitive to 1  $\mu$ M dasatinib than the parental HT144 and Malme-3M cell lines (Table 5.4).

Table 5.4: Percentage inhibition of proliferation induced by dasatinib in HT144 and Malme-3M and the TMZ resistant variants HT144-TMZ and Malme-TMZ.

Cell Line	HT144	HT144-TMZ	Malme-3M	Malme-TMZ
<b>Dasatinib</b>	<b>23</b>	<b>70</b>	<b>14</b>	<b>70</b>
<b>(% inhibition @ 1 <math>\mu</math>M)</b>	$\pm 10$	$\pm 10$	$\pm 10$	$\pm 6$

Dasatinib, as previously described, enhanced response to TMZ in the parent cell line Malme-3M (section 5.2). We compared the effect of dasatinib plus TMZ in Malme-TMZ and Malme-3M (Figure 5.8 A+B).

In the TMZ resistant cell line Malme-TMZ, the combination of dasatinib and TMZ resulted in a significant decrease in the IC<sub>50</sub> for TMZ compared to testing TMZ alone (TMZ alone IC<sub>50</sub> = 267  $\mu$ M  $\pm$  29  $\mu$ M; TMZ IC<sub>50</sub> in combination with dasatinib = 68  $\mu$ M  $\pm$  24  $\mu$ M (p=0.001)) (Figure 5.8A). CI values showed that the combination of dasatinib and TMZ was synergistic in Malme-TMZ at ED<sub>25</sub> and ED<sub>50</sub> concentrations (C.I. @ ED<sub>25</sub> = 0.56  $\pm$  0.24: CI @ ED<sub>50</sub> = 0.79  $\pm$  0.28: CI @ ED<sub>75</sub> = 1.40  $\pm$  0.45) (Figure 5.8B).

A direct comparison of the combination of dasatinib and TMZ in Malme-3M and Malme-TMZ showed that the combination was more effective in Malme-TMZ cells than in Malme-3M cells, at concentrations ranging from 3 nM to 62.5 nM dasatinib (Figure 5.8C).

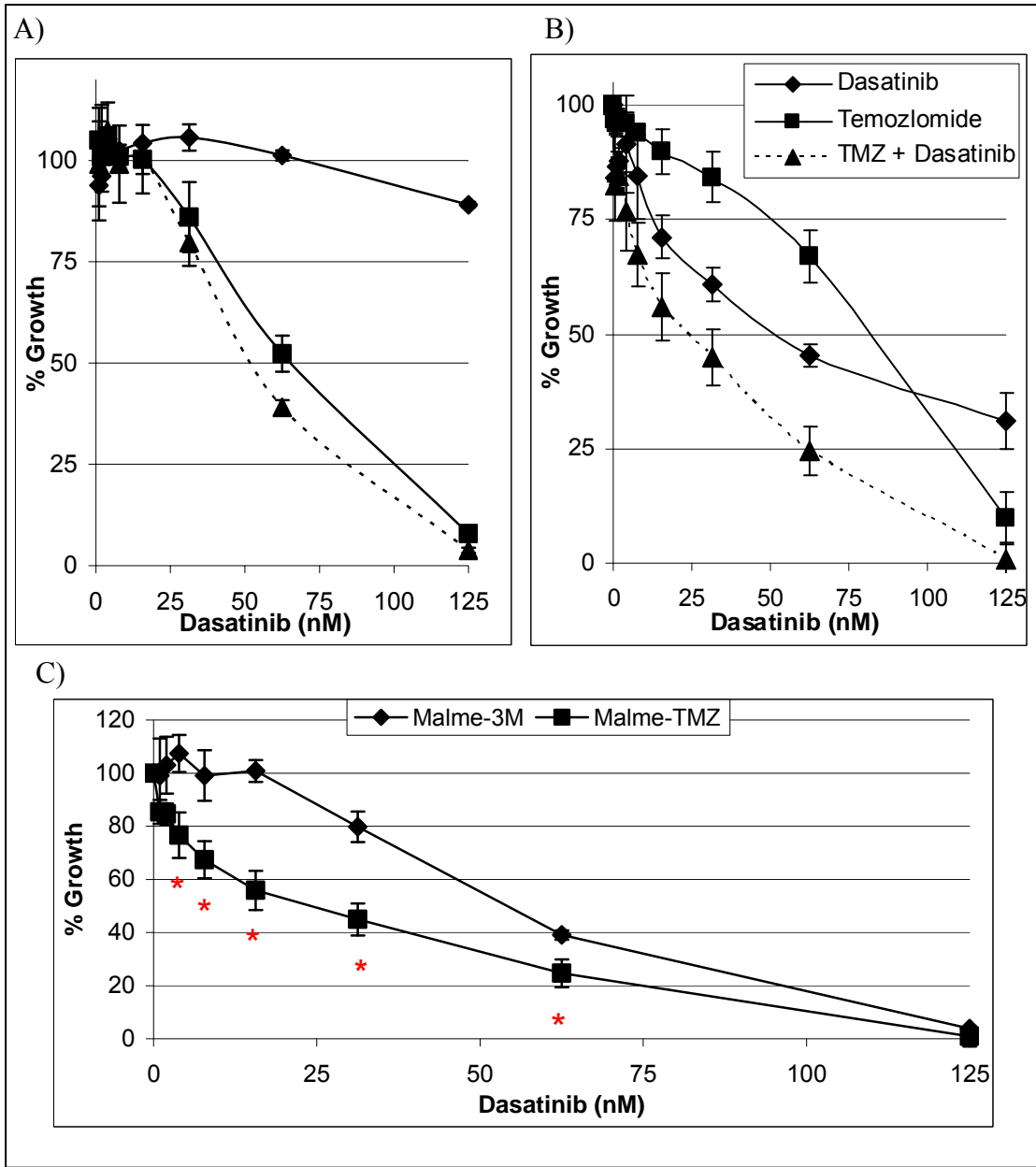


Figure 5.8: Combination assays of dasatinib with TMZ at the specified ratio in A) Malme-3M and B) Malme-TMZ (ratio dasatinib:TMZ - 1:800). C) Comparison of the combination of temozolomide and dasatinib in both Malme-3M and Malme-TMZ. Concentrations of TMZ are represented as a ratio of the dasatinib concentration. Error bars represent the standard deviation of triplicate experiments. '\*' indicates that



the combination of dasatinib and TMZ was significantly more effective in Malme-TMZ than in Malme-3M at the displayed concentrations.

To analyse why TMZ resistant cell lines display greater sensitivity to dasatinib we examined whether the TMZ exposure in the resistant cell lines altered the levels or phosphorylation of SRC kinase in the resistant cells compared to the parent cell lines.

Using western blotting, we showed that exposure to TMZ had no effect on the basal levels of total SRC kinase protein in Malme-TMZ compared to Malme-3M (Figure 5.9A). However, TMZ exposure significantly increased p-SRC levels in Malme-TMZ compared to Malme-3M. Treatment with increasing doses of dasatinib resulted in a decrease in the p-SRC levels in both Malme-3M and Malme-TMZ (Figure 5.9B).

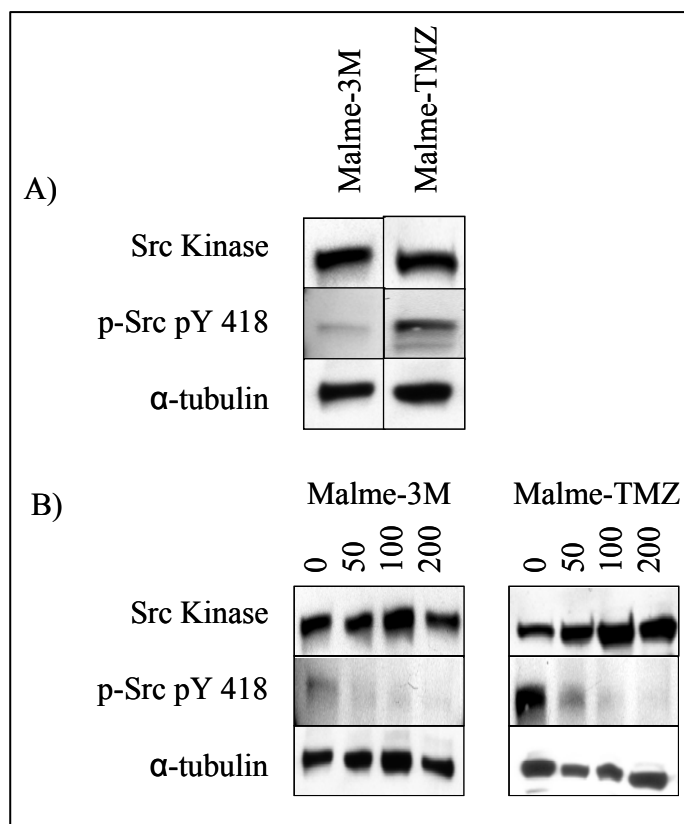


Figure 5.9: Western blotting for total SRC kinase, p-SRC kinase Y119 and  $\alpha$ -tubulin in (A) Malme-3M and Malme-TMZ; and in (B) Malme-3M and Malme-TMZ untreated (control) or treated with increasing doses of dasatinib (nM) for 6 hours.

### 5.5 Summary

Dasatinib in combination with TMZ showed significantly greater efficacy than testing either drug alone in HT144, Lox-IMVI, Malme-3M and M14. Combinations of dasatinib with epirubicin significantly enhanced growth inhibition in two dasatinib sensitive cell lines; however combinations of dasatinib with taxotere only enhanced growth inhibition in Lox-IMVI.

The IC<sub>50</sub> values for sorafenib in the melanoma cell lines range from 1.8  $\mu$ M – 4.1  $\mu$ M. Thus, in dasatinib sensitive melanoma cell lines, dasatinib inhibits growth at significantly lower concentrations than sorafenib. Dasatinib combined with sorafenib slightly enhanced growth inhibition in Lox-IMVI. The triple combination of dasatinib and sorafenib with TMZ also showed improved response in Lox-IMVI and Malme-3M.

Intriguingly cell lines which have acquired TMZ resistance appear to have increased sensitivity to dasatinib compared to the parental cell lines. The combination of dasatinib and TMZ was also more effective in TMZ resistant cell lines compared to the parent cell lines. Phospho-SRC levels are increased in Malme-TMZ when compared to Malme-3M cells, and this may contribute to the TMZ resistance and the increased dasatinib sensitivity observed.

## **Chapter 6**

### **6. Biomarkers for dasatinib treatment in melanoma**

## **6.1 Introduction**

Increasing numbers of novel therapies are emerging from pharmaceutical pipelines and entering clinical trials. The success of such targeted therapies in particular patient subgroups will depend on the availability of appropriate predictive biomarkers to select patients most likely to respond to a specific therapy. Therefore, biomarkers are now of fundamental importance in the road map of drug development.

Huang *et al* [184] identified and validated a six candidate marker genes which predicted response to dasatinib in breast cancer cells lines. Five genes, namely annexin-A1 (ANXA1), caveolin-1 (CAV-1), caveolin-2 (CAV-2), ephrin-A2 (EphA2) and polymerase I and transcript release factor (PTRF) were expressed at higher levels and insulin-like growth factor binding protein 2 (IGFBP2) was expressed at lower levels in dasatinib sensitive breast cancer cell lines. We performed q-RT-PCR and western blotting in our panel of melanoma cell lines to determine whether the 6-gene predictive panel is also predictive of response to dasatinib in melanoma cells. We then selected genes whose expression at either the mRNA or protein level displayed the strongest correlation with dasatinib response in our melanoma cell line panel, and examined expression of these potential biomarkers in melanoma tumour samples using immunohistochemical staining.

## **6.2 Evaluation of Src, EphA2 and FAK as biomarkers for dasatinib therapy in melanoma cell lines**

We have previously shown that EphA2, FAK and SRC kinase are expressed and phosphorylated in the panel of melanoma cell lines (Figure 6.1) and that dasatinib

treatment resulted in changes in phosphorylation status. We therefore examined whether expression or phosphorylation of these proteins correlates with dasatinib sensitivity in the melanoma cell lines HT144, Lox-IMVI, Malme-3M, Sk-Mel-5 and Sk-Mel-28. Of the 5 melanoma cell lines studied, each cell line expressed SRC kinase and had detectable levels of phosphorylation at Y418 (Figure 6.1). However, there was no apparent association between either expression or phosphorylation of SRC kinase and sensitivity to dasatinib in the cell lines studied. FAK expression and phosphorylation were also analysed in the melanoma panel however, again neither expression nor phosphorylation correlated with dasatinib response. Interestingly, EphA2 was expressed and phosphorylated at higher levels in HT144, Lox-IMVI and Malme-3M, which are more sensitive to dasatinib than Sk-Mel-5 and Sk-Mel-28.

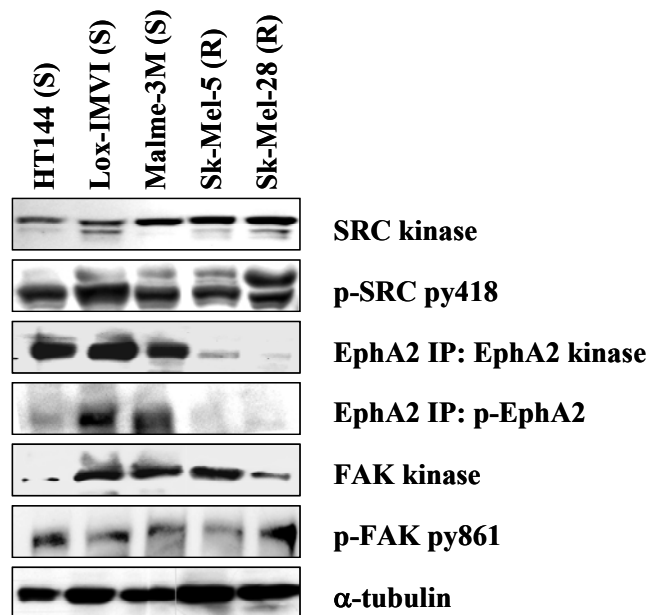


Figure 6.1: Western blotting for SRC kinase, phospho-SRC kinase, immunoprecipitated (IP) EphA2, phospho-EphA2, FAK, phospho-FAK Y861, and  $\alpha$ -tubulin in the panel of melanoma cell lines. (S) indicates that cell lines are sensitive to dasatinib and (R) indicates that cell lines are dasatinib resistant.

### 6.3 Evaluation of a 6-gene predictive biomarker panel by qRT-PCR

Previous work performed by Huang *et al* [184] correlated microarray data and sensitivity to dasatinib in 23 breast cancer cell lines and identified a panel of 6 genes that predicted response to dasatinib. Their results indicated that five genes, ANXA1, CAV1, CAV2, EPHA2 and PTRF, are expressed at higher levels and one gene, IGFBP2, is expressed at lower levels in dasatinib-sensitive breast cancer cell lines compared to dasatinib-resistant cell lines. Levels of mRNA were highest for CAV-1, CAV-2 and EphA2 as detected by qRT-PCR and Affymetrix GeneChip analysis. Levels of mRNA for IGFBP2 were significantly lower in dasatinib sensitive breast cancer cell lines. In an attempt to correlate work by Huang *et al*, (2007) with our melanoma cell line panel, we firstly classified our cell lines as either dasatinib responsive or dasatinib resistant (Table 6.1). The cell lines Lox-IMVI, WM-115, HT144 and Malme-3M were classified as dasatinib responsive as dasatinib treatment (300 nM) causes greater than 20 % inhibition of proliferation. Sk-Mel-28, Sk-Mel-5, WM-266-4 and M14 were classified as dasatinib resistant as less than 20 % inhibition of proliferation was achieved when treated with 300 nM dasatinib.

Table 6.1: Classification of melanoma cell lines as dasatinib responsive or dasatinib resistant based on response to dasatinib at 300 nM.

Dasatinib responsive		Dasatinib Resistant	
Cell Line	% inhibition @ 300 nM	Cell Line	% inhibition @ 300 nM
Lox-IMVI	90 %	Sk-Mel-28	- 50 % <sup>a</sup>
WM-115	60 %	Sk-Mel-5	- 15 % <sup>a</sup>
HT144	50 %	WM-266-4	13 %
Malme-3M	25 %	M14	8 %

<sup>a</sup> recorded values represent that dasatinib resulted in increased levels of proliferation compared to untreated cells.

qRT-PCR analysis (section 2.7) was performed on the 8 melanoma cell lines to determine the mRNA levels of the 6 dasatinib predictive genes (Figure 6.2). Cell lines were compared to a control sample (a pooled sample which consisted of an equal volume of mRNA from each of the cell lines used for analysis) which reflected the average mRNA expression of all the cell lines tested. A result less than 1 indicates lower expression than the control whilst a result of greater than 1 indicates elevated expression relative to the control. qRT-PCR of the 6 gene predictive marker in the melanoma cell lines revealed that EphA2 mRNA levels are higher than the control in dasatinib-sensitive WM-115 and Lox-IMVI, whilst EphA2 mRNA is lower in the remaining cell lines. CAV-1 mRNA levels are higher in Lox-IMVI and WM-115 cells but are also found to be higher in dasatinib resistant M14 and WM-266-4 cells compared to the control. The remaining cell lines have lower CAV-1 mRNA levels compared to the control. ANXA-1 mRNA levels are higher in WM-115 and Lox-IMVI but ANXA1 mRNA levels are also higher in the dasatinib resistant cell line M14. ANXA1 mRNA levels are lower in the remaining cell lines compared to the control. CAV-2 mRNA is higher in Malme-3M and WM-115 which are dasatinib sensitive cell lines but is lower in all other cell lines tested compared to the control. PTRF is lower in all dasatinib sensitive cell lines whilst it is higher in dasatinib resistant WM266-4 and M14 cell lines. IGFBP2 mRNA levels are higher in dasatinib sensitive WM-115 and dasatinib resistant Sk-Mel-5 and WM266-4 but are lower in the remaining cell lines regardless of sensitivity to dasatinib.

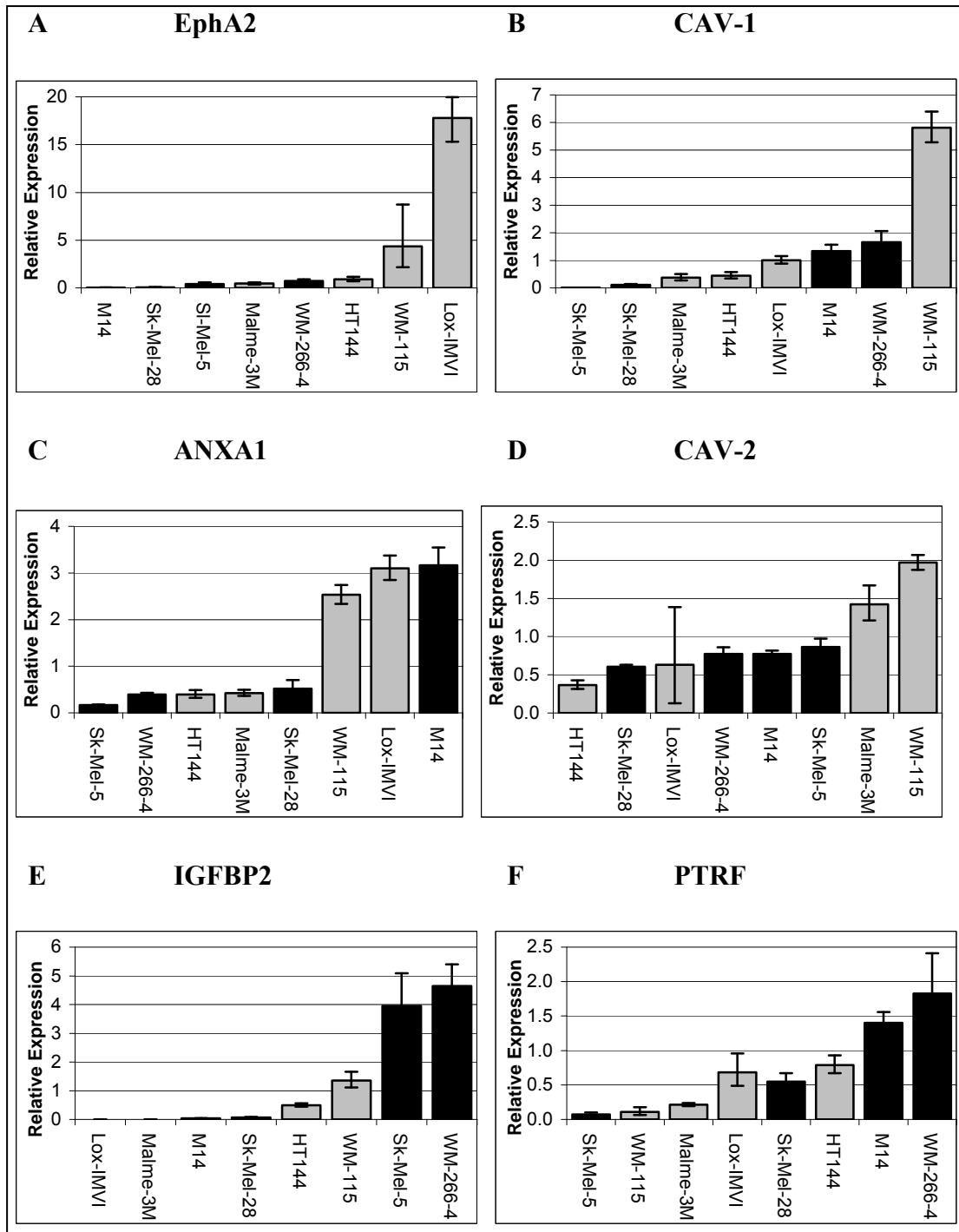


Figure 6.2: Relative expression levels of A) EphA2, B) CAV-1, C) ANXA1, D) CAV-2, E) IGFBP2 and F) PTRF mRNA measured by qRT-PCR. Relative expression is measured compared to the control mix (a combination of equal amounts of mRNA from each cell line tested). Black bars represent dasatinib resistant cell lines; grey samples represent dasatinib responsive samples. Error bars represent standard deviations for technical triplicates of samples.



We also averaged the expression of the 6 gene predictive marker at the mRNA levels in the dasatinib responsive and resistant cell lines to examine their relationship with response to dasatinib in the panel of cell lines. Levels of CAV-1 and EphA2 mRNA were slightly higher and IGFBP2 mRNA levels were slightly lower in dasatinib responsive cell lines compared to dasatinib resistant cell lines (Figure 6.3), however these results were not significant ( $p = 0.446$ ;  $p = 0.265$ ;  $p = 0.639$  respectively). CAV-2 mRNA levels were also lower in dasatinib resistant cell lines compared to dasatinib responsive cell lines but again the results were not significant ( $p = 0.422$ ).

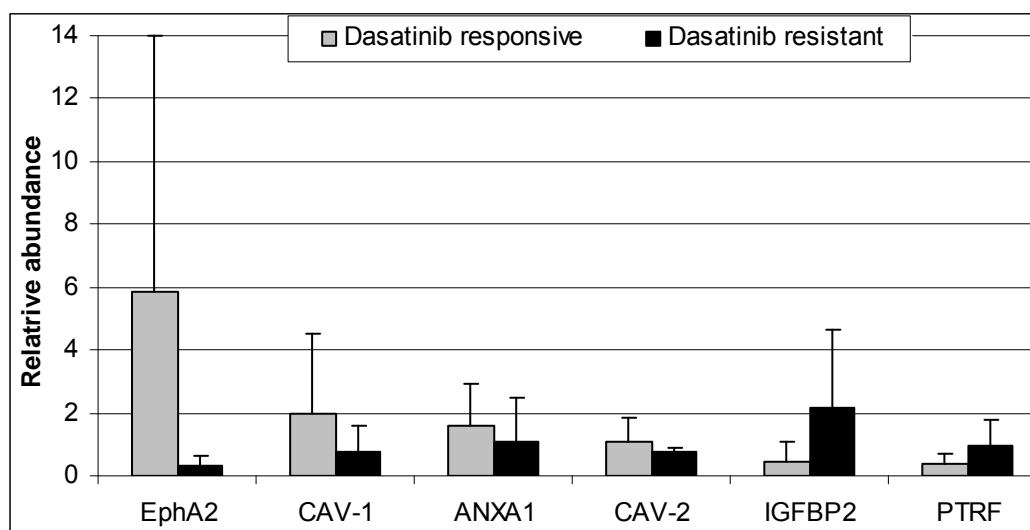


Figure 6.3: Expression levels of PTRF, IGFBP2, EphA2, CAV2, ANXA1 and CAV-1 candidate markers measured by q-RT-PCR. The average expression of technical triplicate results of candidate markers in the dasatinib responsive and resistant cell lines was compared to the control.

#### 6.4 Protein expression of biomarker panel in melanoma cell lines

Western blot analysis was performed for each of the proteins encoded by the 6-gene predictive biomarker panel (Figure 6.5 and Figure 6.6). EphA2 was detected in 6 of the 8 melanoma cell lines tested. Significantly higher levels of EphA2 were detected

in dasatinib responsive cell lines compared to dasatinib resistant cell lines ( $p = 0.02$ ). CAV-1 was detected in all sensitive cell lines but in only 2 of the 4 resistant cell lines, however expression was significantly higher in dasatinib responsive cell lines ( $p = 0.05$ ). ANXA-1 was detected in all cell lines; however significantly higher levels were detected in dasatinib responsive cell lines ( $p = 0.04$ ). Levels of CAV-2 were detected in all cell lines tested with no difference in expression between dasatinib responsive and resistant cell lines ( $p = 0.22$ ). PTRF was detected in the 4 dasatinib responsive cell lines and in 3 out of 4 dasatinib resistant cell lines and there was no significant difference in expression between the cell lines ( $p = 0.14$ ). IGFBP2 was detected in all the cell lines. The expression of IGFBP2 was slightly higher in dasatinib responsive cell lines though the result was not statistically significant ( $p = 0.06$ ).

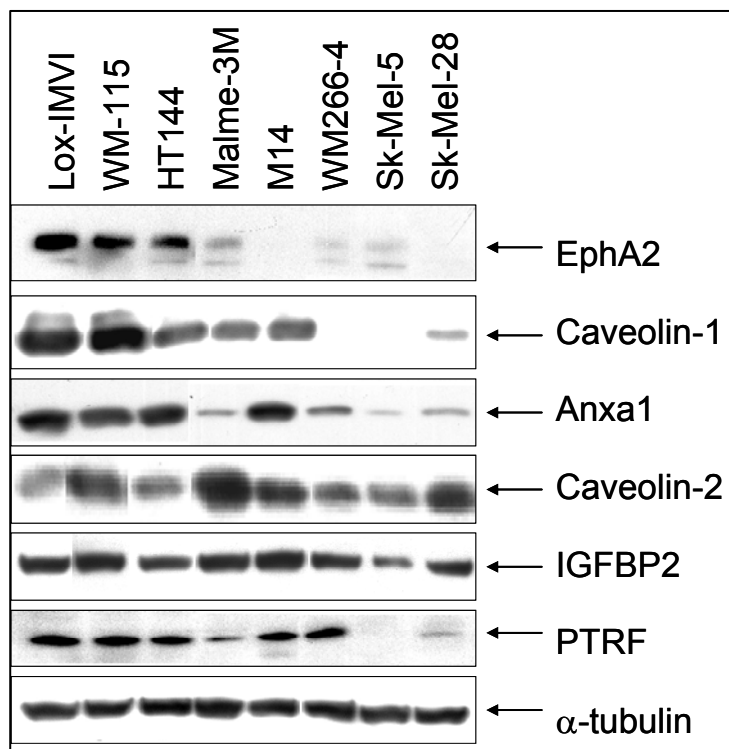


Figure 6.4: Immunoblotting for EphA2, CAV-1, ANXA1, CAV-2, IGFBP2 and PTRF in dasatinib responsive and dasatinib resistant melanoma cell lines.

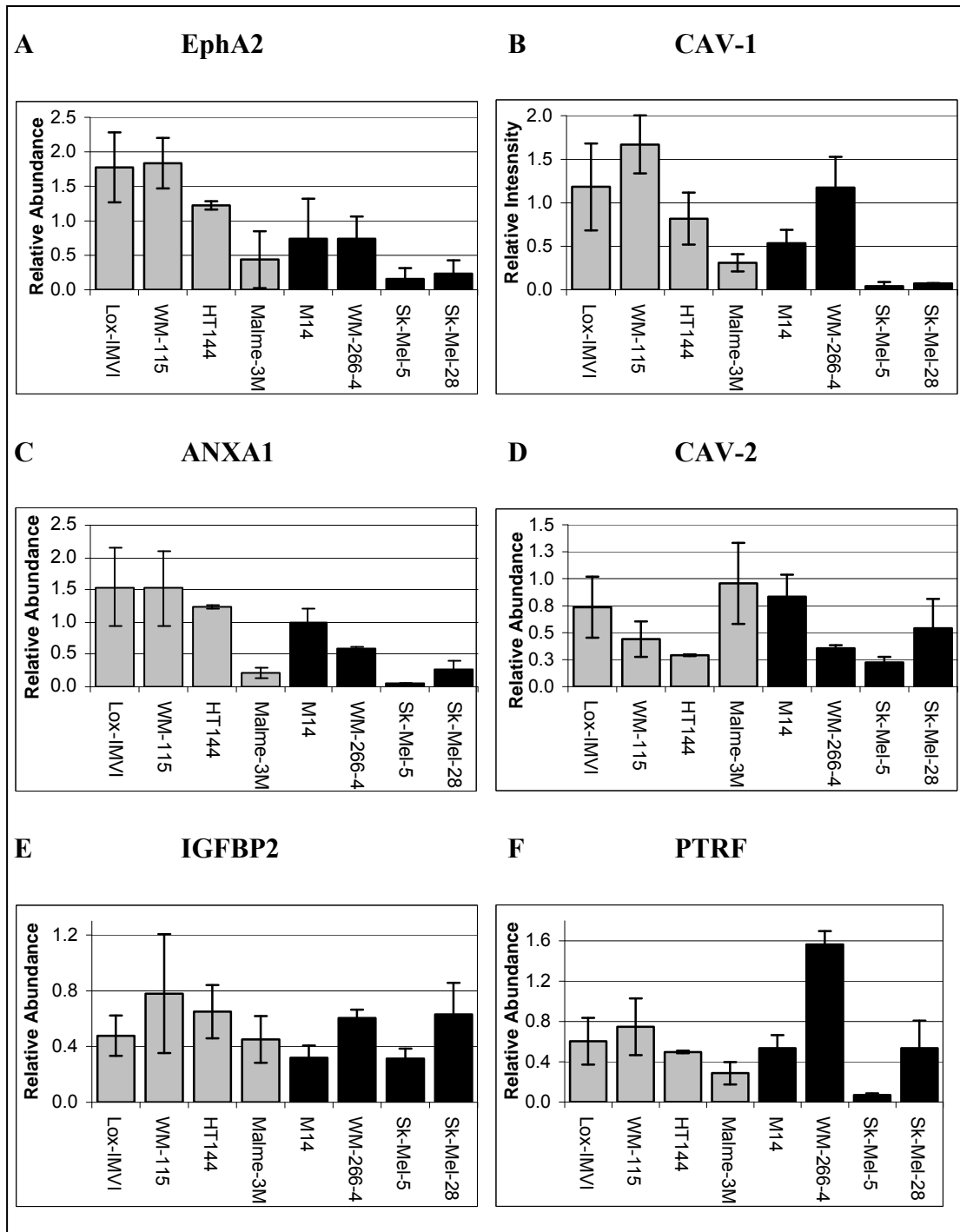


Figure 6.5: Relative expression levels of A) EphA2, B) CAV-1, C) ANXA1, D) CAV-2, E) IGFBP2 and F) PTRF protein levels measured by western blotting. Relative expression was measured by densitometry measurement of band intensities compared to the  $\alpha$ -tubulin endogenous control. Black bars represent dasatinib resistant cell lines; grey samples represent dasatinib sensitive samples. Error bars represent standard deviations for triplicate independent experiments.

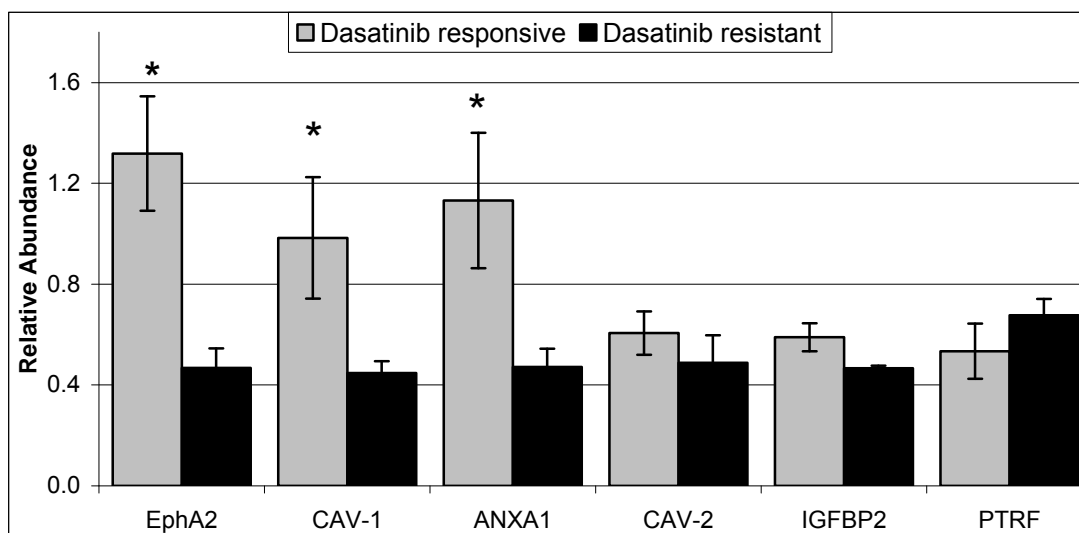


Figure 6.6: Expression levels of PTRF, IGFBP2, EphA2, CAV2, ANXA1 and CAV-1 candidate markers measured by densitometry from triplicate western blots. The average expression of candidate markers in the dasatinib responsive cell lines was compared to the expression in the dasatinib resistant cell lines. ‘\*’ indicates that the p value is < 0.05.

ANOVA analysis was used to determine if there were significant differences between mRNA and protein expression of ANXA1, CAV-1, CAV-2, EphA2, IGFBP2 and PTRF in the dasatinib responsive and resistant cell lines (Figure 6.6). ANXA1 expression was found to be similar at both mRNA and protein levels in dasatinib responsive and resistant cell lines (dasatinib responsive  $p = 0.285$ ; dasatinib resistant  $p = 0.448$ ). mRNA and protein levels of CAV-2 and EphA2 were similar in the dasatinib resistant cell lines; however the mRNA and protein expression were significantly altered in the dasatinib sensitive cell lines (CAV-2 - dasatinib responsive  $p = 0.039$ ; dasatinib resistant  $p = 0.152$ ; EphA2 - dasatinib responsive  $p = 0.003$ ; dasatinib resistant  $p = 0.098$ ). CAV-1, IGFBP2 and PTRF were expressed at similar levels at both the mRNA and protein levels in dasatinib sensitive cell lines. However

in the dasatinib resistant cell lines there were significant differences between protein and mRNA expression (CAV-1 - dasatinib responsive  $p = 0.074$ ; dasatinib resistant  $p = 0.002$ : IGFBP2 - dasatinib responsive  $p = 0.192$ ; dasatinib resistant  $p < 0.001$ : PTRF dasatinib responsive  $p = 0.323$ ; dasatinib resistant  $p = 0.004$ ).

As expression of ANXA1, CAV-1 and EphA2 were significantly higher in dasatinib sensitive melanoma cell lines compared to dasatinib resistant cell lines; we selected CAV-1 for further analysis in melanoma tumour samples, to examine the frequency of expression of the markers in melanoma and their association with melanoma progression. Because SRC has been shown to play an important role in metastasis in melanoma we also examined its expression in the melanoma tumour samples.

## **6.5 Immunohistochemistry analysis of selected biomarkers**

### **6.5.1 Patient characteristics**

A cohort of 126 melanoma tumour samples was used for immunohistochemical analysis. In 7 cases, samples were available from a primary melanoma and a metastatic melanoma from the same patient. Patients are predominantly female and greater than 60 years of age, however 34 % of patients are less than 60 (Table 6.2). Patient tumour samples are mainly from the primary melanoma site (67 %) and 33 % from metastatic melanoma.

Breslow thickness and Clark's level data were not available for 44 % and 49 % of patients respectively. Where data was available, 54 % (n = 38/70) of tumours had a Breslow thickness of less than 2 mm, and 46 % (n = 32/70) had a Breslow thickness of greater than 2 mm. The Clark's level was III or less in 29 % (n = 37/64) of cases and IV or V in 42 % (n = 27/64) of cases.

Of the 52 patients for whom data on lymph node dissection was available, 56 % (n = 28/52) were lymph node positive, whilst 44 % (n = 24/52) were lymph node negative.

Table 6.2: Clinicopathological characteristics of melanoma tumour samples (n=138) used for immunohistochemical analysis of CAV-1 and SRC kinase expression

Characteristic	Number of cases (%)
<b>Age</b>	
< 60	43 (34 %)
≥ 60	83 (66 %)
<b>Sex</b>	
Male	46 (37 %)
Female	80 (63 %)
<b>Tumour type</b>	
Primary melanoma	84 (67 %)
Metastatic melanoma	42 (33 %)
<b>Breslow thickness (mm)</b>	
n/a	56 (44 %)
< 1	28 (40 %)
1 – 1.9	10 (14 %)
2 – 3.9	12 (17 %)
> 4	20 (29 %)
<b>Clarke's Level</b>	
n/a	62 (49 %)
II	8 (13 %)
III	29 (45 %)
IV	20 (31 %)
V	7 (11 %)
<b>Lymph node status</b>	
n/a	74 (59 %)
Positive	28 (56 %)
Negative	22 (44 %)

### 6.6.1 Caveolin-1 expression in melanoma samples

From the 126 samples stained for CAV-1, scores were only obtained for 122, due to a number of slides not containing tumour specimen.

Fifty-four tumour samples (44 %) were positive for CAV-1 expression (Table 6.3). CAV-1 expression was associated with age ( $p = 0.0581$ ) but the result was not significant. Patients who were greater than 60 years of age had lower expression of

CAV-1 than patients who were 60 years or younger (Figure 6.7). CAV-1 expression was not associated with gender or tumour type (primary versus metastatic) (Table 6.4).

In the primary melanoma patient samples Breslow thickness was compared to CAV-1 expression according to the the groups of Breslow thickness (e.g. 1 = <1mm; 2 = 1mm-1.9mm; 3 = 2mm – 4mm; 4 = >4mm) [185] (p = 0.1081) and according to prognostic value (p = 0.4038) (1 = < 2 mm, 5-year survival rate of 80-100%; 2 = ≥ 2mm, 5-survival rate of 50-75%) [186].

CAV-1 expression was compared with grouped Clarkes level (p = 0.7748) where a Clarkes level of III or less correlated with invasion to the dermal junction, and a Clarkes level of greater than III correlated with invasion past the dermal junction into the dermis and subcutaneous fat.



Table 6.3: Relationship between clinico-pathological factors and expression of CAV-1 protein in primary and metastatic melanoma specimens. Breslow thickness, Clarkes levels and lymph node status were only compared in the primary melanoma samples.

P values were determined using the Chi-Squared test.

<b>Characteristic</b>	<b>Caveolin-1 positive (%)</b>	<b>p-value</b>
<b>Total number</b>	54/122 (44 %)	
<b>Age</b>		
≤ 60	24/43 (56 %)	<b>0.0581</b>
> 60	29/76 (38 %)	
<b>Sex</b>		
Male	22/44 (50 %)	0.4
Female	32/78 (41 %)	
<b>Tumour type</b>		
Primary melanoma	39/82 (48 %)	0.2936
Metastatic melanoma	15/40 (38 %)	
<b>Breslow thickness</b>		
n/a	53/122 (43 %)	n/a
< 1 mm	17/28 (61 %)	0.1081
1.0 mm – 1.9 mm	3/9 (33 %)	
2.0 mm – 3.9 mm	3/12 (25 %)	
> 4 mm	12/20 (60 %)	
Grouping 0 – 2 mm	20/37 (55 %)	0.4038
Grouping > 2 mm	15/32 (47 %)	
<b>Clarkes Level</b>		
n/a	59/122 (48 %)	n/a
II	7/8 (88 %)	0.1424
III	13/29 (45 %)	
IV	10/19 (53 %)	
V	5/7 (71 %)	
Grouping I, II, III	20/37 (54 %)	0.7748
Grouping IV, V	15/26 (60 %)	
<b>Lymph node status</b>		
n/a	95/122 (78 %)	n/a
Positive	4/6 (67 %)	0.5346
Negative	11/21 (52 %)	

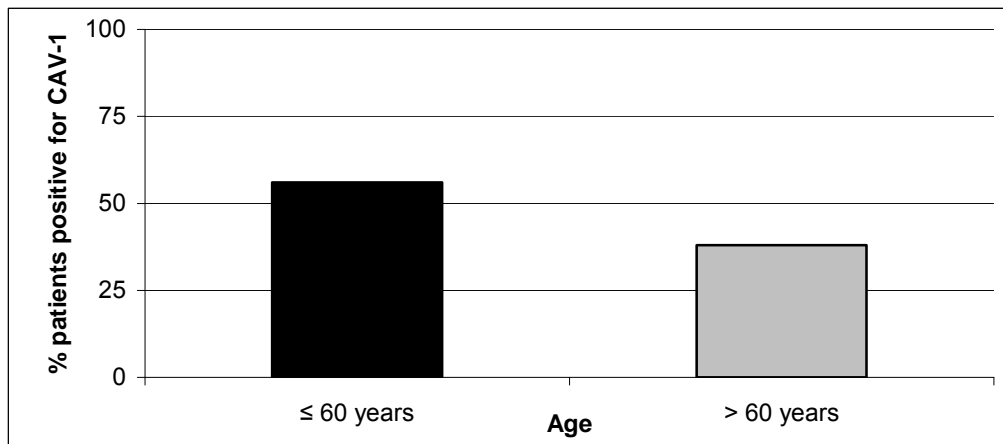


Figure 6.7: Difference in the % of patients who were positive for CAV-1 staining in patients less than or equal to 60 years of age or greater than 60 years of age.

### 6.6.2 Percentage of tumour cells positive for CAV-1 expression in melanoma samples

CAV-1 expression was also graded according to the percentage of tumour cells that were positive for CAV-1 (0 = 0 %; 1 =  $\leq 25$  %; 2 =  $>25$  % -  $\leq 50$  %; 3  $\geq 50$ ). The percentage of tumour cells positive for CAV-1 expression was associated with age ( $p = 0.0587$ ). Patients who were greater than 60 were more frequently negative for CAV-1 staining than patients who were 60 years or younger (Figure 6.8). CAV-1 expression was not associated with gender ( $p = 0.0934$ ) and was also not significantly associated with either metastatic or primary tumours ( $p = 0.4723$ ).

In the primary melanoma tumour samples, the percentage of tumour cells positive for CAV-1 expression did not correlate with Breslow thickness, Clarkes level or lymph node status (Table 6.4).

Table 6.4: Correlation between clinico-pathological factors and the percentage of tumour cells positive for CAV-1 expression in primary and metastatic melanoma specimens. Breslow thickness, Clarkes levels and lymph node status were only compared in the primary melanoma samples. P values were determined using the Chi-Squared test.

Characteristic	% tumours cells positive for CAV-1 expression (%)				p-value
	0 %	≤ 25 %	26 – 50 %	> 50 %	
<b>Age</b>					
≤ 60	19 (44%)	15 (35%)	6 (14%)	3 (7%)	0.0587
> 60	49 (62%)	11 (14%)	13 (16%)	6 (8%)	
<b>Sex</b>					
Male	22 (50%)	14 (32%)	7 (16%)	1 (2%)	0.0934
Female	46 (59%)	12 (15%)	12 (15%)	8 (10%)	
<b>Tumour type</b>					
Primary melanoma	43 (52 %)	20 (24%)	14 (17%)	5 (6%)	0.4723
Metastatic melanoma	26 (63%)	5 (12%)	6 (15%)	4 (10%)	
<b>Breslow thickness</b>					
n/a	53/126 (42 %)				n/a
< 1 mm	11 (32%)	9 (56%)	5 (36%)	3 (60%)	0.2851
1.0 mm – 1.9 mm	6 (18%)	1 (6%)	2 (14%)	0 (0%)	
2.0 mm – 3.9 mm	9 (26%)	2 (12%)	0 (0%)	1 (20%)	
> 4 mm	8 (24%)	4 (26%)	7 (50%)	1 (20%)	
Grouping 0 – 2 mm	17 (50%)	11 (69%)	7 (50%)	3 (60%)	0.6241
Grouping > 2 mm	17 (40%)	5 (31%)	7 (50%)	2 (40%)	
<b>Clarkes Level</b>					
n/a	59/122 (48 %)				n/a
II	1 (3%)	5 (31%)	1 (7%)	1 (20%)	0.1059
III	16 (57%)	6 (38%)	4 (29%)	3 (60%)	
IV	9 (32%)	4 (25%)	5 (36%)	1 (20%)	
V	2 (7%)	1 (6%)	4 (29%)	0 (0%)	
Grouping I, II, III	17 (61%)	11 (69%)	5 (36%)	4 (80%)	0.1950
Grouping IV, V	11 (39%)	5 (31%)	9 (64%)	1 (20%)	
<b>Lymph node status</b>					
n/a	95/122 (78%)				n/a
Positive	2 (17%)	1 (17%)	2 (33%)	1 (33%)	0.8099
Negative	10 (83%)	5 (83%)	4 (67%)	2 (67%)	

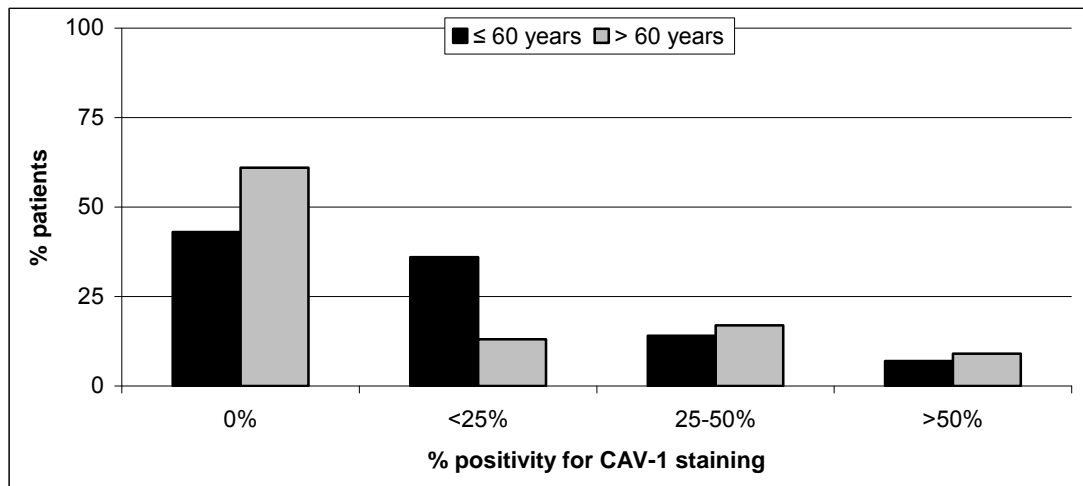


Figure 6.8: % of cells positive for CAV-1 expression in tumours from patients who are less than or equal to 60 years of age compared to patients who are greater than 60 years of age.

### 6.6.3 Intensity of Caveolin-1 expression in melanoma samples

CAV-1 expression was also scored according to the intensity of tumour cell staining (0 = none; 1 = weak; 2 = moderate; 3 = strong). CAV-1 expression was not significantly associated with age ( $p = 0.2707$ ), gender ( $p = 0.6991$ ) or with either metastatic or primary tumours ( $p = 0.2445$ ). In the primary melanoma patient samples CAV-1 expression did not correlate with Breslow thickness, Clarkes level or lymph node status (Table 6.5).

Table 6.5: Correlation between clinico-pathological factors and intensity of staining for CAV-1 protein in primary and metastatic melanoma specimens. Breslow thickness, Clarkes levels and lymph node status were only compared in the primary melanoma samples. P values were determined using the Chi-Squared test.

Characteristic	Caveolin-1 intensity (%)				P-value
	None	Weak	Moderate	Strong	
<b>Age</b>					
≤ 60	23 (53%)	6 (14%)	6 (14%)	8 (19%)	0.2707
> 60	44 (56%)	7 (9%)	20 (25%)	8 (10%)	
<b>Sex</b>					
Male	24 (55%)	3 (7%)	10 (23%)	7 (16%)	0.6991
Female	43 (55%)	10 (13%)	16 (21%)	9 (12%)	
<b>Tumour type</b>					
Primary melanoma	41 (50%)	11 (13%)	20 (24%)	10(12%)	0.1383
Metastatic melanoma	26 (65%)	2 (5%)	6 (15%)	6 (15%)	
<b>Breslow thickness</b>					
n/a	53/122 (43%)				n/a
< 1 mm	10 (30%)	5 (56%)	8 (50%)	5 (46%)	0.5542
1.0 mm – 1.9 mm	6 (18%)	1 (11%)	1 (6%)	1 (9%)	
2.0 mm – 3.9 mm	9 (27%)	1 (11%)	1 (6%)	1 (9%)	
> 4 mm	8 (24%)	2 (22%)	6 (38%)	4 (36%)	
Grouping 0 – 2 mm	16 (49%)	6 (67%)	9 (56%)	6 (55%)	0.4818
Grouping > 2 mm	17 (51%)	3 (33%)	7 (44%)	5 (45%)	
<b>Clarkes Level</b>					
n/a	59/122 (48 %)				n/a
II	1 (4%)	3 (34%)	3 (18%)	1 (9%)	0.3844
III	15 (56%)	4 (44%)	5 (29%)	5 (46%)	
IV	9 (33%)	2 (22%)	5 (29%)	3 (27%)	
V	2 (7%)	0 (0%)	3 (18%)	2 (18%)	
Grouping I, II, III	16 (59%)	7 (78%)	8 (50%)	6 (54%)	0.5864
Grouping IV, V	11 (41%)	2 (22%)	8 (50%)	5 (46%)	
<b>Lymph node status</b>					
n/a	95/122 (78%)				n/a
Positive	2 (17%)	0 (0%)	2 (40%)	2 (29%)	0.5421
Negative	10 (83%)	3 (100%)	3 (60%)	5 (71%)	

### **6.7.1 SRC kinase expression in melanoma samples**

Ninety four tumour samples (76 %) were positive for SRC expression (Table 6.6). SRC expression was not significantly associated with age ( $p = 0.2897$ ), gender ( $p = 0.3554$ ) or with either metastatic or primary tumours ( $p = 0.0890$ ).

In the primary melanoma patient samples, SRC expression did not correlate with Breslow thickness, Clarkes level or lymph node biopsy status (Table 6.6).

Table 6.6: Correlation between clinico-pathological factors and expression of SRC kinase protein in primary and metastatic melanoma specimens. Breslow thickness, Clarkes levels and lymph node status were only compared in the primary melanoma samples. P values were determined using the Chi-Squared test.

<b>Characteristic</b>	<b>SRC kinase positive (%)</b>	<b>p-value</b>
<b>Total number</b>	94/124 (76 %)	
<b>Age</b>		
≤ 60	24/32 (75 %)	0.2897
> 60	59/92 (64 %)	
<b>Sex</b>		
Male	37/46 (80 %)	0.3554
Female	57/78 (73 %)	
<b>Tumour type</b>		
Primary melanoma	66/82 (81 %)	0.0890
Metastatic melanoma	28/42 (67 %)	
<b>Breslow thickness</b>		
n/a	53/122 (43 %)	n/a
< 1 mm	22/27 (82 %)	0.5944
1.0 mm – 1.9 mm	7/10 (70 %)	
2.0 mm – 3.9 mm	10/12 (83 %)	
> 4 mm	18/20 (90 %)	
Grouping 0 – 2 mm	29/37 (78 %)	0.3743
Grouping > 2 mm	28/32 (88 %)	
<b>Clarkes Level</b>		
n/a	59/122 (48 %)	n/a
II	8/8 (100 %)	0.6519
III	23/28 (82 %)	
IV	17/20 (85 %)	
V	6/7 (86 %)	
Grouping I, II, III	31/36 (86 %)	0.9172
Grouping IV, V	23/27 (85 %)	
<b>Lymph node status</b>		
n/a	75/122 (61 %)	n/a
Positive	4/6 (67 %)	0.2895
Negative	18/21 (86 %)	

### **6.7.2 Percentage of tumour cells positive for SRC expression in melanoma samples**

Expression was also graded according to the % of tumour cells that are positive for SRC (0 = 0 %; 1 =  $\leq 25$  %; 2 =  $>25$  % -  $\leq 50$  %; 3  $\geq 50$ ). The percentage of tumours positive for SRC expression was not significantly associated with age ( $p = 0.6102$ ), gender ( $p = 0.7791$ ) or with either metastatic or primary tumours ( $p = 0.1332$ ).

The percentage of tumour cells positive for SRC expression did not correlate with Breslow thickness, Clarkes level or lymph node status (Table 6.7).



Table 6.7: Correlation between clinico-pathological factors and the percentage of tumours positive for SRC expression in primary and metastatic melanoma specimens.

Breslow thickness, Clarkes levels and lymph node status were only compared in the primary melanoma samples. P values were determined using the Chi-Squared test.

Characteristic	% of tumour cells positive for SRC expression (%)				p-value
	0 %	≤ 25 %	26–50%	> 50 %	
<b>Age</b>					
≤ 60	8 (19%)	7 (16%)	9 (21%)	19 (44%)	0.6102
> 60	22 (27%)	13 (16%)	19(24%)	27 (33%)	
<b>Sex</b>					
Male	9 (20%)	7 (15%)	11(24%)	19 (41%)	0.7791
Female	21 (27%)	13 (16%)	17(22%)	27(35%)	
<b>Tumour type</b>					
Primary melanoma	16 (20 %)	13 (16%)	17(20%)	36 (44%)	0.1332
Metastatic melanoma	14 (33%)	7 (17%)	11(26%)	10 (24%)	
<b>Breslow thickness</b>					
n/a	53/122 (43 %)				n/a
< 1 mm	5 (41%)	5 (46%)	5 (33%)	12 (39%)	0.924
1.0 mm – 1.9 mm	3 (25%)	2 (18%)	1 (7%)	4 (13%)	
2.0 mm – 3.9 mm	2 (17%)	1 (9%)	3 (20%)	6 (19%)	
> 4 mm	2 (17%)	3 (27%)	6 (40%)	9 (29%)	0.6693
Grouping 0 – 2 mm	8 (67%)	7 (64%)	6 (67%)	16 (52%)	
Grouping > 2 mm	4 (33%)	4 (36%)	9(33%)	15 (48%)	
<b>Clarkes Level</b>					
n/a	59/122 (48 %)				n/a
II	0 (0%)	2 (20%)	2 (15%)	4 (13%)	0.5405
III	5 (56%)	2 (20%)	6 (46%)	15 (48%)	
IV	3 (33%)	6 (60%)	3 (24%)	8 (26%)	
V	1 (11%)	0 (0%)	2 (15%)	4 (13%)	0.6755
Grouping I, II, III	5 (56%)	4 (36%)	8 (62%)	19 (63%)	
Grouping IV, V	4 (44%)	6 (64%)	5 (38%)	12 (37%)	
<b>Lymph node status</b>					
n/a	75/122 (61%)				n/a
Positive	2 (40%)	1 (25%)	2 (33%)	1 (8%)	0.4402
Negative	3 (60%)	3 (75%)	4 (67%)	11 (92%)	

### **6.7.3 Intensity of SRC kinase expression in melanoma samples**

SRC expression was scored according to the intensity of SRC tumour cell staining (0 = none; 1 = weak; 2 = moderate; 3 = strong). SRC expression was not significantly associated with age ( $p = 0.3677$ ), gender ( $p = 0.8079$ ) or with either metastatic or primary tumours ( $p = 0.3465$ ) (Table 6.8).

SRC expression did not correlate with Breslow thickness, Clarkes level or lymph node status (Table 6.8).

Table 6.8: Correlation between clinico-pathological factors and intensity of staining for SRC kinase in primary and metastatic melanoma specimens. Breslow thickness, Clarkes levels and lymph node status were only compared in the primary melanoma samples. P values were determined using the Chi-Squared test.

Characteristic	SRC kinase intensity (%)				P-value
	None	Weak	Moderate	Strong	
<b>Age</b>					
≤ 60	8 (19 %)	8 (19 %)	16 (36 %)	11 (26 %)	0.3677
> 60	22 (27%)	14(17%)	19 (24 %)	26 (32 %)	
<b>Sex</b>					
Male	9 (20 %)	9 (20 %)	13 (27%)	15(33%)	0.8079
Female	21 (27%)	13 (17%)	22 (28%)	22(28%)	
<b>Tumour type</b>					
Primary melanoma	16 (20%)	15 (17%)	26 (32%)	25(31%)	0.3465
Metastatic melanoma	14 (33%)	7 (17%)	9 (21%)	12(29%)	
<b>Breslow thickness</b>					
n/a	53/122 (45%)				n/a
< 1 mm	5 (41%)	7 (50%)	9 (43%)	6 (27%)	0.2625
1.0 mm – 1.9 mm	3 (25%)	0 (0%)	3 (14%)	4 (18%)	
2.0 mm – 3.9 mm	2 (17%)	1 (7%)	6 (29%)	3 (14%)	
> 4 mm	2 (17%)	6 (43%)	3 (14%)	9 (41%)	0.5690
Grouping 0 – 2 mm	8 (67%)	7 (50%)	12(57%)	10 (46%)	
Grouping > 2 mm	4 (33%)	7 (50%)	9(43%)	12 (54%)	
<b>Clarkes Level</b>					
n/a	59/122 (48 %)				n/a
II	0 (0%)	3 (27%)	2 (10%)	3 (14%)	0.1906
III	5 (56%)	1 (9%)	14(67%)	8 (36%)	
IV	3 (33%)	5 (46%)	4 (18%)	8 (36%)	
V	1 (11%)	2 (18%)	1 (5%)	3 (14%)	0.1376
Grouping I, II, III	5 (55%)	4 (36%)	16(76%)	11 (50%)	
Grouping IV, V	4 (45%)	7 (64%)	5 (24%)	11 (50%)	
<b>Lymph node status</b>					
n/a	75/122 (62%)				n/a
Positive	2 (40%)	3 (50%)	0 (0%)	1 (10%)	0.1036
Negative	3 (60%)	3 (50%)	6 (100%)	9 (90%)	

In the cohort of 138 melanoma patients, both primary and metastatic samples were available for 7 patients. We compared the expression of CAV-1 and SRC in these paired samples. However because the numbers of paired samples were so small, it was not possible to get significant results for these comparisons (Table 6.9).

Table 6.9: Comparison of CAV-1 and SRC expression between the paired primary and metastatic melanoma patient samples.

	<b>CAV-1</b>	<b>SRC</b>
<b>Primary melanoma</b>	1/7	5/7
<b>Metastatic melanoma</b>	0/6	3/7
<b>P - value</b>	0.3352	0.2801

## 6.8 Summary

Our results suggest that neither expression nor phosphorylation of Src kinase or FAK predict response to dasatinib in our panel of melanoma cell lines.

We analysed a 6-gene predictive biomarker, previously validated in breast cancer cell lines, in our melanoma cell line panel. Expression of individual genes at the mRNA level did not correlate with response to dasatinib. However, when protein levels were analysed, expression of ANXA1, CAV-1 and EphA2 was significantly higher in dasatinib sensitive cell lines compared to resistant cell lines.

CAV-1 was detected in 44 % of melanoma tumour samples, and CAV-1 expression was significantly associated with patients over 60 years of age. SRC was detected in 73 % of melanoma tumour samples and was found to be expressed at significantly higher levels in patients who were lymph node negative compared to lymph node positive patients.

## **Chapter 7**

### **7. Phosphoproteomic analysis of dasatinib sensitive WM-115 and dasatinib resistant WM266-4 melanoma cells**

## **7.1 Introduction**

WM-115 is a melanoma cell line derived from the primary site of a melanoma patient. WM-266-4 was derived from a metastatic melanoma from the same patient. We have shown that the primary cell line, WM-115 is sensitive to dasatinib, while the metastatic melanoma cell line, WM-266-4 is resistant to dasatinib (section 4.1). Phosphoproteomic analysis was performed to identify markers of response and resistance to dasatinib in melanoma cell lines. Our model compares two isogenic populations of cells representing both primary and metastatic cell lines.

Following phosphoprotein enrichment, we used two phosphoproteomic approaches to identify phosphoproteins associated with dasatinib response/resistance, namely 2D-DIGE analysis and phosphoprotein staining of 2D gels using the Pro-Q Diamond stain, both followed by protein identification using LC-MS and MALDI-ToF-ToF-MS (section 2.20). The 2D-DIGE analysis provides information on differences in the abundance of particular phosphoproteins identified while the Pro-Q Diamond staining detects differences in the level of phosphorylation of specific proteins.

Finally, using bioinformatics software packages such as PANTHER analysis and Pathway Studio, we interrogated our protein lists to examine associations between specific proteins and melanoma or dasatinib sensitivity.

## **7.2 2-D DIGE analysis**

Protein lysates were prepared from WM-115 and WM-266-4 melanoma cells which were untreated or treated with 100 nM dasatinib for 6 hours (section 2.15).

Phosphoprotein enrichment was performed, and the yield of phosphoprotein was approximately 10 % of total protein. Two-dimensional DIGE proteomic analysis was performed on the phosphoprotein samples as previously described (section 2.17). 2,500 spots were detected on the DIGE gels, and each spot was assigned a unique ID number (Figure 7.1). The results of each set of replicate gels were analysed using the DeCyder differential in-gel analysis (DIA) module, and the difference in protein expression between two samples is expressed as fold-change. The DeCyder software produces 3-D images of protein abundance, and constructs graphs of relative protein abundance of each of the samples analysed.

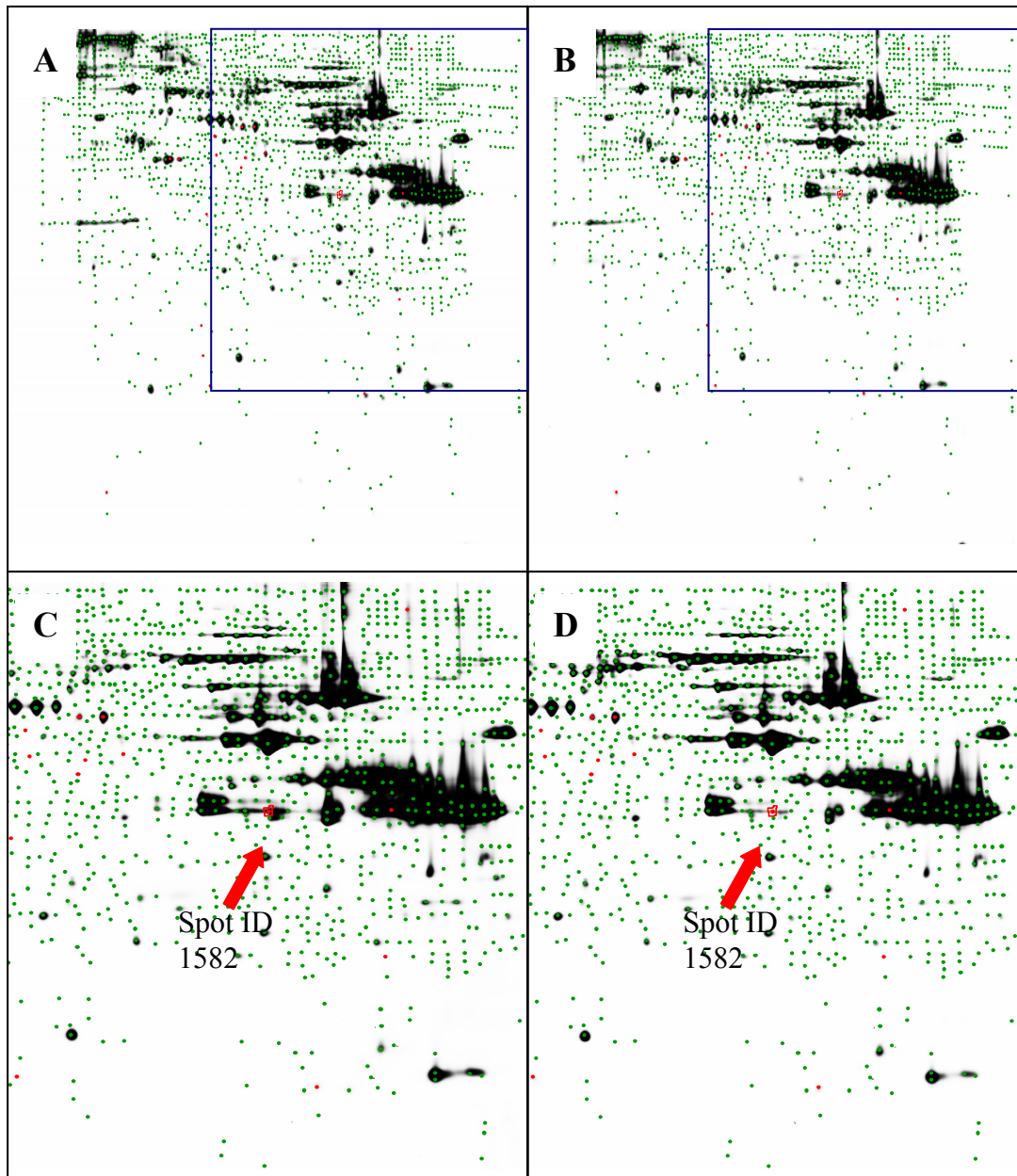


Figure 7.1: Example of DIGE gel images from Gel no. 1 scanned at different wavelengths to reveal spots from **A.** Cy3-labelled WM-115 Ctrl cells, **B.** Cy5-labelled WM-115 dasatinib treated cells. The spots detected by the DeCyder software are marked with green dots. **C.** and **D.** are cropped pictures of A and B, respectively, focusing on the upper region of the gel, with the location of spot ID 1582 (Annexin A2) circled.



### 7.3 Phosphoprotein identification by LC-MS and MALDI-ToF-MS

Comparisons of phosphoprotein levels were performed on WM-115 versus WM-266-4 cells, WM-115 untreated versus dasatinib-treated cells, WM-266-4 untreated versus dasatinib-treated cells and dasatinib-treated WM-115 versus dasatinib-treated WM-266-4 cells (Table 7.1). Triplicate results were analysed by ANOVA. Phosphoproteins which demonstrated a fold-change of  $\geq 1.2$  and a significant p value ( $\leq 0.05$ ) were further analysed. Student t-tests were also performed on each individual comparison and proteins with a significant T-test p value ( $\leq 0.05$ ) were included in the analysis. Of the 2,500 spots detected on the DIGE gels, 203 spots showed significantly altered levels of abundance in one or more comparisons, and were picked for identification by MALDI-ToF-ToF-MS and LC-MS.

Table 7.1: Summary of the comparisons performed in DeCyder software and displayed in Tables 7.2-7.5.

Comparison	Table	Number of spots showing significant change	Number proteins identified by MS
WM-115 vs. WM-266-4	Table 7.2	156	61
WM-115 vs. WM-115 dasat treated	Table 7.3	82	33
WM-266-4 vs. WM-266-4 dasat treated	Table 7.4	21	7
WM-115 dasat vs. WM-266-4 dasat treated	Table 7.5	134	54

In the comparison of WM-115 untreated cells versus WM-266-4 untreated cells, of the 61 significantly altered phosphoproteins identified by LC-MS and MALDI-ToF-MS analysis, 29 proteins were significantly higher in the primary melanoma cell line WM-115 compared to the metastatic melanoma cell line WM-266-4 (Table 7.2). A further 32 proteins were significantly lower in WM-115 cells compared to WM-266-4 cells. The proteins displaying the greatest fold increase in abundance in WM-115

untreated cells were members of the annexin family (ANXA1 and ANXA2) and moesin (MSN) whilst there was also significant decrease in lambda crystallin homolog (CRYL1).

Table 7.2: Identified phosphoproteins altered in untreated WM-266-4 cells compared to untreated WM-115 cells. Phosphoproteins which demonstrated a fold-change of  $\geq 1.2$  and a p value ( $\leq 0.05$ ) were included for analysis.

Master No.	Protein ID	Fold Change	1-ANOVA	Gene I.D.
1193	Actin B	-4.59	2.3E-06	ACTB
1582	Annexin-A2	-3.74	1.4E-06	ANXA2
1619	Annexin-A1	-3.19	1.4E-06	ANXA1
730	Moesin	-3.18	.00012	MSN
1639	Annexin-A1	-3.07	1.4E-05	ANXA1
910	Protein disulfide isomerase-related protein 5	-2.82	3.8E-05	PDIA5
801	Transketolase	-2.68	0.00054	TKT
720	78 kDa glucose-regulated protein	-2.67	1.5E-05	GRP78
1494	Fructose biphosphate aldolase	-2.60	1.3E-05	ALDOA
1618	Glyceraldehyde-3-phosphate dehydrogenase	-2.53	5.4E-07	GAPDH
703	Radixin	-2.52	0.00087	RDX
694	Moesin	-2.50	0.0005	MSN
842	Protein disulfide isomerase-related protein 3	-2.38	0.00014	PDIA3
304	Glyceraldehyde-3-phosphate dehydrogenase	-2.29	1.2E-07	GAPDH
1151	Tryptophanyl-tRNA synthetase	-2.24	7.10E-07	WARS
837	Serum Albumin	-2.19	6.70E-05	ALB
1768	Glyceraldehyde-3-phosphate dehydrogenase	-2.11	0.0044	GAPDH
1620	Annexin-A2	-1.98	2.8E-05	ANXA2
1270	Citrate synthase	-1.96	0.0027	CS
2365	S100 calcium binding protein A10	-1.95	1.2E-06	S100A10
716	Radixin	-1.90	0.0021	RDX
1609	Annexin-A2	-1.88	2.3E-05	ANXA2
909	Protein disulfide isomerase-related protein 5	-1.85	0.0031	PDIA5
1245	Alpha-enolase	-1.81	9.6E-06	ENO1

<b>Master No.</b>	<b>Protein ID</b>	<b>Fold Change</b>	<b>1-ANOVA</b>	<b>Gene I.D.</b>
1024	Alpha-enolase	-1.78	5.5E-05	ENO1
1658	Annexin-A2	-1.73	1.10E-05	ANXA2
1480	Annexin-A1	-1.71	0.0073	ANXA1
683	Radixin	-1.61	0.0083	RDX
2017	Proteasome subunit beta type-1	-1.27	0.00055	PSBM1
1976	High mobility group protein B1	1.23	0.014	HMGB1
2090	Peroxiredoxin-2	1.29	0.0018	PRDX2
2223	Nucleoside diphosphate kinase A	1.42	0.00038	NDKA
855	Succinate dehydrogenase [ubiquinone] flavoprotein subunit	1.44	0.0003	SDHA
2070	Peroxiredoxin-2	1.47	0.0044	PRDX2
1170	Protein disulfide isomerise-related protein 5	1.52	0.016	PDIA5
1415	Actin B	1.54	0.0079	ACTB
975	Pyruvate kinase M2	1.54	0.001	PKM2
1113	Chain A, Human Tryptophanyl-tRNA Synthase	1.58	5.8E-6	WARS
453	Eukaryotic elongation factor 2	1.68	0.0044	EEF-2
1238	Alpha-enolase	1.78	0.012	ENO1
941	Stress-induced-phosphoprotein 1	1.78	3.7E-05	STIP1
1523	Annexin-A1	1.94	0.00038	ANXA1
1095	Protein disulfide isomerise-related protein 5	1.94	0.008	PDIA3
1772	Actin B-related protein 2/3 complex subunit 2	2.02	0.0004	ARPC2
800	Glycerol-3-phosphate dehydrogenase	2.05	0.00016	GPD1
1115	Suppression of tumorigenicity 13	2.07	0.00021	ST13
1139	Fascin 1	2.08	0.00021	FSCN 1
1091	Protein disulfide-isomerase A3	2.14	0.00039	PDIA3
1064	Protein disulfide-isomerase A3	2.2	2.00E-07	PDIA3
1063	Fascin 1	2.29	0.0011	FSCN1
964	Moesin	2.32	0.0001	MSN
1156	Glutathione synthetase	2.33	5.2E-07	GSHB
1083	Glucose-6-phosphate 1-dehydrogenase	2.46	4.3E-08	G6PD
1148	Tryptophanyl tRNA synthase isoform b	2.49	1.10E-08	WARS
1093	Protein disulfide-isomerase A3	2.7	3.30E-06	PDIA3
735	DNA K-type molecular chaperone HSPA5 precursor	2.79	1.7E-05	HSPA5
832	Heat shock cognate 71 kDa protein	3.15	7.3E-08	HSC71
984	Seryl-tRNA synthetase	3.42	1.8E-05	SARS
819	Heat shock-related 70 kDa protein 2	3.78	0.00016	HSPA1A
2148	Peroxiredoxin 2 isoform b	4.32	2.40E-08	PRDX2

Master No.	Protein ID	Fold Change	1-ANOVA	Gene I.D.
1752	Lambda-crystallin homolog	24.17	3.00E-10	CRYL1

In the WM-115 cells, 14 identified phosphoproteins were increased in the dasatinib treated cells compared to the control cells (Table 7.3). A further 18 phosphoproteins were decreased in dasatinib treated WM-115 cells compared to the untreated cells. MSN, peroxiredoxin 2 (PRDX2), 78 kDa glucose-regulated protein (GRP78) and radixin (RDX) displayed the largest fold decrease in abundance. Dasatinib treatment also increased the abundance of ANXA2 and S100 calcium binding protein A10 (S100A10).

Table 7.3: Identified phosphoproteins altered in WM-115 dasatinib treated cells compared to untreated WM-115 cells. Phosphoproteins which demonstrated a fold-change of  $\geq 1.2$  and a significant p value ( $\leq 0.05$ ) were included for analysis.

Master No.	Protein ID	Fold Change	1-ANOVA	Gene I.D.
730	Moesin	-2.98	0.00012	MSN
2148	Peroxiredoxin 2 isoform b	-2.69	2.40E-08	PRDX2
720	78 kDa glucose-regulated protein	-2.68	1.50E-05	GRP78
703	Radixin	-2.46	0.00087	RDX
801	Transketolase	-2.38	0.00054	TKT
694	Moesin	-2.30	0.0005	MSN
683	Radixin	-1.91	0.0083	RDX
837	Serum Albumin	-2.19	6.70E-05	ALB
842	Protein disulfide isomerase-related protein 3	-2.38	0.00014	PDIA3
716	Radixin	-1.84	0.0021	RDX
910	Protein disulfide isomerase-related protein 5	-1.73	3.80E-05	PDIA5
909	Protein disulfide isomerase-related protein 5	-1.66	0.0031	PDIA5
1768	Glyceraldehyde-3-phosphate dehydrogenase	-1.44	0.0044	GAPDH
756	Moesin	-1.41	0.034	MSN

Master No.	Protein ID	Fold Change	1-ANOVA	Gene I.D.
1480	Annexin-A1	-1.37	0.0073	ANXA1
1021	Glucose-6-phosphate 1-dehydrogenase	-1.34	0.02	G6PD
975	Pyruvate kinase M2	-1.34	0.001	PKM2
1245	Alpha-enolase	-1.31	9.60E-06	ENO1
1170	Protein disulfide isomerase-related protein 5	1.34	0.016	PDIA5
2090	Peroxiredoxin-2	1.35	0.0018	PRDX2
1960	Peroxiredoxin-4	1.36	0.0015	PRDX4
429	Alpha-Actinin-4	1.38	0.029	ACTN4
1619	Annexin-A1	1.40	1.40E-05	ANXA1
1618	Glyceraldehyde-3-phosphate dehydrogenase	1.43	5.40E-07	GAPDH
304	Glyceraldehyde-3-phosphate dehydrogenase	1.43	1.20E-07	GAPDH
1415	Actin B	1.51	0.0079	ACTB
784	Stress-70 protein	1.79	0.046	GRP75
1620	Annexin-A2	1.97	2.80E-05	ANXA2
1666	Annexin-A2	2.17	0.013	ANXA2
1609	Annexin-A2	3.02	2.30E-05	ANXA2
1658	Annexin-A2	3.06	1.10E-05	ANXA2
2365	S100 calcium binding protein A10	7.03	1.20E-06	S100A10

Of the proteins identified in WM-266-4 cells, dasatinib treatment decreased 6 and increased 1 phosphoprotein compared to untreated WM-266-4 cells (Table 7.4). The phosphoproteins which displayed the largest decrease in abundance were Annexin-3 (ANXA3), high mobility group protein B1 (HMGB1), whilst there was also an increase in PRDX2.

Table 7.4: Identified phosphoproteins altered in dasatinib treated WM-266-4 cells compared to untreated WM-266-4 cells. Phosphoproteins which demonstrated a fold-change of  $\geq 1.2$  and a significant p value ( $\leq 0.05$ ) were included for analysis.

Master No.	Protein ID	Fold Change	1-ANOVA	Gene I.D.
1671	Annexin-A3	-1.64	0.0018	ANXA3
1976	High mobility group protein B1	-1.57	0.014	HMGB1
719	Radixin	-1.42	0.0055	RXN

Master No.	Protein ID	Fold Change	1-ANOVA	Gene I.D.
832	Heat shock cognate 71 kDa protein	-1.33	7.30E-08	HSC71
720	78 kDa glucose-regulated protein	-1.29	1.50E-05	GRP78
1083	Glucose-6-phosphate 1-dehydrogenase	-1.22	4.30E-08	G6PD
2090	Peroxiredoxin-2	1.33	0.0018	PRDX2

Comparison of phosphoproteins identified in dasatinib treated WM-266-4 and WM-115 cells showed that 20 phosphoproteins were lower and 34 phosphoproteins were higher in dasatinib treated WM-266-4 cells compared to dasatinib treated WM-115 cells (Table 7.5). Four forms of ANXA2, which were identified, showed lower abundance in dasatinib-treated WM-266-4 than dasatinib-treated WM-115 cells, and lower levels of S100A10 were also observed. Significantly higher levels of CRYL1 and PRDX2 were observed in dasatinib treated WM-266-4 cells compared to dasatinib treated WM-115 cells.

Table 7.5: Identified phosphoproteins altered in dasatinib treated WM-266-4 cells compared to dasatinib treated WM-115 cells. Phosphoproteins which demonstrated a fold-change of  $\geq 1.2$  and a significant p value ( $\leq 0.05$ ) were included for analysis.

Master No.	Protein ID	Fold Change	1-ANOVA	Gene I.D.
2365	S100 calcium binding protein A10	-11.80	1.20E-06	S100A10
1658	Annexin-A2	-5.46	1.10E-05	ANXA2
1609	Annexin-A2	-5.35	2.30E-05	ANXA2
1582	Annexin-A2	-5.13	1.40E-06	ANXA2
1619	Annexin-A1	-4.49	1.40E-05	ANXA1
1913	Actin B	-3.98	2.30E-06	ACTB
1639	Annexin-A1	-3.98	1.40E-05	ANXA1
1620	Annexin-A2	-3.72	2.80E-05	ANXA2
304	Glyceraldehyde-3-phosphate dehydrogenase	-3.07	1.20E-07	GAPDH
1618	Glyceraldehyde-3-phosphate dehydrogenase	-3.01	5.40E-07	GAPDH
1024	Alpha Enolase	-2.81	5.50E-05	ENO1

<b>Master No.</b>	<b>Protein ID</b>	<b>Fold Change</b>	<b>1-ANOVA</b>	<b>Gene I.D.</b>
1666	Annexin-A2	-2.41	0.013	ANXA2
1151	Tryptophanyl-tRNA synthetase	-2.18	7.10E-07	WARS
1494	Fructose bisphosphate aldolase	-1.98	1.30E-05	ALDOA
1270	Citrate synthase	-1.6	0.0027	CS
1671	Annexin-A3	-1.58	0.0018	ANXA3
910	protein disulfide isomerase-related protein 5	-1.49	3.80E-05	PDIA5
2017	Proteasome subunit beta type-1	-1.44	0.00055	PSMB1
1245	Alpha Enolase	-1.42	9.60E-06	ENO1
1021	Glucose-6-phosphate 1-dehydrogenase	-1.22	0.02	G6PD
995	HSP60	1.25	0.037	HSP60
1960	Peroxiredoxin-4	1.25	0.0015	PRDX4
1856	Proteasome subunit alpha type a	1.29	0.021	PSMA4
2223	Nucleoside diphosphate kinase A	1.35	0.00038	NDKA
1817	Actin B-related protein 2/3 complex subunit 2	1.43	0.02	ARPC2
1098	Protein disulfide-isomerase A3	1.45	0.0014	PDIA3
855	Succinate dehydrogenase [ubiquinone] flavoprotein subunit	1.49	0.0003	SDHA
2269	Non-metastatic cells 2	1.51	0.012	NM23B
1523	Annexin A1	1.54	0.00038	ANXA1
1238	Alpha-enolase	1.72	0.012	ENO1
1113	Chain A; Human Tryptophanyl-Trna Synthase	1.78	5.80E-06	WARS
800	Glycerol-3-phosphate dehydrogenase	1.79	0.00016	GPDM
1772	Actin-related protein 2/3 complex subunit 2	1.86	0.0004	ARPC2
1095	Protein disulfide-isomerase A3	1.9	0.008	PDIA3
1064	Protein disulfide-isomerase A3	2.02	2.00E-07	PDIA3
453	Elongation factor 2	2.03	0.004	eEF2
1139	Fascin	2.11	0.00021	FSCN1
975	Pyruvate kinase M2	2.12	0.001	PKM2
1083	Glucose-6-phosphate 1-dehydrogenase	2.13	4.30E-08	G6PD
1115	suppression of tumorigenicity 13	2.16	0.00021	ST13
941	Stress-induced-phosphoprotein 1	2.21	3.70E-05	STIP1
1156	Glutathione synthetase	2.33	5.20E-07	GSHB
964	Moesin	2.42	0.0001	MSN
735	DNAK-type molecular chaperone HSPA5 precursor	2.45	1.70E-05	HSPA5
1093	Protein disulfide-isomerase A3	2.57	3.30E-06	PDIA3
1148	Tryptophanyl tRNA synthase isoform b	2.61	1.10E-08	WARS
1063	Fascin 1	2.63	0.0011	FSCN1

Master No.	Protein ID	Fold Change	1-ANOVA	Gene I.D.
832	Heat shock cognate 71 kDa protein	2.68	7.30E-08	HSC71
1091	Protein disulfide-isomerase A3	2.72	0.00039	PDIA3
814	Tryptophanyl-tRNA synthetase	2.77	0.0032	WARS
984	Seryl-tRNA synthetase	3.78	1.80E-05	SARS
819	Heat shock-related 70 kDa protein 2	4.45	0.00016	HSP72
2148	Peroxiredoxin 2 isoform b	9.57	2.40E-08	PRDX2
1752	Lambda-crystallin homolog	28.09	3.00E-10	CRYL1

#### 7.4 Phosphoproteins uniquely associated with dasatinib treatment in sensitive and resistant cell lines

We compared the lists of phosphoproteins altered in dasatinib-treated WM-115 (Table 7.3) and dasatinib-treated WM-266-4 cells (Table 7.4) to identify phosphoproteins that may be uniquely associated with dasatinib response in WM-115 or dasatinib resistance in WM-266-4 (Figure 7.2). Two of the identified phosphoproteins were significantly altered in response to dasatinib in both WM-115 and WM-266-4 cells. However, 31 phosphoproteins were uniquely altered in WM-115 cells (Table 7.6) and 4 phosphoproteins were altered only in WM-266-4 cells (Table 7.7), in response to dasatinib treatment.

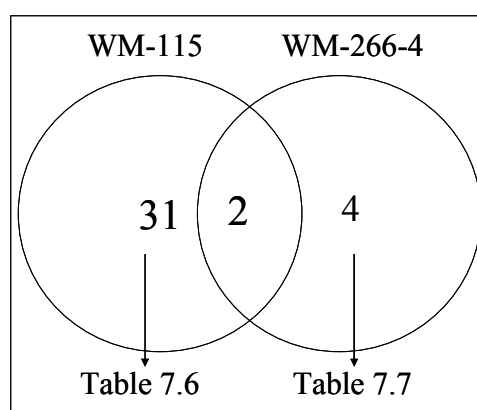


Figure 7.2: Venn diagram displaying the number of altered phosphoproteins in response to dasatinib treatment in WM-115 compared to WM-266-4 cells.



#### 7.4.1 Phosphoproteins uniquely altered in response to dasatinib treatment in sensitive WM-115 cells

Of the 31 phosphoproteins uniquely altered in dasatinib treated WM-115 cells, 17 phosphoproteins were reduced in abundance (Table 7.6). Focussing on the proteins which showed the greatest fold change, 2 spots of protein disulfide isomerase-related protein 5 (PDIA5) were reduced by 1.73 and 1.66 respectively. Abundance of two moesin (MSN) and two radixin (RXN) isoforms were also reduced in dasatinib treated WM-115 cells by 2.98 fold, 2.3 fold, 1.91 fold and 1.84 fold, respectively. Dasatinib treatment of WM-115 cells also resulted in increased abundance of 14 phosphoproteins, which were not altered in dasatinib-treated WM-266-4 cells. Four forms of annexin-2 (ANXA2) were increased by 1.97, 2.17, 3.02 and 3.06 fold when WM-115 cells were treated with dasatinib.

Table 7.6: Identified phosphoproteins uniquely altered in dasatinib treated WM-115 cells. Phosphoproteins which demonstrated a fold-change of  $\geq 1.2$  and a significant p value ( $\leq 0.05$ ) were included for analysis.

Master No.	Protein ID	Fold Change	1-ANOVA	Gene I.D.
730	Moesin	-2.98	0.00012	MSN
2148	Peroxiredoxin 2 isoform b	-2.69	2.40E-08	PRDX2
703	Radixin	-2.46	0.00087	RDX
801	Transketolase	-2.38	0.00054	TKT
694	Moesin	-2.3	0.0005	MSN
683	Radixin	-1.91	0.0083	RXN
837	Serum Albumin	-1.9	6.70E-05	ALB
842	Protein disulfide isomerase-related protein 3	-1.9	0.00014	PDIA3
716	Radixin	-1.84	0.0021	RXN
910	Protein disulfide isomerase-related protein 5	-1.73	3.80E-05	PDIA5
909	Protein disulfide isomerase-related protein 5	-1.66	0.0031	PDIA5

Master No.	Protein ID	Fold Change	1-ANOVA	Gene I.D.
1768	Glyceraldehyde-3-phosphate dehydrogenase	-1.44	0.0044	GAPDH
756	Moesin	-1.41	0.034	MSN
1480	Annexin A1	-1.37	0.0073	ANXA1
975	Pyruvate kinase M2	-1.34	0.001	PKM2
1021	Glucose-6-phosphate 1-dehydrogenase	-1.34	0.02	G6PD
1245	Alpha-enolase	-1.31	9.60E-06	ENO1
1170	Protein disulfide isomerase-related protein 5	1.34	0.016	PDIA5
1960	Peroxiredoxin-4	1.36	0.0015	PRDX4
429	Alpha-actinin-4	1.38	0.029	ACTN4
1619	Annexin-A1	1.4	1.40E-05	ANXA1
304	Glyceraldehyde-3-phosphate dehydrogenase	1.43	1.20E-07	GAPDH
1618	Glyceraldehyde-3-phosphate dehydrogenase	1.43	5.40E-07	GAPDH
1415	Actin B	1.51	0.0079	ACTB
784	Stress-70 protein	1.79	0.046	GRP75
1620	Annexin A2	1.97	2.80E-05	ANXA2
1666	Annexin-A2	2.17	0.013	ANXA2
1609	Annexin-A2	3.02	2.30E-05	ANXA2
1658	Annexin-A2	3.06	1.10E-05	ANXA2
2365	S100A10	7.03	1.20E-06	S100A10

#### 7.4.2 Phosphoproteins uniquely altered in response to dasatinib treatment in resistant WM-266-4 cells

Dasatinib treatment of WM-266-4 cells resulted in the alteration of 4 phosphoproteins which were not altered in WM-115 cells treated with dasatinib (Table 7.7). Of the 4 phosphoproteins that were decreased in response to dasatinib, annexin-A3 (ANXA3) was decreased 1.64 fold and high mobility group protein B1 (HMGB1) was decreased by 1.57 fold. Heat shock cognate 71 (HSC71) was also decreased, by 1.33 fold, in response to dasatinib treatment. No phosphoproteins were increased in WM-266-4 cells treated with dasatinib.

Table 7.7: Identified phosphoproteins uniquely altered in dasatinib treated WM-266-4 cells. Phosphoproteins which demonstrated a fold-change of  $\geq 1.2$  and a significant p value ( $\leq 0.05$ ) were included for analysis.

Master No.	Protein ID	Fold Change	1-ANOVA	Gene I.D.
1671	Annexin-A3	-1.64	0.0018	ANXA3
1976	High mobility group protein B1	-1.57	0.014	HMGB1
832	Heat shock cognate 71 kDa protein	-1.33	7.30E-08	HSC71
1083	Glucose-6-phosphate 1-dehydrogenase	-1.22	4.30E-08	G6PD

### 7.5 PANTHER analysis of identified phosphoproteins

The list of 36 phosphoproteins uniquely altered in dasatinib-treated WM-115 or WM-266-4 cells were annotated to 22 gene symbols using NCBI and submitted to PANTHER (Protein ANalysis THrough Evolutionary Relationships; <http://www.pantherdb.org/>) for functional annotation analysis, to identify the possible cellular functions or pathways impacted by the phosphoproteins which were altered by dasatinib treatment. Dasatinib treatment of WM-115 and WM-266-4 cells resulted in changes to 19 and 3 specific proteins respectively (see Appendix 1), with multiple potential phosphoprotein isoforms detected for some of these proteins, e.g. ANXA2. The 22 individual proteins are associated with 13 biological processes (Table 7.8).

Treatment of WM-115 cells with dasatinib resulted in alterations to several phosphoproteins associated with the biological processes ‘Cell structure and motility (BP00285)’ (6 proteins), ‘Carbohydrate metabolism (BP00001)’ (4 proteins), and ‘Protein metabolism and modification (BP00060)’ (5 proteins) (See appendix 2). In comparison, dasatinib treatment of WM-266-4 cells resulted in no alterations of proteins involved in ‘Cell structure and motility’ and ‘Carbohydrate metabolism’ and 1 protein in ‘Protein metabolism and modification’.

Dasatinib treatment of WM-115 cells altered 6 phosphoproteins associated with the biological process 'Cell structure and motility' (ANXA1, RDX, MSN, ACTB, ACTN4 and ANXA2) whereas no altered proteins were identified in this category for WM-266-4 cells (Appendix 2). 'Cell structure and motility' (BP00285) was further sub-divided into two "child" categories. 'Cell motility' (BP00287) containing ANXA1 and 'Cell structure' (BP00286) containing RDX, MSN, ACTB and ACTN4, with ANXA2 unclassified. This indicates ANXA1 may play a role in dasatinib-mediated effects on motility in WM-115 cells.

Dasatinib treatment of WM-115 resulted in alteration of 5 phosphoproteins related to the biological process 'Protein metabolism and modification' (BP00060) (GRP78, PDIA5, PDIA3, GRP75 and TKT) compared to 1 phosphoprotein which was altered in dasatinib treated WM-266-4 cells (HSC71). Protein metabolism and modification has three "child" categories 'Protein complex assembly' (BP00072), 'Protein folding' (BP00062) and 'Protein modification' (BP00063). In WM-115 cells, dasatinib altered phosphorylation of GRP75 and GRP78 which are associated with 'Protein complex assembly' and 'Protein folding' and PDIA5, PDIA3 and TKT which are associated with 'Protein modification'. Dasatinib treatment of WM-266-4 cells only resulted in an alteration of HSC71, which is related to 'Protein metabolism and modification'.

Four proteins which were altered in response to dasatinib treatment of WM-115 cells (ALDOA, ENO1, G6PD and PKM2) are involved in carbohydrate metabolism (BP00001) while no altered proteins were detected in this category for WM-266-4

cells. Using PANTHER pathway analysis we identified that dasatinib treatment of WM-115 and WM-266-4 cells altered proteins involved in apoptosis signalling (P00006). Two phosphoproteins were altered in dasatinib treated WM-115 cells (GRP75 and GRP78) compared to the alteration of 1 phosphoprotein in WM-266-4 cells (HSC71). All three proteins are members of the HSP70 family.

Table 7.8: Panther analysis of the 22 annotated individual proteins identified by 2D-DIGE analysis. Swiss-Prot IDs were annotated to NCBI human Genbank gene symbols and PANTHER analysis (<http://www.pantherdb.org/>) was performed.

Panther Analysis	Category Name	WM-115 Ctrl vs Dasat	WM-266-4 Ctrl vs Dasat
		# proteins identified in gene ontology	
Biological Process	Cell structure and motility	6	0
	Carbohydrate metabolism	4	0
	Protein metabolism and modification	5	1
	Immunity and defence	4	1
	Signal transduction	2	1
	Lipid, fatty acid and steroid metabolism	1	1
	Developmental processes	2	0
	Intracellular protein traffic	2	0
	Transport	2	0
	Biological process unclassified	1	1
	Cell cycle	1	0
	Amino acid metabolism	1	0
	Coenzyme and prosthetic group metabolism	1	0
Pathway	Apoptosis signalling pathway	2	1
	Glycolysis	2	1
	Parkinson disease	2	1
	Pyruvate metabolism	1	0
	Integrin signalling pathway	1	0

### 7.6 Pathway Studio analysis of phosphoproteins altered in dasatinib treated melanoma cells

We performed literature mining using the list of 22 unique proteins identified from dasatinib treated WM-115 and WM-266-4 cells. We firstly examined the relationship between these proteins and melanoma (Figure 7.3). Pathway Studio analysis showed that of the 22 proteins identified, which were altered in response to

dasatinib, 11 have been previously linked in the literature to melanoma. Two members of the annexin family (ANXA1, ANXA2), and two members of the heat shock family 70 family (HSPA5, HSPA8) were found to be linked to melanoma in the literature.

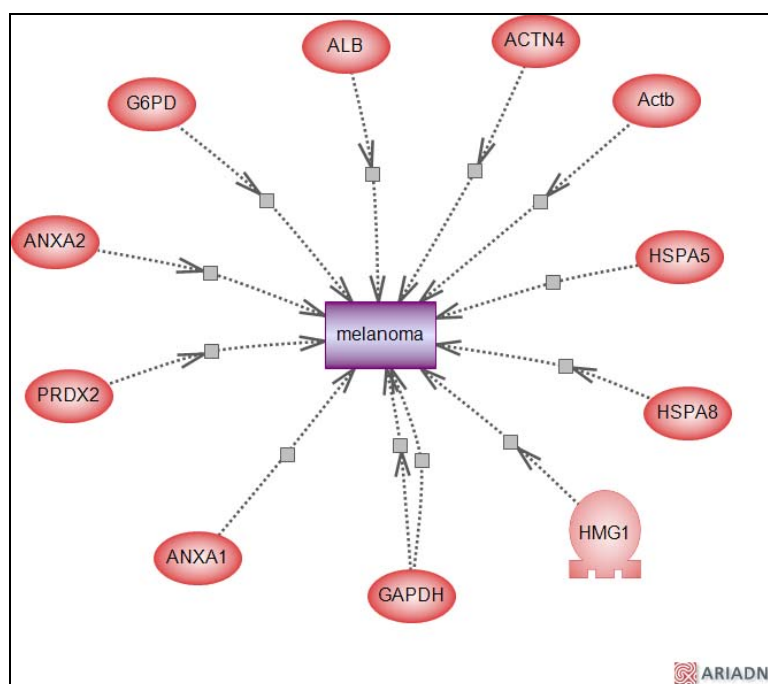
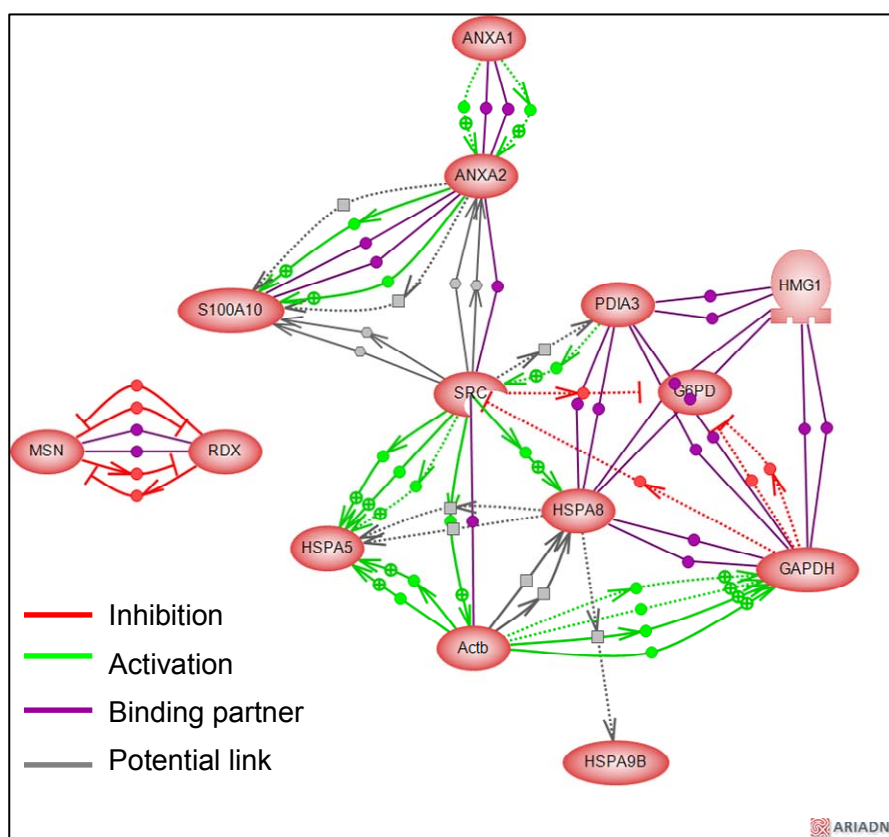


Figure 7.3: Pathway studio literature mining analysis linking melanoma-related studies with proteins from the 22 unique proteins altered in response to dasatinib treatment.

By analysing the direct interactions between the identified phosphoproteins, we found that 13 of the 22 proteins have been shown to have direct interactions with one another. ANXA1 phosphorylates ANXA2, whilst ANXA2 can also phosphorylate S100A10. Members of the HSP 70 family (HSPA8 and HSPA5) have been shown in the literature to directly interact with Src kinase, whilst HSPA8 can bind to PDIA3, GAPDH and HMG1.

SRC kinase was not identified from our proteomic analysis; however dasatinib directly targets it [169]. We therefore examined whether any of our identified targets have been shown to interact with SRC kinase. Interestingly, Pathway Studio analysis have been shown to interact with SRC kinase. Interestingly, Pathway Studio analysis determined that SRC kinase has been previously shown to directly interact with ANXA2, S100A10, PDIA3, G6PD, HSPA8, ACTB, HSPA5 and GAPDH.

Figure 7.4: Direct Interactions between list of 22 phosphoproteins and SRC kinase identified using Pathway Studio literature mining analysis.



### 7.7 Selection of phosphoproteins for further investigation

Due to the multiple spots of ANXA2 identified in the 2D-DIGE analysis, the high fold changes observed, particularly in the dasatinib-treated WM-115 cells, and the literature-based evidence for links between ANXA2 and Src kinase we chose to further analyse the ANXA2 isoforms. Five different ANXA2 spots were identified from phosphoproteomic analysis; 4 which were only altered in WM-115 cells (Spot



ID 1609, 1658, 1620 and 1666) and 1 only altered in WM-266-4 cells (Spot ID 1582) (Table 7.9 and Figure 7.5).

In WM-115 cells, dasatinib treatment resulted in an increase in the levels of 4 of the identified ANXA2 phosphoproteins. Treatment with dasatinib in WM-115 cells did not alter the level of Spot ID 1582; however the abundance of this ANXA2 spot was decreased in response to dasatinib treatment in WM-266-4 cells.

Table 7.9: Protein abundance analysis comparing levels of five annexin-A2 spots in WM-115 versus WM-266-4 cells, untreated versus dasatinib treated WM-115 cells, untreated versus dasatinib treated WM-266-4 cells and dasatinib treated WM-115 cells versus dasatinib treated WM-266-4 cells analysed by the DeCyder software. ‘\*\*’ indicates that the difference in fold change between the two samples is significant as calculated by Students t-test.

Spot ID	WM115 vs WM266-4	WM115 Dasat vs Ctrl	WM266-4 Dasat vs Ctrl	WM115 Dasat vs WM266-4 Dasat
1582	-3.74 *	1.10 *	-1.24 *	-5.13
1609	-1.88 *	3.02 *	1.06	-5.35 *
1620	-1.98 *	1.97 *	1.05	-3.72 *
1658	-1.73 *	3.06 *	-1.03	-5.46 *
1666	-1.26	2.17 *	1.14	-2.41 *

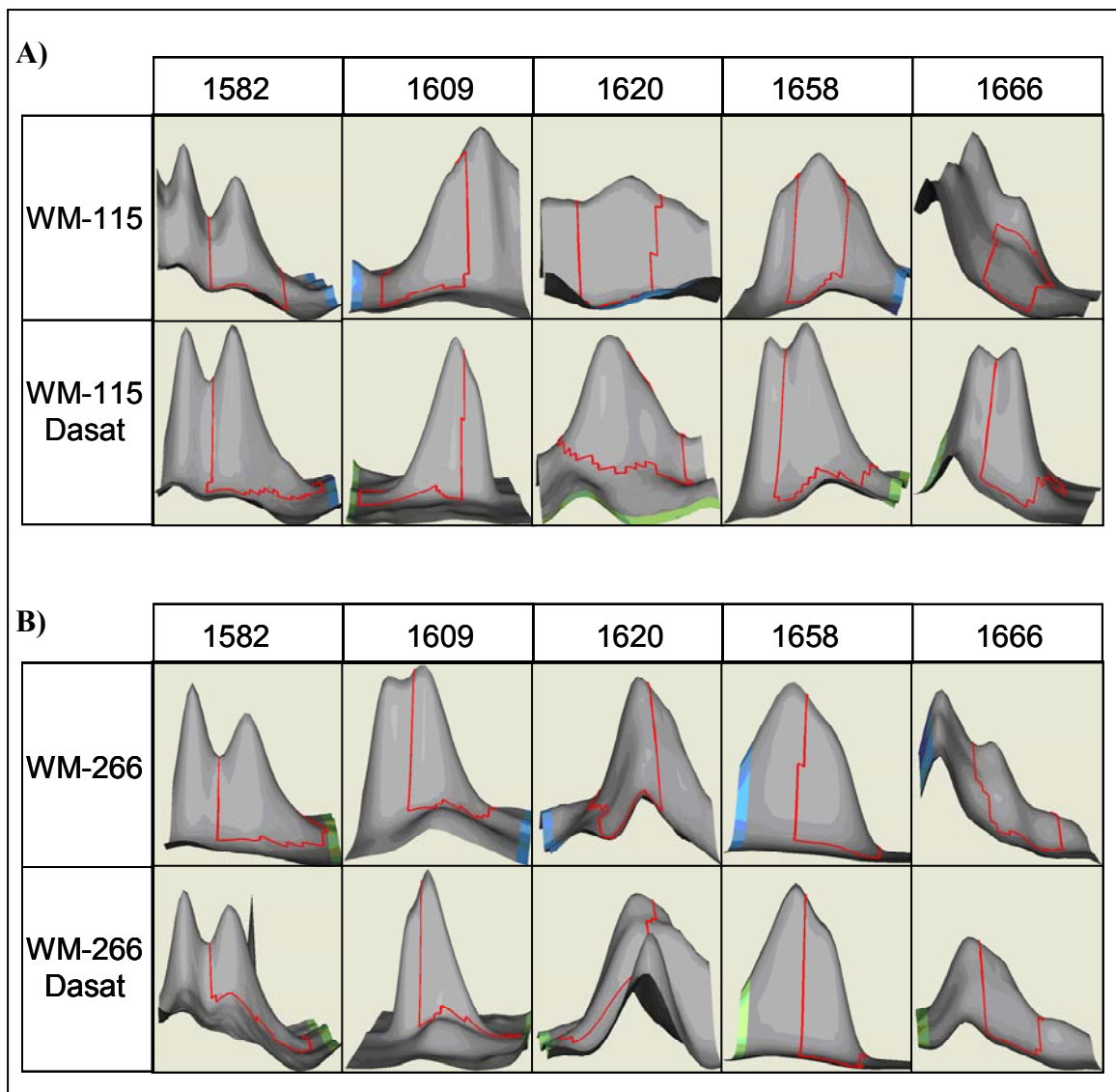


Figure 7.5: A) Protein abundance analysis comparing levels of five annexin-A2 spots in untreated and dasatinib treated WM-115 cells analysed by the DeCyder software. B) Protein abundance analysis comparing levels of five annexin-A2 spots in untreated and dasatinib treated WM-266-4 cells analysed by the DeCyder software.

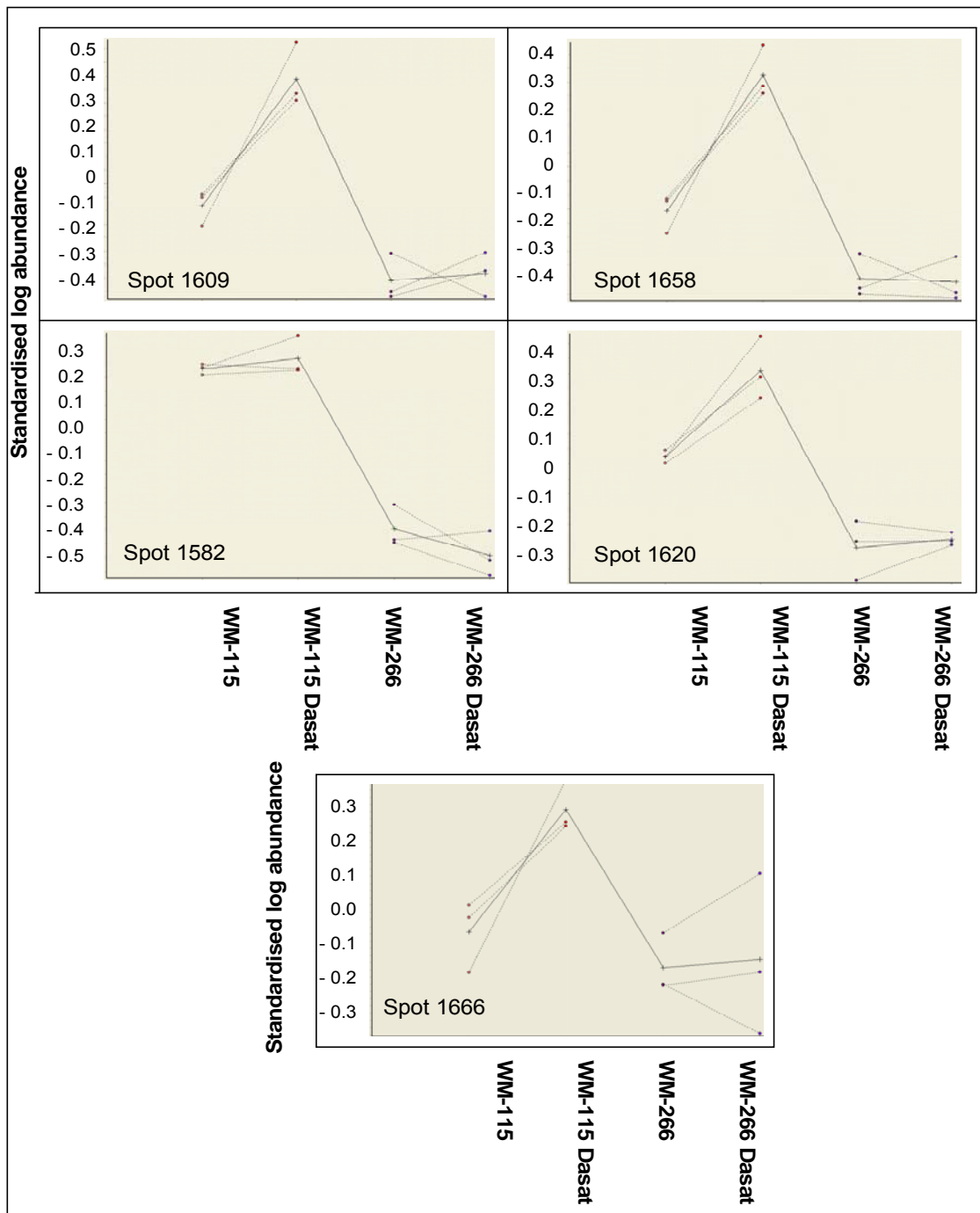


Figure 7.7: Changes in levels of the ANXA2 proteins identified, in untreated and dasatinib treated WM-115 and WM-266-4 cells, analysed by the DeCyder software. The solid line in the graph is the average of triplicate measurements (dotted lines) of protein abundance.

## 7.8 Identification of phosphorylated peptides

The MALDI-ToF-ToF-MS analysis also provides information on the amount of the total protein sequence, or the percent coverage, that was identified for each protein, and on potential post-translational modifications of the identified proteins, such as the presence of potential phosphorylation sites. The average percent coverage of the 4 ANXA2 spots identified was 48.75 %.

A MASCOT score is calculated for each protein identified and reflects the level of confidence in the identification. Figure 7.8 shows an example of an identified protein sequence; protein ID no. 1658 (ANXA2), which had a high MASCOT score of 605, and 59 % protein coverage. Each individual peptide sequenced is also given an ion score, which indicates the level of homology between the peptide sequence and the protein identified.

1	MSTVHEILCK	LSLEGDHSTP	PSAYGSVKAY	TNFDAERDAL	NIETAIKTKG
51	VDEVTIVNIL	TNRSNAQRQD	IAFAYQRRTK	KELASALKSA	LSGHLETVIL
101	GLLKTPAQYD	ASELKASMKG	LGTDEDSLIE	IICSRTNQEL	QEINRVYKEM
151	YKTDLEKDII	SDTSGDFRKL	MVALAKGRRA	EDGSVIDYEL	IDQDARDLYD
201	AGVKRKGTDV	PKWISIMTER	SVPHLQKVFD	RYKSYSPTYDM	LESIRKEVKG
251	DLENAFLNLV	QCIQNKPLYF	ADRLYDSMKG	KGTRDKVLIR	IMVSRSEVDM
301	LKIRSEFKRK	YGKSLYYYYIQ	QDTKGDYQKA	LLYLCEGDD	

Figure 7.8: Protein sequence of protein spot no. 1658, ANXA2, showing the matched peptide sequences are in red (59 % coverage). The green peptide sequence corresponds to amino acids 120 – 135, which had a high ion score of 122, indicating a high level of homology with ANXA2.

MALDI-ToF-ToF-MS data was available for 4 of the identified ANXA2 proteins and was analysed for potential post-translational modifications. MALDI-ToF-ToF-MS analysis did not detect any post-translation modifications on ANXA2 spots no. 1609,

1658 and 1666. One potential phosphorylation site in amino acid residues 232-245 and two potential phosphorylation sites in amino acid residues 274-281 were detected for ANXA2 spot 1658. Sequence 232-245 includes three tyrosine residues and two serine residues, whilst sequence 274-281 contains one serine residue and one tyrosine residue.

Table 7.10: Matched peptide information for identified isoforms of ANXA2 proteins, showing MASCOT scores, % coverage and highest ion score obtained for the matched peptides. Peptide sequences with potential phosphorylation sites and the number of potential phosphorylation sites detected are listed.

<b>Protein I.D.</b>		<b>1609</b>	<b>1620</b>	<b>1658</b>	<b>1666</b>
<b>Fold Change</b>		3.02	1.97	3.06	2.17
<b>MASCOT Score</b>		266	174	605	251
<b>% Coverage</b>		48 %	38 %	59 %	50 %
<b>Highest Ion Score</b>		62	44	122	52
<b>Total no. of phosphate groups identified</b>		0	0	3	0
<b>Peptide sequences and no. of phosphate groups identified</b>					
<b>232-245</b>	R.YKSYSPYDMLLESIR.K	0	0	<b>1</b>	0
<b>274-281</b>	R.LYDSMKGK.G	0	0	<b>2</b>	0

### 7.9 Pro-Q Diamond staining of phosphoproteins in WM-266-4 cells

Pro-Q Diamond is a stain which binds specifically to phosphorylated proteins. We used Pro-Q Diamond staining to identify proteins that display altered phosphorylation in response to dasatinib treatment in WM-266-4 cells. Insufficient phosphoprotein was available to perform this analysis on the WM-115 cells.

Pro-Q Diamond staining was performed on unlabelled phosphoprotein samples separated on duplicate 2D gels (Figure 7.9) (section 2.21). The results of each set of replicate gels were analysed using the ProGenesis SameSpots software where the intensity of the stained proteins was measured. The ProGenesis software produces images which allow comparison of phosphorylation levels between samples, and constructs graphs of phosphorylation levels for each of the proteins analysed (Figure 7.10).

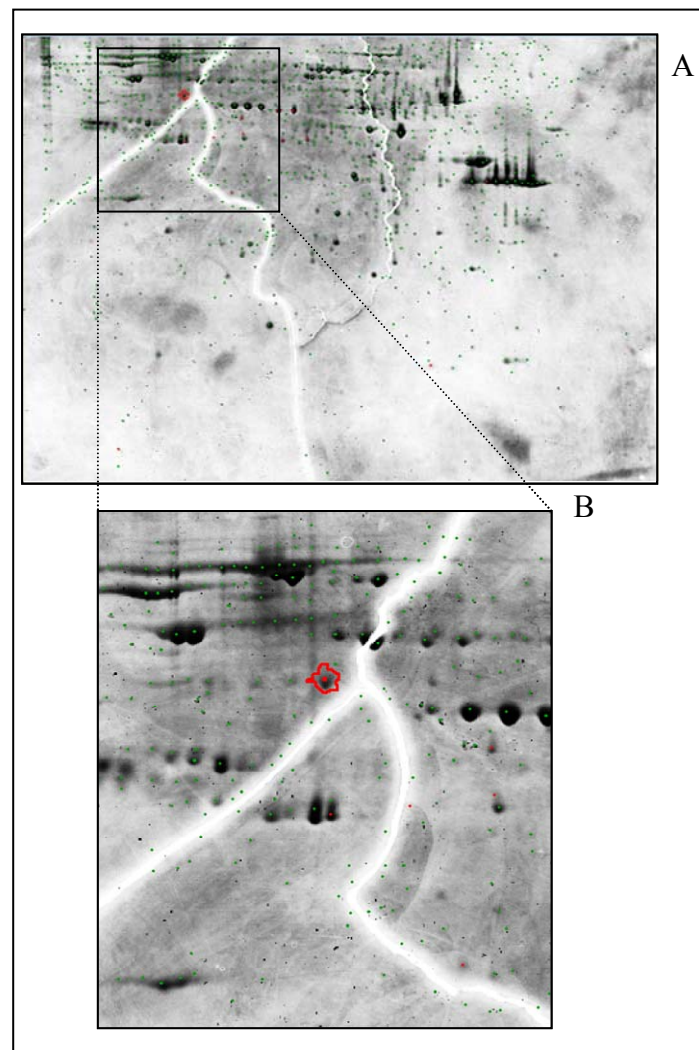


Figure 7.9: (A) 2D gel of WM-266-4 control stained with Pro-Q Diamond. (B) Zoom in on the upper region of the gel, with the location of spot ID 995 (HSP60) circled.

A total of five proteins which displayed altered levels of phosphorylation in response to dasatinib treatment in WM-266-4 cells were identified (Table 7.11). Of the 5 proteins identified, heat shock protein 60 (HSP60) and endoplasmic reticulum protein 29 (ERP29) displayed the highest fold changes; 7.9 fold increase for HSP60 and 5.4 fold increase for ERP29. Other proteins identified which display altered phosphorylation levels included endoplasmic reticulum protein 60 (ERP60) and non-metastatic cells-1 (NM23), however the fold changes observed in phosphorylation levels for both proteins were low in comparison to HSP60 and ERP29.

Table 7.11: Proteins which displayed altered phosphorylation levels in dasatinib-treated compared to control WM-266-4 cells, determined by SameSpots software. Phosphoproteins which demonstrated a fold-change of  $\geq 1.2$  and a significant p value ( $\leq 0.05$ ) were included for analysis.

<b>Master No.</b>	<b>Protein ID</b>	<b>Fold Change</b>	<b>1-ANOVA</b>	<b>Gene I.D.</b>
837	Serum Albumin	1.5	0.0407	SA
1064	Endoplasmic reticulum protein 60	1.6	0.0256	ERP60
2269	Non-metastatic cells 1	2.3	0.00518	NM23
1983	Endoplasmic reticulum protein 29	5.4	0.0071	ERP29
995	Heat Shock protein 60	7.9	0.0022	HSP60

We cross-referenced the change in levels of phosphorylation of both HSP60 and ERP29 with the abundance information previously obtained from the 2D-DIGE analysis on the same phosphoprotein samples (Figure 7.10A and B). The abundance levels of HSP60 (1.14) and ERP29 (-1.15) were not significantly altered in WM-266-4 cells in response to dasatinib treatment, according to the 2D-DIGE analysis.

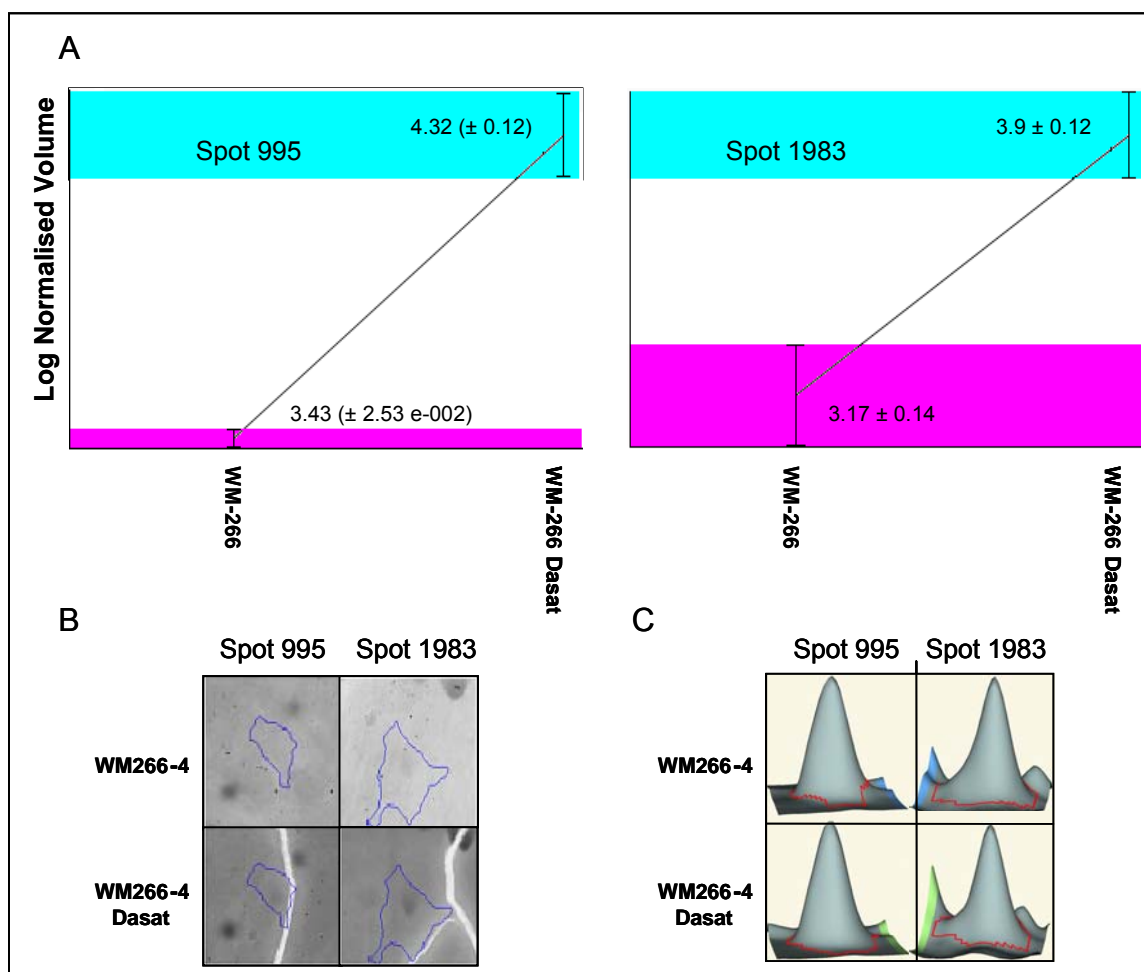


Figure 7.10: A) SameSpots analysis displaying the change in the level of phosphorylation of HSP60 (Spot 995) and ERP29 (Spot 1983) in dasatinib treated compared to untreated WM-266-4 cells. B) Pro-Q Diamond staining of HSP60 and ERP29 in dasatinib untreated and treated WM-266-4 cells C) DeCyder analysis of 2D-DIGE displaying the abundance levels for HSP60 and ERP29 in dasatinib untreated and treated WM-266-4 cells.



## 7.10 Summary

We performed phosphoprotein profiling in a primary melanoma cell line and a metastatic melanoma cell line derived from the same patient. We also studied the effect of dasatinib treatment on both cell lines which display differences in sensitivity to dasatinib.

Using 2-D DIGE analysis of this model 203 phosphoproteins showed altered abundance either between the primary and metastatic cell line, or in response to dasatinib treatment in either cell line. Members of the annexin family, in particular ANXA1, ANXA2 and ANXA3 displayed altered phosphoprotein abundance when treated with dasatinib in both WM-115 and WM-266-4 cells. As the abundance of 4 isoforms of annexin-2 were altered by dasatinib treatment in WM-115 cells, while only 1 isoform was significantly altered in WM-266-4 cells treated with dasatinib, this suggests that alterations in ANXA2 may play a role in response to dasatinib in WM-115 cells.

Pathway Studio analysis confirmed that ANXA1 and ANXA2 have been previously associated with melanoma. PANTHER analysis suggests that ANXA1 and ANXA2 may be associated with motility and cell structure. ANXA2 and S100A10 were also the only identified proteins which are associated with and phosphorylated by SRC.

Using Pro-Q Diamond analysis of untreated versus dasatinib treated WM-266-4 cells we identified a small number of proteins which displayed altered phosphorylation status. Of the identified phosphoproteins, HSP60 and ERP29 displayed the greatest fold change in phosphorylation, although the abundance of both proteins was

unchanged according to the 2D-DIGE analysis. Changes in the phosphorylation status of HSP60 and ERP29 may play a role in dasatinib resistance in WM-266-4 cells.

Appendix 1: NCBI Annotated phosphoproteins identified by 2D-DIGE analysis used for PANTHER and Pathway Studio analysis. Swiss-Prot IDs were annotated to NCBI human Genbank gene symbols

<b>WM-115 dasatinib treatment</b>	<b>WM-266-4 dasatinib treatment</b>
ACTB	ANXA3
ACTN4	HMGB1
ALB	HSC71
ANXA1	
ANXA2	
ENO1	
G6PD	
GAPDH	
GRP75	
GRP78	
MSN	
PDIA3	
PDIA5	
PKM2	
PRDX2	
PRDX4	
RDX	
S100A10	
TKT	

Appendix 2: The biological processes and pathways associated with the annotated list of proteins identified by dasatinib treatment of WM-115 and WM-266-4 melanoma cell lines. Red gene symbols signify proteins that were identified from the WM-266-4 dassatinib treated cells.

<b>PANTHER analysis</b>	<b>Biological Process</b>	<b>Identified Proteins</b>
<b>Biological Process</b>	Cell structure and motility	ANXA2, ANXA1, RDX, MSN, ACTN4, ACTB
	Carbohydrate metabolism	ENO1, PKM2, TKT, G6PD
	Protein metabolism and modification	HSPA5, PDIA5, PDIA3, GRP75, TKT, <b>HSPA8</b>
	Immunity and defence	PRDX4, PRDX2, GRP75, GRP78, <b>HSPA8</b>
	Signal transduction	ANXA1, TKT
	Lipid, fatty acid and steroid metabolism	ANXA1, <b>ANXA3</b>
	Developmental processes	ANXA2, S100A10
	Intracellular protein traffic	ANXA2, ACTB
	Transport	ALB, ACTB
	Biological process unclassified	GAPDH, <b>HMGB1</b>
	Cell cycle	ACTB
	Coenzyme and prosthetic group metabolism	TKT
	<b>Pathway</b>	Apoptosis signalling pathway
Glycolysis		ENO1, PKM2
Parkinson disease		GRP75, GRP78, <b>HSPA8</b>
Pyruvate metabolism		PKM2
Integrin signalling pathway		ACTN4

## **Chapter 8**

### **8. Analysis of targets implicated in dasatinib sensitivity and resistance in melanoma cell lines**

## 8.1 Introduction

Following 2-D DIGE and Pro-Q Diamond phosphoprotein analysis we identified several proteins that may be associated with dasatinib sensitivity or resistance in the melanoma cell lines WM-115 and WM-266-4. The approach we used for functional validation of these targets was immunoblotting followed by siRNA knockdown for selected targets. We initially optimised siRNA transfection in the melanoma cell lines using a range of transfection protocols and reagents, and used the siRNA transfection to examine the effect of SRC knockdown on proliferation in both WM-115 and WM-266-4 cell lines.

The following targets were selected for validation by immunoblotting, ANXA2 which was identified by 2D-DIGE analysis, ERP29 and HSP60 which were identified by Pro-Q Diamond staining. The proteomic results for these three targets are summarised in table 8.1.

Table 8.1: Review of the proteomic analysis by 2-D DIGE analysis and Pro-Q diamond staining for each target selected for validation by immunoblotting.

Target	WM-115 vs. WM-115 dasatinib		WM-266-4 vs. WM-266-4 dasatinib			
ANXA2	2-D DIGE	ID 1609	3.02 fold	2-D DIGE	ID 1609	1.06 fold
		ID 1620	1.97 fold		ID 1620	1.05 fold
		ID 1658	3.06 fold		ID 1658	-1.03 fold
		ID 1666	2.17 fold		ID 1666	1.14 fold
ERP29	2-D DIGE	-1.04		2-D DIGE	-1.15 fold	
	Pro-Q Diamond	N/A		Pro-Q Diamond	5.4 fold	
HSP60	2-D DIGE	1.13		2-D DIGE	1.14 fold	
	Pro-Q Diamond	N/A		Pro-Q Diamond	7.9 fold	

## 8.2 Optimisation studies for siRNA knockdown in melanoma cell lines

SiRNA transfection conditions were optimised using the transfection reagents NeoFX (Ambion), Lipofectamine 2000 (Invitrogen), Genejuice (Novagen), Ribojuice (Novagen) and Interferin (Polyplus transfection) and kinesin siRNA which should cause inhibition of proliferation [187] (section 2.22) (Figure 8.1 and Figure 8.2).

In WM-115 cells Genejuice and NeoFX were both ineffective when tested with kinesin siRNA (Figure 8.1). Kinesin siRNA transfection using Lipofectamine 2000, Ribojuice and Interferin achieved significant inhibition of proliferation in WM-115 cells; however the Ribojuice reagent was also highly toxic to the cells on its own.

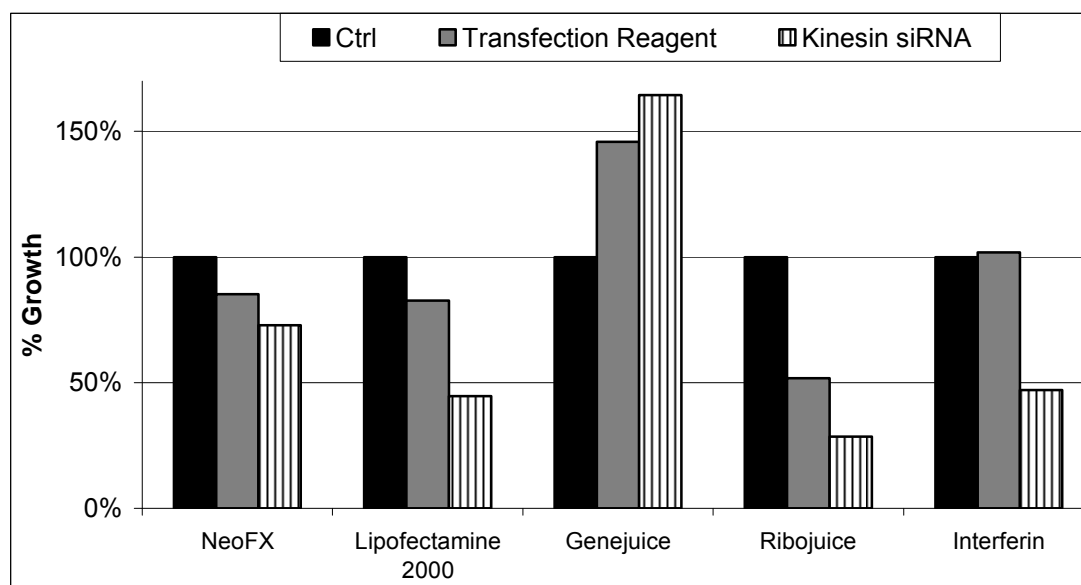


Figure 8.1: Transfection of kinesin siRNA in WM-115 cells using a range of transfection reagents. % growth is expressed relative to control untreated cells.

In WM-266-4 cells, Genejuice and NeoFX were ineffective when tested with kinesin siRNA (Figure 8.2). Transfection of kinesin siRNA with Lipofectamine 2000,

Ribojuice and Interferin showed significant inhibition of proliferation in WM-266-4, but the Ribojuice transfection reagent was again highly toxic on its own.

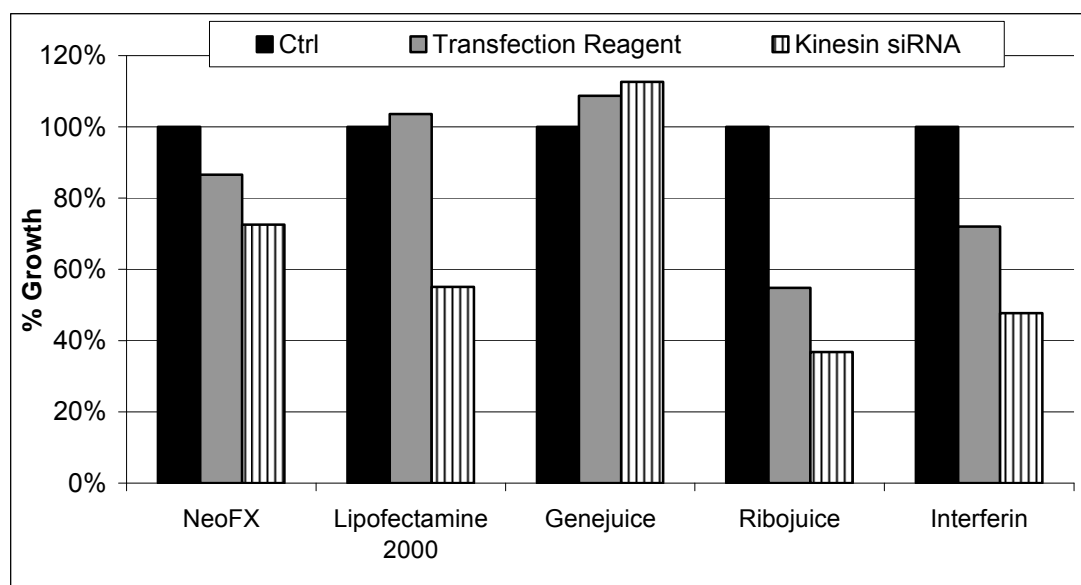


Figure 8.2: Transfection of kinesin siRNA in WM-266-4 cells using a range of transfection reagents. % growth is expressed relative to control untreated cells. These results are from a single experiment.

In WM-115 cells, Interferin was non-toxic to the cells, but it was more toxic than Lipofectamine 2000 in WM-266-4 cells. Due to the efficient inhibition of growth achieved with kinesin siRNA and low toxicity to the cells, Lipofectamine 2000 was selected as the transfection reagent for future siRNA experiments.

### 8.3 SRC siRNA

#### 8.3.1 SRC siRNA in WM-115

The effect of SRC knockdown on proliferation was assessed using three commercial siRNAs (Ambion) (section 2.22). The three siRNAs were also combined to create a siRNA pool. The efficiency of SRC knockdown was examined by western blotting.

The negative control siRNA (scrambled) had little effect on SRC levels (Figure 8.3). SRC siRNAs 1 and 2 (SRC1 and SRC2) significantly reduced SRC levels compared to scrambled siRNA ( $p = 0.04$ ;  $p = 0.05$ ). However, neither SRC3 nor SRC pool siRNAs significantly reduced levels of SRC as determined by western blotting.

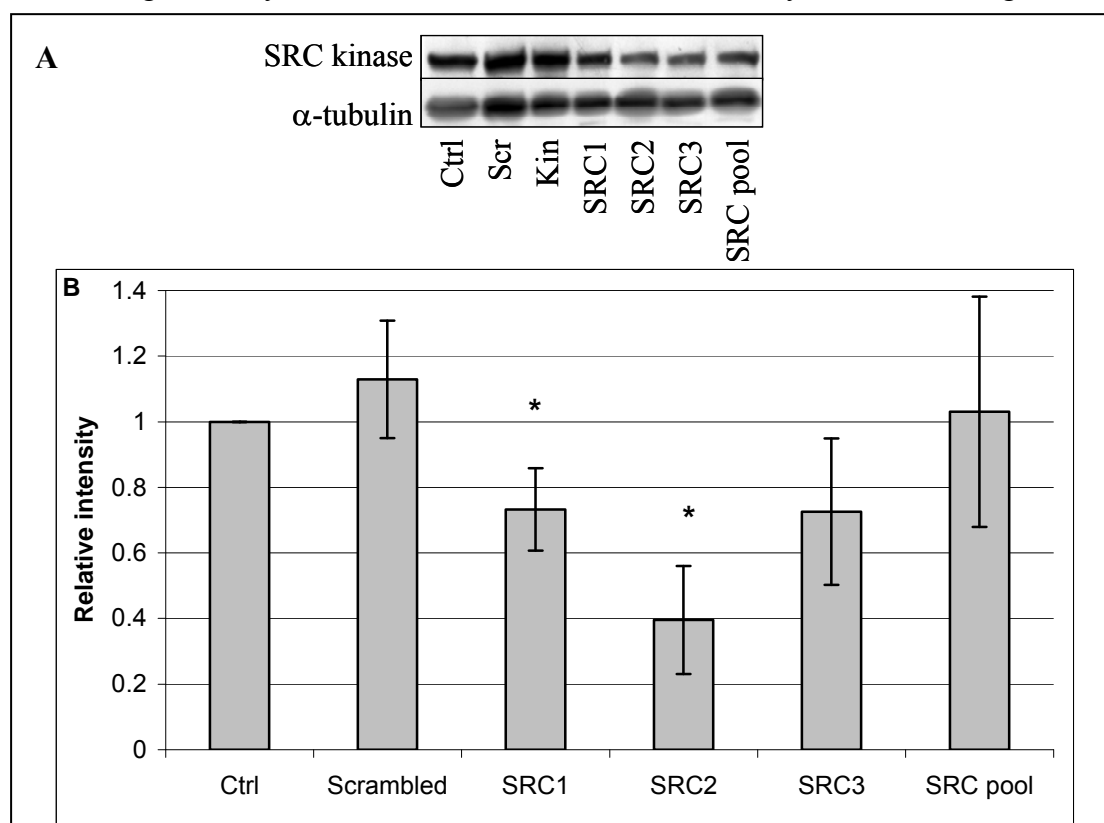


Figure 8.3: (A) Representative western blotting analysis of SRC knockdown by three independent siRNAs or a pool of the three siRNAs in WM-115 melanoma cells. (B) Densitometry analysis of SRC bands (normalised to  $\alpha$ -tubulin). Error bars represent the standard deviation of triplicate siRNA transfection experiments. ‘\*’ indicates that  $p < 0.05$ .

Kinesin siRNA reduced proliferation by approximately  $71.8 \% \pm 3.3 \%$  in WM-115 cells (Figure 8.4). Only SRC2 siRNA significantly reduced proliferation by  $24.6 \% \pm 2.7 \%$  ( $p = 0.0006$ ) in WM-115 cells (Figure 8.4). SRC3 siRNA also reduced



proliferation by  $22.4 \% \pm 11.9 \%$  but this did not achieve statistical significance ( $p = 0.07$ ).

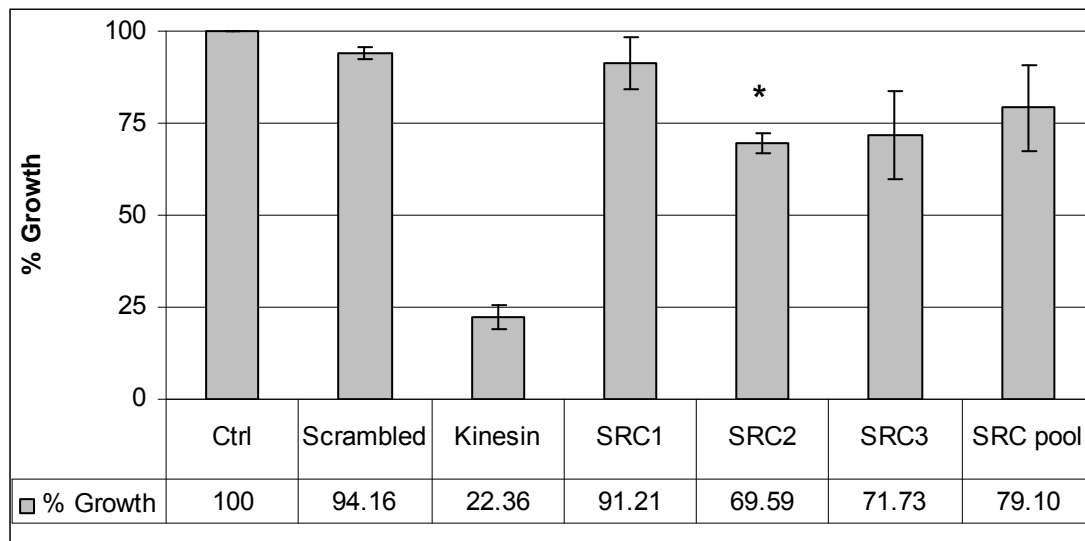


Figure 8.4: Effect of SRC siRNA on growth of WM-115 melanoma cells. Error bars represent the standard deviation of triplicate experiments. . ‘\*’ indicates that  $p < 0.05$  for any SRC siRNA compared to scrambled siRNA.

### 8.3.2 SRC siRNA in WM-266-4

SRC2 siRNA significantly reduced SRC expression compared to scrambled siRNA in WM-266-4 cells ( $p = 0.03$ ) (Figure 8.5). However SRC1, SRC3 or SRC pool siRNA knockdown did not have a significant effect on SRC expression as determined by western blotting ( $p = 0.64$ ;  $p = 0.26$ ;  $p = 0.86$ ).

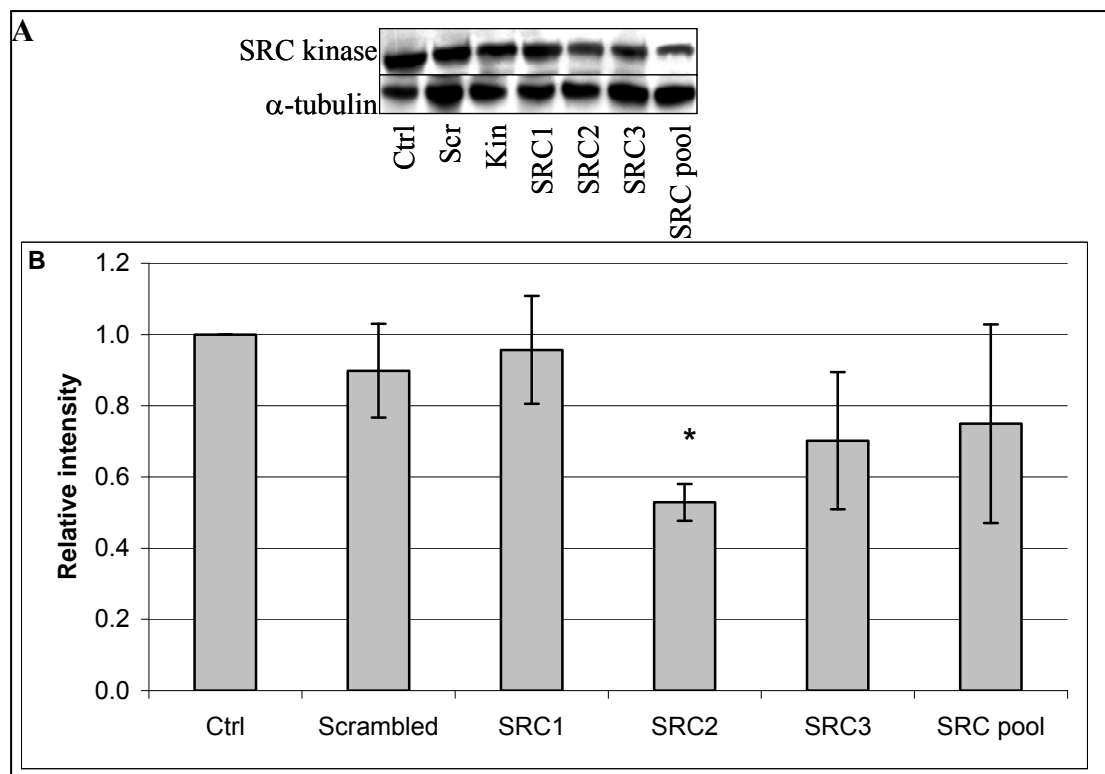


Figure 8.5: (A) Western blotting analysis of SRC knockdown by three independent siRNAs or a pool of the three siRNAs in WM-266-4 melanoma cells. (B) Densitometry analysis of SRC bands (normalised to  $\alpha$ -tubulin). Error bars represent the standard deviation of triplicate siRNA transfection experiments. ‘\*’ indicates that  $p < 0.05$ .

Kinesin siRNA reduced proliferation by  $69.2 \% \pm 5.1 \%$  in WM-266-4 cells. Significant knockdown of SRC by SRC2 siRNA, resulted in significant inhibition of proliferation in WM-266-4 ( $16.4 \% \pm 1.0 \%$  inhibition ( $p = 0.01$ )) (Figure 8.6). Although SRC1 siRNA did not significantly reduce SRC levels in WM-266-4 based on the western blotting results, it caused a significant  $25.2 \% \pm 3.8 \%$  reduction of proliferation ( $p = 0.03$ ). Neither SRC3 nor the SRC siRNA pool had a significant effect on proliferation in WM-266-4.

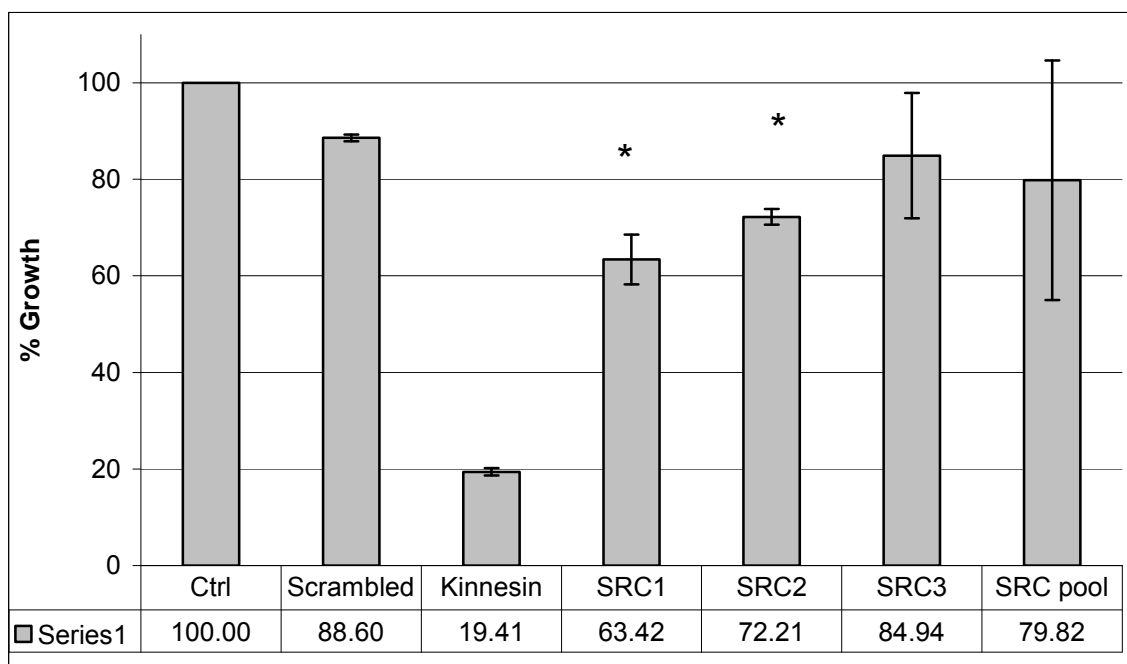


Figure 8.6: Effect of siRNA SRC knockdown on growth in WM-266-4 melanoma cell line. Error bars represent the standard deviation of triplicate experiments. ‘\*’ indicates that  $p < 0.05$  for any SRC siRNA compared to scrambled siRNA.

#### 8.4 Validation of targets identified by Pro-Q Diamond staining

To examine if the selected candidate phosphoproteins were up-regulated or down-regulated in dasatinib treated or untreated WM-155 and WM-266-4 cells, we analysed protein levels by western blotting.

No difference in expression of ERP29 was observed between WM-115 and WM-266-4 cells (Figure 8.7). The Pro-Q Diamond proteomic analysis showed that dasatinib treatment increased the levels of ERP29 phosphorylation by 5.4 fold in WM-266-4 cells. Based on previous phosphoproteomic analyses ERP29 contains 2 potential tyrosine phosphorylation sites ([www.phosphosite.org](http://www.phosphosite.org)) [188]. However, no tyrosine

phosphorylation was detected on immunoprecipitated ERP29, in either cell line or in response to dasatinib treatment. Analysis to date has not detected any other potential phosphorylation sites of ERP29.

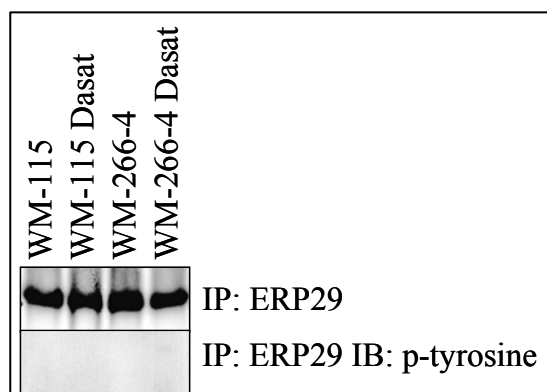


Figure 8.7: Western blotting analysis of ERP29 as detected by immunoprecipitation (IP) and detection of the ERP29 tyrosine residues by immunoblotting using a phosphotyrosine antibody in WM-115 and WM-266-4 cells untreated and treated with 100 nM dasatinib for 6 hours.

HSP60 is expressed at similar levels in both WM-115 and WM-266-4 cell lines and its expression is unaffected by dasatinib treatment (Figure 8.8). Pro-Q Diamond staining showed that dasatinib treatment increased the level of phosphorylation of HSP60 in WM-266-4 cells by 7.9 fold. Based on previous phosphoproteomic analyses HSP60 contains 2 potential serine phosphorylation sites and 3 potential tyrosine phosphorylation sites ([www.phosphosite.org](http://www.phosphosite.org)) [189]. Immunoprecipitation of HSP60 followed by immunoblotting with anti-phosphotyrosine and anti-phosphoserine antibodies detected low levels of both tyrosine and serine phosphorylation in WM-115 and WM-266-4 cells. The levels of phosphorylation were unchanged after treatment with dasatinib in both WM-115 and WM-266-4 cells.

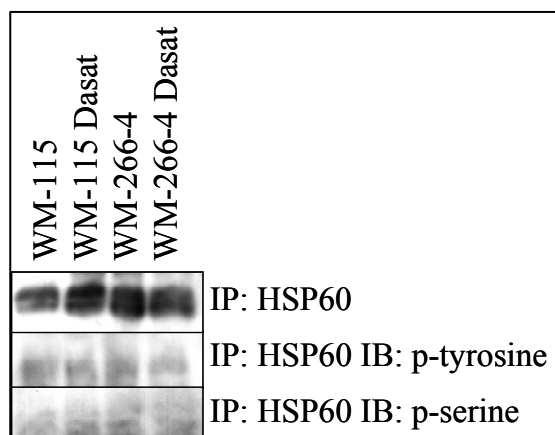


Figure 8.8: Western blotting analysis of HSP60 as detected by immunoprecipitation (IP) and detection of the HSP60 tyrosine and serine residues by immunoblotting using either a phosphotyrosine or phosphoserine antibody in WM-115 and WM-266-4 cells untreated and treated with 100 nM dasatinib for 6 hours.

### 8.5 Validation of ANXA2 in melanoma cell lines

ANXA2 was detected in a panel of melanoma cell lines and ANXA2 was detected in both WM-115 and WM-266-4 cell lines by western blotting. Dasatinib treatment does not appear to affect total expression of ANXA2 (Figure 8.9).

Based on previous phosphoproteomic analyses ANXA2 contains 5 potential serine phosphorylation sites and 14 potential tyrosine phosphorylation sites ([www.phosphosite.org](http://www.phosphosite.org)) [190]. 2D-DIGE proteomic results showed that ANXA2 phosphoprotein levels were higher in WM-115 cells compared to WM-266-4 cells (Table 8.1). In WM-115 cells treated with dasatinib, 4 of the identified phospho-

ANXA2 spots were increased by 3.06, 3.02, 2.17 and 1.97 fold, based on the 2D-DIGE analysis.

Immunoblotting following immunoprecipitation of ANXA2 detected tyrosine phosphorylated ANXA2 in both WM-115 and WM-266-4. Dasatinib treatment resulted in a slight increase in phosphotyrosine levels in WM-115. Immunoblotting for phosphotyrosine showed a slight decrease in tyrosine phosphorylation levels in dasatinib treated WM-266-4 cells.

Very low levels of serine phosphorylation were detected on ANXA2 in both WM-115 and WM-266-4 cells.

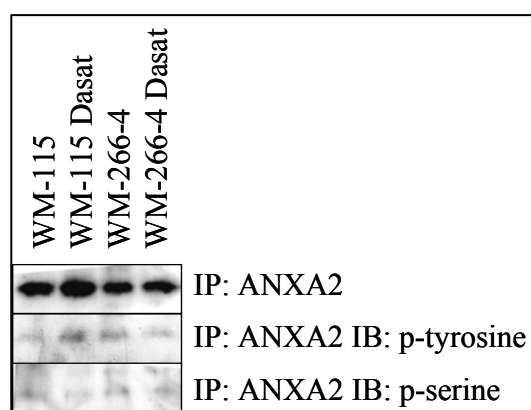


Figure 8.9: Western blotting analysis of ANXA2 as detected by immunoprecipitation (IP) and detection of the ANXA2 tyrosine and serine residues by immunoblotting using either a phosphotyrosine or phosphoserine antibody in WM-115 and WM-266-4 cells untreated and treated with 100 nM dasatinib for 6 hours.

ANXA2 expression was examined in the melanoma cell line panel (Figure 8.10) and was detected in 3 out of the 4 dasatinib responsive cell lines and in 2 out of 4 dasatinib resistant melanoma cell lines.

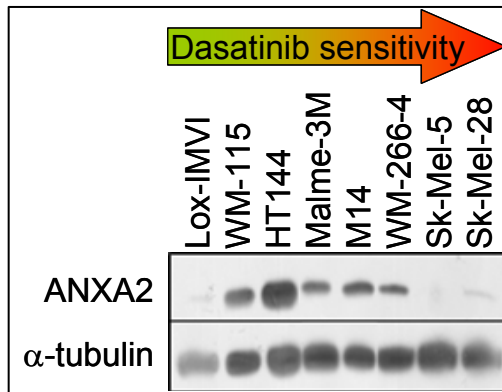


Figure 8.10: Expression of ANXA2 and  $\alpha$ -tubulin in the panel of melanoma cell lines.

### 8.5.1 ANXA2 siRNA in WM-115

We assessed the effects of ANXA2 siRNA on proliferation and sensitivity to dasatinib in both WM-115 and WM-266-4 cells. ANXA2 siRNA significantly knocked down ANXA2 expression compared to scrambled siRNA ( $p = 0.04$ ) (Figure 8.11) in WM-115 cells. Lipofectamine 2000 or scrambled siRNA did not significantly affect the expression of ANXA2 in WM-115 cells.

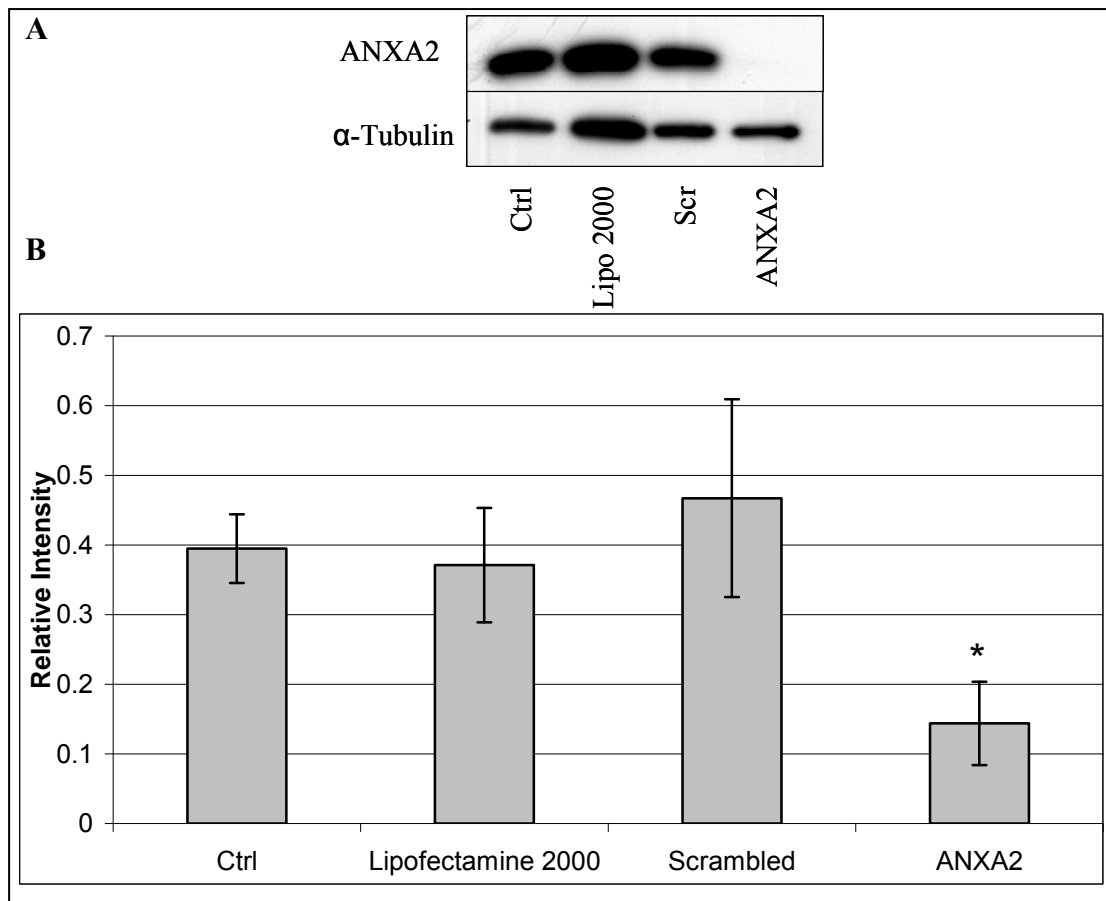


Figure 8.11: (A) Western blotting analysis of ANXA2 knockdown by siRNA SMARTpool in WM-115 melanoma cells. (B) Densitometry analysis of ANXA2 bands (normalised to  $\alpha$ -tubulin). Error bars represent the standard deviation of triplicate siRNA transfection experiments. ‘\*’ indicates that  $p < 0.05$  for ANXA2 siRNA compared to scrambled siRNA.

Kinesin siRNA reduced proliferation by approximately  $63.2 \% \pm 4.1 \%$  in WM-115 cells. ANXA2 siRNA caused significant inhibition of proliferation in WM-115 cells ( $33.3 \% \pm 14.8 \%$  inhibition ( $p = 0.04$ )) (Figure 8.12).



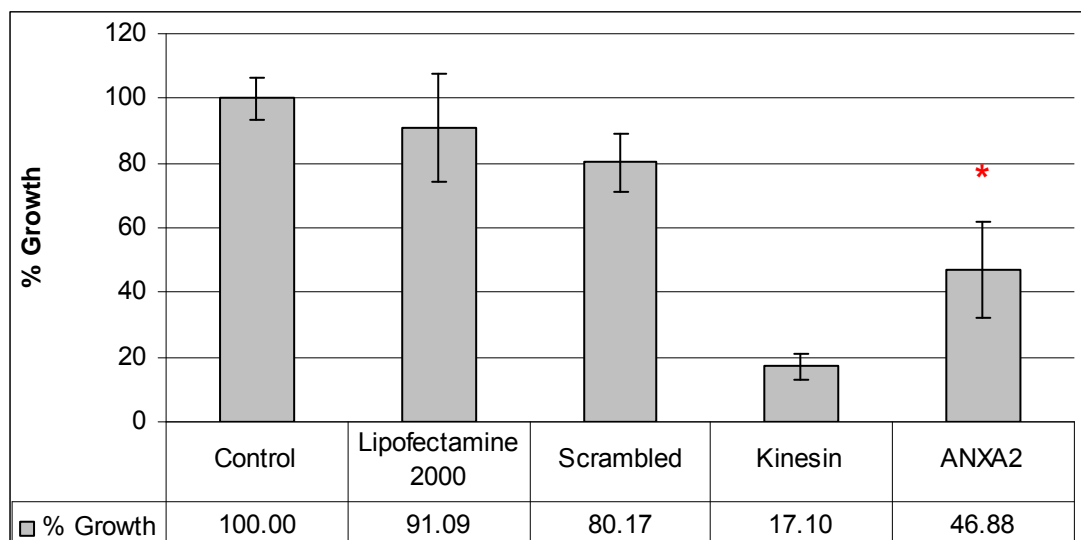


Figure 8.12: Effect of siRNA SRC knockdown on growth in WM-115 melanoma cell line. Error bars represent the standard deviation of triplicate experiments. ‘\*’ indicates that  $p < 0.05$  for ANXA2 siRNA compared to scrambled siRNA.

Under the conditions of the siRNA experiment, treatment with dasatinib did not significantly reduce proliferation of WM-115 cells (16.6 %) compared to untreated control cells ( $p = 0.06$ ) (Figure 8.13). Treatment with scrambled siRNA and dasatinib did not significantly reduce proliferation (18.1 %) compared to WM-115 cells treated with scrambled siRNA alone ( $p = 0.12$ ). ANXA2 siRNA significantly decreased proliferation (28.5 %) of WM-115 cells compared to cells treated with scrambled siRNA alone ( $p = 0.0008$ ). Dasatinib treatment combined with ANXA2 siRNA further inhibited proliferation by 24.7 %, compared to untreated cells combined with ANXA2 siRNA, however, this difference was not statistically significant ( $p = 0.067$ ).

Lipofectamine 2000 alone resulted in a 26.8 % decrease in proliferation compared to untreated WM-115 cells. However, lipofectamine 2000 combined with dasatinib, had a greater effect on proliferation than WM-115 cells treated with dasatinib alone

(dasatinib alone = 26.8 % proliferation inhibition; dasatinib and lipofectamine 2000 = 42.9 % proliferation inhibition), thus lipofectamine 2000 may affect the response to dasatinib in WM-115 cells (results not shown).

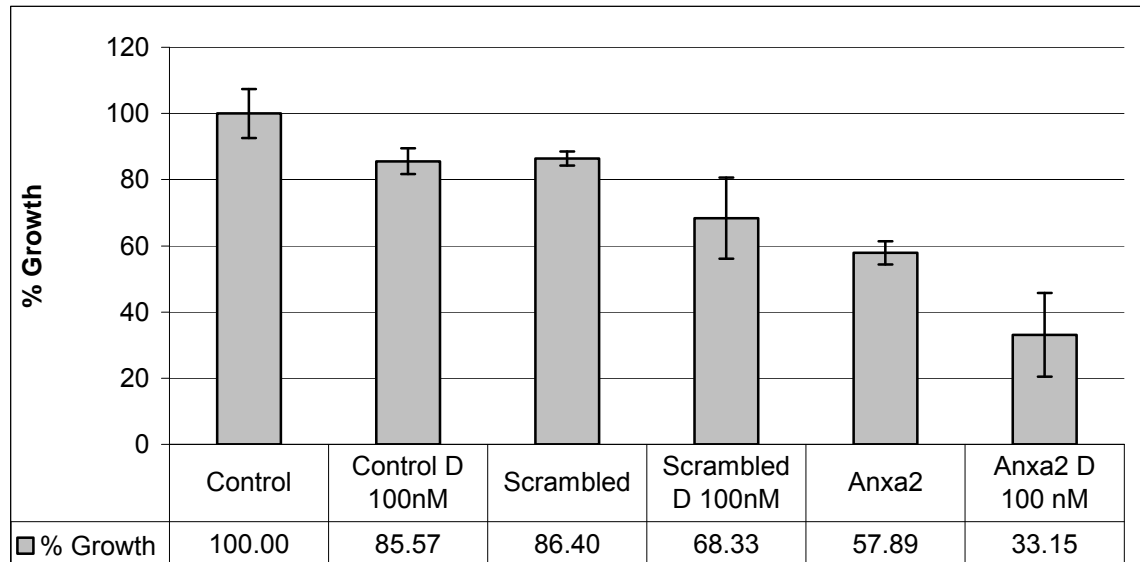


Figure 8.13: The effect of dasatinib on proliferation inhibition when combined with ANXA2 siRNA in WM-115 cells. Error bars represent the standard deviation of duplicate experiments. ‘\*’ indicates that  $p < 0.05$  for ANXA2 siRNA compared to scrambled siRNA.

### 8.5.2 ANXA2 siRNA in WM-266-4

ANXA2 siRNA significantly reduced ANXA2 expression compared to scrambled siRNA ( $p = 0.01$ ) (Figure 8.14) in WM-266-4 cells. Lipofectamine 2000 or scrambled siRNA did not significantly affect the expression of ANXA2 in WM-266-4 cells.

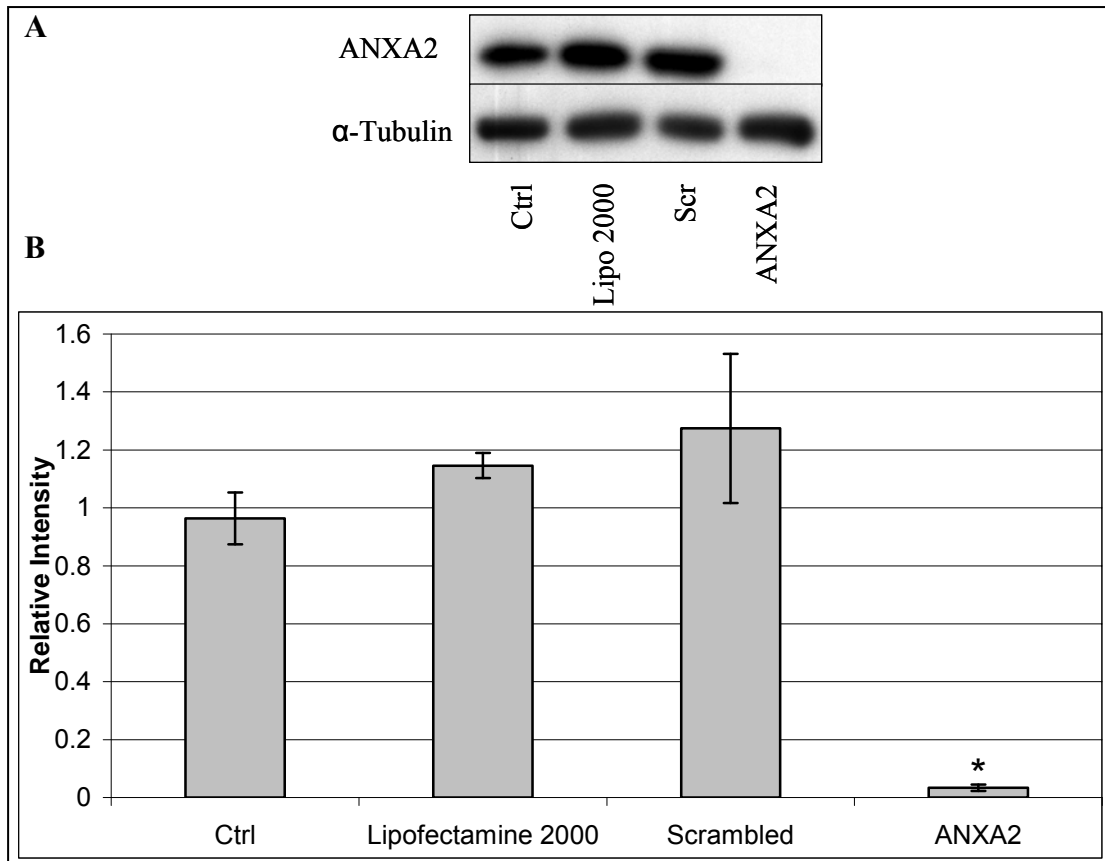


Figure 8.14: (A) Western blotting analysis of ANXA2 knockdown by siRNAs in WM-266-4 melanoma cells. (B) Densitometry analysis of ANXA2 bands (normalised to  $\alpha$ -tubulin). Error bars represent the standard deviation of triplicate siRNA transfection experiments. ‘\*’ indicates that  $p < 0.05$  for ANXA2 siRNA compared to scrambled siRNA.

Kinesin siRNA reduced proliferation by approximately  $64.2 \% \pm 4.3 \%$  in WM-266-4 cells. ANXA2 siRNA alone did not significantly reduce proliferation ( $11.6 \% \pm 9.8 \%$ ) in WM-266-4 cells ( $p = 0.36$ ) (Figure 8.15).

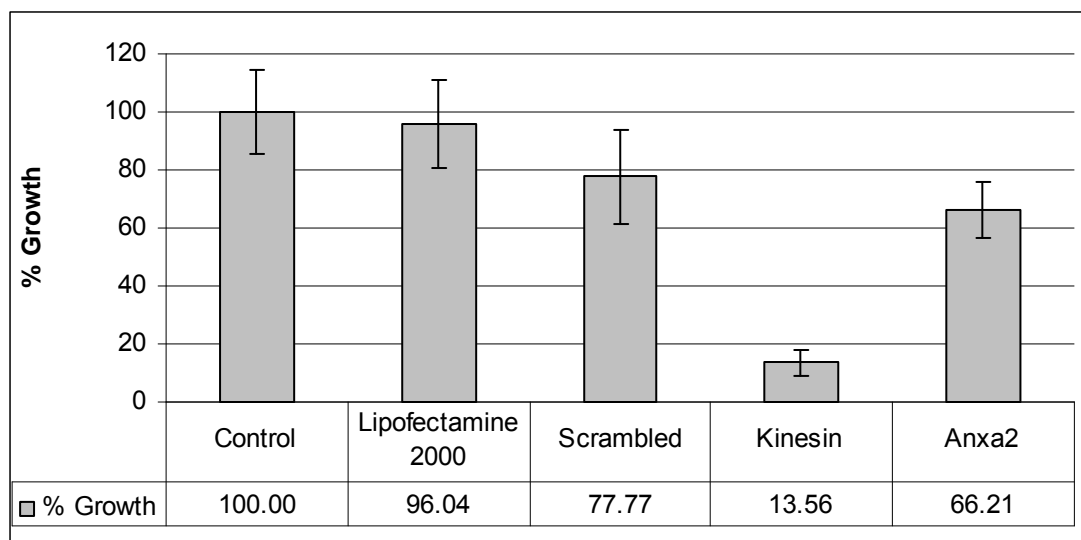


Figure 8.15: Effect of siRNA ANXA2 knockdown on growth in WM-266-4 melanoma cell line. Error bars represent the standard deviation of triplicate experiments. ‘\*’ indicates that  $p < 0.05$  for ANXA2 siRNA compared to scrambled siRNA.

Dasatinib alone did not significantly reduce proliferation of WM-266-4 cells ( $31.2 \% \pm 16.3 \%$ ) compared to untreated control cells ( $p = 0.07$ ) (Figure 8.16). Scrambled siRNA combined with dasatinib did not significantly reduce proliferation ( $23.2 \% \pm 10.7 \%$ ) compared to WM-266-4 cells treated with scrambled siRNA alone ( $p = 0.13$ ). ANXA2 siRNA did not result in a significant decrease in proliferation ( $19.4 \% \pm 15.9 \%$ ) compared to scrambled siRNA ( $p = 0.26$ ), however scrambled siRNA did account for a  $39.0 \% \pm 17.0 \%$  inhibition of proliferation on its own compared to the control sample. Dasatinib treatment combined with ANXA2 siRNA did not significantly inhibit proliferation ( $11.3 \% \pm 12.0 \%$ ) compared to cells treated with ANXA2 siRNA alone ( $p = 0.36$ ).

Lipofectamine 2000 alone resulted in a 13 % decrease in proliferation compared to untreated WM-266-4 cells. However, lipofectamine 2000 combined with dasatinib,

had a greater effect on proliferation than WM-266-4 cells treated with dasatinib alone (dasatinib alone = 12.6 % proliferation inhibition; dasatinib and lipofectamine 2000 = 43.6 % proliferation inhibition), thus lipofectamine 2000 may affect the response to dasatinib in WM-266-4 cells (Data not shown).

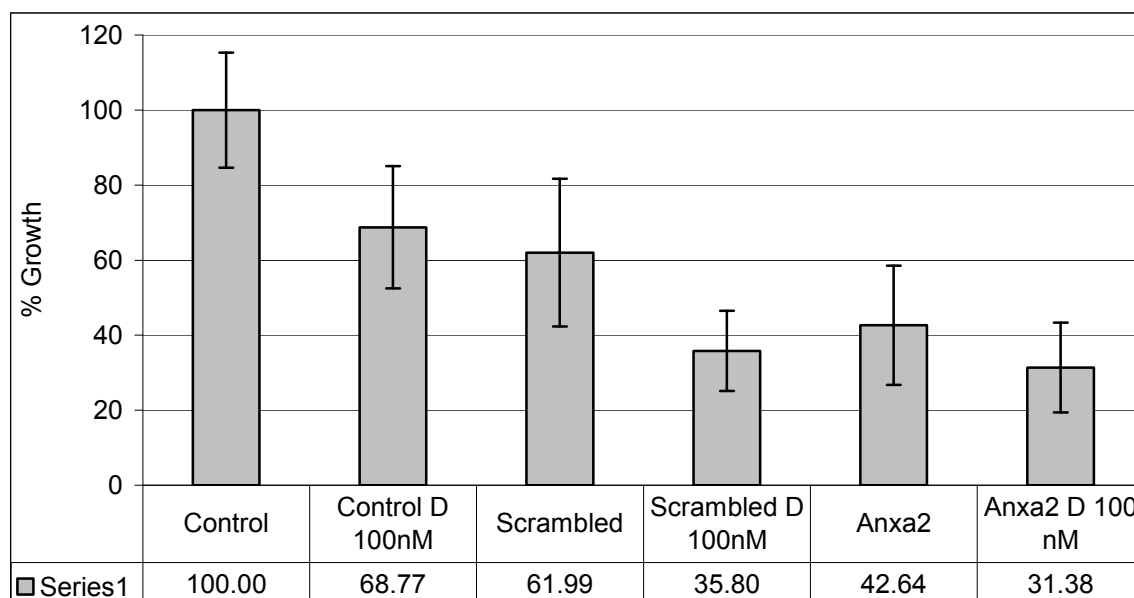


Figure 8.16: The effect of dasatinib on proliferation inhibition when combined with ANXA2 siRNA in WM-266-4 cells. Error bars represent the standard deviation of triplicate experiments. ‘\*’ indicates that  $p < 0.05$  for ANXA2 siRNA compared to scrambled siRNA.

## 8.6 Summary

Lipofectamine 2000 resulted in the good transfection efficiency in both of the melanoma cell lines and was minimally toxic to the cells.

SRC knockdown resulted in a significant decrease in proliferation in both the dasatinib sensitive WM-115 and the dasatinib resistant WM-266-4 cells.

Two proteins were selected for further analysis from the Pro-Q Diamond phosphoprotein staining. Both ERP29 and HSP60 were expressed in WM-115 and WM-266-4 cells. However, the levels of tyrosine and serine phosphorylation detected by immunoblotting did not correlate with the apparent changes in phosphorylation observed on the Pro-Q Diamond gel analysis.

Several spots of ANXA2 were identified by 2-D DIGE analysis of WM-115 cells treated with dasatinib. ANXA2 was detected in both WM-115 and WM-266-4 by immunoblotting, and low levels of phosphorylation of tyrosine and serine were detected in the melanoma cells.

ANXA2 tyrosine phosphorylation levels were slightly increased in response to dasatinib in WM-115 cells and unchanged in dasatinib treated WM-266-4 cells, based on phosphotyrosine immunoblotting results, which correlated with the 2D-DIGE results. siRNA knockdown of ANXA2 resulted in significant inhibition of proliferation in WM-115 cells, but did not significantly inhibit proliferation in WM-266-4 cells.

Finally ANXA2 knockdown of WM-115 and WM-266-4 cells did not significantly alter response to dasatinib in either cell line. However, the transfection reagents used may have improved the response to dasatinib, thus limiting the ability to assess any specific effect of ANXA2 siRNA on dasatinib response.

## **Chapter 9**

### **9. Discussion**

The overall aim of this thesis was to develop novel therapeutic strategies for metastatic melanoma. The main focus of the research was on the evaluation of targeted therapies, in particular the multi-target kinase inhibitor dasatinib. We examined the effects of dasatinib on melanoma cell growth, apoptosis, invasion and migration. In order to identify optimal rational therapeutic combinations, we tested combinations of dasatinib with other therapies. We investigated potential mechanisms of response and resistance to dasatinib in melanoma cells by interrogating signalling pathways targeted by dasatinib and by phosphoproteomic profiling of sensitive and resistant cell lines. Potential predictive biomarkers for dasatinib therapy were assessed in both cell lines and melanoma tumour specimens.

### **9.1 Characterisation of melanoma cell lines**

Malignant melanoma is characterised as an aggressive, invasive cancer [191]. The panel of melanoma cell lines were derived from metastatic tumours, which is consistent with the migratory and invasive phenotype observed *in vitro*. Within the panel of melanoma cell lines there was some variation in migration and invasion capacity which could be related to the number of genetic mutations associated with motility in each cell line. The COSMIC database contains information on somatic mutation in human cancers and cancer cell lines. Based on the data available in the COSMIC database, all of the melanoma cell lines tested are B-RAF mutated, whilst HT144 is PTEN mutated. None of the cell lines in our panel are NRAS mutated (COSMIC). The altered mutational status of genes such as B-Raf, NRas and PTEN have been implicated in determining the migratory and invasive potential of cell lines [191]. Sk-Mel-28 and M14, which display high levels of invasion and migration have



mutated P53, which has previously been implicated in increased invasion and migration in lung cancer cell lines [192] and A375P melanoma cell lines [193].

Metastatic melanoma is notoriously resistant to treatment in the clinical setting, with TMZ only achieving a 10-15 % response rate [194], and other drugs such as taxotere achieving 12-18 % responses [71]. We found that the IC<sub>50</sub> concentrations of TMZ, whilst similar in melanoma and glioma cell lines, were in the high  $\mu\text{M}$  range in both cases. Previous studies testing TMZ in two melanoma cell lines found the IC<sub>50</sub> concentration of TMZ to be approximately 800  $\mu\text{M}$  [195] which is consistent with the values observed in our cell line panel (TMZ IC<sub>50</sub> ranged from 250  $\mu\text{M}$  to 800  $\mu\text{M}$ ). However, in the clinical setting plasma levels of TMZ only reach concentrations approaching 80  $\mu\text{M}$  [196, 197]. The half-life of TMZ is less than two hours [198] which would reduce the efficacy of the drug in patients and may also explain the high IC<sub>50</sub> values observed *in vitro*.

The IC<sub>50</sub> concentrations for taxotere and epirubicin reveal that our melanoma cell lines have comparable sensitivity to other cancer types tested. However, despite this finding, melanoma patients do not respond to these drugs in the clinic. Previous studies have shown that tumour cells in cancer patients and cell lines can differ greatly not only in their cell cycle times but also in their ability to apoptose and their sensitivity to chemotherapeutic drugs [199]. Another reason for higher sensitivity in cell lines could be that expression of P-gP and MRP-1 may be lost in melanoma cell lines, as both of these transporters are detected frequently in melanoma tumours [200].

In order to study potential mechanisms of resistance to TMZ, which is frequently used to treat metastatic melanoma, two TMZ resistant cell lines were established using two different selection methods. Although the level of resistance induced was low, these two cell lines provide unique models to study acquired TMZ resistance in melanoma. Pulse selection of cell lines with chemotherapeutic drugs has been shown to lead to altered drug resistance to a range of chemotherapies in the selected cell lines [201, 202]. However, the effect of acquired TMZ resistance on altered drug sensitivity has not been investigated. Pulse selection of the two melanoma cell lines with TMZ resulted in increased resistance to cisplatin. As TMZ and cisplatin are both DNA damaging agents, there may be common mechanisms of resistance to the DNA damage induced by these agents.

ABC transporters have been implicated in chemotherapy drug resistance in cancer. However their role in TMZ resistance has not been extensively studied. Our studies revealed that repeated exposure to TMZ resulted in the decreased mRNA expression of the ABC transporters MRP1, MRP2 and ABCB5 whilst increasing mRNA expression of P-gP. Studies in glioma have shown that treatment with TMZ can increase MRP-1 mRNA expression [203], whilst studies in astrocytoma cells revealed that TMZ treatment led to increases in the transcription levels of BCRP, MRP3 and MRP-1 [204]. Therefore our results suggest that TMZ exposure alters the expression of ABC transporters. However, the role this altered expression plays in TMZ resistance, if any, remains to be determined.

Exposure to taxotere also caused some changes in expression of ABC transporters. The increase in BCRP levels observed in HT144-Tax may contribute to the slight

decrease in sensitivity to taxotere observed as taxotere is also a substrate for BCRP [82].

Interestingly, we found that BCRP and MRP-2 are highly expressed in the melanoma cell line panel tested. The role of BCRP and MRP-2 in melanoma is not well tested. We therefore tested specific inhibitors of BCRP and MRP-2 to determine if inhibition enhanced response to substrate chemotherapy drugs in the melanoma cell lines. Inhibition of BCRP has been achieved by using fumitremorgin C (FTC) in a breast cancer cell line [205]. Mitoxantrone which is transported by BCRP [89, 205] was used to assess the impact of BCRP inhibition. Whilst inhibition of BCRP was effective in a mitoxantrone selected cell line, DLKP-Mitox, no effect was observed in the melanoma cell lines, Malme-3M and Sk-Mel-5. The lack of effect in the melanoma cell lines could be due to FTC not efficiently inhibiting the BCRP pump mechanism, or that despite BCRP inhibition other ABC transporters are capable of transporting mitoxantrone as ABC transporters have overlapping substrate profiles [206].

MRP-2, a known transporter of vincristine [89], was expressed in Malme-3M and Sk-Mel-5 in the melanoma panel. MK571 has been shown to inhibit the transport of MRP-1 substrate drugs in melanoma cells and MRP-2 substrate drugs in liver cells [207, 208]. Our studies revealed that combination of vincristine and MK571 was ineffective in all cell lines tested. MK571 alone at a concentration of 7.5  $\mu$ M inhibited growth by 17 % ( $\pm$  10 %). The 2008 MRP-2, Sk-Mel-5 and Malme-3M cells express MRP-2 but MK-571 did not enhance response to vincristine in any of these cell lines.

MK-571 may not entirely inhibit the activity of MRP-2, or vincristine may be transported by MRP-1 or P-gP.

Our study of the melanoma cell lines *in vitro* suggests that the aggressive invasive phenotype of metastatic melanoma is also evident in the cell lines, whereas the inherent chemotherapy resistant phenotype does not appear to be retained in melanoma cells in culture. This may be due in part to loss of expression of specific ABC transporters *in vitro* as we found low levels of MRP-1 and P-gP mRNA expression in the cell lines and studies of tumour tissues have reported high levels of these two transport proteins in melanoma [200]. Thus melanoma cell lines may not be appropriate models to investigate mechanisms of resistance to chemotherapy drugs.

## **9.2 *In vitro* evaluation of dasatinib and imatinib in melanoma**

Targeted therapies may improve prognosis in chemotherapy resistant tumours such as melanoma. We focussed on examining the effects of multi-target kinase inhibitors in melanoma cells, as novel potential therapies for melanoma treatment. We examined the effects of dasatinib, which targets BCR-Abl, SRC, c-KIT, PDGFR, Ephrin-A receptors, and imatinib mesylate, which targets Bcr-Abl, c-Kit and PDGFR in melanoma cell lines

In a previous study in breast cancer cell lines, sensitivity to 1  $\mu$ M dasatinib was defined as at least 60 % inhibition of cell proliferation, moderate sensitivity as 40-59 % inhibition and resistance as less than 40 % inhibition [172] (assuming that higher concentrations than 1  $\mu$ M would not be achievable *in vivo*) [172]. However, we also included cell lines which displayed a lower level of response to dasatinib and we

classified cell lines which displayed greater than 25 % inhibition of proliferation at 300 nM as dasatinib responsive (Lox-IMVI, WM-115, HT144 and Malme-3M) and cell lines with less than 25 % inhibition of proliferation at 300 nM as dasatinib resistant (M14, WM-266-4, Sk-Mel-5 and Sk-Mel-28). We set the highest dasatinib concentration at 300 nM dasatinib due to recent studies identifying that the peak plasma concentration of dasatinib was only 100 ng/ml [209]. Consistent with our findings, a recent study which tested dasatinib in a different panel of melanoma cell lines, also reported that both Sk-Mel-5 and Sk-Mel-28 were resistant to dasatinib up to concentrations of 2  $\mu$ M [210].

Dasatinib inhibition of SRC has been implicated in reducing invasion and migration in human sarcoma [182], lung cancer [183] whilst specific SRC inhibition by PP2 reduced invasion and migration in breast cancer cells [211]. Dasatinib reduced the level of invasion and migration in HT144 and Sk-Mel-28 cell lines, at concentrations that were non-toxic to the cells. Interestingly, although Sk-Mel-28 showed no response to dasatinib in proliferation assays, very low concentrations of dasatinib (15 nM) inhibited invasion and migration of these cells.

Studies in lung cancer [212], head and neck squamous cell carcinoma [183] and malignant pleural mesothelioma [134] have revealed that dasatinib induces both cell cycle arrest and apoptosis. Our results show that dasatinib induces both apoptosis and G1 cell cycle arrest in Lox-IMVI (the most dasatinib responsive cell line), whilst inducing either G1 arrest in HT144 or apoptosis in Malme-3M (moderately responsive). Therefore, optimal response to dasatinib in melanoma cells may require efficient induction of both cell cycle arrest and apoptosis.

Imatinib, which targets Bcr-Abl, c-Kit and PDGFR, does not inhibit the growth of either HT144 or Lox-IMVI cells. This raised the possibility that the sensitivity of melanoma cell lines to dasatinib may be due to targeting SRC or EphA receptors.

SRC has been shown to be activated by the phosphorylation of tyrosine 418, which can control proliferation and invasion [134, 163]. After six hours of treatment, we found that dasatinib inhibited phosphorylation of SRC in all 3 dasatinib sensitive cell lines tested but also in the dasatinib resistant cell line Sk-Mel-5. Furthermore a recent study [210] showed that longer incubation with dasatinib inhibits phosphorylation of SRC in all melanoma cell lines tested. Thus inhibition of p-SRC alone does not predict sensitivity to inhibition of proliferation by dasatinib in melanoma cells. In contrast to our results inhibition of c-SRC activation in prostate cancer cell lines was linked with a reduction in proliferation [213].

In the panel of cell lines, treatment with dasatinib for 6 hours had no effect on expression of EphA2. In a time course experiment in the dasatinib-sensitive cell line, Lox-IMVI, phosphorylation of EphA2 appeared to be transiently decreased, but was restored by 6 hours. These results suggest that inhibition of EphA2 does not play a key role in the response to dasatinib observed in Lox-IMVI. In contrast dasatinib has been shown to decrease the phosphorylation of EphA2 and EphA2 kinase activity in A2058 and A375 melanoma cell lines [210]. Thus EphA2 may play a role in dasatinib sensitivity; however this may be cell line specific.

In colon cancer cells, inhibition of SRC was associated with reduced phosphorylation of FAK at tyrosine 861, which in turn was implicated in inhibiting migration and invasion [173]. Treatment with dasatinib reduced the level of FAK phosphorylation of tyrosine 861 in all melanoma cell lines tested; therefore inhibition of FAK phosphorylation may play a role in mediating the inhibitory effects of dasatinib on invasion and migration in melanoma cells. Recently enzyme assays have shown that dasatinib is a potent inhibitor of several additional kinases, including FAK ( $IC_{50} = 0.2$  nM) [214]. Therefore, dasatinib may directly target FAK, independently of SRC, resulting in inhibition of migration/invasion without inhibition of proliferation as we observed in the Sk-Mel-28 cells.

Differences in the level or activation status of SRC do not appear to predict sensitivity to dasatinib in the melanoma panel. Tsao *et al* [134] have also found that SRC expression does not predict response to dasatinib in malignant pleural mesothelioma. Serrels *et al* [173] showed that inhibition of p-SRC in peripheral blood mononuclear cells correlated with inhibition of p-SRC in colon tumours. Measuring changes in phospho-SRC in peripheral blood mononuclear cells may therefore serve as a surrogate marker for response to dasatinib. However dasatinib treatment inhibited p-SRC in dasatinib responsive and dasatinib resistant cell lines, indicating that p-SRC inhibition does not correlate with response to dasatinib.

### **9.3 Dasatinib in combination with current targeted therapies**

Targeted therapies have been shown to be effective at inhibiting tumour growth when combined with chemotherapy. We studied the effect of dasatinib in combination with chemotherapy and targeted therapies. In the dasatinib sensitive Lox-IMVI and HT144

cells, combining dasatinib with TMZ showed a significantly greater inhibition of cellular proliferation than either drug tested alone. In the partially responsive M14 and Malme-3M cells, there is a small but significant improvement in response when dasatinib is combined with TMZ. In the dasatinib-resistant cell line Sk-Mel-28, the combination was slightly more inhibitory than TMZ alone although the difference was not significant. Of note, although dasatinib alone appeared to increase growth of Sk-Mel-28 cells, this effect did not result in any antagonism when combined with TMZ. A study by Homsy *et al*, (2009) reported that the combination of dasatinib and temozolomide was not synergistic in a panel of melanoma cell lines though interestingly combinations of cisplatin, a DNA damaging agent, and dasatinib were found to be synergistic. This could indicate that inhibition of SRC may enhance response to DNA damaging agents as has been previously shown in glioma, breast and lung cancer [215, 216].

Dasatinib was also tested in combination with taxotere and epirubicin. Some enhancement of the effect of epirubicin was observed in Lox-IMVI and HT144 cell lines, but the combination of dasatinib and taxotere did not result in a substantial improvement when compared to either drug alone. Studies in melanoma cell lines which tested dasatinib in combination with paclitaxel also showed that the combination was not synergistic [217].

Sorafenib which targets several tyrosine kinase inhibitors including BRAF is presently being assessed alone and in combination in clinical trials for the treatment of melanoma [218]. We tested sorafenib in a panel of melanoma cell lines which are



BRAF mutated. Interestingly the dasatinib sensitive cell lines were sensitive to lower concentrations of dasatinib than sorafenib.

The combination of dasatinib and sorafenib was also tested but did not produce an improved response compared to the single agents suggesting that this combination may not be beneficial clinically. However, the triple combination of dasatinib, sorafenib and TMZ displayed improved response compared to testing each drug on its own in both Lox-IMVI and Malme-3M, suggesting that this may be a rational combination for testing in clinical trials in melanoma patients.

Prolonged exposure of melanoma cells to TMZ altered the sensitivity to other chemotherapy drugs. Interestingly TMZ exposure also sensitised cells to dasatinib. We tested the combination of TMZ and dasatinib in the parent and TMZ resistant cell line and found the combination was more effective in Malme-TMZ compared to the parent cell line Malme-3M. Expression of SRC was unchanged but phosphorylation of SRC was increased in the resistant cell line. This may indicate that repeated exposure to TMZ increases SRC signalling. Radiation of lung cancer cell line A549 has been shown to activate SRC [215] and cisplatin has been previously shown to increase SRC phosphorylation [216]. These results indicate a link between DNA damage and the increased phosphorylation of SRC, which could underpin the mechanism whereby TMZ treated cells become more sensitive to dasatinib. Importantly despite TMZ resistant cells displaying increased levels of phosphorylation of SRC, treatment with 100 nM dasatinib still inhibited SRC phosphorylation. These results suggest that dasatinib therapy may be of benefit to

melanoma patients whose tumours have progressed on TMZ-based chemotherapy regimes.

#### **9.4 Biomarkers for dasatinib treatment in melanoma**

Dasatinib is effective at inhibiting proliferation in 50 % of melanoma cell lines tested. To determine the effectiveness of dasatinib in the clinical setting it will be important to identify biomarkers that can be used to select patients that are more likely to respond to dasatinib therapy. We found a potential link between inhibition of FAK phosphorylation by dasatinib and the reduction of migration and invasion in melanoma cell lines. We also showed a potential link between EphA2 expression and dasatinib sensitivity in the panel of melanoma cell lines.

We then examined a panel of genes which have been tested as biomarkers for dasatinib sensitivity in 23 breast cancer cell lines [184]. Based on microarray analysis, 161 genes which were associated with dasatinib sensitivity were identified. From the list of 161 genes, ANXA1, CAV-1, CAV-2, EphA2, IGFBP2 and PTRF were chosen to develop a biomarker panel whose combined expression profile predicted response to dasatinib.

Other studies have also identified biomarkers of response to dasatinib *in vitro*. One study found that elevated expression of CAV-1, moesin and yes associated protein-1 predicted sensitivity to dasatinib in 39 breast cancer cell lines [172]. A second study in 16 prostate cancer cell lines found 171 genes were correlated with *in vitro* sensitivity to dasatinib. Of the 171 genes, elevated expression of androgen receptor, prostate specific antigen, cytokeratin 5, urokinase-type plasminogen activator and

EphA2 was found to significantly correlate with dasatinib sensitivity [219]. Finally a study in ovarian cancer found that elevated expression of CAV-1, ANXA1 and EphA2 correlated with sensitivity to dasatinib [220].

We tested the 6-gene dasatinib sensitivity biomarker panel as these genes are either targets of dasatinib; SRC substrates; or part of the downstream SRC pathway. It was also validated in 11 additional breast cancer cell lines and 23 lung cancer cell lines, predicting response to dasatinib in greater than 85 % of cases [184].

mRNA expression of ANXA1, CAV-1, CAV-2, EphA2, IGFBP2 and PTRF did not correlate with response to dasatinib in our panel of melanoma cell lines. However the number of cell lines in the panel was limited to 8 and this may be too small to detect correlations with dasatinib response. Interestingly, protein expression of ANXA1, CAV-1 and EphA2, determined by semi-quantitative immuno-blotting, correlated with dasatinib sensitivity. Protein based detection systems are generally more favourable in the clinical setting, for example by immunohistochemical staining in tumour tissues or by ELISA on serum samples. Therefore, the development of ANXA1, CAV-1 and EphA2 as a panel of protein markers for predicting response to dasatinib should be investigated further in clinical specimens.

The possible reasons for a lack of correlation between mRNA expression and dasatinib sensitivity are that Huang et al (2007) classified cells as being dasatinib sensitive if they achieved an  $IC_{50}$  at 600 nM dasatinib; however we classified cell lines as responsive if they achieved greater than 25 % growth inhibition at 300 nM dasatinib. The less stringent definition of sensitivity may affect the accuracy of the

sensitivity biomarker in our panel of melanoma cell lines. The lack of correlation between protein and mRNA expression could be due to mRNAs not being translating into protein.

Interestingly the elevated expression of ANXA1, CAV-1 and EphA2 in our melanoma cell lines has been recorded in the other dasatinib biomarker studies as mentioned above. CAV-1 expression was elevated in breast and ovarian cell lines that are responsive to dasatinib [172, 220]. Elevated ANXA1 expression was found in dasatinib sensitive ovarian cell lines [220], whilst EphA2 was elevated in ovarian and prostate cancer cell lines [219, 220]. Because CAV-1 expression was elevated in breast and ovarian cancer studies which used large numbers of cell lines and CAV-1 is associated with SRC kinase, we selected CAV-1 and SRC as preliminary markers to assess in melanoma patient samples.

CAV-1 was expressed in 43 % of melanoma patient tumours. A previous study of exosomes from melanoma patient plasma found that CAV-1 was expressed at higher levels in melanoma patients compared to healthy volunteers [221] and in hepatocellular carcinoma CAV-1 expression increased with disease progression [222]. There was, however, no correlation between CAV-1 expression and metastatic or primary melanoma in our study. Therefore CAV-1 expression may be increased at an early stage of melanoma and does not appear to be a marker of melanoma progression.

SRC was expressed in 73 % of melanoma tumours and was expressed at slightly higher levels in primary tumours compared to metastatic tumours. A recent study also

found that p-SRC Y418 was detected in 17/35 patient tumours and in 5/9 metastatic tumours [217]. We also determined that SRC kinase expression is lower in lymph node positive patients compared to lymph node negative patients. These results suggest that SRC expression in melanoma is associated with a better prognosis. We found that 41 % of melanoma tumours express both SRC and CAV-1. To determine the percentage of patients that will possibly benefit from dasatinib therapy, future work will include measuring ANXA1 and EphA2 in the melanoma samples.

Previous studies in breast cancer have shown that SRC expression and phosphorylation are increased with disease progression [223, 224]. Studies have also shown that SRC kinase expression and phosphorylation are associated with decreased survival [225-227]. However in one study of bladder cancer, SRC kinase expression was lost with disease progression [228].

To determine if expression of ANXA1, CAV-1 and EphA2 correlate with dasatinib sensitivity in melanoma, this panel of potential biomarkers would need to be assessed in melanoma patients who receive dasatinib treatment.

### **9.5 Proteomic profiling of dasatinib sensitive and resistant melanoma cells and functional validation of targets identified from phosphoproteomic analysis**

Analysis of the effects of dasatinib on cell signalling did not reveal specific markers or pathways which are responsible for sensitivity or resistance to dasatinib. Furthermore, siRNA knockdown of SRC did not correlate with dasatinib sensitivity in the two melanoma cell lines tested. Other SRC family members may also play a role in proliferation control and may also play a role in sensitivity to dasatinib. SRC

siRNAs used in this experiment only inhibited the expression of c-SRC. Specific targeting of other SRC family members may be required to determine if other SRC family members are involved in dasatinib sensitivity.

Therefore, in an attempt to identify mechanisms of response or resistance to dasatinib, we performed phosphoproteomic profiling on two cell lines representing a model of dasatinib sensitivity and dasatinib resistance. The model selected was the isogenic pair of melanoma cell lines WM-115, which is dasatinib sensitive, and WM-266-4, which is dasatinib resistant. WM-115 was derived from a primary tumour and WM-266-4 was derived from a metastatic tumour from the same patient [229]. Two hundred and nine phosphoproteins were significantly altered in the comparisons of WM-115 and WM-266-4 with and without dasatinib treatment and we successfully identified 82 phosphoproteins. The 209 phosphoproteins detected were identified by 2D-DIGE analysis which has some limitations. Novel techniques such as stable isotope labelling by amino acids in cell culture (SILAC) may be useful for identification of smaller and less abundant proteins.

In our studies moesin (MSN) and radixin (RDX) phosphoprotein levels were higher in untreated WM-115 cells compared to untreated WM-266-4 cells. Dasatinib treatment reduced the phosphoprotein levels (2.98, 2.3 and 1.41 fold) of MSN and RDX (2.4 and 2.3 fold) in WM-115 cells compared to untreated cells. Moesin and radixin are members of the ezrin, moesin, radixin (ERM) family of molecules involved in the association of actin filaments with the plasma membrane [230]. Moesin is constitutively activated by phosphorylation of threonine 555 [231] and the activation of ERM family members links actin filaments to CD43, CD44 and ICAM-1 which are

involved in adhesion [232]. Moesin is critical for invasion in 3-D matrices [233], and the phosphorylation of moesin has also been linked with invasion in endometrial cells [234]. Dasatinib reduced invasion and migration in the three melanoma cell lines tested, regardless of their sensitivity to dasatinib. Therefore MSN and RDX may play a role in invasion in WM-115 and WM-266-4 cells and in dasatinib mediated inhibition of invasion and motility.

PRDX2 was increased in untreated WM-266-4 cells compared to untreated WM-115 cells (1.29, 1.47 and 4.32 fold). The two identified PRDX2 spots in dasatinib treated WM-115 cells were increased by 1.35 fold and decreased by 2.69 fold. The peroxiredoxase (PRDX) family protects cells against peroxide oxidative damage and regulates H<sub>2</sub>O<sub>2</sub> mediated signalling [235]. PRDX2 is a cellular peroxidase that eliminates endogenous H<sub>2</sub>O<sub>2</sub> produced in response to growth factors such as platelet derived growth factor (PDGF) and epidermal growth factor (EGF) [236]. PRDX2 is expressed in melanocytes, however its expression is lost in advanced melanoma [237, 238]. PRDX2 is a negative regulator of PDGFR and the silencing of PRDX2 increased levels of PDGFR which resulted in increased growth of melanoma cells [237] and migration of mice cells [236].

In WM-115 cells dasatinib reduced the phosphoprotein levels of one spot of PRDX2 by 2.69 fold. This phosphorylated form of PRDX2 could therefore be implicated in response to dasatinib. However to fully elucidate this role it would be necessary to identify the specific residue of PRDX2 that was phosphorylated and assess its affect on dasatinib sensitivity in melanoma.

Heat shock protein A5 (HSPA5, GRP78) phosphoprotein levels were both increased and decreased in untreated WM-266-4 cells compared to untreated WM-115 cells (2.67 fold increase and 2.79 fold decrease) and dasatinib treatment of WM-115 cells resulted in increased levels of phospho-HSPA9A (GRP75) (1.79 fold). HSPA8 (HSC71) phosphoprotein levels were decreased in untreated WM-266-4 cells when compared to untreated WM-115 cells (2.67 fold) and dasatinib treatment of WM-266-4 cells resulted in increased levels of HSPA8 (1.33 fold).

Heat shock protein (HSP) 70 family consists of 8 members, which enhance the recovery of stressed cells by catalysing the reassembly of damaged ribosomal proteins [239]. HSPA5, an essential housekeeping gene, is localised in the endoplasmic reticulum protein and is involved in protein folding and facilitating the transport of new proteins [239]. Interestingly chemotherapy induces the unfolded protein response which increases levels of HSPA5 in melanoma cell lines. HSPA5 inhibits apoptosis by preventing the activation of caspase 4 and 7 [240]. siRNA knockdown of HSPA5 resulted in apoptosis induction and sensitised cells to cisplatin [240]. c-SRC has been linked to activation of HSPA5 in kidney and fibroblast cells [241].

HSPA8 (HSC71) is expressed constitutively in most cell types and is an essential housekeeping protein. Its functions include amongst others protein folding and the prevention of protein aggregation which we confirmed by PANTHER analysis. Its importance is illustrated in mice, where knockout of HSPA8 is lethal [239]. Interestingly the simultaneous inhibition of HSPA1A and HSPA8 resulted in the inhibition of proliferation and apoptotic induction in colon, ovarian and glioblastoma cell lines [242].



Phosphoprotein levels of HSPA9A (GRP75) were reduced in response to dasatinib in WM-115 cells. This may implicate HSPA9A in response to dasatinib in melanoma. Previous studies have implicated HSPA9A in the progression of brain cancer [243], however no studies have been performed to assess its impact on drug sensitivity.

Levels of phospho-HSPA8 were decreased in WM-266-4 cells when compared to WM-115 cells and dasatinib resulted in the decrease in levels of HSPA8 in WM-266-4 cells. WM-266-4 is a dasatinib resistant cell line, and the reduction of phosphoprotein levels of HSPA8 by dasatinib would be expected to decrease proliferation and increase apoptosis [242]. Because WM-266-4 cells do not respond to dasatinib it would seem unlikely that HSPA8 is mediating resistance to dasatinib.

ANXA2 is expressed at higher levels in WM-115 cells compared to WM-266-4 cells (3.74, 1.98, 1.88 and 1.73 fold). We found that dasatinib increased the level of ANXA2 phosphorylation in WM-115 cells (3.06, 3.02, 2.17 and 1.97 fold), whilst dasatinib did not significantly affect ANXA2 in WM266-4 cells.

The annexin family are calcium sensitive proteins that can bind negatively charged phospholipids and establish interactions with other lipids. The annexin family have been previously implicated in proliferation, migration, apoptosis and chemoresistance in cancer [244, 245]. The annexin family have also been implicated in signalling through several pathways that are heavily linked with cancer and metastasis such as the vascular endothelial growth factor (VEGF), protein kinase C (PKC), EGFR and SRC kinase pathways [244, 246, 247].

Annexin-2 (ANXA2) linked with invasion, metastasis and angiogenesis is a substrate for PKC, PDGFR and SRC kinase and acts in a calcium dependant manner whereby it can interact with the cell surface and affect the movement of phospholipids [244]. ANXA2 is usually found in a tetrameric construct consisting of two ANXA2 chains and two S100A10 chains and the complex of ANXA2-S100A10 has a channel modulating effect on the cell surface which can affect the membrane interactions of lipids [248]. The role of S100A10 is not fully understood, however it is known that the calcium binding site of S100A10 is constitutively active and as such its actions are calcium independent [249]. SRC kinase has also been shown to phosphorylate S100A10 [250] and ANXA1 and ANXA2 have also been shown to interact with each other as they can both bind in a calcium dependent manner [251].

The expression of ANXA2 has been shown to be increased in glioma, pancreatic and colorectal cancer, whilst its expression was reduced in prostate cancer [244]. The expression of ANXA2 is also shown to be lower in metastatic samples when compared to primary samples in lung cancer [244]. Expression of ANXA2 therefore does not correlate with progression of cancer in all solid tumours. In our study, the levels of phosphorylated ANXA2 are slightly lower in the metastatic cell line WM-266-4 compared to the primary cell line WM-115. This indicates that ANXA2 phosphorylation may be lost with melanoma progression. Further analysis in a larger group of melanoma cell lines by immuno-blotting and studying phosphorylated ANXA2 in primary and metastatic melanoma patient samples by immunohistochemistry may help to elucidate the role of ANXA2 in cancer metastasis.

Treatment with dasatinib increased phosphorylation levels of ANXA2 in WM-115 cells but not in WM-266-4 cells. This may indicate that phosphorylated ANXA2 plays a role in dasatinib sensitivity. ANXA2 can be phosphorylated on both serine and tyrosine residues, and the phosphorylation of each residue can have different effects on ANXA2 function. Our immuno-blotting results suggest that dasatinib increased phosphorylation of tyrosine residues in WM-115 but not in WM-266-4 cells; whilst phosphorylation levels of serine residues were reduced by dasatinib treatment in both WM-115 and WM-266-4 cells. The levels of tyrosine and serine phosphorylation though were very low in both cases. Alterations in tyrosine phosphorylation therefore may be important in response to dasatinib in melanoma cell lines.

Phosphorylation of ANXA2 at tyrosine 23 (Y23) is associated with actin remodelling [252], proper endosomal association [190] and the translocation of ANXA2 to the membrane [253]. These factors implicate ANXA2 Y23 in the control of cancer cell motility. Interestingly SRC can directly phosphorylate ANXA2 on Y23 [253, 254], which negatively modulates ANXA2 function and inhibits the ability of ANXA2 to bind F-actin [254]. However another study found that phosphorylation of ANXA2 Y23 is essential for ANXA2 function and its association with the endosome [190]. Phosphorylation of ANXA2 Y23 has not been previously implicated in control of proliferation. However 12 other potential tyrosine phosphorylation sites have been identified by phosphoproteomic studies ([www.phosphosite.org](http://www.phosphosite.org)) and the function of these sites are not fully explored. ANXA2 Y274 was found to be altered in SRC transformed mice [255] and ANXA2 Y237 has been associated with migration [256]. This may indicate that tyrosine phosphorylation of ANXA2 may play a role in

proliferation inhibition in dasatinib sensitive melanoma cell lines, however further studies of individual tyrosine phosphorylation residues is required.

ANXA2 can exist as either a tetramer bound to S100-A10 or as a monomer [257]. Phosphorylation of serine 25 (S25) of the ANXA2 monomer by the PKC pathway [258] has been associated with ANXA2 nuclear entry [259]. The entry of ANXA2 to the nucleus has been associated with control of proliferation and DNA synthesis [260]. Studying nuclear localisation of ANXA2 in melanoma cells in response to dasatinib may clarify if S25 ANXA2 phosphorylation plays a role in dasatinib sensitivity.

ANXA2 has been associated with control of proliferation, apoptosis and the invasive potential of multiple myeloma and ANXA2 knockdown can reduce proliferation and migration whilst increasing apoptosis in a range of cancer types [261-264]. We found that ANXA2 siRNA caused significant inhibition of growth in the dasatinib sensitive WM-115 cells. In the dasatinib resistant WM-266-4 cells there was a slight decrease in growth but the affect was not significant. Inhibition of ANXA2 function may play a role in dasatinib mediated inhibition of growth in WM-115 cells. However, further investigation would be required to determine the effects of the altered phosphorylation of ANXA2 on its function and response to dasatinib.

Our attempts to study the effect of ANXA2 knockdown on sensitivity to dasatinib were unsuccessful. The transfection reagent Lipofectamine 2000 increased the sensitivity of both WM-155 and WM-266-4 cell lines to dasatinib. Previous studies increased the time between transfection and drug treatment allowing the cells a

chance to recover from transfection [265]. If the knockdown of ANXA2 by siRNA can be maintained it may be possible to further study the role of ANXA2 in dasatinib sensitivity. Alternatively stable transfection of short hairpin RNA to knockdown ANXA2 may be required to study the effects on dasatinib sensitivity.

Pro-Q diamond staining of dasatinib treated WM-266-4 cells compared to untreated cells was performed to identify proteins that had altered phosphorylation levels in response to dasatinib. Analysis of dasatinib treated WM-115 cells could not be performed due to insufficient quantities of phosphoprotein required to perform duplicate gels. For the comparison of dasatinib treatment of WM-266-4 cell lines duplicate gels were analysed and SameSpots analysis used to identify significantly altered phosphorylation status between untreated and treated WM-266-4 cell lines.

Pro-Q Diamond staining though was not a reliable technique. Staining between gels often varied despite even loading concentrations and similar incubation times for the Pro-Q Diamond stain causing concerns over the reliability of results. From the limited number of proteins identified by Pro-Q Diamond staining of dasatinib treated WM-266-4 cells, two proteins showed increased phosphorylation levels in response to dasatinib.

Endoplasmic reticulum protein 29 (ERP29) a general endoplasmic reticulum marker usually localised to the endoplasmic reticulum or nuclear envelope is implicated in secretory protein synthesis [266, 267]. Studies in breast cancer xenografts have demonstrated that ERP29 contributes to the growth of MCF-7 induced tumours. [268].

Pro-Q Diamond results demonstrated that dasatinib significantly increased the phosphorylation of ERP29 in WM-266-4 (5.4 fold). However, using immuno-blotting we failed to detect tyrosine phosphorylation in either dasatinib untreated or treated WM-155 or WM-266-4 cells. The discrepancy between these results may be due to two factors. Replicate staining of untreated and dasatinib treated WM-266-4 gels with Pro-Q diamond failed to produce repeatable results due to irregular binding of the stain to the phosphorylated proteins. This may indicate that the identified phosphorylated proteins are artefacts and that dasatinib does not alter the phosphorylation level of ERP29. Alternatively previous analysis has only identified one tyrosine phosphorylation site for ERP29 ([www.phosphosite.org](http://www.phosphosite.org)). The basal level of phosphorylation for ERP29 in untreated WM-266-4 cells by Pro-Q Diamond staining (section 2.21) was very low and dasatinib treatment only resulted in a slight but significant increase in phosphorylation of ERP29 in WM-266-4 cells. Therefore, detection of ERP29 tyrosine residues by immuno-blotting may not be possible due to low levels of phosphorylation.

Heat shock protein 60 (HSP60) is a mitochondrial chaperone that functions by preventing the aggregation and promoting proteolytic degradation of misfolded or denatured proteins [269, 270]. An increase in the levels of HSP60 has been associated with apoptotic survival and increased proliferation [271].

In WM-266-4 cells dasatinib treatment resulted in an increase in the phosphorylation of HSP60, according to the Pro-Q Diamond analysis. This could possibly implicate HSP60 in resistance to dasatinib in melanoma cell lines. However immuno-blotting

of HSP60 tyrosine and serine residues failed to confirm this result. Pro-Q-Diamond staining identified low basal levels of phosphorylated HSP60 in untreated WM-266-4 cells and the resulting increase in phosphorylation of HSP60 after dasatinib treatment was low. Previous analysis has identified two potential serine and three potential tyrosine phosphorylation sites ([www.phosphosite.org](http://www.phosphosite.org)). A limitation of our study is that immuno-blotting with phospho-tyrosine and phospho-serine antibodies detects total tyrosine and serine phosphorylation levels of HSP60. Alterations in the phosphorylation of multiple sites may not be detected by immunoblotting if there are multiple changes in phosphorylation. Further analysis to identify specific phosphorylation sites which are important in cancer would be required to identify if HSP60 plays a role in dasatinib resistance.

Comparison of the lists of phosphoproteins identified in the primary and metastatic cell lines WM-115 and WM-266-4 may also lead to identification of phosphoproteins associated with metastasis.

Fascin 1 (FSCN1) phosphoprotein levels were increased in WM-266-4 cells compared to WM-115 cells indicating that FSCN1 could be a marker of metastasis for melanoma. FSCN1, which functions in the formation of actin based structures, [272] is increased in breast, lung and ovary cancer. Increased expression correlates with tumour progression and aggressiveness in colorectal cancer [273].

Lambda crystallin homolog (CRYL1) was found to be 24.17 fold higher in WM-266 cells compared to WM-115 cells. CRYL1 is a tumour suppressor gene known to be related to small heat shock proteins [274]. No studies have been performed in

melanoma, however expression of CRYL1 was lower in hepato-cellular carcinoma (HCC) compared to non-tumour liver samples, and low expression of CRYL1 was associated with poor response in liver cancer. The increased expression of CRYL1 observed in WM-266-4 may implicate CRYL1 expression in melanoma metastasis.

Three alpha-enolase (ENO1) spots were detected by phosphoproteomic analysis. Two spots showed increased phosphoprotein levels whilst one spot showed decreased phosphoprotein levels in WM-115 cells compared to WM-266-4 cells. (ENO1) is an enzyme involved in the glycolytic pathway and is frequently down-regulated in lung cancer, and low levels of ENO1 are predictive of aggressive behaviour of the tumour [275]. ENO1 has been shown to direct the migration and invasion of monocytic cells in inflammatory responses [276]. Further studies are required to analyse the role of ENO1 in melanoma in melanoma growth and metastasis.

## **9.6 Summary and Conclusion**

In summary, our data suggests that melanoma cell lines are not an appropriate model to study chemotherapy drug resistance.

We found that dasatinib has anti-proliferative and anti-invasive effects in melanoma cell lines, and that the combination of dasatinib and TMZ is more effective at inhibiting proliferation than either drug alone. We believe that the use of dasatinib in combination with TMZ represents a viable alternative to current therapeutic regimens for metastatic melanoma and should be further studied to determine its efficacy in patients.



From analysis of previously studied dasatinib sensitivity biomarkers we identified a 3-gene marker of sensitivity in melanoma cell lines. We analysed expression of CAV-1 and SRC in patient samples and found that they were expressed in 44 % and 73 % of melanoma tumours respectively. Further analysis of ANXA1 and EphA2 in patient samples will determine the percentage of patients who express all three markers and classify them as the group who may respond to dasatinib therapy.

Finally phosphoproteomic analysis revealed that levels of phosphorylated ANXA2 were lower in dasatinib responsive WM-115 cells compared to dasatinib resistant WM-266-4 cells. SiRNA knockdown of ANXA2 resulted in decreased proliferation in WM-115 cells compared to WM-266-4 cells possibly implicating ANXA2 in mediating response to dasatinib in melanoma cell lines. To determine the role of ANXA2 in dasatinib response or resistance it would be necessary to identify specific phosphorylation residues affected by dasatinib therapy. By specifically inhibiting these residues we could determine their effect on proliferation, invasion and migration in melanoma cell lines.

## **References**

1. Garbe, C. and U. Leiter, *Melanoma epidemiology and trends*. Clin Dermatol, 2009. **27**(1): p. 3-9.
2. Perlis, C. and M. Herlyn, *Recent advances in melanoma biology*. Oncologist, 2004. **9**(2): p. 182-7.
3. Freeman, S.E., et al., *Wavelength dependence of pyrimidine dimer formation in DNA of human skin irradiated in situ with ultraviolet light*. Proc Natl Acad Sci U S A, 1989. **86**(14): p. 5605-9.
4. Jhappan, C., F.P. Noonan, and G. Merlino, *Ultraviolet radiation and cutaneous malignant melanoma*. Oncogene, 2003. **22**(20): p. 3099-112.
5. Cummins, D.L., et al., *Cutaneous malignant melanoma*. Mayo Clin Proc, 2006. **81**(4): p. 500-7.
6. Balch, C.M., et al., *Final version of the American Joint Committee on Cancer staging system for cutaneous melanoma*. J Clin Oncol, 2001. **19**(16): p. 3635-48.
7. Mitchell, M.S., *Chemotherapy for melanoma: the resultant of conflicting vectors*. J Clin Oncol, 2004. **22**(11): p. 2043-5.
8. Hsu, M.Y., F. Meier, and M. Herlyn, *Melanoma development and progression: a conspiracy between tumor and host*. Differentiation, 2002. **70**(9-10): p. 522-36.
9. Chin, L., *The genetics of malignant melanoma: lessons from mouse and man*. Nat Rev Cancer, 2003. **3**(8): p. 559-70.
10. Kincannon, J. and C. Boutzale, *The physiology of pigmented nevi*. Pediatrics, 1999. **104**(4 Pt 2): p. 1042-5.
11. Gray-Schopfer, V., C. Wellbrock, and R. Marais, *Melanoma biology and new targeted therapy*. Nature, 2007. **445**(7130): p. 851-7.
12. Neville, J.A., E. Welch, and D.J. Leffell, *Management of nonmelanoma skin cancer in 2007*. Nat Clin Pract Oncol, 2007. **4**(8): p. 462-9.
13. Roewert-Huber, J., et al., *Epidemiology and aetiology of basal cell carcinoma*. Br J Dermatol, 2007. **157** Suppl 2: p. 47-51.
14. Wong, C.S., R.C. Strange, and J.T. Lear, *Basal cell carcinoma*. Bmj, 2003. **327**(7418): p. 794-8.
15. von Domarus, H. and P.J. Stevens, *Metastatic basal cell carcinoma. Report of five cases and review of 170 cases in the literature*. J Am Acad Dermatol, 1984. **10**(6): p. 1043-60.
16. Shelton, R.M., *Skin cancer: a review and atlas for the medical provider*. Mt Sinai J Med, 2001. **68**(4-5): p. 243-52.
17. Callen, J.P., D.R. Bickers, and R.L. Moy, *Actinic keratoses*. J Am Acad Dermatol, 1997. **36**(4): p. 650-3.
18. Anwar, J., et al., *The development of actinic keratosis into invasive squamous cell carcinoma: evidence and evolving classification schemes*. Clin Dermatol, 2004. **22**(3): p. 189-96.
19. Rinker, M.H., et al., *Histologic variants of squamous cell carcinoma of the skin*. Cancer Control, 2001. **8**(4): p. 354-63.
20. Hara, H., et al., *Detection of human papillomavirus type 34 in Bowen's disease on the pubic area*. J Eur Acad Dermatol Venereol, 2006. **20**(2): p. 206-8.
21. McGuire, J.F., N.N. Ge, and S. Dyson, *Nonmelanoma skin cancer of the head and neck I: histopathology and clinical behavior*. Am J Otolaryngol, 2009. **30**(2): p. 121-33.

22. Kinsler, V. and N. Bulstrode, *The role of surgery in the management of congenital melanocytic naevi in children: a perspective from Great Ormond Street Hospital*. J Plast Reconstr Aesthet Surg, 2009. **62**(5): p. 595-601.
23. Armour, K., S. Mann, and S. Lee, *Dysplastic naevi: to shave, or not to shave? A retrospective study of the use of the shave biopsy technique in the initial management of dysplastic naevi*. Australas J Dermatol, 2005. **46**(2): p. 70-5.
24. Chudnovsky, Y., P.A. Khavari, and A.E. Adams, *Melanoma genetics and the development of rational therapeutics*. J Clin Invest, 2005. **115**(4): p. 813-24.
25. Kelly, J.W., et al., *Nodular melanoma. No longer as simple as ABC*. Aust Fam Physician, 2003. **32**(9): p. 706-9.
26. Redondo, P., et al., *Amelanotic melanoma presenting as a scar*. Arch Intern Med, 2001. **161**(15): p. 1912-3.
27. Chamberlain, A. and J. Ng, *Cutaneous melanoma--atypical variants and presentations*. Aust Fam Physician, 2009. **38**(7): p. 476-82.
28. Woodman, S.E. and M.A. Davies, *Targeting KIT in melanoma: A paradigm of molecular medicine and targeted therapeutics*. Biochem Pharmacol.
29. Gershenwald, J.E., S.J. Soong, and C.M. Balch, *2010 TNM Staging System for Cutaneous Melanoma...and Beyond*. Ann Surg Oncol.
30. Gogas, H., et al., *Biomarkers in melanoma*. Ann Oncol, 2009. **20 Suppl 6**: p. vi8-13.
31. Ugurel, S., J. Utikal, and J.C. Becker, *Tumor biomarkers in melanoma*. Cancer Control, 2009. **16**(3): p. 219-24.
32. Janku, F., et al., *KIT receptor is expressed in more than 50% of early-stage malignant melanoma: a retrospective study of 261 patients*. Melanoma Res, 2005. **15**(4): p. 251-6.
33. Dai, D.L., M. Martinka, and G. Li, *Prognostic significance of activated Akt expression in melanoma: a clinicopathologic study of 292 cases*. J Clin Oncol, 2005. **23**(7): p. 1473-82.
34. Mikhail, M., et al., *PTEN expression in melanoma: relationship with patient survival, Bcl-2 expression, and proliferation*. Clin Cancer Res, 2005. **11**(14): p. 5153-7.
35. Andersen, K., et al., *Expression of S100A4 combined with reduced E-cadherin expression predicts patient outcome in malignant melanoma*. Mod Pathol, 2004. **17**(8): p. 990-7.
36. Guo, H.B., et al., *Clinical significance of serum S100 in metastatic malignant melanoma*. Eur J Cancer, 1995. **31A**(11): p. 1898-902.
37. Stahlecker, J., et al., *MIA as a reliable tumor marker in the serum of patients with malignant melanoma*. Anticancer Res, 2000. **20**(6D): p. 5041-4.
38. Lee, J.T. and M. Herlyn, *Microenvironmental influences in melanoma progression*. J Cell Biochem, 2007. **101**(4): p. 862-72.
39. Berking, C., et al., *Basic fibroblast growth factor and ultraviolet B transform melanocytes in human skin*. Am J Pathol, 2001. **158**(3): p. 943-53.
40. Ruiter, D., et al., *Melanoma-stroma interactions: structural and functional aspects*. Lancet Oncol, 2002. **3**(1): p. 35-43.
41. Lazar-Molnar, E., et al., *Autocrine and paracrine regulation by cytokines and growth factors in melanoma*. Cytokine, 2000. **12**(6): p. 547-54.
42. Chin, L., G. Merlino, and R.A. DePinho, *Malignant melanoma: modern black plague and genetic black box*. Genes Dev, 1998. **12**(22): p. 3467-81.
43. Herlyn, M., *Metastatic melanoma cells. Introduction*. Cancer Metastasis Rev, 2005. **24**(2): p. 193-4.

44. Rodolfo, M., M. Daniotti, and V. Vallacchi, *Genetic progression of metastatic melanoma*. *Cancer Lett*, 2004. **214**(2): p. 133-47.
45. Ronnstrand, L., *Signal transduction via the stem cell factor receptor/c-Kit*. *Cell Mol Life Sci*, 2004. **61**(19-20): p. 2535-48.
46. Giehl, A., et al., *Protein expression of melanocyte growth factors (bFGF, SCF) and their receptors (FGFR-1, c-kit) in nevi and melanoma*. *Journal of Cutaneous Pathology*, 2007. **34**(1): p. 7-14.
47. Grichnik, J.M., et al., *The SCF/KIT pathway plays a critical role in the control of normal human melanocyte homeostasis*. *J Invest Dermatol*, 1998. **111**(2): p. 233-8.
48. Marquette, A., et al., *Recent discoveries in the genetics of melanoma and their therapeutic implications*. *Arch Immunol Ther Exp (Warsz)*, 2007. **55**(6): p. 363-72.
49. Becker, J.C., et al., *Imatinib in melanoma: A selective treatment option based on KIT mutation status?* *Journal of Clinical Oncology*, 2007. **25**(7): p. E9-E9.
50. Rivera, R.S., et al., *C-kit protein expression correlated with activating mutations in KIT gene in oral mucosal melanoma*. *Virchows Arch*, 2008. **452**(1): p. 27-32.
51. Janku, F., et al., *KIT receptor is expressed in more than 50% of early-stage malignant melanoma: a retrospective study of 261 patients*. *Melanoma Research*, 2005. **15**(4): p. 251-256.
52. Curtin, J.A., et al., *Somatic activation of KIT in distinct subtypes of melanoma*. *J Clin Oncol*, 2006. **24**(26): p. 4340-6.
53. Holden, J.A., C. Willmore-Payne, and L.J. Layfield, *Tyrosine kinase activating mutations in human malignancies: implications for diagnostic pathology*. *Exp Mol Pathol*, 2008. **85**(1): p. 68-75.
54. Smalley, K.S., et al., *Identification of a novel subgroup of melanomas with KIT/cyclin-dependent kinase-4 overexpression*. *Cancer Res*, 2008. **68**(14): p. 5743-52.
55. Hilmi, C., et al., *IGF1 promotes resistance to apoptosis in melanoma cells through an increased expression of BCL2, BCL-X(L), and survivin*. *J Invest Dermatol*, 2008. **128**(6): p. 1499-505.
56. Yuen, J.S. and V.M. Macaulay, *Targeting the type I insulin-like growth factor receptor as a treatment for cancer*. *Expert Opin Ther Targets*, 2008. **12**(5): p. 589-603.
57. Ullrich, A., et al., *Insulin-like growth factor I receptor primary structure: comparison with insulin receptor suggests structural determinants that define functional specificity*. *Embo J*, 1986. **5**(10): p. 2503-12.
58. Ciampolillo, A., C. De Tullio, and F. Giorgino, *The IGF-I/IGF-I receptor pathway: Implications in the Pathophysiology of Thyroid Cancer*. *Curr Med Chem*, 2005. **12**(24): p. 2881-91.
59. Kanter-Lewensohn, L., et al., *Expression of the insulin-like growth factor-I receptor and its anti-apoptotic effect in malignant melanoma: a potential therapeutic target*. *Melanoma Res*, 1998. **8**(5): p. 389-97.
60. Maloney, E.K., et al., *An anti-insulin-like growth factor I receptor antibody that is a potent inhibitor of cancer cell proliferation*. *Cancer Res*, 2003. **63**(16): p. 5073-83.
61. Yeh, A.H., E.A. Bohula, and V.M. Macaulay, *Human melanoma cells expressing V600E B-RAF are susceptible to IGF1R targeting by small interfering RNAs*. *Oncogene*, 2006. **25**(50): p. 6574-81.

62. Kasper, B., et al., *Novel treatment strategies for malignant melanoma: a new beginning?* Crit Rev Oncol Hematol, 2007. **62**(1): p. 16-22.
63. Smalley, K.S. and M. Herlyn, *Loitering with intent: new evidence for the role of BRAF mutations in the proliferation of melanocytic lesions.* J Invest Dermatol, 2004. **123**(4): p. xvi-xvii.
64. Houben, R., et al., *Constitutive activation of the Ras-Raf signaling pathway in metastatic melanoma is associated with poor prognosis.* J Carcinog, 2004. **3**(1): p. 6.
65. Luo, J., B.D. Manning, and L.C. Cantley, *Targeting the PI3K-Akt pathway in human cancer: rationale and promise.* Cancer Cell, 2003. **4**(4): p. 257-62.
66. Curtin, J.A., et al., *PI3-kinase subunits are infrequent somatic targets in melanoma.* J Invest Dermatol, 2006. **126**(7): p. 1660-3.
67. Singh, R.S., et al., *Phosphoinositide 3-kinase is not overexpressed in melanocytic lesions.* J Cutan Pathol, 2007. **34**(3): p. 220-5.
68. Robertson, G.P., *Functional and therapeutic significance of Akt deregulation in malignant melanoma.* Cancer Metastasis Rev, 2005. **24**(2): p. 273-85.
69. Chung, J.H., et al., *The ERK1/2 pathway modulates nuclear PTEN-mediated cell cycle arrest by cyclin D1 transcriptional regulation.* Hum Mol Genet, 2006. **15**(17): p. 2553-9.
70. Chin, P.C. and S.R. D'Mello, *Brain chemotherapy from the bench to the clinic: targeting neuronal survival with small molecule inhibitors of apoptosis.* Front Biosci, 2005. **10**: p. 552-68.
71. Becker, J.C., E. Kampgen, and E. Brocker, *Classical chemotherapy for metastatic melanoma.* Clin Exp Dermatol, 2000. **25**(6): p. 503-8.
72. Maxwell, J.A., et al., *Mismatch repair deficiency does not mediate clinical resistance to temozolomide in malignant glioma.* Clin Cancer Res, 2008. **14**(15): p. 4859-68.
73. Naumann, S.C., et al., *Temozolomide- and fotemustine-induced apoptosis in human malignant melanoma cells: response related to MGMT, MMR, DSBs, and p53.* Br J Cancer, 2009. **100**(2): p. 322-33.
74. Brock, C.S., et al., *Phase I trial of temozolomide using an extended continuous oral schedule.* Cancer Res, 1998. **58**(19): p. 4363-7.
75. Qirt, I., et al., *Temozolomide for the treatment of metastatic melanoma: a systematic review.* Oncologist, 2007. **12**(9): p. 1114-23.
76. Gogas, H.J., J.M. Kirkwood, and V.K. Sondak, *Chemotherapy for metastatic melanoma: time for a change?* Cancer, 2007. **109**(3): p. 455-64.
77. Gajewski, T.F., et al., *Phase II trial of the O6-alkylguanine DNA alkyltransferase inhibitor O6-benzylguanine and 1,3-bis(2-chloroethyl)-1-nitrosourea in advanced melanoma.* Clin Cancer Res, 2005. **11**(21): p. 7861-5.
78. Larkin, J.M., et al., *A phase I/II study of lomustine and temozolomide in patients with cerebral metastases from malignant melanoma.* Br J Cancer, 2007. **96**(1): p. 44-8.
79. Li, Y. and E.F. McClay, *Systemic chemotherapy for the treatment of metastatic melanoma.* Semin Oncol, 2002. **29**(5): p. 413-26.
80. Clark, J.I., et al., *Phase 2 trial of combination thalidomide plus temozolomide in patients with metastatic malignant melanoma: Southwest Oncology Group S0508.* Cancer. **116**(2): p. 424-31.
81. Leslie, E.M., R.G. Deeley, and S.P. Cole, *Multidrug resistance proteins: role of P-glycoprotein, MRP1, MRP2, and BCRP (ABCG2) in tissue defense.* Toxicol Appl Pharmacol, 2005. **204**(3): p. 216-37.

82. Zhou, S.F., et al., *Substrates and inhibitors of human multidrug resistance associated proteins and the implications in drug development*. *Curr Med Chem*, 2008. **15**(20): p. 1981-2039.
83. Molinari, A., et al., *Detection of P-glycoprotein in the Golgi apparatus of drug-untreated human melanoma cells*. *Int J Cancer*, 1998. **75**(6): p. 885-93.
84. Helmbach, H., et al., *Drug-resistance in human melanoma*. *Int J Cancer*, 2001. **93**(5): p. 617-22.
85. Schadendorf, D., R. Herfordt, and B.M. Czarnetzki, *P-glycoprotein expression in primary and metastatic malignant melanoma*. *Br J Dermatol*, 1995. **132**(4): p. 551-5.
86. Ichihashi, N. and Y. Kitajima, *Chemotherapy induces or increases expression of multidrug resistance-associated protein in malignant melanoma cells*. *Br J Dermatol*, 2001. **144**(4): p. 745-50.
87. Jedlitschky, G., U. Hoffmann, and H.K. Kroemer, *Structure and function of the MRP2 (ABCC2) protein and its role in drug disposition*. *Expert Opin Drug Metab Toxicol*, 2006. **2**(3): p. 351-66.
88. Gerk, P.M. and M. Vore, *Regulation of expression of the multidrug resistance-associated protein 2 (MRP2) and its role in drug disposition*. *J Pharmacol Exp Ther*, 2002. **302**(2): p. 407-15.
89. Choudhuri, S. and C.D. Klaassen, *Structure, function, expression, genomic organization, and single nucleotide polymorphisms of human ABCB1 (MDR1), ABCC (MRP), and ABCG2 (BCRP) efflux transporters*. *Int J Toxicol*, 2006. **25**(4): p. 231-59.
90. Liedert, B., et al., *Overexpression of cMOAT (MRP2/ABCC2) is associated with decreased formation of platinum-DNA adducts and decreased G2-arrest in melanoma cells resistant to cisplatin*. *J Invest Dermatol*, 2003. **121**(1): p. 172-6.
91. Sarkadi, B., et al., *Human multidrug resistance ABCB and ABCG transporters: participation in a chemoimmunity defense system*. *Physiol Rev*, 2006. **86**(4): p. 1179-236.
92. Diestra, J.E., et al., *Frequent expression of the multi-drug resistance-associated protein BCRP/MXR/ABCP/ABCG2 in human tumours detected by the BXP-21 monoclonal antibody in paraffin-embedded material*. *J Pathol*, 2002. **198**(2): p. 213-9.
93. Frank, N.Y., et al., *ABCB5-mediated doxorubicin transport and chemoresistance in human malignant melanoma*. *Cancer Res*, 2005. **65**(10): p. 4320-33.
94. Bush, J.A. and G. Li, *The role of Bcl-2 family members in the progression of cutaneous melanoma*. *Clin Exp Metastasis*, 2003. **20**(6): p. 531-9.
95. Giannetti, L., et al., *Apoptosis: escaping strategies in human skin cancer (Review)*. *Oncol Rep*, 2004. **11**(2): p. 401-5.
96. Nachmias, B., et al., *Caspase-mediated cleavage converts Livin from an antiapoptotic to a proapoptotic factor: implications for drug-resistant melanoma*. *Cancer Res*, 2003. **63**(19): p. 6340-9.
97. Grossman, D., et al., *Inhibition of melanoma tumor growth in vivo by survivin targeting*. *Proc Natl Acad Sci U S A*, 2001. **98**(2): p. 635-40.
98. Hussein, M.R., A.K. Haemel, and G.S. Wood, *Apoptosis and melanoma: molecular mechanisms*. *J Pathol*, 2003. **199**(3): p. 275-88.
99. Komenaka, I., H. Hoerig, and H.L. Kaufman, *Immunotherapy for melanoma*. *Clin Dermatol*, 2004. **22**(3): p. 251-65.

100. Morton, D.L., et al., *Improved long-term survival after lymphadenectomy of melanoma metastatic to regional nodes. Analysis of prognostic factors in 1134 patients from the John Wayne Cancer Clinic.* Ann Surg, 1991. **214**(4): p. 491-9; discussion 499-501.
101. Lee, P.P., et al., *Characterization of circulating T cells specific for tumor-associated antigens in melanoma patients.* Nat Med, 1999. **5**(6): p. 677-85.
102. Chiao, E.Y. and S.E. Krown, *Update on non-acquired immunodeficiency syndrome-defining malignancies.* Curr Opin Oncol, 2003. **15**(5): p. 389-97.
103. Fang, L., A.S. Lonsdorf, and S.T. Hwang, *Immunotherapy for advanced melanoma.* J Invest Dermatol, 2008. **128**(11): p. 2596-605.
104. Atkins, M.B., et al., *High-dose recombinant interleukin 2 therapy for patients with metastatic melanoma: analysis of 270 patients treated between 1985 and 1993.* J Clin Oncol, 1999. **17**(7): p. 2105-16.
105. Petrella, T., et al., *Single-agent interleukin-2 in the treatment of metastatic melanoma: a systematic review.* Cancer Treat Rev, 2007. **33**(5): p. 484-96.
106. Acquavella, N., et al., *Toxicity and activity of a twice daily high-dose bolus interleukin 2 regimen in patients with metastatic melanoma and metastatic renal cell cancer.* J Immunother, 2008. **31**(6): p. 569-76.
107. Schadendorf, D., et al., *Immunotherapy of distant metastatic disease.* Ann Oncol, 2009. **20 Suppl 6**: p. vi41-50.
108. Tsao, H., M.B. Atkins, and A.J. Sober, *Management of cutaneous melanoma.* N Engl J Med, 2004. **351**(10): p. 998-1012.
109. Sznol, M., *Betting on immunotherapy for melanoma.* Curr Oncol Rep, 2009. **11**(5): p. 397-404.
110. Eggermont, A.M., et al., *Utility of adjuvant systemic therapy in melanoma.* Ann Oncol, 2009. **20 Suppl 6**: p. vi30-4.
111. Ascierto, P.A. and J.M. Kirkwood, *Adjuvant therapy of melanoma with interferon: lessons of the past decade.* J Transl Med, 2008. **6**: p. 62.
112. Wheatley, K., et al., *Does adjuvant interferon-alpha for high-risk melanoma provide a worthwhile benefit? A meta-analysis of the randomised trials.* Cancer Treat Rev, 2003. **29**(4): p. 241-52.
113. Legha, S.S., *The role of interferon alfa in the treatment of metastatic melanoma.* Semin Oncol, 1997. **24**(1 Suppl 4): p. S24-31.
114. Ascierto, P.A., et al., *Adjuvant treatment of malignant melanoma: where are we?* Crit Rev Oncol Hematol, 2006. **57**(1): p. 45-52.
115. Marincola, F.M., et al., *Combination therapy with interferon alfa-2a and interleukin-2 for the treatment of metastatic cancer.* J Clin Oncol, 1995. **13**(5): p. 1110-22.
116. Cranmer, L.D. and E. Hersh, *The role of the CTLA4 blockade in the treatment of malignant melanoma.* Cancer Invest, 2007. **25**(7): p. 613-31.
117. Weber, J., *Ipilimumab: controversies in its development, utility and autoimmune adverse events.* Cancer Immunol Immunother, 2009. **58**(5): p. 823-30.
118. Kaufmann, R., et al., *Temozolomide in combination with interferon-alfa versus temozolomide alone in patients with advanced metastatic melanoma: a randomized, phase III, multicenter study from the Dermatologic Cooperative Oncology Group.* J Clin Oncol, 2005. **23**(35): p. 9001-7.
119. Hauschild, A., et al., *Combined treatment with pegylated interferon-alpha-2a and dacarbazine in patients with advanced metastatic melanoma: a phase 2 study.* Cancer, 2008. **113**(6): p. 1404-11.



120. Spieth, K., et al., *Temozolomide plus pegylated interferon alfa-2b as first-line treatment for stage IV melanoma: a multicenter phase II trial of the Dermatologic Cooperative Oncology Group (DeCOG)*. *Ann Oncol*, 2008. **19**(4): p. 801-6.
121. Ives, N.J., et al., *Chemotherapy compared with biochemotherapy for the treatment of metastatic melanoma: a meta-analysis of 18 trials involving 2,621 patients*. *J Clin Oncol*, 2007. **25**(34): p. 5426-34.
122. Rosenberg, S.A., et al., *Prospective randomized trial of the treatment of patients with metastatic melanoma using chemotherapy with cisplatin, dacarbazine, and tamoxifen alone or in combination with interleukin-2 and interferon alfa-2b*. *J Clin Oncol*, 1999. **17**(3): p. 968-75.
123. Robert, C., et al., *Phase I/II study of the association of sorafenib and temozolomide (extended schedule) in patients with metastatic melanoma: A new clinical response profile with massive tumor necroses.*, in *J Clin Oncol* 2009.
124. Sharma, A., et al., *Mutant V599EB-Raf regulates growth and vascular development of malignant melanoma tumors*. *Cancer Res*, 2005. **65**(6): p. 2412-21.
125. Murphy, D.A., et al., *Inhibition of tumor endothelial ERK activation, angiogenesis, and tumor growth by sorafenib (BAY43-9006)*. *Am J Pathol*, 2006. **169**(5): p. 1875-85.
126. Eisen, T., et al., *Sorafenib in advanced melanoma: a Phase II randomised discontinuation trial analysis*. *Br J Cancer*, 2006. **95**(5): p. 581-6.
127. McDermott, D.F., et al., *Double-blind randomized phase II study of the combination of sorafenib and dacarbazine in patients with advanced melanoma: a report from the 11715 Study Group*. *J Clin Oncol*, 2008. **26**(13): p. 2178-85.
128. Hauschild, A., et al., *Results of a phase III, randomized, placebo-controlled study of sorafenib in combination with carboplatin and paclitaxel as second-line treatment in patients with unresectable stage III or stage IV melanoma*. *J Clin Oncol*, 2009. **27**(17): p. 2823-30.
129. Tsai, J., et al., *Discovery of a selective inhibitor of oncogenic B-Raf kinase with potent antimelanoma activity*. *Proc Natl Acad Sci U S A*, 2008. **105**(8): p. 3041-6.
130. Dhillon, A.S., et al., *MAP kinase signalling pathways in cancer*. *Oncogene*, 2007. **26**(22): p. 3279-90.
131. Adjei, A.A., et al., *Phase I pharmacokinetic and pharmacodynamic study of the oral, small-molecule mitogen-activated protein kinase kinase 1/2 inhibitor AZD6244 (ARRY-142886) in patients with advanced cancers*. *J Clin Oncol*, 2008. **26**(13): p. 2139-46.
132. Dummer, R., et al., *AZD6244 (ARRY-142886) vs temozolomide (TMZ) in patients (pts) with advanced melanoma: An open-label, randomized, multicenter, phase II study.*, in *2008 ASCO Annual Meeting*. 2008, *J Clin Oncol*
133. Stahl, J.M., et al., *Deregulated Akt3 activity promotes development of malignant melanoma*. *Cancer Res*, 2004. **64**(19): p. 7002-10.
134. Tsao, A.S., et al., *Inhibition of c-Src expression and activation in malignant pleural mesothelioma tissues leads to apoptosis, cell cycle arrest, and decreased migration and invasion*. *Mol Cancer Ther*, 2007. **6**(7): p. 1962-72.

135. Goel, V.K., et al., *Examination of mutations in BRAF, NRAS, and PTEN in primary cutaneous melanoma*. J Invest Dermatol, 2006. **126**(1): p. 154-60.
136. Karbowniczek, M., et al., *mTOR is activated in the majority of malignant melanomas*. J Invest Dermatol, 2008. **128**(4): p. 980-7.
137. Dancey, J.E., *Molecular targeting: PI3 kinase pathway*. Ann Oncol, 2004. **15 Suppl 4**: p. iv233-9.
138. McCormick, F., *Cancer: survival pathways meet their end*. Nature, 2004. **428**(6980): p. 267-9.
139. Yap, T.A., et al., *Targeting the PI3K-AKT-mTOR pathway: progress, pitfalls, and promises*. Curr Opin Pharmacol, 2008. **8**(4): p. 393-412.
140. Wulff, B.C., et al., *Sirolimus reduces the incidence and progression of UVB-induced skin cancer in SKH mice even with co-administration of cyclosporine A*. J Invest Dermatol, 2008. **128**(10): p. 2467-73.
141. Bundscherer, A., et al., *Antiproliferative and proapoptotic effects of rapamycin and celecoxib in malignant melanoma cell lines*. Oncol Rep, 2008. **19**(2): p. 547-53.
142. Romano, M.F., et al., *Rapamycin inhibits doxorubicin-induced NF-kappaB/Rel nuclear activity and enhances the apoptosis of melanoma cells*. Eur J Cancer, 2004. **40**(18): p. 2829-36.
143. Molhoek, K.R., D.L. Brautigan, and C.L. Slingsluff, Jr., *Synergistic inhibition of human melanoma proliferation by combination treatment with B-Raf inhibitor BAY43-9006 and mTOR inhibitor Rapamycin*. J Transl Med, 2005. **3**: p. 39.
144. Thallinger, C., et al., *Comparison of a treatment strategy combining CCI-779 plus DTIC versus DTIC monotreatment in human melanoma in SCID mice*. J Invest Dermatol, 2007. **127**(10): p. 2411-7.
145. Thallinger, C., et al., *CCI-779 plus cisplatin is highly effective against human melanoma in a SCID mouse xenotransplantation model*. Pharmacology, 2007. **79**(4): p. 207-13.
146. Margolin, K., et al., *CCI-779 in metastatic melanoma: a phase II trial of the California Cancer Consortium*. Cancer, 2005. **104**(5): p. 1045-8.
147. Krasilnikov, M., et al., *Contribution of phosphatidylinositol 3-kinase to radiation resistance in human melanoma cells*. Mol Carcinog, 1999. **24**(1): p. 64-9.
148. Bedogni, B., et al., *The hypoxic microenvironment of the skin contributes to Akt-mediated melanocyte transformation*. Cancer Cell, 2005. **8**(6): p. 443-54.
149. Baumann, P., et al., *The novel orally bioavailable inhibitor of phosphoinositol-3-kinase and mammalian target of rapamycin, NVP-BEZ235, inhibits growth and proliferation in multiple myeloma*. Exp Cell Res, 2008.
150. Maira, S.M., et al., *Identification and characterization of NVP-BEZ235, a new orally available dual phosphatidylinositol 3-kinase/mammalian target of rapamycin inhibitor with potent in vivo antitumor activity*. Mol Cancer Ther, 2008. **7**(7): p. 1851-63.
151. Serra, V., et al., *NVP-BEZ235, a dual PI3K/mTOR inhibitor, prevents PI3K signaling and inhibits the growth of cancer cells with activating PI3K mutations*. Cancer Res, 2008. **68**(19): p. 8022-30.
152. Molckovsky, A. and L.L. Siu, *First-in-class, first-in-human phase I results of targeted agents: Highlights of the 2008 American Society of Clinical Oncology meeting*. J Hematol Oncol, 2008. **1**: p. 20.

153. Ernst, D.S., et al., *Phase II study of perifosine in previously untreated patients with metastatic melanoma*. Invest New Drugs, 2005. **23**(6): p. 569-75.
154. Lasithiotakis, K.G., et al., *Combined inhibition of MAPK and mTOR signaling inhibits growth, induces cell death, and abrogates invasive growth of melanoma cells*. J Invest Dermatol, 2008. **128**(8): p. 2013-23.
155. Bedogni, B., et al., *Inhibition of phosphatidylinositol-3-kinase and mitogen-activated protein kinase kinase 1/2 prevents melanoma development and promotes melanoma regression in the transgenic TPRas mouse model*. Mol Cancer Ther, 2006. **5**(12): p. 3071-7.
156. Meier, F., et al., *Combined targeting of MAPK and AKT signalling pathways is a promising strategy for melanoma treatment*. Br J Dermatol, 2007. **156**(6): p. 1204-13.
157. Uziel, O., et al., *Imatinib mesylate (Gleevec) downregulates telomerase activity and inhibits proliferation in telomerase-expressing cell lines*. Br J Cancer, 2005. **92**(10): p. 1881-91.
158. Eton, O., et al., *Phase II trial of imatinib mesylate (STI-571) in metastatic melanoma (MM)*. Journal of Clinical Oncology, 2004. **22**(14): p. 717S-717S.
159. Kim, K.B., et al., *Phase II trial of imatinib mesylate in patients with metastatic melanoma*. Br J Cancer, 2008. **99**(5): p. 734-40.
160. Barnekow, A., E. Paul, and M. Scharfl, *Expression of the c-src protooncogene in human skin tumors*. Cancer Res, 1987. **47**(1): p. 235-40.
161. Marchetti, D., et al., *Stimulation of the protein tyrosine kinase c-Yes but not c-Src by neurotrophins in human brain-metastatic melanoma cells*. Oncogene, 1998. **16**(25): p. 3253-60.
162. Huang, J., et al., *Cooperative roles of Fyn and cortactin in cell migration of metastatic murine melanoma*. J Biol Chem, 2003. **278**(48): p. 48367-76.
163. Qi, J., et al., *Involvement of Src family kinases in N-cadherin phosphorylation and beta-catenin dissociation during transendothelial migration of melanoma cells*. Mol Biol Cell, 2006. **17**(3): p. 1261-72.
164. Wellbrock, C., et al., *Activation of p59(Fyn) leads to melanocyte dedifferentiation by influencing MKP-1-regulated mitogen-activated protein kinase signaling*. J Biol Chem, 2002. **277**(8): p. 6443-54.
165. Loganzo, F., Jr., et al., *Elevated expression of protein tyrosine kinase c-Yes, but not c-Src, in human malignant melanoma*. Oncogene, 1993. **8**(10): p. 2637-44.
166. Homsy, J., C. Cubitt, and A. Daud, *The Src signaling pathway: a potential target in melanoma and other malignancies*. Expert Opin Ther Targets, 2007. **11**(1): p. 91-100.
167. Deconti, M., Decker et al. *Expression of STAT proteins and interferon- $\alpha$  receptors in benign and malignant melanocytic lesions: correlation with recurrence*. . in ASCO Annual Meeting Proceedings (2004). 2004.
168. Niu, G., et al., *Roles of activated Src and Stat3 signaling in melanoma tumor cell growth*. Oncogene, 2002. **21**(46): p. 7001-10.
169. Lombardo, L.J., et al., *Discovery of N-(2-chloro-6-methyl-phenyl)-2-(6-(4-(2-hydroxyethyl)-piperazin-1-yl)-2-methylpyrimidin-4-ylamino)thiazole-5-carboxamide (BMS-354825), a dual Src/Abl kinase inhibitor with potent antitumor activity in preclinical assays*. J Med Chem, 2004. **47**(27): p. 6658-61.
170. Eustace, A.J., et al., *Preclinical evaluation of dasatinib, a potent Src kinase inhibitor, in melanoma cell lines*. J Transl Med, 2008. **6**(1): p. 53.

171. Nam, S., et al., *Action of the Src family kinase inhibitor, dasatinib (BMS-354825), on human prostate cancer cells.* Cancer Res, 2005. **65**(20): p. 9185-9.
172. Finn, R.S., et al., *Dasatinib, an orally active small molecule inhibitor of both the src and abl kinases, selectively inhibits growth of basal-type/"triple-negative" breast cancer cell lines growing in vitro.* Breast Cancer Res Treat, 2007. **105**(3): p. 319-26.
173. Serrels, A., et al., *Identification of potential biomarkers for measuring inhibition of Src kinase activity in colon cancer cells following treatment with dasatinib.* Mol Cancer Ther, 2006. **5**(12): p. 3014-22.
174. Serrels, B., et al., *A novel Src kinase inhibitor reduces tumour formation in a skin carcinogenesis model.* Carcinogenesis, 2009. **30**(2): p. 249-57.
175. Hennequin, L.F., et al., *N-(5-chloro-1,3-benzodioxol-4-yl)-7-[2-(4-methylpiperazin-1-yl)ethoxy]-5-(tetrahydro-2H-pyran-4-yloxy)quinazolin-4-amine, a novel, highly selective, orally available, dual-specific c-Src/Abl kinase inhibitor.* J Med Chem, 2006. **49**(22): p. 6465-88.
176. Jallal, H., et al., *A Src/Abl kinase inhibitor, SKI-606, blocks breast cancer invasion, growth, and metastasis in vitro and in vivo.* Cancer Res, 2007. **67**(4): p. 1580-8.
177. Hopert, A., et al., *Specificity and sensitivity of polymerase chain reaction (PCR) in comparison with other methods for the detection of mycoplasma contamination in cell lines.* J Immunol Methods, 1993. **164**(1): p. 91-100.
178. Glynn, S.A., et al., *A new superinvasive in vitro phenotype induced by selection of human breast carcinoma cells with the chemotherapeutic drugs paclitaxel and doxorubicin.* Br J Cancer, 2004. **91**(10): p. 1800-7.
179. Martin, A. and M. Clynes, *Acid phosphatase: endpoint for in vitro toxicity tests.* In Vitro Cell Dev Biol, 1991. **27A**(3 Pt 1): p. 183-4.
180. Alban, A., et al., *A novel experimental design for comparative two-dimensional gel analysis: two-dimensional difference gel electrophoresis incorporating a pooled internal standard.* Proteomics, 2003. **3**(1): p. 36-44.
181. Scheffer, G.L., et al., *Specific detection of multidrug resistance proteins MRP1, MRP2, MRP3, MRP5, and MDR3 P-glycoprotein with a panel of monoclonal antibodies.* Cancer Res, 2000. **60**(18): p. 5269-77.
182. Shor, A.C., et al., *Dasatinib inhibits migration and invasion in diverse human sarcoma cell lines and induces apoptosis in bone sarcoma cells dependent on SRC kinase for survival.* Cancer Res, 2007. **67**(6): p. 2800-8.
183. Johnson, F.M., et al., *Dasatinib (BMS-354825) tyrosine kinase inhibitor suppresses invasion and induces cell cycle arrest and apoptosis of head and neck squamous cell carcinoma and non-small cell lung cancer cells.* Clin Cancer Res, 2005. **11**(19 Pt 1): p. 6924-32.
184. Huang, F., et al., *Identification of candidate molecular markers predicting sensitivity in solid tumors to dasatinib: rationale for patient selection.* Cancer Res, 2007. **67**(5): p. 2226-38.
185. Balch, C.M., et al., *Prognostic factors analysis of 17,600 melanoma patients: validation of the American Joint Committee on Cancer melanoma staging system.* J Clin Oncol, 2001. **19**(16): p. 3622-34.
186. Rousseau, D.L., Jr., et al., *Revised American Joint Committee on Cancer staging criteria accurately predict sentinel lymph node positivity in clinically node-negative melanoma patients.* Ann Surg Oncol, 2003. **10**(5): p. 569-74.

187. Nakai, R., et al., *K858, a novel inhibitor of mitotic kinesin Eg5 and antitumor agent, induces cell death in cancer cells*. *Cancer Res*, 2009. **69**(9): p. 3901-9.
188. Guo, A., et al., *Signaling networks assembled by oncogenic EGFR and c-Met*. *Proc Natl Acad Sci U S A*, 2008. **105**(2): p. 692-7.
189. Rush, J., et al., *Immunoaffinity profiling of tyrosine phosphorylation in cancer cells*. *Nat Biotechnol*, 2005. **23**(1): p. 94-101.
190. Morel, E. and J. Gruenberg, *Annexin A2 binding to endosomes and functions in endosomal transport are regulated by tyrosine 23 phosphorylation*. *J Biol Chem*, 2009. **284**(3): p. 1604-11.
191. Gaggioli, C. and E. Sahai, *Melanoma invasion - current knowledge and future directions*. *Pigment Cell Res*, 2007. **20**(3): p. 161-72.
192. Mukhopadhyay, T. and J.A. Roth, *Functional inactivation of p53 by antisense RNA induces invasive ability of lung carcinoma cells and downregulates cytokeratin synthesis*. *Anticancer Res*, 1996. **16**(4A): p. 1683-9.
193. Gadea, G., et al., *Loss of p53 promotes RhoA-ROCK-dependent cell migration and invasion in 3D matrices*. *J Cell Biol*, 2007. **178**(1): p. 23-30.
194. Kute, T., et al., *Development of Herceptin resistance in breast cancer cells*. *Cytometry A*, 2004. **57**(2): p. 86-93.
195. Azzabi, A., et al., *Phase I study of temozolomide plus paclitaxel in patients with advanced malignant melanoma and associated in vitro investigations*. *Br J Cancer*, 2005. **92**(6): p. 1006-12.
196. Friedman, H.S., T. Kerby, and H. Calvert, *Temozolomide and treatment of malignant glioma*. *Clin Cancer Res*, 2000. **6**(7): p. 2585-97.
197. Aoki, T., et al., *Pharmacokinetic study of temozolomide on a daily-for-5-days schedule in Japanese patients with relapsed malignant gliomas: first study in Asians*. *Int J Clin Oncol*, 2007. **12**(5): p. 341-9.
198. Dhodapkar, M., et al., *Phase I trial of temozolomide (NSC 362856) in patients with advanced cancer*. *Clin Cancer Res*, 1997. **3**(7): p. 1093-100.
199. Baguley, B.C. and E.S. Marshall, *In vitro modelling of human tumour behaviour in drug discovery programmes*. *Eur J Cancer*, 2004. **40**(6): p. 794-801.
200. Walsh, N., et al., *Expression of multidrug resistance markers ABCB1 (MDR-1/P-gp) and ABCC1 (MRP-1) in renal cell carcinoma*. *BMC Urol*, 2009. **9**: p. 6.
201. Breen, L., et al., *Development of taxane resistance in a panel of human lung cancer cell lines*. *Toxicol In Vitro*, 2008. **22**(5): p. 1234-41.
202. Ghadersohi, A., et al., *Prostate derived Ets transcription factor shows better tumor-association than other cancer-associated molecules*. *Oncol Rep*, 2004. **11**(2): p. 453-8.
203. Trog, D., et al., *Expression of ABC-1 transporter is elevated in human glioma cells under irradiation and temozolomide treatment*. *Amino Acids*, 2005. **28**(2): p. 213-9.
204. Chua, C., et al., *Characterization of a side population of astrocytoma cells in response to temozolomide*. *J Neurosurg*, 2008. **109**(5): p. 856-66.
205. Rabindran, S.K., et al., *Fumitremorgin C reverses multidrug resistance in cells transfected with the breast cancer resistance protein*. *Cancer Res*, 2000. **60**(1): p. 47-50.
206. Robey, R.W., et al., *ABCG2: determining its relevance in clinical drug resistance*. *Cancer Metastasis Rev*, 2007. **26**(1): p. 39-57.

207. Depeille, P., et al., *Combined effects of GSTP1 and MRP1 in melanoma drug resistance*. Br J Cancer, 2005. **93**(2): p. 216-23.
208. Sergent, T., et al., *Differential modulation of ochratoxin A absorption across Caco-2 cells by dietary polyphenols, used at realistic intestinal concentrations*. Toxicol Lett, 2005. **159**(1): p. 60-70.
209. Demetri, G.D., et al., *Phase I dose-escalation and pharmacokinetic study of dasatinib in patients with advanced solid tumors*. Clin Cancer Res, 2009. **15**(19): p. 6232-40.
210. Buettner, R., et al., *Inhibition of Src family kinases with dasatinib blocks migration and invasion of human melanoma cells*. Mol Cancer Res, 2008. **6**(11): p. 1766-74.
211. Tan, M., et al., *ErbB2 promotes Src synthesis and stability: novel mechanisms of Src activation that confer breast cancer metastasis*. Cancer Res, 2005. **65**(5): p. 1858-67.
212. Song, L., et al., *Dasatinib (BMS-354825) selectively induces apoptosis in lung cancer cells dependent on epidermal growth factor receptor signaling for survival*. Cancer Res, 2006. **66**(11): p. 5542-8.
213. Recchia, I., et al., *Pyrrolopyrimidine c-Src inhibitors reduce growth, adhesion, motility and invasion of prostate cancer cells in vitro*. Eur J Cancer, 2003. **39**(13): p. 1927-35.
214. Bantscheff, M., et al., *Quantitative chemical proteomics reveals mechanisms of action of clinical ABL kinase inhibitors*. Nat Biotechnol, 2007. **25**(9): p. 1035-44.
215. Dittmann, K., et al., *Radiation-induced caveolin-1 associated EGFR internalization is linked with nuclear EGFR transport and activation of DNA-PK*. Mol Cancer, 2008. **7**: p. 69.
216. Benhar, M., D. Engelberg, and A. Levitzki, *Cisplatin-induced activation of the EGF receptor*. Oncogene, 2002. **21**(57): p. 8723-31.
217. Homsy, J., et al., *Src activation in melanoma and Src inhibitors as therapeutic agents in melanoma*. Melanoma Res, 2009. **19**(3): p. 167-75.
218. Flaherty, K.T., *Sorafenib: delivering a targeted drug to the right targets*. Expert Rev Anticancer Ther, 2007. **7**(5): p. 617-26.
219. Wang, X.D., et al., *Identification of candidate predictive and surrogate molecular markers for dasatinib in prostate cancer: rationale for patient selection and efficacy monitoring*. Genome Biol, 2007. **8**(11): p. R255.
220. Konecny, G.E., et al., *Activity of the multikinase inhibitor dasatinib against ovarian cancer cells*. Br J Cancer, 2009. **101**(10): p. 1699-708.
221. Logozzi, M., et al., *High levels of exosomes expressing CD63 and caveolin-1 in plasma of melanoma patients*. PLoS One, 2009. **4**(4): p. e5219.
222. Cokakli, M., et al., *Differential expression of Caveolin-1 in hepatocellular carcinoma: correlation with differentiation state, motility and invasion*. BMC Cancer, 2009. **9**: p. 65.
223. Campbell, E.J., et al., *Phosphorylated c-Src in the nucleus is associated with improved patient outcome in ER-positive breast cancer*. Br J Cancer, 2008. **99**(11): p. 1769-74.
224. Diaz, N., et al., *Activation of stat3 in primary tumors from high-risk breast cancer patients is associated with elevated levels of activated SRC and survivin expression*. Clin Cancer Res, 2006. **12**(1): p. 20-8.

225. Elsberger, B., et al., *Is expression or activation of Src kinase associated with cancer-specific survival in ER-, PR- and HER2-negative breast cancer patients?* Am J Pathol, 2009. **175**(4): p. 1389-97.
226. Tatarov, O., et al., *SRC family kinase activity is up-regulated in hormone-refractory prostate cancer.* Clin Cancer Res, 2009. **15**(10): p. 3540-9.
227. Ben-Izhak, O., V. Cohen-Kaplan, and R.M. Nagler, *The prognostic role of phospho-Src family kinase analysis in tongue cancer.* J Cancer Res Clin Oncol, 2009.
228. Wu, Y., et al., *Src phosphorylation of RhoGDI2 regulates its metastasis suppressor function.* Proc Natl Acad Sci U S A, 2009. **106**(14): p. 5807-12.
229. Westermark, B., et al., *Human melanoma cell lines of primary and metastatic origin express the genes encoding the chains of platelet-derived growth factor (PDGF) and produce a PDGF-like growth factor.* Proc Natl Acad Sci U S A, 1986. **83**(19): p. 7197-200.
230. Ichikawa, T., et al., *Moesin and CD44 expression in cutaneous melanocytic tumours.* Br J Dermatol, 1998. **138**(5): p. 763-8.
231. Niggli, V. and J. Rossy, *Ezrin/radixin/moesin: versatile controllers of signaling molecules and of the cortical cytoskeleton.* Int J Biochem Cell Biol, 2008. **40**(3): p. 344-9.
232. Hoefflich, K.P., et al., *Insights into a single rod-like helix in activated radixin required for membrane-cytoskeletal cross-linking.* Biochemistry, 2003. **42**(40): p. 11634-41.
233. Estecha, A., et al., *Moesin orchestrates cortical polarity of melanoma tumour cells to initiate 3D invasion.* J Cell Sci, 2009. **122**(Pt 19): p. 3492-501.
234. Flamini, M.I., et al., *Differential actions of estrogen and SERMs in regulation of the actin cytoskeleton of endometrial cells.* Mol Hum Reprod, 2009. **15**(10): p. 675-85.
235. Manta, B., et al., *The peroxidase and peroxynitrite reductase activity of human erythrocyte peroxiredoxin 2.* Arch Biochem Biophys, 2009. **484**(2): p. 146-54.
236. Choi, M.H., et al., *Regulation of PDGF signalling and vascular remodelling by peroxiredoxin II.* Nature, 2005. **435**(7040): p. 347-53.
237. Furuta, J., et al., *Silencing of Peroxiredoxin 2 and aberrant methylation of 33 CpG islands in putative promoter regions in human malignant melanomas.* Cancer Res, 2006. **66**(12): p. 6080-6.
238. Carta, F., et al., *Analysis of candidate genes through a proteomics-based approach in primary cell lines from malignant melanomas and their metastases.* Melanoma Res, 2005. **15**(4): p. 235-44.
239. Daugaard, M., M. Rohde, and M. Jaattela, *The heat shock protein 70 family: Highly homologous proteins with overlapping and distinct functions.* FEBS Lett, 2007. **581**(19): p. 3702-10.
240. Jiang, C.C., et al., *Glucose-regulated protein 78 antagonizes cisplatin and adriamycin in human melanoma cells.* Carcinogenesis, 2009. **30**(2): p. 197-204.
241. Hong, M., et al., *Transcriptional regulation of the Grp78 promoter by endoplasmic reticulum stress: role of TFII-I and its tyrosine phosphorylation.* J Biol Chem, 2005. **280**(17): p. 16821-8.
242. Powers, M.V., P.A. Clarke, and P. Workman, *Dual targeting of HSC70 and HSP72 inhibits HSP90 function and induces tumor-specific apoptosis.* Cancer Cell, 2008. **14**(3): p. 250-62.

243. Takano, S., et al., *Elevated levels of mortalin expression in human brain tumors*. *Exp Cell Res*, 1997. **237**(1): p. 38-45.
244. Mussunoor, S. and G.I. Murray, *The role of annexins in tumour development and progression*. *J Pathol*, 2008. **216**(2): p. 131-40.
245. Monastyrskaya, K., E.B. Babiychuk, and A. Draeger, *The annexins: spatial and temporal coordination of signaling events during cellular stress*. *Cell Mol Life Sci*, 2009. **66**(16): p. 2623-42.
246. Biener, Y., et al., *Annexin II is a novel player in insulin signal transduction. Possible association between annexin II phosphorylation and insulin receptor internalization*. *J Biol Chem*, 1996. **271**(46): p. 29489-96.
247. Huang, K.S., et al., *Two human 35 kd inhibitors of phospholipase A2 are related to substrates of pp60v-src and of the epidermal growth factor receptor/kinase*. *Cell*, 1986. **46**(2): p. 191-9.
248. Monastyrskaya, K., et al., *Annexins sense changes in intracellular pH during hypoxia*. *Biochem J*, 2008. **409**(1): p. 65-75.
249. Rescher, U. and V. Gerke, *S100A10/p11: family, friends and functions*. *Pflugers Arch*, 2008. **455**(4): p. 575-82.
250. Powell, M.A. and J.R. Glenney, *Regulation of calpactin I phospholipid binding by calpactin I light-chain binding and phosphorylation by p60v-src*. *Biochem J*, 1987. **247**(2): p. 321-8.
251. Lee, K.H., D.S. Na, and J.W. Kim, *Calcium-dependent interaction of annexin I with annexin II and mapping of the interaction sites*. *FEBS Lett*, 1999. **442**(2-3): p. 143-6.
252. de Graauw, M., et al., *Annexin A2 phosphorylation mediates cell scattering and branching morphogenesis via cofilin Activation*. *Mol Cell Biol*, 2008. **28**(3): p. 1029-40.
253. Deora, A.B., et al., *An annexin 2 phosphorylation switch mediates p11-dependent translocation of annexin 2 to the cell surface*. *J Biol Chem*, 2004. **279**(42): p. 43411-8.
254. Hubaishy, I., et al., *Modulation of annexin II tetramer by tyrosine phosphorylation*. *Biochemistry*, 1995. **34**(44): p. 14527-34.
255. Luo, W., et al., *Global impact of oncogenic Src on a phosphotyrosine proteome*. *J Proteome Res*, 2008. **7**(8): p. 3447-60.
256. Wolf-Yadlin, A., et al., *Effects of HER2 overexpression on cell signaling networks governing proliferation and migration*. *Mol Syst Biol*, 2006. **2**: p. 54.
257. Eberhard, D.A., et al., *Control of the nuclear-cytoplasmic partitioning of annexin II by a nuclear export signal and by p11 binding*. *J Cell Sci*, 2001. **114**(Pt 17): p. 3155-66.
258. Gould, K.L., et al., *The protein-tyrosine kinase substrate p36 is also a substrate for protein kinase C in vitro and in vivo*. *Mol Cell Biol*, 1986. **6**(7): p. 2738-44.
259. Luo, W., et al., *Epstein-Barr virus latent membrane protein 1 mediates serine 25 phosphorylation and nuclear entry of annexin A2 via PI-PLC-PKCalpha/PKCbeta pathway*. *Mol Carcinog*, 2008. **47**(12): p. 934-46.
260. Liu, J., et al., *Nuclear annexin II negatively regulates growth of LNCaP cells and substitution of ser 11 and 25 to glu prevents nucleo-cytoplasmic shuttling of annexin II*. *BMC Biochem*, 2003. **4**: p. 10.
261. Huang, Y., et al., *Involvement of Annexin A2 in p53 induced apoptosis in lung cancer*. *Mol Cell Biochem*, 2008. **309**(1-2): p. 117-23.



262. Tatenhorst, L., et al., *Knockdown of annexin 2 decreases migration of human glioma cells in vitro*. *Neuropathol Appl Neurobiol*, 2006. **32**(3): p. 271-7.
263. Bao, H., et al., *Overexpression of Annexin II affects the proliferation, apoptosis, invasion and production of proangiogenic factors in multiple myeloma*. *Int J Hematol*, 2009. **90**(2): p. 177-85.
264. Chiang, Y., et al., *Specific down-regulation of annexin II expression in human cells interferes with cell proliferation*. *Mol Cell Biochem*, 1999. **199**(1-2): p. 139-47.
265. Pierce, A., et al., *Identification of a novel, functional role for S100A13 in invasive lung cancer cell lines*. *Eur J Cancer*, 2008. **44**(1): p. 151-9.
266. Shnyder, S.D. and M.J. Hubbard, *ERp29 is a ubiquitous resident of the endoplasmic reticulum with a distinct role in secretory protein production*. *J Histochem Cytochem*, 2002. **50**(4): p. 557-66.
267. Hermann, V.M., J.F. Cutfield, and M.J. Hubbard, *Biophysical characterization of ERp29. Evidence for a key structural role of cysteine 125*. *J Biol Chem*, 2005. **280**(14): p. 13529-37.
268. Mkrtchian, S., et al., *ERp29, an endoplasmic reticulum secretion factor is involved in the growth of breast tumor xenografts*. *Mol Carcinog*, 2008. **47**(11): p. 886-92.
269. Deocaris, C.C., S.C. Kaul, and R. Wadhwa, *On the brotherhood of the mitochondrial chaperones mortalin and heat shock protein 60*. *Cell Stress Chaperones*, 2006. **11**(2): p. 116-28.
270. Garrido, C., et al., *Heat shock proteins: endogenous modulators of apoptotic cell death*. *Biochem Biophys Res Commun*, 2001. **286**(3): p. 433-42.
271. Cappello, F., et al., *Hsp60 expression, new locations, functions and perspectives for cancer diagnosis and therapy*. *Cancer Biol Ther*, 2008. **7**(6): p. 801-9.
272. Hwang, J.H., et al., *The role of fascin in the migration and invasiveness of malignant glioma cells*. *Neoplasia*, 2008. **10**(2): p. 149-59.
273. Tsai, W.C., et al., *Overexpression of fascin-1 in advanced colorectal adenocarcinoma: tissue microarray analysis of immunostaining scores with clinicopathological parameters*. *Dis Markers*, 2007. **23**(3): p. 153-60.
274. Chen, J., et al., *Human CRYL1, a novel enzyme-crystallin overexpressed in liver and kidney and downregulated in 58% of liver cancer tissues from 60 Chinese patients, and four new homologs from other mammals*. *Gene*, 2003. **302**(1-2): p. 103-13.
275. Ejeskar, K., et al., *Introduction of in vitro transcribed ENO1 mRNA into neuroblastoma cells induces cell death*. *BMC Cancer*, 2005. **5**: p. 161.
276. Wygrecka, M., et al., *Enolase-1 promotes plasminogen-mediated recruitment of monocytes to the acutely inflamed lung*. *Blood*, 2009. **113**(22): p. 5588-98.